Design and Synthesis of Lossy Microwave Filters

Meng Meng

Submitted in accordance with the requirements for the degree of
Doctor of philosophy

The University of Leeds
School of Electrical and Electronic Engineering

July, 2014

The candidate confirms that the work submitted is her own, except where work which has formed part of jointly-authored publications has been included. The contribution of the candidate and the other authors to this work has been explicitly indicated below. The candidate confirms that appropriate credit has been given within the thesis where reference has been made to the work of others.

The work presented in this thesis is co-authored with my supervisor Professor Ian Hunter. The candidate is responsible for the work presented in Chapter 3 and 4 and section 5.1. The synthesis of directional filters presented in section 5.2 is a combined work with Mr. Evaristo Musonda who has worked on the derivation of circuit equivalence. The candidate has worked on the circuit analysis, lossy examples and the EM modeling. The work presented in Chapter 6 is co-authored with Professor John. D. Rhodes. The candidate has worked on formulation of lumped element analysis and the examples.

Acknowledgements

I would like to express sincere gratitude to my advisor Prof. Ian Hunter for his invaluable guidance and support throughout out the period of research and study.

I'm also extremely grateful to Filtronic plc for sponsoring my work.

I would also like to thank Prof J. D. Rhodes and Mr. Evaristo Musonda for the collaborated work.

Special thanks go to Mr. Graham Brown in the department workshop for the fabrication of the filters.

Finally, I would like to thank my family and friend for their encouragement and support.

Abstract

The design of microwave filters starts from the derivation of a defined lowpass prototype network. A general lossy synthesis method is given which can 1) derive the reflection function from the transfer function when the unitary condition is not satisfied; 2) find the expressions for the complex admittance parameters and 3) synthesize the lossy coupling matrix (CM) with prescribed loss distributions. Two special cases are discussed for solving the refection function from a prescribed transfer function.

An alternative approach to cope with loss is studied. In a transversal array, some resonators can be replaced by their low-Q alternatives to reduce the manufacture cost as well as the cavity size. The exact values for the dissipations of resonators or couplings can be determined analytically or by methods of gradient based optimizations.

A method of CM synthesis with non-ideal load is given which can be used in designing diplexers or multiplexers. Filter networks matching to complex load impedances can be found by renormalizing reference impedances. An iteration method is introduced which can deal with frequency variant load and can deliver the required reflection zeros.

A method for the synthesis of directional filters is presented which can be used for designing combiners. While each section of directional filters provides a 1^{st} order response, more complex filter characteristics can be realized by cascading those single sections. By proper transformations, directional filter networks can be realized using normal resonators and couplings. An example utilizing coaxial resonator is given.

A method for the analysis of 2-D lumped element networks is presented. The method is based on the general telegrapher's equations of multi-wire transmission lines. A 2-D lumped element network is equivalent to a combination of sub-networks which support single mode propagations. The method can be applied to the analysis of metamaterials and can be used for the design of waffle-iron filters.

Table of Contents

List of Tables

List of Figures

Chapter 1
Introduction

1.1 Microwave filters in communication systems

Microwave filters are frequency selective devices implemented in most communication systems. It allows signals of certain frequency band to pass though and blocks or attenuates the signal transmission of other frequencies [1][2]. Generally speaking, the vast literatures on microwave filters concentrate on one of the following aspects: 1) material and structure related to the filter design, 2) performance of transmission and rejection related to the filter synthesis and 3) issues of cost and size related to the manufacture.

Since the 1950s, the development of communication systems requires the implementation of microwave filters of high performance. While filter design in the past involves much lab work on cut-and-try, filter design nowadays has been influenced by the developments of two areas including the applications of EM modelling and simulation software and the use of CMs as a general representation of narrow band filter networks. The field of filter design and synthesis is to convert the specifications to a circuit network and to realize the network by a physical filter through modelling and tuning.

In satellite communication systems, the frequency division architecture illustrated in Fig. 1.1 is used due to the linearity requirement of high power amplifiers[2][3]. Filters are integrated into input/output multiplexers so that signals can be channelized. Due to the stringent requirement on loss, common designs use waveguide or dielectric filters as they provide the highest Q. Dual-mode waveguide filters are also used for size reduction.

In most mobile communication systems, filters implemented in base stations are integrated as a diplexer [4][5] as illustrated in Fig. 1.2. Typically, the requirements for a diplexer include the high isolation between the two channels, high rejection of the transmit filter in the receiver band and low passband insertion loss of the transmit filter. These requirements can be fulfilled by filters with transmission zeros which are generated by cross couplings. Coaxial resonators are usually used as they can be easily

arranged into desired configurations. Also, the requirement for loss is not as stringent as that in satellite communication systems.

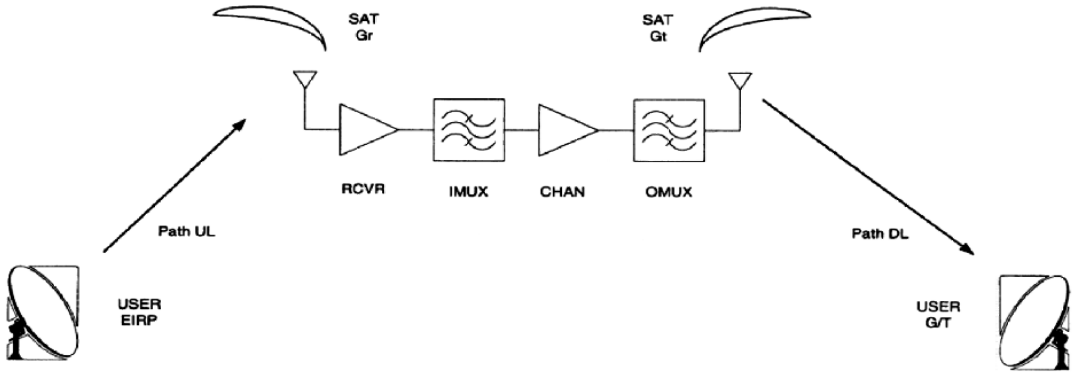

Fig. 1.1 Illustration of multiplexers in a satellite communication system [3].

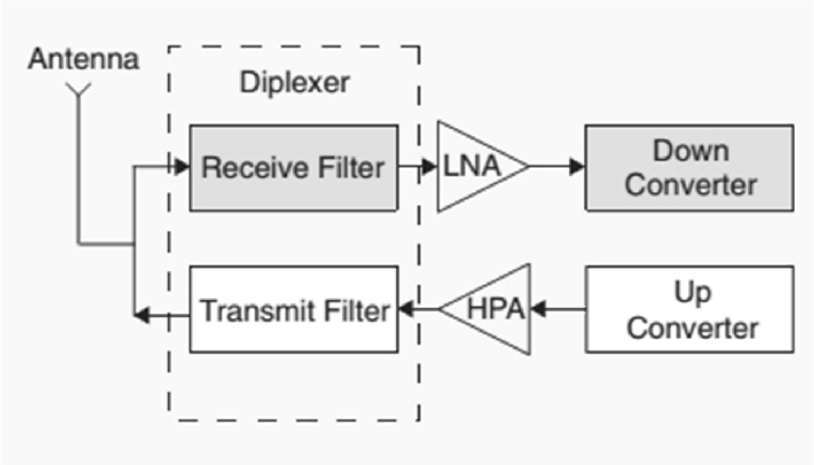

Fig. 1.2 Diplexer in base station for mobile communication system [4].

1.2 Overview on filter design and synthesis

Starting from the specifications of a certain communication channel, the goal of filter design and synthesis is to find a physical realization that can fulfil those requirements. This problem has been divided into two categories, the filter synthesis which concentrates on the derivation of networks based on standard characteristics, and the filter design which concentrates on the physical realisation of the network. Various techniques proposed in the literature on microwave filters usually deal with a specific section of that sequence.

Developed since the 1930s, modern filter synthesis techniques as illustrated in Fig. 1.3 involve the approximation of the filter specifications by a transfer function and the derivation of lowpass prototype networks. The requirements for a bandpass filter include the centre frequency, the percentage bandwidth, the maximum insertion loss in the passband, and the minimum rejection levels in the stopband.

First, those specifications are fulfilled by a filter characteristic which is a mathematical expression usually in the form of rational polynomials[6]. The standard characteristics can be derived analytically and the non-standard ones can be found by optimizations. Much of the work is summarized in [1] with design charts for various filter characteristics.

Next, a low pass prototype network can be synthesized in an approximated or exact manner according to the characteristic. Nowadays, CMs are used for coupled resonator filters of varied configurations [7], and analytical procedures are found to derive the corresponding coupling matrix (CM) from a given characteristic [8].

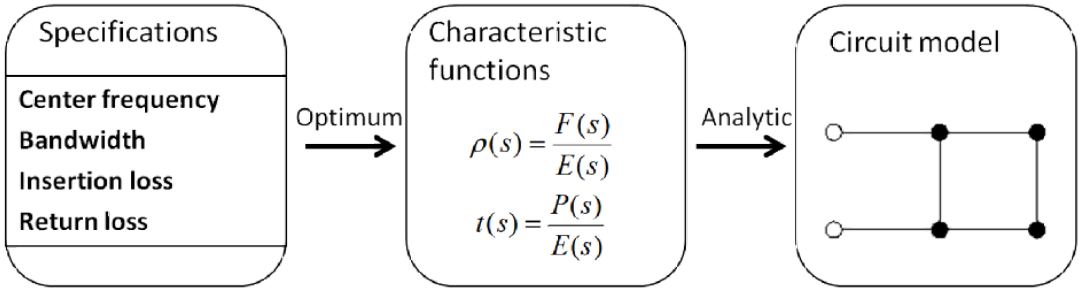

Fig. 1.3 Procedures for filter synthesis.

The procedures for filter design are illustrated in Fig. 1.4. First, varied denormalizations are applied to the synthesized lowpass prototype network, so that it can be transformed into desired frequency bands. For the lumped element network, standard transformations between lowpass, bandpass, highpass and band stop configurations can be found in [1]. Richard's transformation can be used to transform the lumped elements to distributed elements [9].

Then physical realisation of the network can be found by utilizing various microwave elements including TEM transmission lines, waveguides, coaxial and dielectric resonators. Design equations can be found for some standard filter structures in [1]. Nowadays, filter design utilizes EM simulation software that can provide results close to measurements. For narrow band design, filter networks can be treated as coupled resonators [7]. With desired technologies, resonators and coupling elements are modelled separately according to their values in the synthesized network [10]. For desired configurations, connecting the resonators with coupling elements provides an initial design.

Finally, computer aided tunings [11] can be applied to the initial designs utilizing various optimization techniques until the desired response is achieved. Computer aided tunings are also useful to tune the physical devices in order to compensate the manufacturing tolerance.

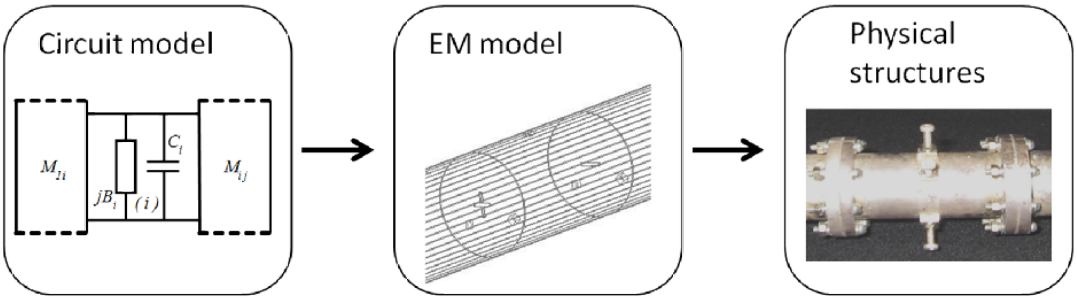

Fig. 1.4 Procedures for filter design.

Circuit models are important for the filter design and synthesis because they link between the mathematical expressions and the physical devices. A filter network that is suitable for a CM representation is shown in Fig. 1.5. The resonators are multiple coupled and non-synchronized tuned. M_{ij} represents the coupling between i^{th} and j^{th} resonators. jB_i is the frequency invariant reactance. G_s and G_L are the unitary source and load admittances. It's defined as an N+2 type network in [8] as there are two invertors connecting to the input and output loads. Ideally, the coupling matrix M is purely real and symmetric.

The current filter design and synthesis techniques dealing with ideal CMs have been proven to be effective. However, the requirements of purely real

CM and unitary loads in circuit models are not true for physical filters and thus limit the applications of CMs in filter design and synthesis. For example, for filters of high performance in insertion loss or the ones with reduced size, as the dissipation incorporated in resonators and couplings can no longer be neglected, CM can no longer be purely real. Also, filters in communication systems are usually integrated with other devices at the output end. As a result, the unitary load admittance is only an approximation to the actual condition.

A more practical network is shown in Fig. 1.6 with dissipations included in resonators and a non-ideal load admittance. While the procedures for the synthesis of ideal CMs are described in section 2.1 and 2.2, the derivation of CMs considering these non-ideal effects remains to be problematic.

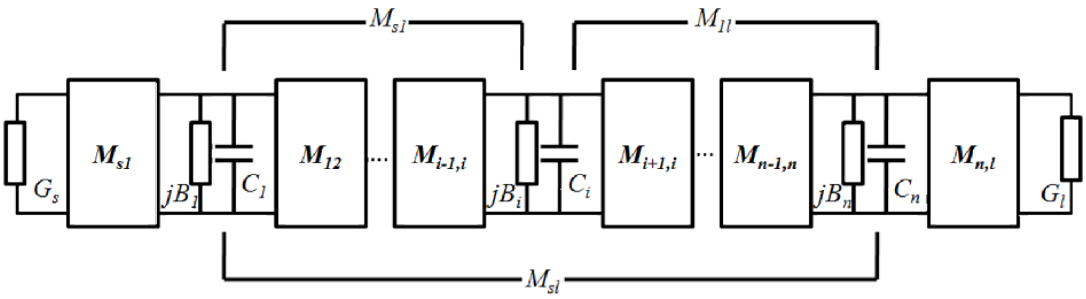

Fig. 1.5 Illustration of an N+2 prototype network.

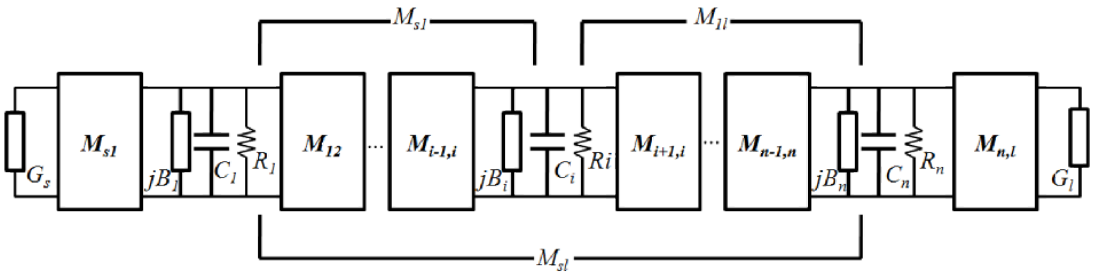

Fig. 1.6 Illustration of an N+2 prototype network with lossy resonators.

1.3 Overview of the thesis

The purpose of the work presented in this thesis is to provide a synthesis method for a modified circuit model in which some of the physical effects are included, so that the application of CM can be extended to more general cases. Besides the method for the synthesis of lossy filter networks, various

techniques are proposed for the design of diplexers or lowpass waveguide filters.

For lossless networks, the reflection function can be found from the transfer function according to the condition of power conservation. Rational polynomial expressions for admittance parameters can then be derived [8]. The partial expansion of admittance parameters provides purely real residues and purely imaginary poles. Then a transversal array can be formed and can be transformed to other configurations. However, for lossy networks, the power conservation is not satisfied. The procedure [8] for the derivation of admittance parameters is no longer valid.

The lossy synthesis method is general in this paper. A condition for the characteristic polynomials is introduced to replace the use the power conservation. As a result, the rational polynomial transformation between the S and admittance parameters for an N^{th} degree filter network is modified to be capable of dealing with losses. When the polynomials of S parameters satisfy a given condition, it is guaranteed that the admittance parameters as well as the CM can be derived from the S parameters.

Two special cases are discussed for solving the refection function from a prescribed transfer function. In the first case, F_{11} (the numerator of S_{11}) equals to F_{22} (the numerator of S_{22}). This is the case that is equivalent to the even/odd mode analysis but is extended to be applied for asymmetric filter responses. In the second case, the loss distribution among a filter network is given. A method of iteration is applied to derive the CM with the prescribed loss distribution. The method is an extension to the conventional method of predistortion with non-uniform resonator Qs and lossy invertors.

An alternative approach to cope with loss is also studied. It is noticed that in a transversal array, the effect of loss of each resonator on the filter response is independent of each other. The effect of loss of each resonator depends on its bandwidth and resonant frequency. As a result, some resonators can be replaced by their low-Qu alternatives to reduce the manufacture cost as well as the cavity size. A new type of transfer function is introduced. Circuit model synthesized according to this transfer function exhibits parallel

connected resonators with great bandwidth variations thus suitable for the design using varied Qu distributions.

The exact values for the Qu distributions or lossy invertors can be determined by methods of gradient based optimizations. Previously, optimizations of CM are used to replace the series rotations for a desired configuration and the responses achieved are based on ideal Chebyshev function. The methods presented in this thesis can optimize the dissipation distribution for a parallel connected network. The cost function is defined not to get an ideal Chebyshev response but one with proper insertion and return loss. By tuning the weightings of different terms in the cost function, various goals can be achieved.

The design method is also applied to configurations other than parallel connected networks. Using CM rotations, transversal arrays can be transformed into other parallel connected networks by grouping the residues and poles. Various examples are given in the thesis. One of the 4^{th} order example is implemented with mixed coaxial and microstrip technology. Examples of filters realized by mixed coaxial and dielectric resonators are also provided.

Since the size and weight of a filter is an important aspect of filter implementation, compensations between filter's performance and dissipation is critical in practical design. The introduction of non-uniform Q provides extra variables that can be tuned so that filter size can be reduced without losing performance.

A method of CM synthesis with non-ideal load is given which can be used in the design of a diplexer or a multiplexer. Contracting to the lowpass prototype networks which begin and end in uniform resistances, a channel filter is synthesized with a non-ideal load impedance which represents the manifold connected.

Since the S parameters of any two port network are defined with reference impedances, the filter network matching to a complex load impedance can be easily derived by a renormalization of reference impedance. For more

practical cases, the complex reference impedance should be a function of frequency over a specified frequency band. However, when the frequency variant load is taken into consideration, the response of the network is of a higher degree which violates the methods for the CM synthesis. As a result, various optimizations such as curve fittings are used to maintain the original degree of the filter network.

In this thesis, an iteration method is introduced which doesn't involve any curve fitting and can deliver the required reflection zeros thus maintain the required return loss level. This can provide better results comparing to previous methods.

The method for the synthesis of directional filters is presented in this thesis. While each section of directional filters provides a 1^{st} order response, more complex filter characteristics can be realized by cascading those single sections. It is also demonstrated that directional filters can be used as a novel approach for designing combiners which is used in Long Term Evolution (LTE) base stations.

A method for the analysis of 2-D lumped element networks is presented. The method is based on general telegrapher's equation of the multi-wire transmission line. The 2-D lumped element network is equivalent to a combination of sub-networks which support a single mode of propagation. The method can be applied to the analysis of certain types of metamaterials and can be used for the study of waffle-iron filters.

1.4 Organization of the thesis

The thesis is arranged to have six chapters with the first one being the introduction.

Chapter 2 provides background information on filter synthesis and design. Traditional synthesis methods in which the resonators are of high Qus or lossless are reviewed first. The synthesis methods are based on low pass prototype networks. With the introduction of CMs, the coupled resonator

networks can be synthesized and analyzed by various matrix operations. Using the transversal array network, the synthesis of CMs is greatly simplified. Then, techniques for the synthesis and design of lossy filters are reviewed including the method of predistortion, the use of even and odd mode networks and some modifications applied to CMs. These loss filters are designed to have dissipative resonators and cross couplings based on lossy transfer functions.

Chapter 3 provides the generalized CM synthesis method for lossy filters. A condition for the characteristic polynomials is introduced to replace the use the power conservation. And a rational polynomial transformation between the S and admittance parameters for an N^{th} degree filter network is given. Then two special cases of solutions are discussed. The first one corresponds to the even and odd mode analysis method with asymmetrical responses. The second one corresponds to a more generalized method of predistortion with non-uniform dissipations. Examples of mixed coaxial and dielectric resonator filters are designed.

In Chapter 4, the synthesis of lossy parallel connected network is discussed. The effect of loss in parallel connected network is studied. It is found that for a filter networks, some of its resonators are more critical than the others considering the effect of loss. As a result an optimum Q distribution with minimum number of higher Qu resonators can be implemented. Then an analytic solution to the Q distribution is given for parallel connected networks with small losses. When non-uniform Q is applied to other types of networks, a gradient based optimization can be used to derive the optimum loss distribution. Various numerical examples are given with two physical designs.

Chapter 5 presents the method for the synthesis of CM with non-ideal load effects which can be applied in the design of diplexer. The transformation between S and Y parameters with a frequency variant reference impedance are reviewed first. Then an iteration is applied for the synthesis of CM with which the reflection zeros are solved thus obtaining a similar return loss level.

The method for the design of diplexers based on directional filters is revisited. Explicit synthesis procedures are given so that any filter

characteristic can be realized by a cascading of single section DFs. Transformation and circuit equivalence are then applied so that the DF networks can be realized by standard filter technologies using resonators, couplings and TLs. An example is given for a 4^{th} degree DF and is realized by combline resonators.

Chapter 6 presents the method for the analysis of 2-D lumped element networks which can be used in the design of waffle-iron filters. First, analysis is given for the multi-mode propagation in multi-wire lines. 2-D network consisting of lumped elements are studied which shows that this kind of network supports multi-mode of propagation. Waffle-iron filters are examples of these 2-D networks and simulations results are given and compared with circuit analysis.

Chapter 2
Filter Design and Synthesis

In this chapter, the theories for the design and synthesis of microwave filters will be reviewed. Traditionally, as presented in [1], filter design consists of the following steps. The first is the approximation of the specifications by a transfer function. Specifications include requirements on the rejection level, the in-band insertion loss level and the return loss level. Transfer functions satisfying given specifications are usually solved approximately by optimizations [12]. Standard types of transfer functions are reviewed first.

The second step is the synthesis of a network which can realize the transfer function and is solved with the knowledge of network synthesis. Lowpass prototype networks are defined which is usually a cascading of series inductance and shunt capacitance. Design charts for lowpass prototypes with standard transfer functions are given in [1]. Other networks can be derived directly from them. When inverters are introduced to lowpass prototypes [13], the cascaded inductance and capacitance network is transformed to coupled resonators which can be synthesized by Darlington's insertion loss method [1][2] using series of element extractions.

Finally, with the prototype networks, the problem of filter design aims to transform the network representation into a variety of microwave elements including TEM transmission lines, waveguides and dielectric resonators. This is achieved by the denormalization of prototype networks based on the equivalence of lumped and distributed elements. [1] provides design charts for most standard filter responses and physical structures.

Nowadays, CMs introduced in [7] and developed in [8] are used as a general representation of coupled resonator filters. Its definition is reviewed first. Then the procedures for the synthesis of transversal arrays are reviewed. The next section is on the introduction of various transformations applied to transversal arrays so that various network configurations can be achieved.

With the aid of EM simulation software, filter designs depend more and more on the efficient modelling of microwave components. [14] provides recent examples for the design of various microwave filters. Initial EM models of bandpass or distributed networks which are obtained by the demoralisation

of lowpass prototypes. Then tuning is applied to the initial model so that the required response can be achieved.

When dissipations are taken into consideration, sets of conditions used in the synthesis of filter networks are violated. Commonly used methods for the synthesis of lossy networks are reviewed including the predistortion, the lossy CM synthesis and the even/odd mode analysis.

2.1 Filter characteristics

The synthesis of microwave filter starts with the filter functions which are defined in a normalized frequency domain [1]. An ideal filter response has perfect transmission in the passband defined from ω=-1 to ω=1. The perfect transmission in the passband and complete rejection in the stopband leads to an infinite group delay at the band edge which is impossible to achieve by finite degree networks [15].

This ideal response can be approximated by functions of rational polynomials. The rational polynomial expressions for S parameters of a filter network are given in (2.1) in which the polynomials F_{11} and E are of degree N (which is defined as the filter order) and the polynomial P is of degree Nfz (which defines the transmission zeros and is less than N). In addition to the S parameters responses, it is useful to study the roots of these polynomials and this can be done in a plot of roots distributions in the complex plane of $s=\sigma+j\omega$ with the x-axis denoting the real part σ and y-axis denoting the imaginary part $j\omega$.

$$S_{11}=\frac{F_{11}(s)}{E(s)},\quad S_{21}=\frac{\mathrm{P}(s)}{E(s)},\quad S_{22}=\frac{F_{22}(s)}{E(s)} \tag{2.1}$$

For lossless characteristics, S parameters must satisfy the condition of power conservation given in (2.2). As a result, the polynomial F_{22} is the complex conjugate of F_{11} with its highest coefficient be equal to that of F_{11} as given in (2.3).Also the polynomial E satisfies the Hurwitz condition that all its roots lie in the left half of the complex plane. According to (2.4), when F_{11} and P are known, E can be found by an alternative roots method [16].

$$\begin{aligned} S_{11}S_{11}^{*}+S_{21}S_{21}^{*}&=1\\ S_{22}S_{22}^{*}+S_{12}S_{12}^{*}&=1\\ S_{11}S_{21}^{*}+S_{21}S_{22}^{*}&=0 \end{aligned} \tag{2.2}$$

$$F_{11} = (-1)^N F_{22}^* \tag{2.3}$$

$$F_{11} \cdot F_{11}^* + P \cdot P^* = E \cdot E \tag{2.4}$$

To approximate the ideal shape, various functions of rational polynomial are used [1] such as Maximum Flat and Chebyshev functions. For these standard filter characteristics, the polynomials F_{11} and P could be derived according to defined procedures [12]. Some examples of filter characteristics are given in the following.

1). Maximum flat

For a maximum flat characteristic, its polynomials are given in (2.5). The denominator can be found according to (2.4). A typical response and roots distribution for a 4th degree response is shown in Fig. 2.1(a).

$$\begin{aligned} F_{11} &= s^N \\ P &= 1 \end{aligned} \tag{2.5}$$

2). Chebyshev

For Chebyshev response, the polynomial F can be found from a Chebyshev polynomial as in (2.6) which could be derived according to the recursive procedure given in [1]. A 4th degree response is shown in Fig. 2.1(b).

$$\begin{aligned} F_{11} &= T_n \\ P &= 1 \end{aligned} \tag{2.6}$$

3). Characteristics with transmission zeros

Transmission zeros are included in designing filter responses as they have several advantages and are realized by modifying the constant P in (2.5) and (2.6) to a polynomial of certain degree. Purely imaginary transmission zeros are included to provide sharpened transitions at bandedges. Fig. 2.1(c) shows the example of a 4th order maximum flat response with two transmission zeros at ±1.6j.

Transmission zeros can also be introduced into Chebyshev responses. It is then called a general Chebyshev response and the derivation is given in [16]. When the positions of transmission zeros are arranged properly, the rejection in stopband can be equal-ripple. The example of a 4th degree with three transmission zeros at 1.7j, 2.2j and 3.6j is shown in Fig. 2.1(d).

Complex transmission zeros can also be introduced to provide equalized group delay [17][18]. They must appear in a conjugate pair.

4). Other characteristics

Besides the standard filter characteristics, other functions may have advantages for specific applications. The example is the characteristic polynomials in (2.7) that will be used in the design of lossy parallel connected network to be discussed in Chapter 4. The response of a typical example is given in Fig. 2.1(e).

$$F_{11}(s) = (-js+1)^N$$
$$P(s) = (js+1)^N \tag{2.7}$$

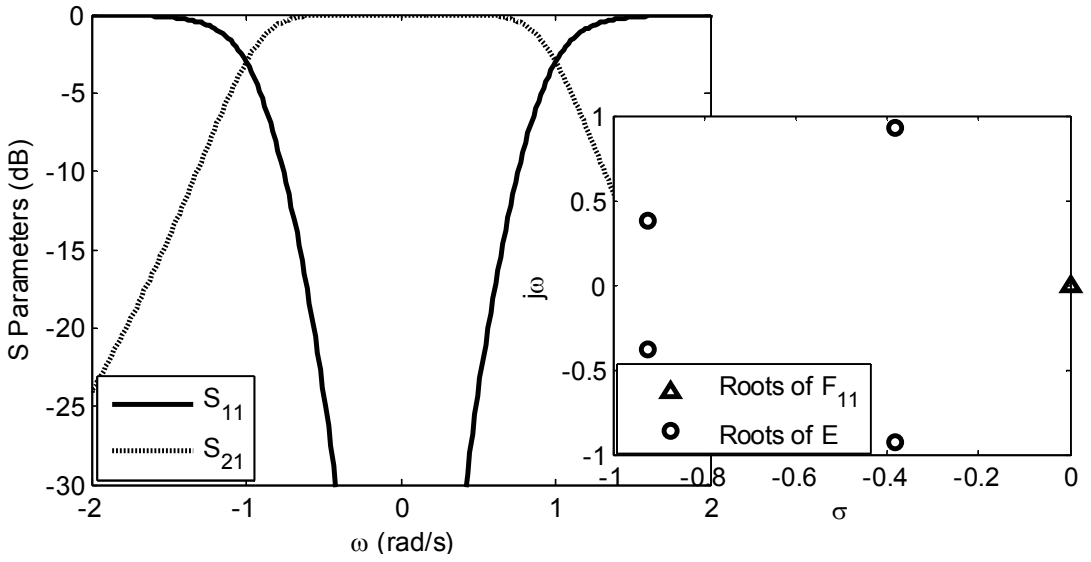

(a)

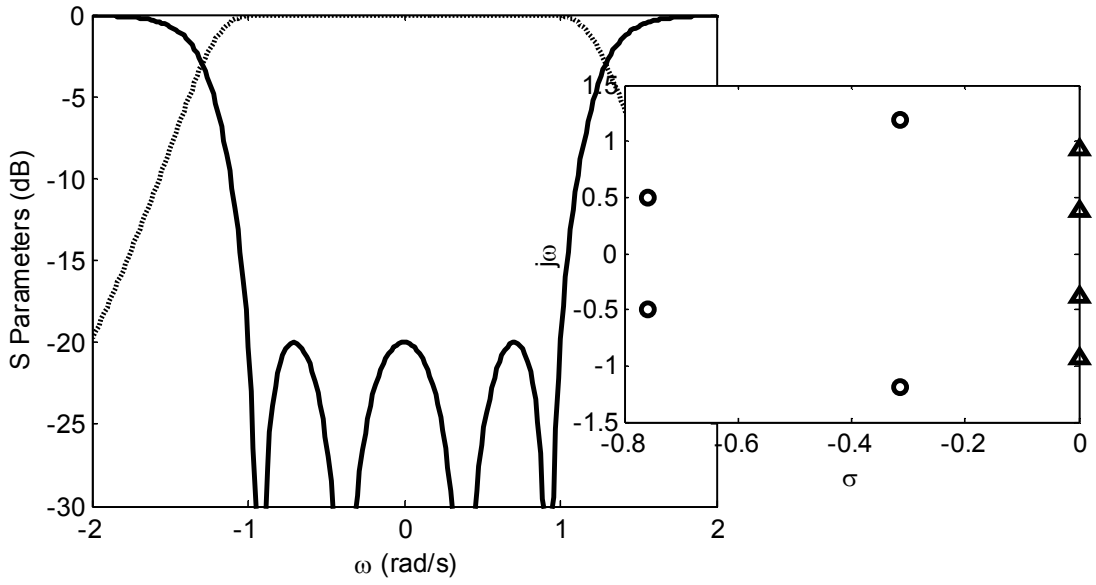

(b)

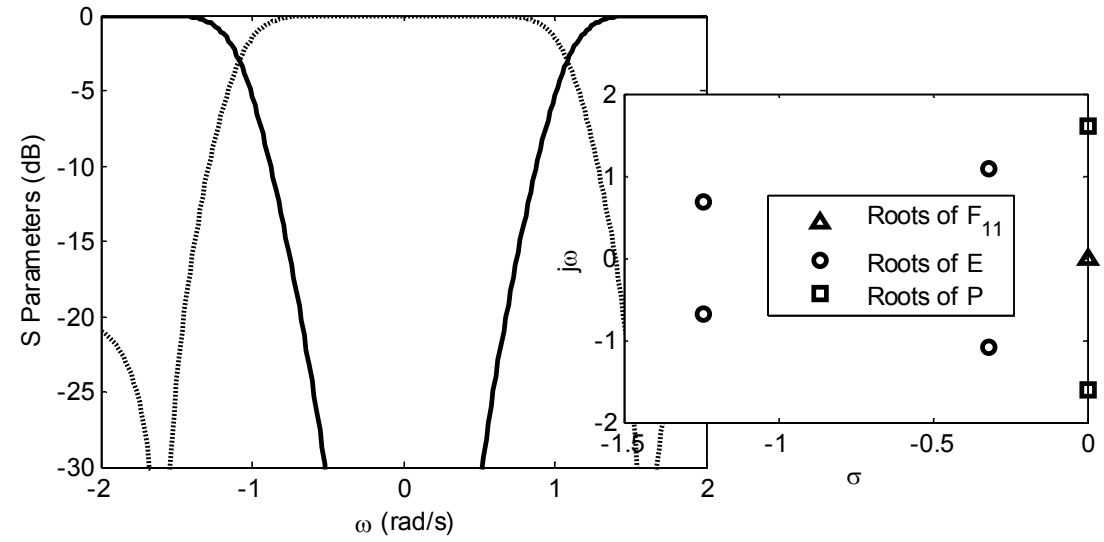

(c)

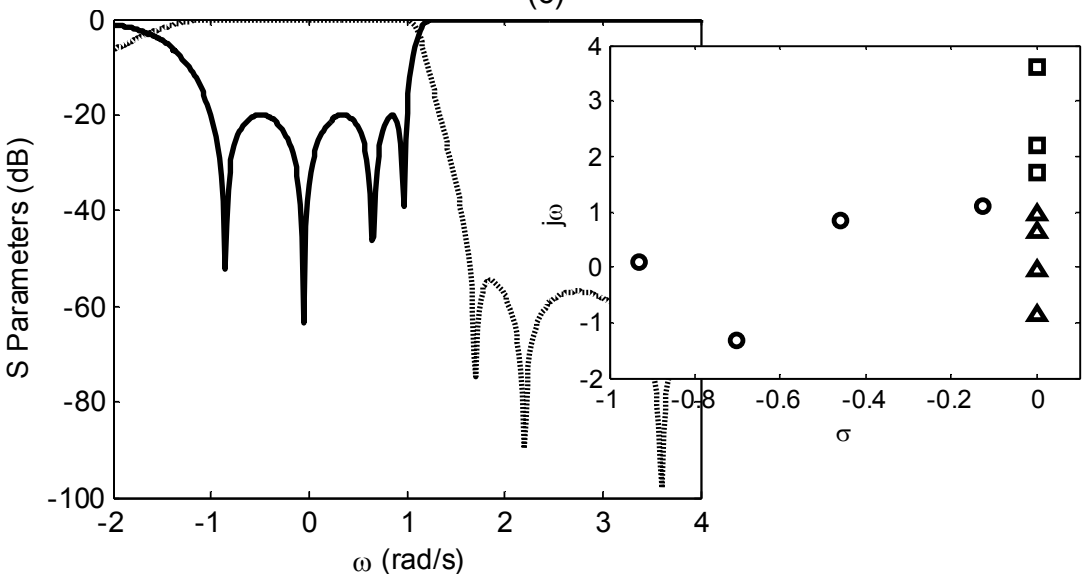

(d)

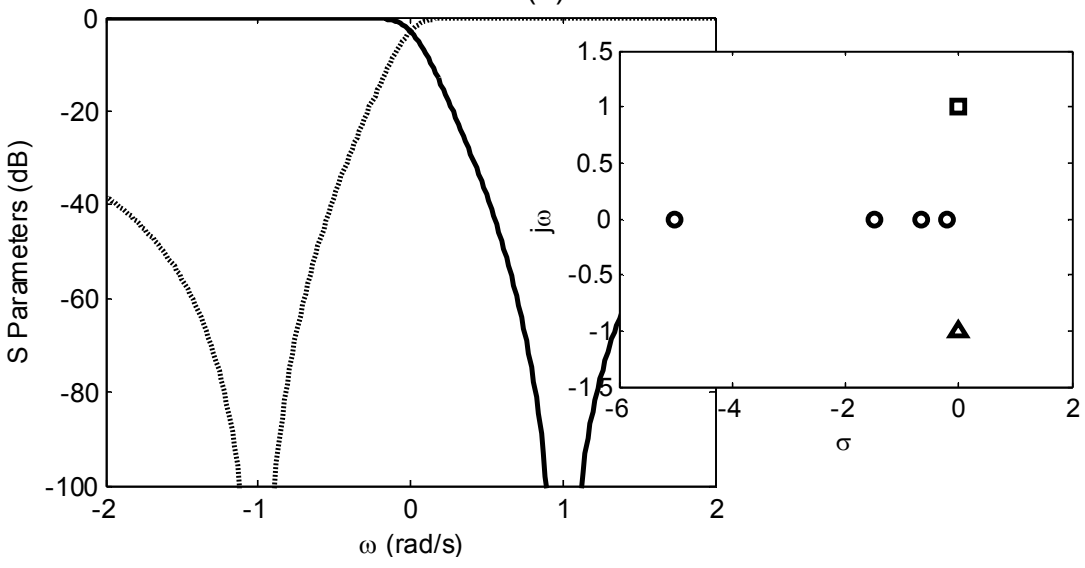

(e)

Fig. 2.1 Various standard filter responses and their roots distributions.

2.2 Filter networks of coupled resonators

With the defined N^{th} degree functions, a corresponding N^{th} degree lowpass prototype network can be derived. The lowpass prototype network is a cascading of series inductances and shunt capacitances and can be derived by extractions of elements. Introducing inverters into the network to represent couplings can provide a coupled resonator network.

With the requirement of high performance filters, transmission zeros are introduced into filter characteristics to provide steep transitions into stop bands or equalized group delays. Transmission zeros are generally realized by signal passes from two separated paths that have cancelled with each other at a specific frequency. As a result, the all-pass coupled resonators can be modified to included couplings between non-adjacent resonators.

Atia and Williams in 1972 [7] presented a filter synthesis method based on the CM which is a general representation of cross coupled resonators. The complete network of multi-coupled resonators is described by its admittance matrix which is the sum of the CM, the source/load resistant matrix and the diagonalized resonator matrix. The problem of filter synthesis is to find the bridge linking the admittance matrix and the S parameters. The method of analysis given by Atia and Williams is reviewed first in this section followed by a simplified procedure given by Cameron [8]. Using these procedures, filters can be represented by CMs with various responses of rational polynomials.

2.2.1 Lowpass prototype networks

For standard filter characteristics, a lowpass prototype network can be synthesized according to the exact formulas given in [19][20]. These prototype networks are of two-port and consist of cascaded lumped elements of inductance and capacitance as shown in Fig. 2.2.

The network consists of coupled resonators is first introduced by Dishal in 1951 [21]. In the reference, a narrow band bandpass filter is defined with three kinds of parameters including the synchronous resonant frequencies for resonators, the couplings between adjacent resonators and the external Qs of the first and last resonators. The method of designing narrow band filters with no finite transmission zeros using sequentially coupled resonators is shown in [13][22].

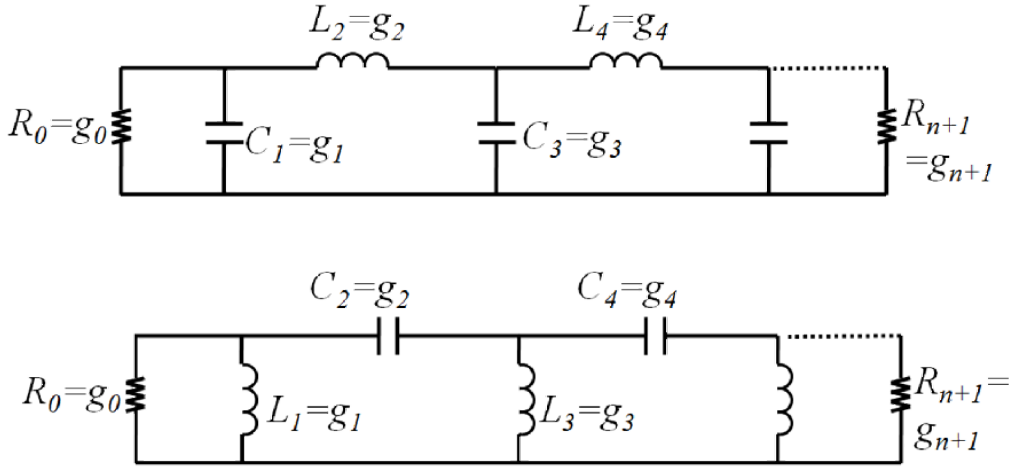

Fig. 2.2 Lowpass prototype network for minimum phase filters.

For the lowpass prototype network, there are both shunt and series elements that are difficult for the implementation. Inverters [13] are inserted into the circuit so that the circuit can be transformed to coupled resonators in which only series or shunt resonators are required. The transfer matrix of an inverter is given in (2.8).

$$[T]=\begin{bmatrix} 0 & jK \\ j/K & 0 \end{bmatrix} \tag{2.8}$$

An inverter is ideally a quarter wavelength transmission line. With the narrowband approximations, equivalence between lumped and distributed resonators can be found based on the reactance slope parameter. Then an inverter can be realized accordingly by the lumped or distributed equivalence as shown in [13]. The negative capacitances and inductances can be emerged with adjacent resonator elements of the lowpass prototype. The negative length of transmission lines could also be emerged with the length of adjacent cavities in waveguide filters.

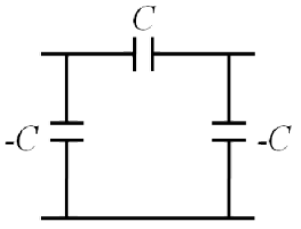

$K=1/\omega C$

(a)

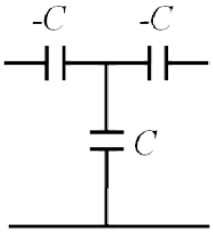

$K=1/\omega C$

(b)

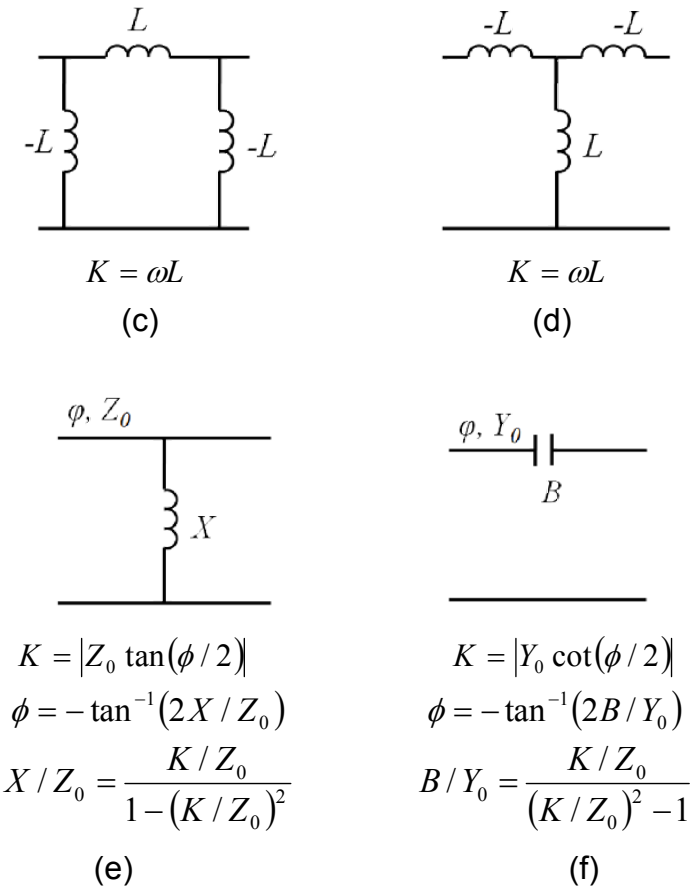

Fig. 2.3 Equivalence of invertors [13].

As a result, the design of lowpass prototype is transformed into the design of tuned resonators and coupling elements as shown in Fig. 2.4.

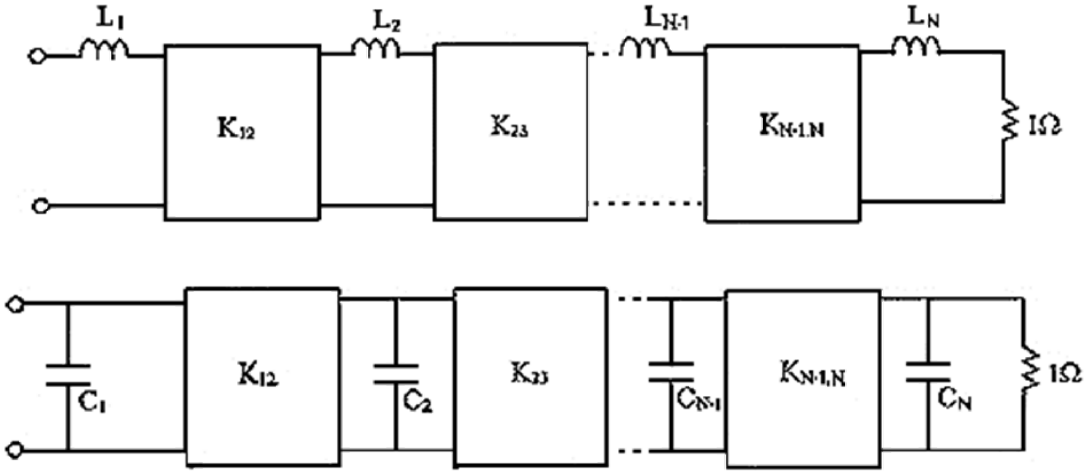

Fig. 2.4 Lowpass prototype network with invertors.

This technique significantly simplified the design process [13]. However, as the approximations of ideal inverters by coupling elements set limitations to

the bandwidth that a filter can be designed accurately, the choice of equivalent networks depends on the frequency band. In narrow band applications, lowpass to bandpass transformation could be applied to the resonators while the inverters are considered to be constant. In this way, the coupled resonator filter network can be designed.

2.2.2 Introduction of CM

If the frequency band of interest is narrow, each cavity can be treated as a single resonant with multiple couplings to other cavities. A generalized lowpass filter network was introduced by a series of paper [7][23][24] and is shown in Fig. 2.5. The method of analysis is reviewed in this section.

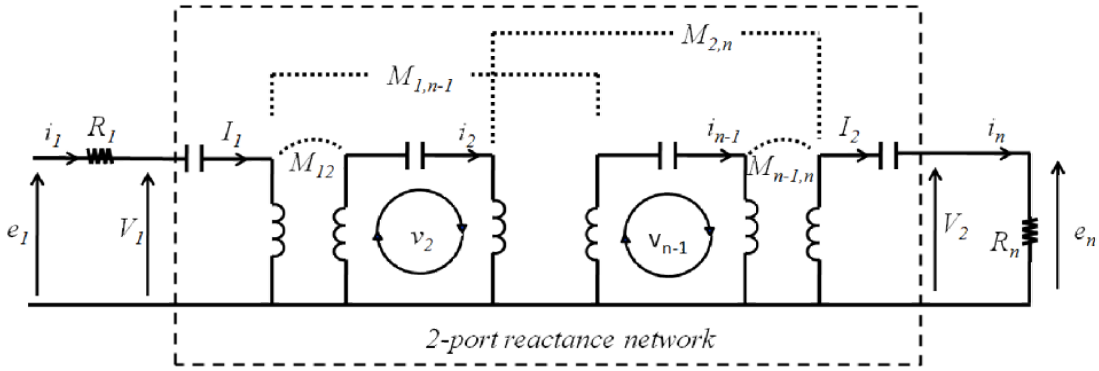

Fig. 2.5 Illustration of a prototype network suitable to be represented by a CM [7].

The series connected LC resonators are all normalized to a centre frequency of $\omega_0=1rad/sec$ thus giving $1F$ capacitance and $1H$ inductance for each loop. The couplings between i^{th} and j^{th} resonators are denoted by a coupling coefficient M_{ij}. For narrow band applications, the couplings are assumed to be frequency invariant. Each resonator forms a loop with coupling elements and the N loop voltage are denoted as $e_1, v_2, \ldots, e_n$ with the loop current $i_1, i_2, \ldots, i_n$. The source and load resistance are R_1 and R_n.

For an N^{th} degree network with input voltage applied only at the first loop, the complete set of loop equations according to Kirchhoff's voltage law is given in (2.9) with s defined in (2.10) and M_{ij} explained in (2.11).

$$\begin{bmatrix} e_1 \\ 0 \\ 0 \\ \dots \\ 0 \\ 0 \end{bmatrix} = \begin{bmatrix} s+R_1 & jM_{12} & jM_{13} & \dots & jM_{1,n-1} & jM_{1,n} \\ jM_{12} & s & jM_{23} & \dots & jM_{2,n-1} & jM_{2,n} \\ jM_{13} & jM_{23} & s & \dots & jM_{3,n-1} & jM_{3,n} \\ \dots & \dots & \dots & \dots & \dots & \dots \\ jM_{1,n-1} & jM_{2,n-1} & jM_{3,n-1} & \dots & s & jM_{n-1,n} \\ jM_{1,n} & jM_{2,n} & jM_{3,n} & \dots & jM_{n-1,n} & s+R_n \end{bmatrix} \cdot \begin{bmatrix} i_1 \\ i_2 \\ i_3 \\ \dots \\ i_{n-1} \\ i_n \end{bmatrix} \tag{2.9}$$

$$s = j\left(\omega - \frac{1}{\omega}\right) \tag{2.10}$$

$$jM_{ij} = j\omega_0 M_{ij} \quad \text{with} \quad \omega_0 = 1 \,\text{rad/sec} \tag{2.11}$$

For a two port reactance network shown in Fig. 2.5, its short circuit admittance parameters are defined in (2.12) with port voltages and currents V_1, I_1, V_2 and I_2.

$$\begin{aligned} I_1 &= Y_{11}V_1 + Y_{12}V_2 \\ I_2 &= Y_{21}V_1 + Y_{22}V_2 \end{aligned} \tag{2.12}$$

The admittances Y_{11} and Y_{21} can be found as in (2.13) when $V_2=0$. Then (2.13) can be further derived using the loop voltage and current e_1, i_1 and i_n of Fig. 2.5 since $e_1=V_1$ when $R_1=0$.

$$\begin{aligned} Y_{11} &= \frac{I_1}{V_1} = \frac{i_1}{e_1} \\ Y_{21} &= \frac{I_2}{V_1} = \frac{i_n}{e_1} \end{aligned} \tag{2.13}$$

Then with $R_1=R_n=0$, the loop equation in (2.9) is simplified to (2.14). By matrix inversion, an admittance matrix can be found as in (2.15). y_l and z_l represent the N-by-N admittance and impedance matrix in the following texts.

$$\begin{bmatrix} e_1 \\ 0 \\ 0 \\ \dots \\ 0 \\ 0 \end{bmatrix} = \begin{bmatrix} s & jM_{12} & jM_{13} & \dots & jM_{1,n} \\ jM_{12} & s & jM_{23} & \dots & jM_{2,n} \\ jM_{13} & jM_{23} & s & \dots & jM_{3,n} \\ \dots & \dots & \dots & \dots & \dots \\ & & & \dots & \\ jM_{1,n} & jM_{2,n} & jM_{3,n} & \dots & s \end{bmatrix} \cdot \begin{bmatrix} i_1 \\ i_2 \\ i_3 \\ \dots \\ i_{n-1} \\ i_n \end{bmatrix} \tag{2.14}$$

$$\begin{bmatrix} i_1 \\ i_2 \\ i_3 \\ \dots \\ i_{n-1} \\ i_n \end{bmatrix} = \begin{bmatrix} y_{11} & y_{12} & y_{13} & \dots & y_{1,n} \\ y_{12} & y_{22} & y_{23} & \dots & y_{2,n} \\ y_{13} & y_{23} & y_{33} & \dots & y_{3,n} \\ \dots & \dots & \dots & \dots & \dots \\ & & & \dots & \\ y_{1,n} & y_{2,n} & y_{3,n} & \dots & y_{nn} \end{bmatrix} \cdot \begin{bmatrix} e_1 \\ 0 \\ 0 \\ \dots \\ 0 \\ 0 \end{bmatrix} \tag{2.15}$$

With the admittance matrix in (2.15), the Y_{11} and Y_{21} of (2.13)can be found as in (2.16) where I is an N-by-N identity matrix and M is the CM.

$$\begin{aligned} Y_{11} &= \frac{i_1}{e_1} = y_{11} = \left[sI + jM\right]^{-1}_{11} \\ Y_{21} &= \frac{i_n}{e_1} = y_{n1} = \left[sI + jM\right]^{-1}_{n1} \end{aligned} \tag{2.16}$$

From the definition of the filter network, the matrix M is real and symmetric. As a result, it can be diagonalized as in (2.17). Matrix Λ is a diagonal matrix with its diagonal element being the eigenvalues of matrix M as in (2.18). Matrix T is the orthogonal eigenvector matrix.

$$M = T\Lambda T^t \tag{2.17}$$

$$\Lambda = \begin{bmatrix} \lambda_1 & 0 & \dots & 0 \\ 0 & \lambda_2 & \dots & 0 \\ \dots & \dots & \dots & \dots \\ 0 & 0 & \dots & \lambda_n \end{bmatrix}, \; TT^t = I \tag{2.18}$$

The admittance matrix y_l of (2.15) is the reversion of the impedance matrix and with (2.17), the inversion can be derived as in (2.19) utilizing the eigenvalues and eigenvectors of CM M.

$$\begin{aligned} \left[y_l\right] = \left[z_l\right]^{-1} &= \left[sI + jM\right]^{-1} = \left[sI + jT\Lambda T^t\right]^{-1} \\ &= T\begin{bmatrix} \dfrac{1}{s + j\lambda_1} & 0 & & \\ 0 & \dfrac{1}{s + j\lambda_2} & & \\ & & \dots & \\ & & & \dfrac{1}{s + j\lambda_n} \end{bmatrix} T^t \end{aligned} \tag{2.19}$$

$$
\begin{aligned}
[y_l] &= \begin{bmatrix} T_{11} & T_{12} & \dots & T_{1n} \\ T_{21} & T_{22} & \dots & T_{2n} \\ & & \dots & \\ T_{n1} & T_{n2} & \dots & T_{nn} \end{bmatrix} \begin{bmatrix} \frac{1}{s+j\lambda_1} & 0 & & \\ 0 & \frac{1}{s+j\lambda_2} & & \\ & & \dots & \\ & & & \frac{1}{s+j\lambda_n} \end{bmatrix} \begin{bmatrix} T_{11} & T_{21} & \dots & T_{n1} \\ T_{12} & T_{22} & \dots & T_{n2} \\ & & \dots & \\ T_{1n} & T_{2n} & \dots & T_{nn} \end{bmatrix} \\
&= \begin{bmatrix} \frac{T_{11}}{s+j\lambda_1} & \frac{T_{12}}{s+j\lambda_2} & \dots & \frac{T_{1n}}{s+j\lambda_n} \\ \frac{T_{21}}{s+j\lambda_1} & \frac{T_{22}}{s+j\lambda_2} & \dots & \frac{T_{2n}}{s+j\lambda_n} \\ & & \dots & \\ \frac{T_{n1}}{s+j\lambda_1} & \frac{T_{n2}}{s+j\lambda_2} & \dots & \frac{T_{nn}}{s+j\lambda_n} \end{bmatrix} \begin{bmatrix} T_{11} & T_{21} & \dots & T_{n1} \\ T_{12} & T_{22} & \dots & T_{n2} \\ & & \dots & \\ T_{1n} & T_{2n} & \dots & T_{nn} \end{bmatrix}
\end{aligned}
\tag{2.20}
$$

And the matrix multiplications in (2.19) can be further derived when the elements of T is given as in (2.20). As a result, Y_{11} and Y_{21} can be calculated as in (2.21). A conclusion can be drawn that for the network as in Fig. 2.5, its admittance parameters are rational polynomials with a common denominator of degree N.

$$
\begin{aligned}
Y_{11} &= \frac{T_{11}^2}{s+j\lambda_1} + \frac{T_{12}^2}{s+j\lambda_2} + \dots + \frac{T_{1n}^2}{s+j\lambda_n} = \sum_{k=1}^{N} \frac{T_{1k}^2}{s+j\lambda_k} \\
Y_{21} &= \frac{T_{11}T_{n1}}{s+j\lambda_1} + \frac{T_{12}T_{n2}}{s+j\lambda_2} + \dots + \frac{T_{1n}T_{nn}}{s+j\lambda_n} = \sum_{k=1}^{N} \frac{T_{1k}T_{nk}}{s+j\lambda_k}
\end{aligned}
\tag{2.21}
$$

In the synthesis of filter networks, the S parameters are known and the admittance parameters can be found according to (2.22) in which polynomial V is given in (2.23) for lossless case.

$$
\begin{aligned}
Y_{21}(s) &= \frac{-2P(s)}{E(s)+F_{11}(s)+F_{22}(s)-V(s)} \\
Y_{11}(s) &= \frac{E(s)-F_{11}(s)+F_{22}(s)+V(s)}{E(s)+F_{11}(s)+F_{22}(s)-V(s)}
\end{aligned}
\tag{2.22}
$$

$$
V(s) = E(s)\big(S_{12}(s)S_{21}(s) - S_{11}(s)S_{22}(s)\big) = (-1)^{N+1}\big(E(s)\big)^{*} \tag{2.23}
$$

A partial expansion could then be applied to Y parameters as in (2.24). Comparing (2.21) with (2.24), λ_k can be found from the poles of Y parameter and T_{1k} and T_{nk} can be found from the residues. With matrix Λ and T, the matrix M can be found.

$$
Y = \begin{bmatrix} Y_{11} & Y_{12} \\ Y_{21} & Y_{22} \end{bmatrix} = \sum_{k=1}^{N} \frac{1}{s-p_k} \begin{bmatrix} r_{11} & r_{12} \\ r_{21} & r_{22} \end{bmatrix} \tag{2.24}
$$

According to the derivation above, there are some constraints for the poles and residues of Y parameters. Because matrix M is real and symmetric, its eigenvalues must be real and its eigenvector matrix T must be real and orthogonal.

1). As λ_k is real, the poles p_k must be purely imaginary.

2). As the trace of M equals zero, $\sum \lambda_k = -j\sum p_k = 0$.

3). As matrix T is real, the residues r_{11}, r_{12} and r_{22} are all real and positive.

4). $r_{11}r_{22} - r_{21}^2 = 0$.

5). As T is orthogonal, $\sum T_{1k}T_{nk} = 0$ and $\sum r_{21k} = 0$.

6). As $M_{11} = M_{nn} = 0$, $\sum \lambda_k r_{11k} = \sum \lambda_k r_{22k} = 0$.

2.2.3 Synthesis of CM

The synthesis procedure in last section can be greatly simplified using the network of transversal array given in Fig. 2.6. It is a prototype of coupled resonator network and is generally a parallel connection of N resonators. Each of the resonators consists of two inverters J_{sk} , one capacitor C_k , and one frequency invariant reactance jB_k .

For lossy circuit that will be discussed in the following section, a resistor G_k is also included in each resonator as in Fig. 2.7. The synthesis procedure in [8] is reviewed here. The transfer matrix of each resonator in Fig. 2.7 is derived in (2.25) by matrix multiplications of the transfer matrix of each element.

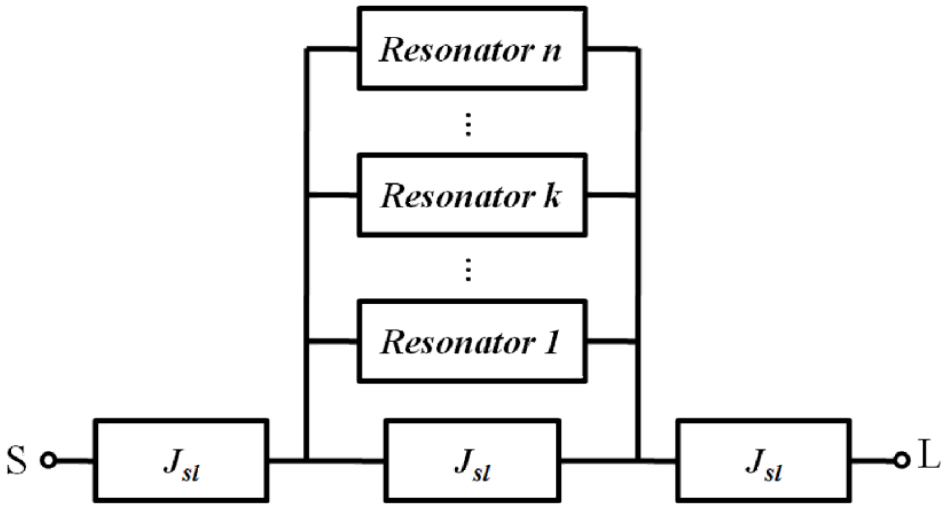

Fig. 2.6 Transversal array model of coupled resonator microwave filter [8].

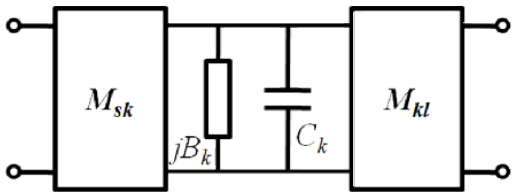

Fig. 2.7 Circuit model of each resonator in Fig. 2.6 [8].

$$[ABCD]_k = \begin{bmatrix} 0 & jM_{Sk} \\ \frac{j}{M_{Sk}} & 0 \end{bmatrix} \begin{bmatrix} 1 & 0 \\ -sC_k & 1 \end{bmatrix} \begin{bmatrix} 1 & 0 \\ -\frac{1}{jB_k} & 1 \end{bmatrix} \begin{bmatrix} 0 & jM_{Lk} \\ \frac{j}{M_{Lk}} & 0 \end{bmatrix}$$
$$= -\begin{bmatrix} \frac{M_{Lk}}{M_{Sk}} & \frac{sC_k + jB_k}{M_{Sk}M_{Lk}} \\ 0 & \frac{M_{Sk}}{M_{Lk}} \end{bmatrix} \tag{2.25}$$

So the admittance parameters of each resonator can be derived using the standard ABCD to Y transformations. The admittance matrix of a resonator is thus given in (2.26).Comparing it with the partial expansion of (2.24), the values of the elements in the circuit model can then be found as $C_k = 1$, $B_k = -\lambda_k$, $M_{Lk}^2 = r_{22k}$, and $M_{Sk}M_{Lk} = r_{21k}$.

$$[Y]_k = \frac{1}{sC_k + jB_k} \begin{bmatrix} M_{Sk}^2 & M_{Sk}M_{Lk} \\ M_{Sk}M_{Lk} & M_{Lk}^2 \end{bmatrix} \tag{2.26}$$

This method of synthesis CM is based on an N+2 CM in which the first and last nodes are representing the source and load. As a result, the method is capable of designing of filter with couplings to or between source and load.

2.2.4 Transformation of CM

For better rejection, transmission zeros are introduced by meanings of cross couplings. Then the basic matrices (full matrix derived from N-by-N network and parallel connected matrix from N+2 network) can be transformed to other configurations by means of similarity transformations. Similarity transformation is a series of matrix rotation applied sequentially to annihilating specific element in CM.

Fig. 2.8 shows some of the filter configurations that are used in most practical design. These configurations are illustrated by node diagrams which show the coupling schemes. The solid circles represent resonators

and the hollow circles represent the non-resonating nodes that are usually the input and output nodes. The solid and dash lines are the positive and negative couplings respectively.

To the standard configurations, sequence of rotations is given. Folded configuration [25] in Fig. 2.8(a) is generally used in filter that requires the presence of transmission zeros and can be easily implemented by waveguide or other structures. A corresponding CM is also shown with its responses.

The configuration in (b) can be derived directly from transversal array for symmetric response [8]. It is similar to transversal array but has reduced number of parallel connected sub-networks. The Cud-de-sac [26] configuration is shown in (c). Trisection in (d) has the advantage that each transmission zero is assigned to one cross coupling. It can be further transformed to the configuration in (e). The rotation for trisection is given in [27] and [28]. The extended box configuration [29] is shown in (f). Arbitrary transmission zeros can also be introduced into the network by non-resonating nodes [30] as shown (g).

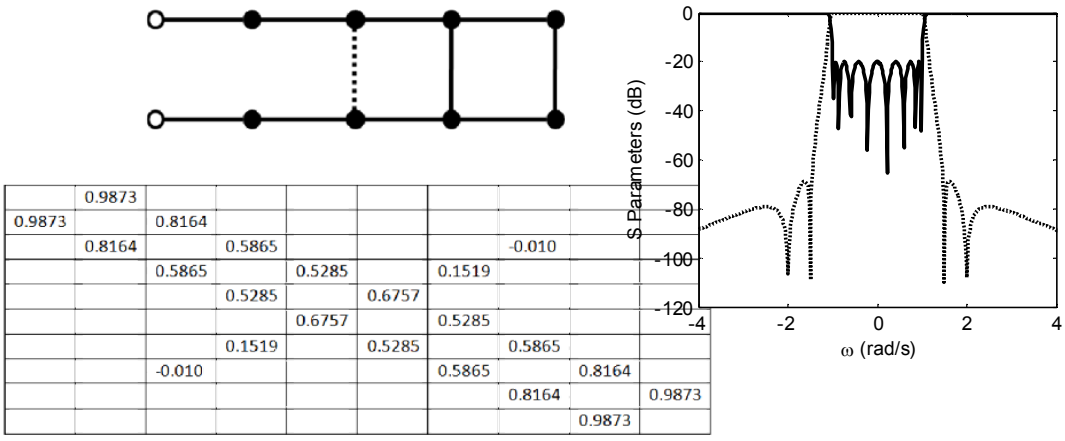

(a)

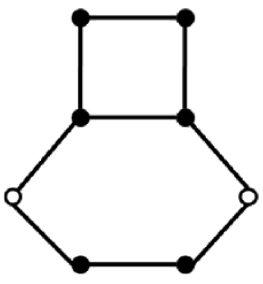

(b)

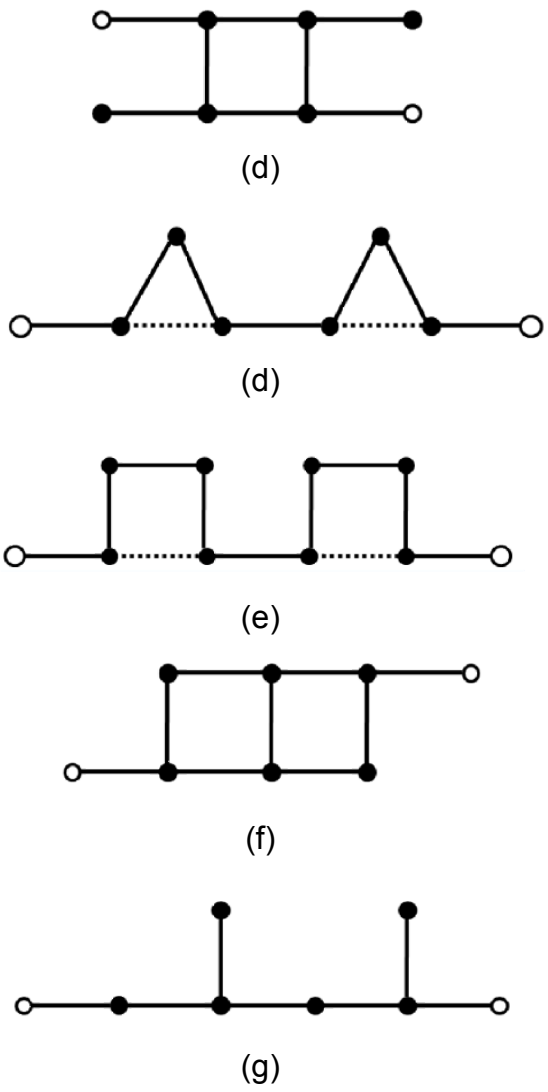

Fig. 2.8 Various CM configurations [25]-[30].

2.2.5 The application of optimization

For other configurations that are difficult to be achieved by matrix rotations, various optimizations can be used to find the required CM. In [31], gradient based optimization is applied to an initial CM, and the cost function is defined in (2.27) for perfect reflection and transmission zeros. A_i and B_j represent the refection and transmission zeros. ε is the current ripple of insertion loss in the passband while ε_0 is the desired value.

$$cf = \sum_{i=1}^{N} [S_{11}(A_i)]^2 + \sum_{j=1}^{N} [S_{21}(B_i)]^2 + [\varepsilon - \varepsilon_0]^2 \tag{2.27}$$

[32] and [33] provides a more effective optimization by giving the gradient of response with respect to elements in CM (2.28). A is the complete

admittance matrix as $[A]=\omega[I]-j[R]+[M]$. Matrix P defines the desired CM configurations.

$$\frac{\partial S_{11}}{\partial M_{pq}} = -4jR_1 P_{pq}\left[A^{-1}\right]_{1p}\left[A^{-1}\right]_{q1}$$
$$\frac{\partial S_{21}}{\partial M_{pq}} = 2j\sqrt{R_1 R_2}\,P_{pq}\left(\left[A^{-1}\right]_{Np}\left[A^{-1}\right]_{q1}+\left[A^{-1}\right]_{Np}\left[A^{-1}\right]_{p1}\right) \quad (2.28)$$

Based on the optimization, it has been shown in [33]-[37] that various CM configurations can be achieved without similarity transformations.

2.3 The synthesis of lossy filter networks

Filter networks can be implemented by different technologies. However, all the physical filters deal with certain level of losses. The use of lossy resonator can greatly reduce the size of manufactured filter cavities [38] [39]. It is thus desirable to include losses in the filter synthesis to compensate the performance degradation. The problem of synthesizing lossy filter networks has been completely solved by reflection mode device [40]-[42]. No general solutions have been found for two-port transmission type devices.

Followed by the definition of Qu, various techniques for the synthesis of lossy filter networks are reviewed. The first one is predistortion described in 2.4.2. By realizing a transfer function whose poles are shifted to the right to compensate the effect of loss, lossless transfer function can be recovered at the expense of high return loss. The previous CM synthesis technique is not valid when the circuit is lossy. The lossy circuit synthesis method in 2.4.3 uses the decomposition of even and odd mode and thus non-uniform dissipations can be included in the circuit with hyperbolic transformations. A specific case of lossy CM synthesis is discussed in 2.4.4 which is valid for a specific response. Finally, optimization can also be used in the derivation of lossy CM.

2.3.1 The definition of Qu

For a lumped element resonator consisting series connected capacitor and inductance, loss is included by an additional resistance R as given in Fig.

2.9. Then the quality factor Q is defined by the stored and dissipated energy [9] as in (2.29).

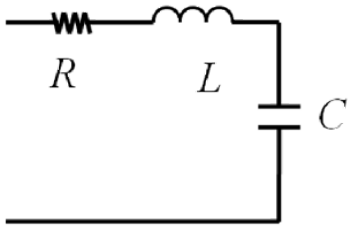

Fig. 2.9 Definition of lossy resonator [9].

$$Q = \frac{\omega L}{R} = \omega \frac{\frac{1}{2} L i^2}{\frac{1}{2} R i^2} \tag{2.29}$$

For physical implementations of microwave filters, the existence of loss is inevitable. For cavity filters, losses introduced by metal cavities can be found by (2.30) where b refers to the dimension of the cavity, K is a chosen constant for various resonator types and f is the resonant frequency [43]. Loss due to coupling apertures, tuning screws, and surface roughness can be found experimentally [44].

$$Q = Kb\sqrt{f} \tag{2.30}$$

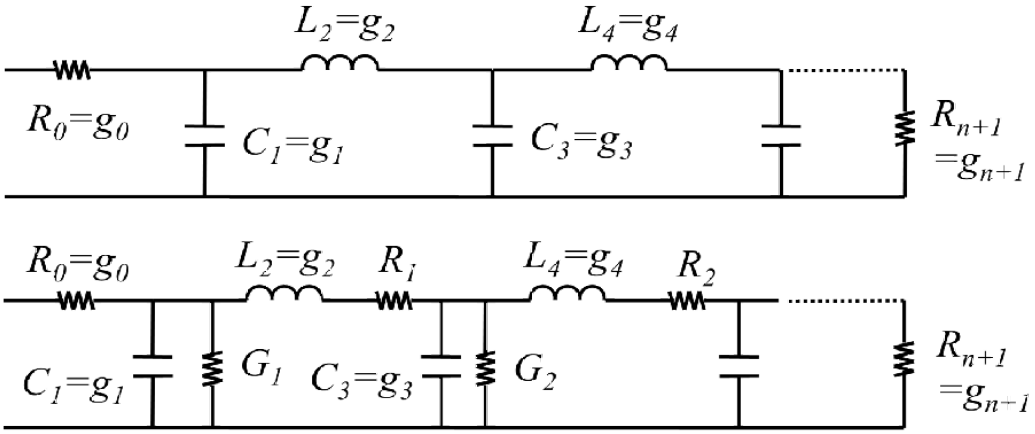

Fig. 2.10 A typical lowpass prototype network compared to one with loss.

A lossy lowpass prototype network is illustrated in Fig. 2.10 with comparison to the lossless one. Insertion loss due to dissipation can be evaluated at the centre of the pass band using (2.31) according to the method given in [45]. f_0

is the center frequency, Δf is the bandwidth and g_i is the element values of the lowpass prototype.

$$L = \frac{4.343 f_0}{\Delta f Q_u} \sum_{r=1}^{N} g_r \tag{2.31}$$

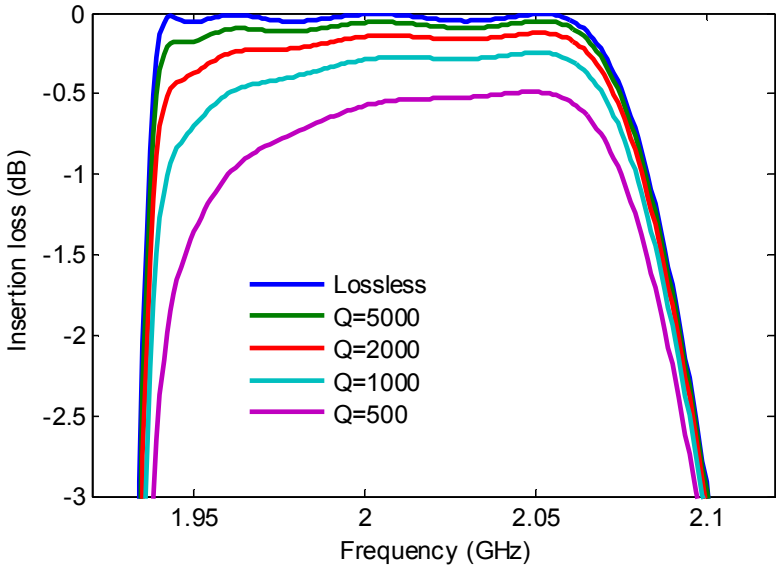

Fig. 2.11 Insertion loss of a typical filter with Qu of infinity, 5000, 2000, 1000 and 500 for a center frequency of 2 GHz and bandwidth of 0.12 GHz.

Typical filter responses with various loss levels are depicted in Fig. 2.11. The example uses 4th order Chebyshev response with 3 transmission zeros at -$1.7j$, -$2.2j$ and -$3.6j$ in the lowpass domain. For a center frequency of 2 GHz and bandwidth of 0.12 GHz, The Qs used are infinity, 5000, 2000, 1000 and 500. The dissipation loss is nearly proportional to the group delay in the passband [46][1]. The decrease of selectivity is much greater in the lower bandedge due to the steep transition in this side caused by the transmission zeros. General effect of loss to the nature frequencies and eigenmodes can be found in [47].

2.3.2 The method of predistortion

The basic idea of predistortion [48] is to modify the filter network so that the effect of losses can be compensated. The first order perturbation of filter characteristics due to uniform losses can be derived. And the predistorted network can be found from the characteristics containing a reverse perturbation.

The method given in [49] enforces the poles and zeros of the transmittance of the lossy network to be the same as the lossless one. The method in [50] uses transfer immittances. In [51], insertion loss ratio was used for which the ideal response was given in (2.32a) and the predistorted one was given in (2.32b) by a first order approximation. The relationship between circuit elements and coefficients of insertion loss ratio can be found by Taylor series expansion [52]. The change of the natural frequencies which refers to the roots of the E polynomial due to dissipation can also be found by a sensitivity analysis [53].

$$\Lambda(p) = \frac{V_{20}}{V_2} = \frac{E(p)}{P(p)} \tag{2.32a}$$

$$\Lambda_p = K\frac{2E(p) - E_L(p)}{P(p)} \tag{2.32b}$$

The method of predistortion was applied to CM for uniform dissipations in [54][3].Since the effect of losses is to add a real part to the frequency variable of the transfer function and thus to move the poles and zeros to the left in the complex plane, this effect can be compensated by moving the poles and zeros to the right in the design of the transfer function. Then the high Q performance can be recovered using relatively low Q resonators.

The denominator of S_{21} can be expressed by its roots as in (2.33a), where E_{rk} is the k^{th} root of the polynomial $E(s)$. In predistortion, the roots of the denominator are moved to the right by a factor δ which is related to the value of Q that need to be compensated. The new $E'(s)$ is now given in (2.33b).

$$E(s) = \prod_{k=1}^{N}(s - E_{rk}) \tag{2.33a}$$

$$E'(s) = \prod_{k=1}^{N}\left(s - \left(E_{rk} + \delta\right)\right) \tag{2.33b}$$

Since the circuit to be synthesized is lossless, the polynomial $F(s)$ can be found according to (2.34). Then a lossless CM can be synthesized using $F(s)$, $P(s)$ and $E(s)$.

$$F_{11}'(s)\left(F_{11}'(s)\right)^*/\varepsilon_R^2 + P'(s)\left(P'(s)\right)^*/\varepsilon^2 = E'(s)\left(E'(s)\right)^* \tag{2.34}$$

An example of 4th order Chebyshev filter with two transmission zeros at $\pm 1.6j$ is given in the following. The centre frequency is 0.956 MHz, and the bandwidth is 60 MHz. A Q of 250 is assumed. The synthesized CM is shown in Table 2.1.

Table 2.1 CM of the predistorted circuit

	-0.1020	0.1020	-0.3942	0.3942	
-0.1020	-1.3715				0.6159
0.1020		1.3715			0.6159
-0.3942			0.8658		0.6708
0.3942				-0.8658	0.6708
	0.6159	0.6159	0.6708	0.6708	

Fig. 2.12 shows the S_{21} of four different circuits. The green one is the response of original lossless circuit. When loss in included in each resonator, the response is the red one with round-ups at band edges. To compensate the roundings, the response of the predistorted circuit shows two peaks at band edges. Then when loss is added, the response at band edges will be flattened as the blue curve. Fig. 2.13 shows the original lossless response and the lossy response using the predistorted circuit. As shown in the figure, the effect of predistorted circuit is to flatten the S_{21} at band edge, but also results in a high return loss.

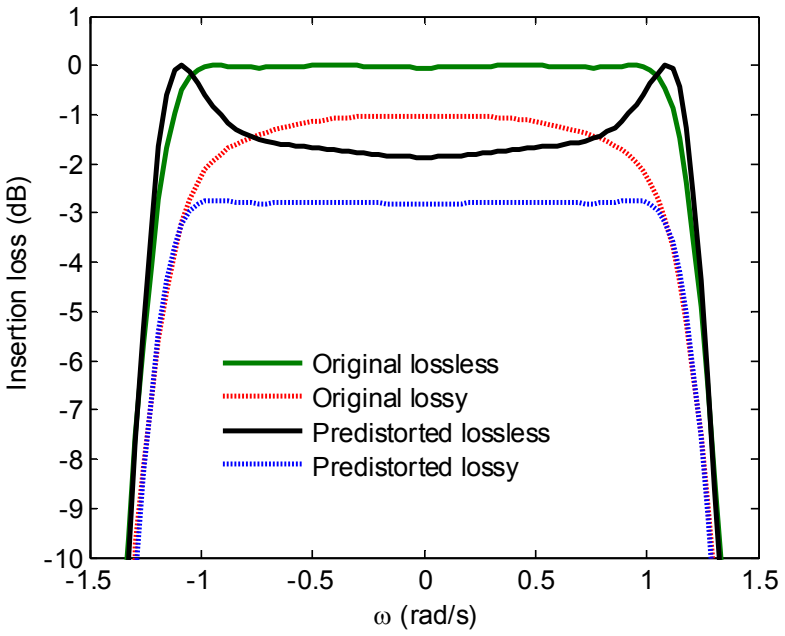

Fig. 2.12 S parameters of original and predistorted circuit.

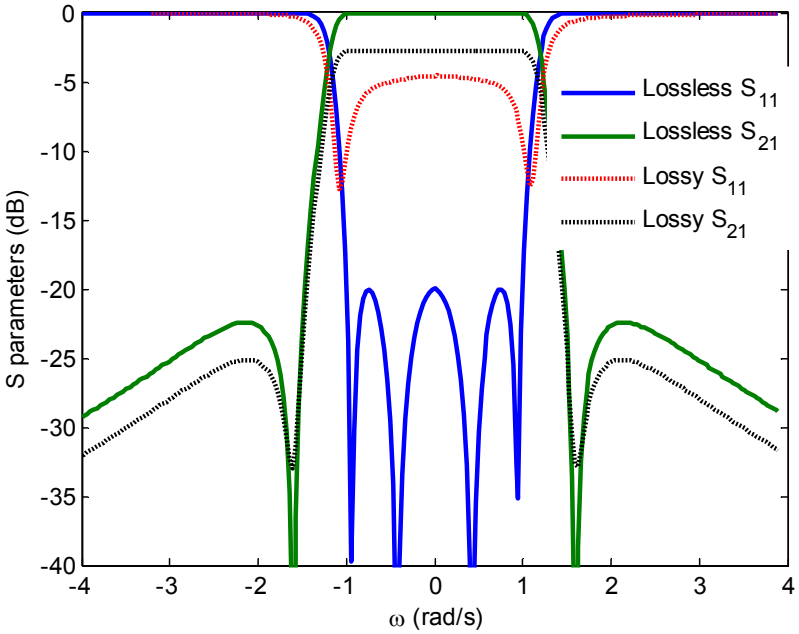

Fig. 2.13 S parameters of original and predistorted circuits.

2.3.3 The method based on even/odd mode analysis

Using predistortion, the synthesized circuit has equal losses on resonators and the return loss is usually not good. To improve the return loss and to distribute losses into resonators, the method of lossy circuit synthesis with non-uniform dissipation is introduced in [55].

This method is based on even and odd mode analysis of two port network and can give even and odd mode circuit of any given lossy transfer functions. In [56], the method is extended to a more general case where a complimentary all pass function is added to the original transfer function and thus providing a network of higher degrees. The S parameters of a two ports network can be expressed by its even and odd mode of admittance parameters as in (2.35). As a result, we have the even and odd mode of S parameters as in (2.36)

$$S_{11} = \frac{1 - Y_e Y_o}{(1+Y_e)(1+Y_o)}$$
$$S_{21} = \frac{Y_o - Y_e}{(1+Y_e)(1+Y_o)} \tag{2.35}$$

$$S_e = S_{11} + S_{21} = \frac{F_{11}(s)/\varepsilon_R + P(s)/\varepsilon}{E(s)} = \frac{(1-Y_e)(1+Y_o)}{(1+Y_e)(1+Y_o)}$$
$$S_o = S_{11} - S_{21} = \frac{F_{11}(s)/\varepsilon_R - P(s)/\varepsilon}{E(s)} = \frac{(1+Y_e)(1-Y_o)}{(1+Y_e)(1+Y_o)} \tag{2.36}$$

The roots of E(s) can be divided into two groups. R_e represents the roots of $(1+Y_e)$ and Ro represents the roots of $(1+Y_o)$. According to (2.36), we have the equations in (2.37).

$$\begin{aligned} F_{11}'(s)/\varepsilon_R + P'(s)/\varepsilon = 0 \text{ at } R_o \\ F_{11}'(s)/\varepsilon_R - P'(s)/\varepsilon = 0 \text{ at } R_e \end{aligned} \tag{2.37}$$

In the following, we denote N_e as the order of even mode and N_o as the order of odd mode. The problem of determining the even mode roots to choose N_e elements from a set of N elements. This can be solved in Matlab using the function combnts. Only one combination of R_e will result in an $F_{11}(s)$ that leads to a passive S_{11}. Assuming the highest coefficient of $F_{11}(s)$ is unit. The other coefficients of $F_{11}(s)$ can be found by solving the linear equations above. Then we can derive the expressions for S_e and S_o as in (2.38).The admittance of even and odd mode can be found as in (2.39).

$$\begin{aligned} S_e &= \frac{S_{en}}{S_{ed}} \\ S_o &= \frac{S_{on}}{S_{od}} \end{aligned} \tag{2.38}$$

$$\begin{aligned} Y_e &= \frac{S_{ed} + S_{en}}{S_{ed} - S_{en}} \\ Y_o &= \frac{S_{od} + S_{on}}{S_{od} - S_{on}} \end{aligned} \tag{2.39}$$

Using the partial expansion of the admittance parameters the even and odd mode circuit can be found. They can be connected in parallel to form the transversal array of the complete circuit. However, when transformed to ladder networks, the circuit contains lossy elements only in the first and last resonators. This condition is equivalent to add attenuators at the input and output resonators.

In order to distribute dissipations within the network, two methods are given in the literature. The first one is to include an all pass term to the transfer function [56]. An example of such a transfer function is given in (2.40).We can derive $P'(s) = kP(s)(p-\delta)$ and $E'(s) = kP(s)(p-\delta)$. Then $F_{11}'(s)$ can be derived and the corresponding network can be found. The second method is to apply the hyperbolic transformations [57] until proper loss distribution is achieved.

$$S_{21}(s) = \frac{kP(s)(s-\delta)}{\varepsilon E(s)(s+\delta)} \tag{2.40}$$

The following is an example of 4th order Chebyshev filter with $k=0.5$ and $\delta=9$. The response of the original lossless circuit is compared with the lossy response in Fig. 2.14. The synthesized circuit is shown in Fig. 2.15 and the elements values are given in the following.

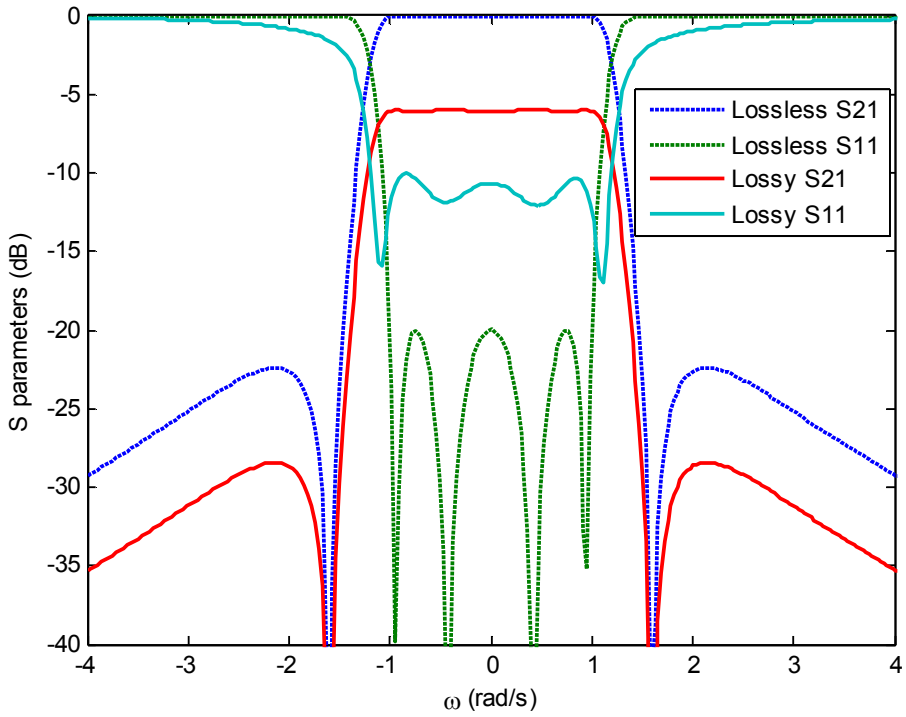

Fig. 2.14 S parameters of the original Chebyshev circuit and the synthesized lossy circuit.

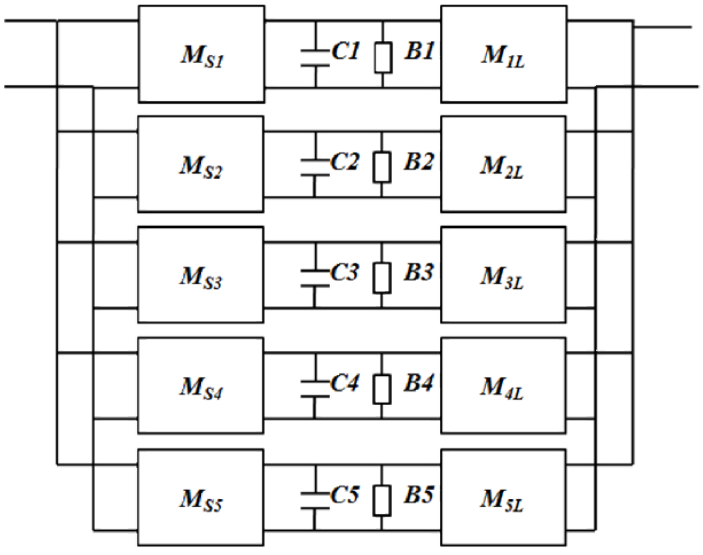

Fig. 2.15 Circuit synthesized according to the lossy response.

$M_{s1}=M_{1L}=0.1923+0.1950j$, $M_{s2}=M_{2L}=0.3596-0.0063j$, $M_{s3}=M_{3L}=0.7147-0.0188j$,
$M_{s4}=-M_{4L}=0.3609+0.0098j$, $M_{s5}=-M_{5L}=0.7136+0.0256j$,
$C1=C2=C3=C4=C5=2$, $B1=18.0012-0.1617j$, $B2=0.1731+2.4138j$,
$B3=0.6168-1.3028j$, $B4=0.1729-2.4163j$, $B5=0.6168+1.2927j$

Filter can be designed to contain separated high *Qu* and low *Qu* paths [58]. While the higher *Qu* path corresponds to response near the bandedge, the low *Qu* path corresponds to the response in the centre of passband. The method is extended in Chapter 4 for the design of lossy parallel connected networks.

With the lossy even and odd mode responses, the network of predistortion can be applied for the sub-networks so that non-uniform dissipation can be obtained [59]. A similar method is given in [60] and [61] for non-symmetric responses in which the derivation of lossy networks is based on (2.34). It is stated in [60] that even/odd mode analysis of filter network can be applied to asymmetrical response as long as $F_{11}=F_{22}$. However the method requires the use of hybrid in the implementation to combine the subnetworks.

2.3.4 Lossy synthesis based on CM

A method of synthesizing lossy CMs is provided in [62] and [63]. The method is based on specifically assigned lossy response that is derived by shifting the lossless response with a given amount. When the synthesized network is transformed into a folded array, only the first and last resonators are lossy. Hyperbolic rotations can then be applied to distribute losses among the resonators and couplings. As a result, the final circuit contains both lossy inverters and resonators.

The synthesis starts with the lossy response in (2.41) where k and α are constants. The admittance parameters can be derived as in (2.42).

$$S_{21}(s)=\frac{kP(s)}{\varepsilon E(s)},\ S_{11}(s)=\frac{k\alpha F_{11}(s)}{\varepsilon_R E(s)},\ S_{22}(s)=\frac{kF_{22}(s)}{\alpha\varepsilon_R E(s)} \tag{2.41}$$

$$\begin{aligned} Y_{21}(s)&=\frac{-2kP(s)}{E(s)+k\alpha F_{11}(s)+(k/\alpha)F_{22}(s)-k^2(-1)^{N+1}(E(s))^*} \\ Y_{11}(s)&=\frac{E(s)-k\alpha F_{11}(s)+(k/\alpha)F_{22}(s)+k^2(-1)^{N+1}(E(s))^*}{E(s)+k\alpha F_{11}(s)+(k/\alpha)F_{22}(s)-k^2(-1)^{N+1}(E(s))^*} \end{aligned} \tag{2.42}$$

The key point is that by using the lossy responses of (2.41), the numerator and denominator the admittance parameters in (2.42) are of the same

degrees as in the lossless case, so that the CM of the same order can be derived using the same procedures as in lossless. The partial expansions of the admittance parameters will result complex λ_k and residues. As a result, in the synthesized circuit, the inverters and the resonators are both lossy in the transversal array.

The same 4th order example is given here with $k=0.5$ and $\alpha=1.3$. The responses of the original lossless circuit and the synthesized lossy circuit are shown in Fig. 2.16. The CM of the transversal array is shown in Table 2.2. The couplings are complex. After rotations, only the first and last resonators are lossy. The CM is shown in Table 2.3.

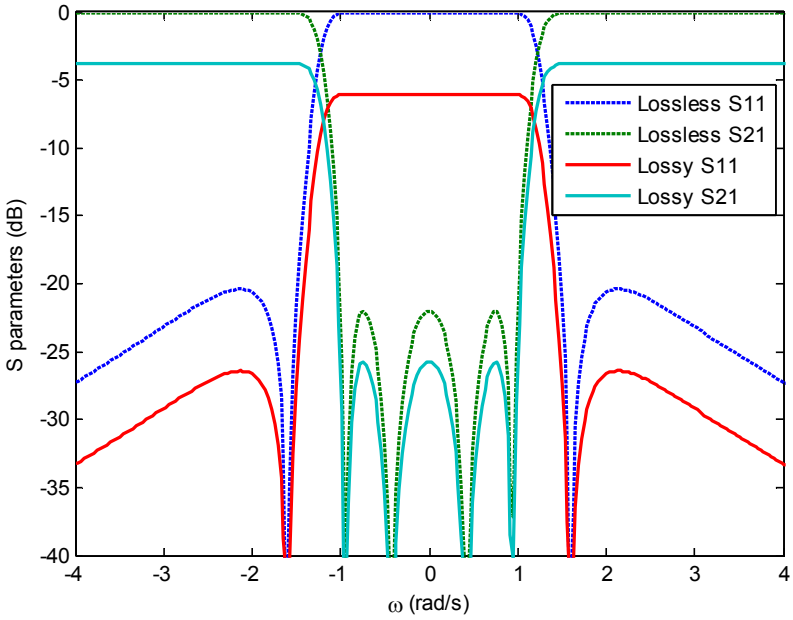

Fig. 2.16 S parameters of the original Chebyshev circuit and the synthesized lossy circuit.

Table 2.2 CM of the synthesized transversal array.

	0.3707 - 0.0092i	-0.3707 - 0.0092i	-0.6323 - 0.0090i	0.6323 - 0.0090i	
0.3707 - 0.0092i	-1.2865 - 0.0748i				0.2724 + 0.0940i
-0.3707 - 0.0092i		1.2865 - 0.0748i			0.2724 - 0.0940i
-0.6323 - 0.0090i			-0.7813 - 0.2944i		0.6226 + 0.0423i
0.6323 - 0.0090i				0.7813 - 0.2944i	0.6226 - 0.0423i
	0.2724 + 0.0940i	0.2724 - 0.0940i	0.6226 + 0.0423i	0.6226 - 0.0423i	

Table 2.3 CM of the synthesized lossy circuit.

	1.0364				
1.0364	- 0.2386i	-0.8620		0.3437	
	-0.8620		-0.8499		
		-0.8499		-0.8620	
	0.3437		-0.8620	- 0.4999i	0.9500
				0.9500	

2.3.5 Methods of optimizations

While analytic methods of deriving lossy filter networks have certain limitations as discussed earlier, methods of optimizations were introduced in [64] in which the element values of ladder networks were modified so that the magnitude of the transfer function of the lossy network is proportional to that of the lossless one.

The basic design equation is given in (2.43) in which T_1 is the transfer function of a lossless network and T_2 is the transfer function of a lossy network with its magnitude proportional to that of the ideal one. The changes of element values are given by ε_p. The magnitude of the transfer function is a linear combination of ε_p described by γ_p which can then be found by comparing the response with and without ε_p. A least square or gradient based minimization can be used to derive the values of ε_p.

$$|T_2(j\omega)| = |T_1(j\omega)| + \sum_{p=1}^{2n+1} \gamma_p(\omega)\varepsilon_p + 0(\varepsilon_i\varepsilon_k) \tag{2.43}$$

A method of optimization was formulated in [65] using various minimization techniques with constraints of inequalities. The method was applied to ladder networks whose characteristics are expressed by the cascading of transfer matrices. Different cost functions are given in [66][67].

For the design of waveguide filter introduced in [68], the dissipations due to various physical structures such as the cavities and coupling screws are modelled separately. Then a filter was designed using the CM which gives the optimum insertion loss. This method utilized the fact that for a give configuration and transfer function, there are numbers of CMs with changed element values.

2.4 Filter design based on CM

When the required specifications are met by a synthesized lowpass prototype network, the next step is to design the filter's physical structure. There are various technologies available [69] and the choice is made based on the operating band. When there are multiple technologies available, the choice can be made through a trade-off between the performance and the cost.

The first step in filter design based on CM is the demoralization of lowpass prototype to the required frequency band. For a bandpass filter, this can be achieved by a standard lowpass to bandpass transformation of lumped elements. Then, various technologies may be applied for the realization of bandpass resonators which are coupled correspondingly for the realization of couplings. For transmission line type of networks, the lowpass prototype may also be transformed into a distributed network. The design of waveguide filter is a typical example.

Finally, with the coarse model based on direct transformation, various tuning methods can be applied. Most tuning methods are based on an extraction of equivalent circuit from the responses. By comparing the extracted circuit to the designed one, corresponding elements can be tuned accordingly. After the manufacture of physical filters, tuning can also be applied to compensate manufacture tolerance.

2.4.1 Design of coarse models

With the standard lowpass to bandpass transformations in (2.44) [1], a lowpass resonator denoted by a capacitor in Fig. 2.17 (a) is transformed to a bandpass resonator consisting of a parallel connected capacitor and inductor as in Fig. 2.17 (b) which is a typical example of a coupled resonator bandpass filter.

$$\omega = \frac{f_0}{BW}\left(\frac{f}{f_0} - \frac{f_0}{f}\right) \tag{2.44}$$

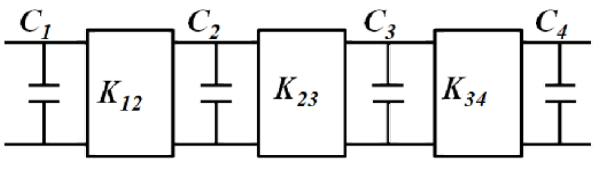

(a)

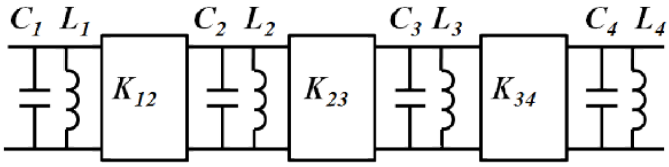

(b)

Fig. 2.17 Illustration of the lowpass-bandpass transformation of coupled resonator network.

Bandpass resonators can then be realized by various technologies. A microstrip resonator discussed in [1] is shown in Fig. 2.18 consisting of cascaded half-wave length transmission line. The resonant frequency is determined by the length and the couplings are realized by gaps between the microstrip lines. Filters based on microstrip lines have smaller size but are usually of higher loss.

The EM model for a coaxial resonator is shown in Fig. 2.19. Its resonant frequency is mainly determined by the stub length and is affected by the cavity size and the tuning screw. When two of the resonators are cascaded, there are both electrical and magnetic couplings in between and different couplings may be realized by a window between the two cavities or an inserted stub. Coaxial resonators can be cascaded to form a combline filter [70] which is usually used in mobile communication systems for its ability to realize various coupling configurations.

The EM model of a TE_{01} dielectric resonator is shown in Fig. 2.20. The resonant frequency is determined by the size of the dielectric bulk structure and various couplings can be realized by windows or probes between the cavities[71]. Dielectric filters have the best performance regarding loss and is typically used in satellite communication systems.

A method is given by Cohn [13] for the design of narrow band waveguide filters. The bandpass resonators can be replaced by the equivalent half-wavelength transmission lines. And the ideal inverters can be replaced by their equivalence of reactances as in Fig. 2.3. The negative lines of inverters can be emerged with adjacent length of transmissions. The result is a cascading of shunt reactances with lengths of transmission lines. The shunt reactances can then be realized by various discontinuities in the waveguide.

A cascading of waveguide cavities and is only capable of realising the mainline couplings. As a result, the filter is synchronously tuned with no transmission zeros. A dual mode waveguide introduced in [72] can be used

for realizing more complex filter configurations. A typical diagram for an 8th order dual-mode waveguide filter is shown in Fig. 2.21.

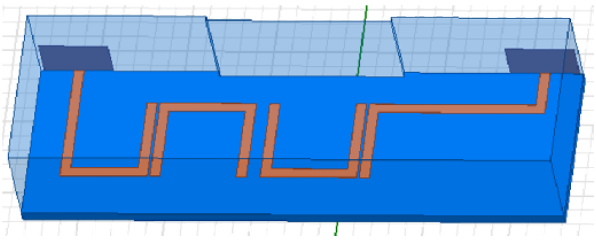

Fig. 2.18 A typical microstrip filter of cascaded half-wavelength lines [1].

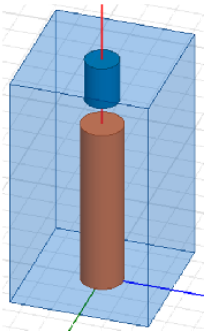

Fig. 2.19 EM model of a coaxial resonator with air cavity and tuning screw.

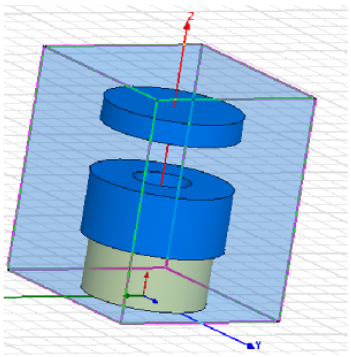

Fig. 2.20 The EM model of a dielectric resonator.

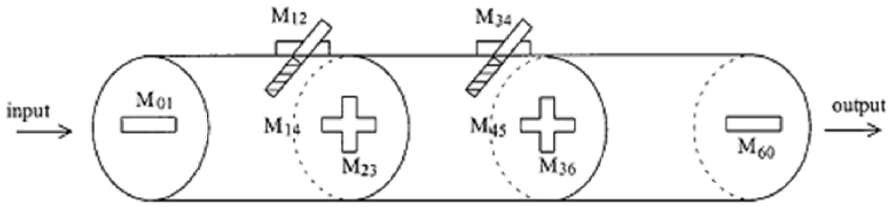

Fig. 2.21 A dual-mode waveguide filter [72].

2.4.2 Filter tuning based on CM extractions

Based on the coarse model, various computer aided tuning techniques can be applied. An example utilizing parameter extraction is shown in Fig. 2.22 [11][73]. First, S parameters are obtained from EM simulations or real time measurements. Data gathered should be rationalized by removing the effects induced by the input and output connections.

CMs or other circuit models can then be extracted from the responses using an appropriate method. Various analytical or optimization methods can be used for this purpose. The differences between the extracted circuits and the designed ones can indicate which structures should be adjusted.

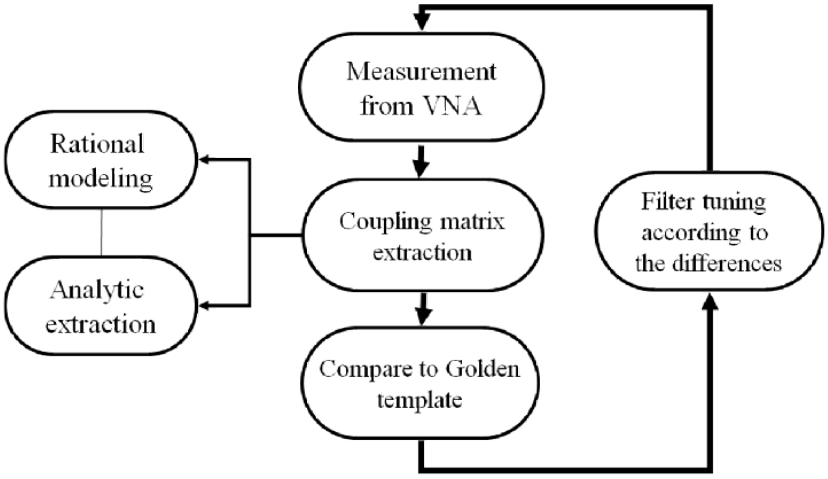

Fig. 2.22 Flow chart of filter tuning process using CM extractions.

Chapter 3
Generalized Coupling Matrix Synthesis for Lossy Microwave Filters

Generally speaking, there are two problems in the synthesis of lossy CMs: the determination of lossy transfer functions that can be realized by lossy networks and the derivation of lossy circuits based on the given responses. The lossy synthesis methods reviewed earlier solve these problems partially and are only applicable within certain constants. The method of predistortion [54] in 2.4.2 provides the denominator polynomial of lossy transfer functions with uniform resonator losses. The method given in 2.4.3 determines lossy circuits based on even and odd modes analysis [55]. The filter networks realized either have dissipations only at the input and output resonators or have complex cross couplings which are difficult to implement. In [60][61], the even and odd mode analysis which is originally only valid for symmetrical responses is extended to the case when $S_{11}=S_{22}$. However, the lossy network synthesized requires the use of hybrids to combine sub-networks. The method in 2.4.4 is based on a very specific type of lossy responses for which the characteristic polynomials are multiplied by certain constants so that the lossless synthesis method is still valid.

A generalized lossy synthesis technique is presented in this chapter. The method can (1) find the reflection function from the transfer function when unitary condition is not satisfied; (2) derive the expressions for the complex Y parameters and (3) synthesize the lossy CM with prescribed loss distribution. The method is based on a condition set for the polynomials of S parameters which replaces the use of power conservation in the lossless case and it is guaranteed that the admittance parameters and corresponding CMs can be derived.

Two special cases are given for solving the refection function with a prescribed transfer function. In the first case, F_{11} the numerator of S_{11} equals to F_{22} the numerator of S_{22}. The method is equivalent to the even and odd mode analysis given in [55] and [60] for asymmetric filter responses. Since the networks are transversal arrays which have a parallel connection of the even and odd mode sub-networks, they can be transformed to any realizable

configurations. In the second case, loss distributions are given. An method of iteration is applied so that the synthesized CM has the prescribed loss distribution. The method is equivalent to an extension of conventional method of predistortion with non-uniform resonator Qs and lossy invertors.

The lossy synthesis method provided is capable of synthesizing lossy networks with prescribed non-uniform Qs. The application of this method is found in the implementation of filter networks consisting of two different kinds of resonators. Filters with both dielectric and coaxial resonators is used in to provide improved spurious [74][75]. Various examples of synthesizing CMs are given in this section to illustrate the design processes. A 6^{th} degree filter with TM dielectric and coaxial resonators is modeled in HFSS [76] and simulated. A 4^{th} degree filter with dual-mode dielectric resonator and coaxial resonator is also given.

3.1 Lossy transfer functions

The method of lossy synthesis starts with a given transfer function. As dissipations included in filter networks introduce rounding at bandedge and thus deteriorate the filter's performance, an insertion loss which is proportional to the lossless one as shown in Fig. 3.1 is chosen to maintain the selectivity. This kind of transfer function is used in the receiver pass as the degraded insertion loss can be easily compensated by an additional LNA [42] as illustrated in Fig. 3.2.

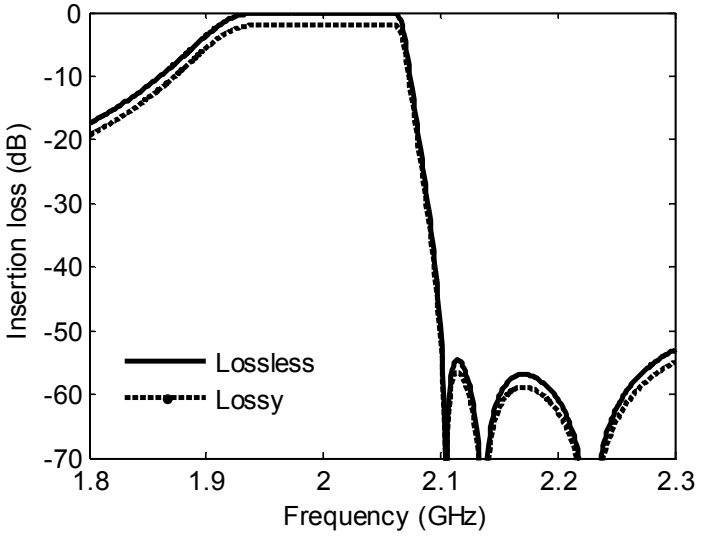

Fig. 3.1 A typical lossy insertion loss compared to the lossless one.

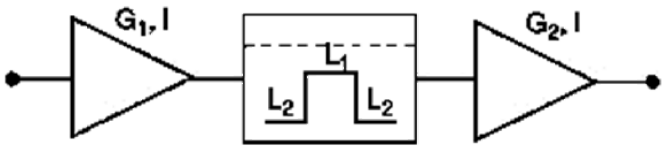

Fig. 3.2 Loss compensation by LNA [42].

S parameters in (2.1) are used in which S_{21} is the general Chebyshev response or other desired filter characteristics, S_{21}' in (3.1) represents the lossy response and k_{21} is a constant smaller than one that determines the insertion loss level. Using the polynomials in (2.1), the transfer function can be expressed by polynomials in (3.2) in which the denominator polynomial E is the same as the lossless one and the numerator polynomial P is the lossless one multiplied by k_{21}.

$$S_{21}' = k_{21} S_{21} \tag{3.1}$$

$$\begin{aligned} P_s(s)' &= k_{21} \cdot P_s(s) \\ E_s(s)' &= E_s(s) \end{aligned} \tag{3.2}$$

A new lossless characteristic can also be used which has a similar insertion loss as the general Chebyshev response but a different return loss. It is derived by shifting the poles of the original Chebyshev response non-uniformly as in (3.3) until the flatness of passband insertion loss is achieved. The insertion loss shown in (3.3) has the same numerator as the standard response. r_{ei} is the pole and δ_i is the corresponding modification. k_{21} is a constant used to renormalize the insertion loss level. For lossy responses, k_{21} equals to one and the insertion loss level is determined by the value of δ_i.

$$\begin{aligned} S_{21n} &= k_{21} \frac{P_s(s)}{\prod_{i=1}^{N} (s - r_{ei} + \delta_i)} \\ k_{21} &= \max\left(\prod_{i=1}^{N} (s - r_{ei} + \delta_i) \Big/ P_s(s) \right) \end{aligned} \tag{3.3}$$

A similar response is discussed in [77] where a lossy filter is realized by including non-uniform losses to lossless parallel connected networks. Because the sensitivity of insertion loss is different regarding resonator dissipations and is a parameter of resonator bandwidth, a parallel connected network with non-uniform Q and selective insertion loss can be derived. The detail of the design method will be given in Chapter 4.

The following is an example of the new characteristic which is originally a 4th order general Chebyshev response with three transmission zeros at -1.7j, -2.2j and -3.6j. The poles of the insertion loss are shifted to the left by 0.0709; 0.0730; 0.0024; 0.0135 in the complex plane while the zeros are kept at the original positions. According to power conservation in (3.4), the polynomial F_{11} can be derived. The poles and zeros of these characteristics are compared with the original ones in Table 3.1 and Table 3.2. The roots of F_{11} are complex and form complex conjugate pairs with the roots of F_{22}.

$$F_{11}(s)\cdot F_{11}(s)^{*} + P(s)\cdot P(s)^{*} = E(s)\cdot E(s)^{*} \tag{3.4}$$

Table 3.1 Roots of the polynomials of the original characteristics.

E	P	F_{11}	F_{22}
-0.7034+1.3183j	-3.6000j	+0.8569j	+0.8569j
-0.9291-0.0812j	-2.2000j	-0.9644j	-0.9644j
-0.1248-1.0961j	-1.7000j	-0.6517j	-0.6517j
-0.4608-0.8483j		+ 0.0519j	+0.0519j

Table 3.2 Roots of the polynomials of the new characteristics.

E_n	P_n	F_{11n}	F_{22n}
-0.7743+1.3183j	-3.6000j	-0.3474+0.8890j	0.3474+0.8890j
-1.0021-0.0812j	-2.2000j	-0.9639j	-0.9667j
-0.1272-1.0961j	-1.7000j	-0.1580-0.6940j	0.1580-0.6940j
-0.4743-0.8483j		-0.4766+0.0630j	0.4766+0.0630j

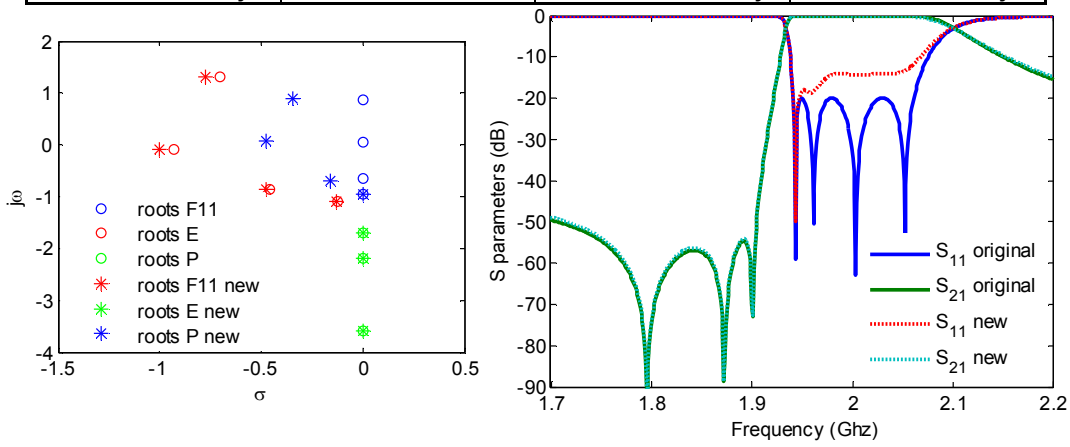

(a) (b)

Fig. 3.3 Roots distribution (a) and response (b) of the new characteristic.

Fig. 3.3(a) shows the root distributions compared to the original ones in the complex plane. The insertion loss of this new characteristic in Fig. 3.3(b) is the same as the general Chebyshev response while the return loss is no longer equal-ripple.

It is noted that the new characteristics can be derived by shifting the poles with amounts proportional to the ones given earlier. Poles can even be shifted to the right as shown in Fig. 3.4(a). The response is shown in Fig. 3.4(b). Though these new responses have higher return loss levels, they can be used in the synthesis of lossy filters and some new properties can be found that will be discussed later.

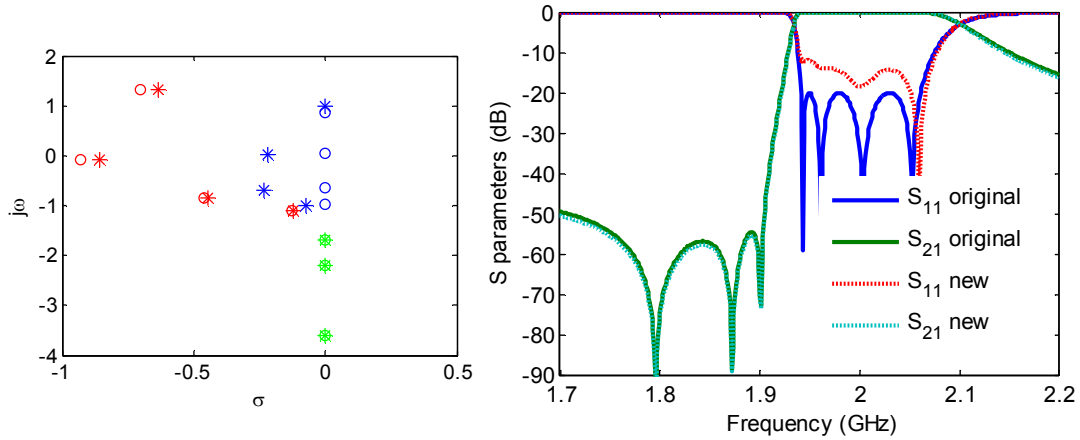

(a) (b)

Fig. 3.4 Roots distribution (a) and response (b) of the new characteristic when the roots are shifted to the left in the complex plane.

3.2 Synthesis of lossy CMs

The problem of CM synthesis with given transfer functions involve three steps. The first one is to derive the corresponding reflection function. For lossless cases, this can be easily solved using the condition of power conservation. The second one is to derive the rational polynomial expressions of the admittance parameters from S parameters. And the third one is to build up the transversal array using the residues and poles of the admittance parameters. A general procedure for CM synthesis is given in this section. It is based on an S to Y transformation and a modified condition for the polynomials of S parameters can be found for which the power conservation in (3.4) is only a special case.

3.2.1 Generalized S to Y transformation

The transformation between scattering and impedance matrices for multi-port networks is given in (3.5) [78] where Z_s is the reference impedance. *F* and *G* are diagonal matrices with diagonal elements $1/2\sqrt{|Re(Z_s)|}$ and Z_s. For a two-port network with unitary reference impedance, the transformation between scattering and admittance matrices can be simplified to (3.6).

$$Z = F^{-1}(I - S)^{-1}(SG + G^*)F \tag{3.5}$$

$$\begin{aligned} Y_{11} &= \frac{(1 - S_{11})(1 + S_{22}) + S_{12}S_{21}}{(1 + S_{11})(1 + S_{22}) - S_{12}S_{21}} \\ Y_{21} &= \frac{-2S_{21}}{(1 + S_{11})(1 + S_{22}) - S_{12}S_{21}} \\ Y_{22} &= \frac{(1 + S_{11})(1 - S_{22}) + S_{12}S_{21}}{(1 + S_{11})(1 + S_{22}) - S_{12}S_{21}} \end{aligned} \tag{3.6}$$

According to the polynomial expressions of S parameters in (2.1), for an N^{th} degree network, the admittance parameters are rational polynomials whose denominators are of degree *2N* as in (3.7).

$$\begin{aligned} Y_{11} &= \frac{(E - F_{11})(E + F_{22}) + P^2}{(E + F_{11})(E + F_{22}) - P^2} \\ Y_{21} &= \frac{-2PE}{(E + F_{11})(E + F_{22}) - P^2} \\ Y_{22} &= \frac{(E + F_{11})(E - F_{22}) + P^2}{(E + F_{11})(E + F_{22}) - P^2} \end{aligned} \tag{3.7}$$

For lossless responses, substituting the power conservation of (3.4) into (3.7), we have (3.8) in which the admittance parameters are rational polynomials of degree N. Then the CM synthesis in [9] can be applied which is based on the partial expansions of the admittance parameters.

$$\begin{aligned} Y_{11} &= \frac{Y_{11n}}{Y_d} = \frac{E(s) - F_{11}(s) + F_{22}(s) - E(s)^*}{E(s) + F_{11}(s) + F_{22}(s) + E(s)^*} \\ Y_{21} &= \frac{Y_{21n}}{Y_d} = \frac{-2\mathrm{P}(s)}{E(s) + F_{11}(s) + F_{22}(s) + E(s)^*} \\ Y_{22} &= \frac{Y_{22n}}{Y_d} = \frac{E(s) + F_{11}(s) - F_{22}(s) - E(s)^*}{E(s) + F_{11}(s) + F_{22}(s) + E(s)^*} \end{aligned} \tag{3.8}$$

Since the power conservation is no longer valid for lossy cases, a new condition for the polynomials of S parameters is given in (3.9). E_x is a newly defined polynomial of degree *N* and it can be found from the F, P and E polynomials according to (3.10). When this new condition in (3.9) is satisfied, Nth degree admittance parameters can always be found as in (3.11).

$$F_{11}(s)\cdot F_{22}(s)-P(s)\cdot P(s)=E(s)\cdot E_x(s) \tag{3.9}$$

$$E_x=\frac{F_{11}(s)F_{22}(s)-P(s)\cdot P(s)}{E(s)} \tag{3.10}$$

$$\begin{aligned} Y_{11}&=\frac{Y_{11n}}{Y_d}=\frac{E(s)-F_{11}(s)+F_{22}(s)-E_x}{E(s)+F_{11}(s)+F_{22}(s)+E_x}\\ Y_{21}&=\frac{Y_{21n}}{Y_d}=\frac{-2\mathrm{P}(s)}{E(s)+F_{11}(s)+F_{22}(s)+E_x}\\ Y_{22}&=\frac{Y_{22n}}{Y_d}=\frac{E(s)+F_{11}(s)-F_{22}(s)-E_x}{E(s)+F_{11}(s)+F_{22}(s)+E_x} \end{aligned} \tag{3.11}$$

3.2.2 Discussions on the polynomial E_x

For *Nth* degree responses, (3.9) provides the condition with which *Nth* degree admittance parameters can be derived. It is general for both lossless and lossy cases. For a lossless response, due to the condition of power conservation, the roots of F_{11} and F_{22} are of conjugate pairs and thus the polynomial F_{22} is the complex conjugate of F_{11} as in (3.12) [8]. The polynomial P can be expressed by its roots r_{pi} as in (3.13). If r_{pi} are purely imaginary, the complex conjugate of P could be expressed as in (3.14) where *nfz* is the number of transmission zeros.

$$F_{22}(s)=(-1)^N F_{11}(s)^* \tag{3.12}$$

$$P(s)=\prod(s-r_{pi}) \tag{3.13}$$

$$P(s)^*=\prod(-s-r_{pi}^*)=\prod(-s+r_{pi})=(-1)^{nfz}\prod(s-r_{pi})=(-1)^{nfz}P(s) \tag{3.14}$$

Substituting the expressions of (3.12) and (3.14) into (3.4), we have (3.15) which is a modified version of power conservation. When *(N-nfz)* is odd, (3.16) can be easily derived. When *(N-nfz)* is even, the polynomial *P* is multiplied by *j* in the synthesis of filter characteristic polynomials [8] and (3.16) is still satisfied. Thus the expression in (3.15) is equivalent to (3.16)

for any N and nfz. Comparing (3.16) to the original power conservation in (3.4), we can easily see that for lossless cases, polynomial E_x is the complex conjugate of E as in (3.17).

$$(-1)^N F_{11}(s)\cdot F_{22}(s)+(-1)^{nfz} P(s)\cdot P(s)=E(s)\cdot E(s)^* \tag{3.15}$$

$$F_{11}(s)\cdot F_{22}(s)-P(s)\cdot P(s)=(-1)^N E(s)\cdot E(s)^* \tag{3.16}$$

$$E_x=(-1)^N E(s)^* \tag{3.17}$$

For lossy responses, the polynomial E_x is not the same as in the lossless case and its roots are shifted according to the dissipations. Substituting the insertion loss of (3.1) into (3.9), we have the condition in (3.18).

$$F_{11}(s)'\cdot F_{22}(s)'-k_{21}^2 P(s)'\cdot P(s)'=E(s)'\cdot E_x(s)' \tag{3.18}$$

For a synthesis problem, P' and E' are given while F_{11}', F_{22}' and E_x are unknown. The expression for F_{11}' and F_{22}' can be derived in two different cases given in the following sections. Then with the complete set of polynomials of S parameters, corresponding admittance parameters can be found from (3.10) and can be synthesized as an N^{th} degree parallel connected network according to [8]. It will also be shown that with the condition in (3.18), it is guaranteed that an N^{th} degree network can be synthesized. (3.18) is the basis for the synthesis of CMs for which the condition of power conservation is a special case.

3.2.3 Realizable conditions for CMs

For lossless networks, the derivation of the CMs in [7], [8] and [79] requires the poles and residues of the admittance parameters satisfying the conditions given in (3.19). For the lossy networks, since the poles and residues are complex, those conditions are violated. It will be proved in this section that the condition given in (3.18) is sufficient that the prescribed lossy characteristics can be realized by a lowpass prototype networks with distributed dissipations.

$$\begin{gathered} r_{11},\ r_{12} \text{ and } r_{22} \text{ are real} \\ r_{11}, r_{22} \geq 0 \\ r_{11}r_{22}-r_{12}^2=0 \end{gathered} \tag{3.19}$$

$$\sum r_{12} = 0$$

The synthesis method given in [8] is based on the equivalence of the admittance parameters derived from S parameters and from parallel connected networks. The rational polynomials of admittance parameters in (3.10) can be expressed by partial expansions as in (3.20) where λ_k is a pole. r_{11k}, r_{21k} and r_{22k} are corresponding residues of Y_{11}, Y_{21} and Y_{22}. For transversal arrays, the admittance parameters consisting of *N* resonators are the summation of the admittance parameters of each resonator as in (3.21).

$$[Y] = \sum_{k=1}^{N} \frac{1}{s - j\lambda_k} \begin{bmatrix} r_{11k} & r_{12k} \\ r_{21k} & r_{22k} \end{bmatrix} \tag{3.20}$$

$$[Y] = \sum_{k=1}^{N} \frac{1}{sC_k - jB_k} \begin{bmatrix} M_{sk}^2 & M_{sk}M_{Lk} \\ M_{sk}M_{Lk} & M_{Lk}^2 \end{bmatrix} \tag{3.21}$$

For admittance parameters to be realized by a parallel connected network, the two expression in (3.20) and (3.21) should be equivalent to each other. Thus it is required that the condition in (3.22) is satisfied. For lossy networks, the residues no longer need to be positive since the invertors can be lossy and complex. As a result, the realizable conditions in (3.19) are simplified to the one in (3.22) for more general cases.

$$r_{11k} r_{22k} = r_{12k}^2 \tag{3.22}$$

We will show next that with (3.9), the realizable condition in (3.22) is always satisfied. That is to say with (3.9), the responses can always be synthesized as a network of transversal array. The residues can be calculated according to (3.23) where Y_{11n}, Y_{21n} and Y_{22n} are the numerators of admittance parameters and Y_d' is the first order derivative of the denominator [8]. Then the condition in (3.22) on the residues is equivalent to the one in (3.24) which relates the values of numerators at each pole.

$$r_{11k} = \left(\frac{Y_{11n}}{Y_d'} \right)_{s=j\lambda_k}, r_{21k} = \left(\frac{Y_{21n}}{Y_d'} \right)_{s=j\lambda_k}, r_{22k} = \left(\frac{Y_{22n}}{Y_d'} \right)_{s=j\lambda_k} \tag{3.23}$$

$$\text{At } Y_d = 0,\ Y_{11n} Y_{22n} = Y_{21n}^2 \tag{3.24}$$

According the polynomial expressions of the admittance parameters of (3.11) into (3.24), a pole is achieved at the frequency when (3.25) is satisfied. Then the polynomial E_x can be found as in (3.26).

$$E(s)+F_{11}(s)+F_{22}(s)+E_x(s)=0 \tag{3.25}$$

$$E_x(s)=-E(s)-F_{11}(s)-F_{22}(s) \tag{3.26}$$

Substituting (3.26) into the condition in (3.9), we have (3.27) which can be rearranged to give the polynomial *P* as in (3.28). Factorizing the right-hand side of (3.28), we have (3.29) which is equivalent to (3.24). As a result, we have proven that under (3.9), the realizable condition in (3.24) is always satisfied and the S parameters can be synthesized as a parallel connected network.

$$\begin{aligned} F_{11}(s)\cdot F_{22}(s)-P(s)^2 &= -E(s)\cdot\left(E(s)+F_{11}(s)+F_{22}(s)\right) \\ &= -E(s)^2-E(s)F_{11}(s)-E(s)F_{22}(s) \end{aligned} \tag{3.27}$$

$$\begin{aligned} P(s)^2 &= F_{11}(s)\cdot F_{22}(s)+E(s)^2+E(s)F_{11}(s)+E(s)F_{22}(s) \\ &= \left(E(s)+F_{11}(s)\right)\left(E(s)+F_{22}(s)\right) \end{aligned} \tag{3.28}$$

$$\begin{aligned} &Y_{21n}^2 = 4P(s)^2 \\ &= \left(E(s)-F_{11}(s)+F_{22}(s)-E_x(s)\right)\left(E(s)+F_{11}(s)-F_{22}(s)-E_x(s)\right) \\ &= Y_{11n}Y_{22n} \end{aligned} \tag{3.29}$$

3.3 Case I: $F_{11}=kF_{22}$

With a given insertion loss as in section 3.1, the condition in (3.18) can be used to solve the reflection functions of F_{11} and F_{22}. The first solution is found when $F_{11}=kF_{22}$. For lossless responses discussed in [13], roots of F_{11} and F_{22} are the same and lie on the imaginary axis of the complex plane. Additional losses in the network make the roots of F_{11} and F_{22} be shifted away from the original positions and are complex in general. It will be shown in this section that when the roots of F_{11} lie in the same positions as those of F_{22}, an even/odd mode analysis that is originally only applicable to symmetrical responses [55][80] can now be used for the synthesis of lossy networks. Also, there is no need for hybrids to combine the even/odd mode sub-networks as in [60].

3.3.1 Methods of synthesis

When $F_{22}=F_{11}$, or more generally as in (3.30) where k_{11} is a constant, (3.31) can be derived from the left hand side of (3.18). The two factors in (3.31)

which are a combination of F_{11} and P consists polynomial E. As a result, at a root of E, either of the two factors should be zero as in (3.32) where r_{ei} represents part of the roots of E and r_{ej} represents the others. For an N^{th} degree response, using the roots of E, the coefficients of F_{11} can be solved from the N linear equations without knowing the expression for E_x.

$$F_{22}(s)' = k_{11}F_{11}(s)' \tag{3.30}$$

$$\begin{aligned} E(s)'\cdot E_x(s)' &= k_{11}F_{11}(s)'\cdot F_{11}(s)' - k_{21}^2 P(s)'\cdot P(s)' \\ &= \left(\sqrt{k_{11}}F_{11}(s)' + k_{21}P(s)'\right)\left(\sqrt{k_{11}}F_{11}(s)' - k_{21}P(s)'\right) \end{aligned} \tag{3.31}$$

$$\begin{aligned} \left(\sqrt{k_{11}}F_{11}(s)' + k_{21}P(s)'\right)_{s=rei} &= 0 \\ \left(\sqrt{k_{11}}F_{11}(s)' - k_{21}P(s)'\right)_{s=rej} &= 0 \end{aligned} \tag{3.32}$$

The 4th order example used in section 3.1 with the new characteristics is used as an example to illustrate the synthesis procedures. Given $k_{21}=0.8$ and $k_{11}=0.7$, the characteristic polynomials are listed in Table 3.3 and their roots are plotted in Fig. 3.5(a) in the complex plane compared to the standard general Chebyshev responses. The derived F_{11} and F_{22} have the same coefficients except for a constant k_{11}. E_x can also be found from (3.26) which is no longer the complex conjugate of E due to the existence of losses as shown in Fig. 3.5b.

The CM synthesized in given in Table 3.4. The response of the synthesized lossy network is given in Fig. 3.6. The insertion loss is the equivalent to the lossless one shifted by a constant k_{21}. The S_{11} and S_{22} are no longer the same and are shifted by constant k_{11}. In designing a lossy network, the value of k_{21} determines the insertion loss level and thus the amount of included dissipations. The values k_{11} determines the difference between S_{11} and S_{22} and thus has effect on the loss distribution.

Table 3.3 Polynomials for the 4th order example

E'	P'	F_{11}'	F_{22}'	E_x
-0.7743 +1.3183j	-3.6000j	-0.0339 +1.0005j	-0.0339 +1.0005j	0.5366 +1.3945j
-1.0021 -0.0812j	-2.2000j	0.1005 -1.0046j	0.1005 -1.0046j	0.6800 -0.0542j
-0.1272 -1.0961j	-1.7000j	-0.0920 -0.8028j	-0.0920 -0.8028j	0.1265 -1.1424j
-0.4743 -0.8483j		-0.3113 +0.0804j	-0.3113 +0.0804j	0.3616 -0.9438j

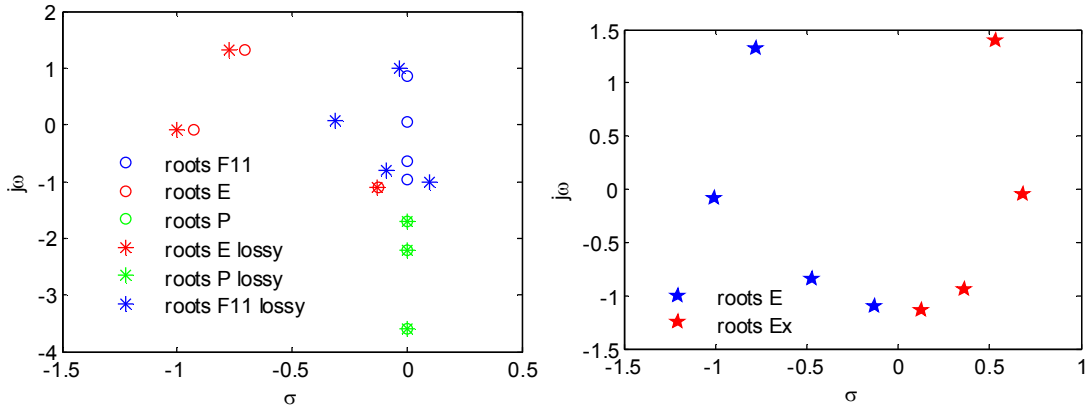

Fig. 3.5 (a) Roots of the characteristic polynomials for the 4th order network synthesized comparing to the lossless ones. (b) Roots of E and E_x.

Table 3.4 CM synthesized for the 4th order example.

	-1.0103 + 0.0048i				
-1.0103 + 0.0048i	-0.1510 - 0.1765i	0.9471 + 0.0026i		-0.3422 - 0.0208i	0.0513 + 0.0002i
	0.9471 + 0.0026i	0.1359 + 0.0112i	0.3181 - 0.0022i	0.6623 - 0.0002i	
		0.3181 - 0.0022i	0.8573 + 0.0027i	-0.6272 - 0.0035i	
	-0.3422 - 0.0208i	0.6623 - 0.0002i	-0.6272 - 0.0035i	-0.1173 - 0.3541i	0.9931 - 0.0047i
	0.0513 + 0.0002i			0.9931 - 0.0047i	

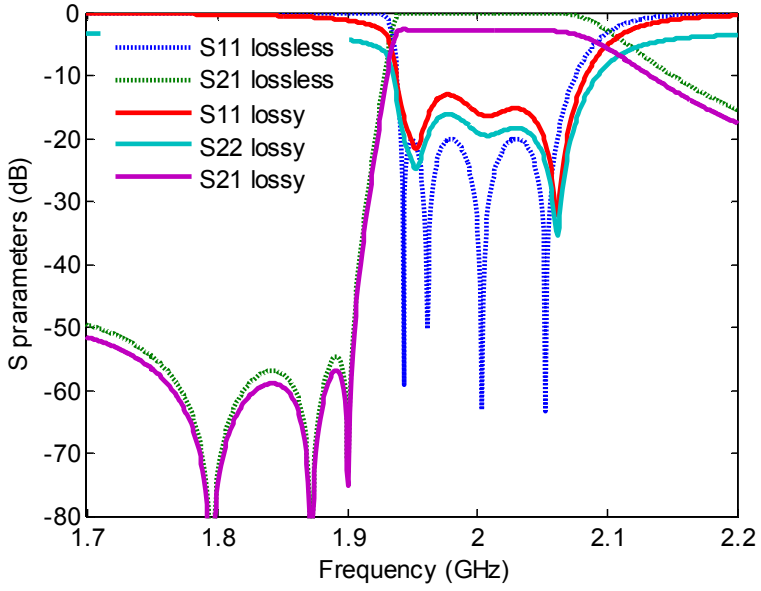

Fig. 3.6 Response of the 4th order network synthesized when $F_{11}=k_{11}F_{22}$.

When the lossy transfer function is derived from the lossless one by $S_{21}'=k_{21}S_{21}$, the synthesized CM either have dissipations concentrated at the input and output resonators or have complex cross couplings which are difficult to implement.

3.3.2 Relations to even/odd mode analysis

This method of deriving the reflection function is more general than the ones given in [55] and [60] that the filter response doesn't need to be symmetric. Based on the synthesis procedure, the even and odd mode analysis which is originally used for symmetric networks could be applied to asymmetric networks when the response satisfies the conditions in (3.18) and (3.30).

The even and odd mode of this asymmetric network is defined based on the equation in (3.33) which is derived from (3.31) by dividing E. The even and odd mode S parameters can then be defined as in (3.34) where $E_x=E_{xe}E_{xo}$ and $E_s=E_{se}E_{so}$.

$$\left(\sqrt{k_{11}}S_{11}+S_{21}\right)\left(\sqrt{k_{11}}S_{11}-S_{21}\right)=\frac{E_x(s)}{E(s)} \tag{3.33}$$

$$\begin{aligned} S_e &= \left(\sqrt{k11}S_{11}+S_{21}\right)=\frac{E_{xe}}{E_{se}} \\ S_o &= \left(\sqrt{k_{11}}S_{11}-S_{21}\right)=\frac{E_{xo}}{E_{so}} \end{aligned} \tag{3.34}$$

With the even and odd mode S parameters, the corresponding even and odd mode admittance parameters can be defined according to (3.35). For S parameters of this asymmetric network, the condition in (3.36) which is for the symmetrical response is still satisfied.

$$\begin{aligned} S_e &= \frac{1-Y_e}{1+Y_e} \\ S_o &= \frac{1-Y_o}{1+Y_o} \end{aligned} \tag{3.35}$$

$$\begin{aligned} S_{11} &= \frac{1}{2}\left(S_e+S_o\right)=\frac{1-Y_eY_o}{\left(1+Y_e\right)\left(1+Y_o\right)} \\ S_{21} &= \frac{1}{2}\left(S_e-S_o\right)=\frac{Y_e-Y_o}{\left(1+Y_e\right)\left(1+Y_o\right)} \end{aligned} \tag{3.36}$$

By substituting (3.36) into standard transformation from S parameters to admittance parameters, we have (3.37), which shows that the filter network is the parallel connection of the even and odd mode sub-networks as for symmetric networks.

$$Y_{11} = \frac{1}{2}(Y_e + Y_o)$$
$$Y_{21} = \frac{1}{2}(Y_e - Y_o) \tag{3.37}$$

The lossy characteristic of (3.2) could be extended to the ones that are of higher degree than *N*. In this case, the polynomials of P and E are multiplied by additional terms of X_p and X_e as in (3.38). Those additional terms only change the phase of the insertion loss and thus are equivalent to an all pass network. The same procedure can be applied to synthesize lossy circuits. When the network synthesized by even and odd mode method has loss distributed only at the input and output resonators, this method can be used to distribute losses into the internal of the network.

$$\begin{aligned} P(s)' &= k \cdot P(s) \cdot X_p \\ E(s)' &= E(s) \cdot X_e \\ \left|\frac{X_p}{X_e}\right| &= 1 \end{aligned} \tag{3.38}$$

3.4 Case II: given loss distribution

Solution to (3.18) could also be found when the polynomial E_x is given. For lossless networks, it is shown that E_x is the complex conjugate of *E*. For lossy networks, this relation is not valid. We will show in this section that with the prescribed loss distribution and transfer function, a network can be synthesized with losses only at resonators.

3.4.1 Generalized Y to S transformation

Based on the transformation from S parameters to admittance parameters in (3.11), the polynomial expressions for the numerator and denominator of the admittance parameters can be found as in (3.39).

$$\begin{aligned} Y_{11n} &= E(s) - F_{11}(s) + F_{22}(s) - E_x \\ Y_{21n} &= \text{-2P}(s) \\ Y_{22n} &= E(s) + F_{11}(s) - F_{22}(s) - E_x \\ Y_d &= E(s) + F_{11}(s) + F_{22}(s) + E_x \end{aligned} \tag{3.39}$$

Then a similar condition as in (3.18) can be found for the admittance parameters as in (3.40) with Y_x defined in (3.41).

$$\begin{aligned} Y_{11n}Y_{22n} - Y_{21n}^2 &= \left(E(s) - F_{11}(s) + F_{22}(s) - E_x\right) \\ &\quad \cdot \left(E(s) + F_{11}(s) - F_{22}(s) - E_x\right) - 4\mathrm{P}^2(s) \\ &= \left(E(s) - E_x\right)^2 - \left(F_{11}(s) - F_{22}(s)\right)^2 - 4\mathrm{P}^2(s) \\ &= \left(E(s) + E_x\right)^2 - \left(F_{11}(s) + F_{22}(s)\right)^2 \\ &= \left(E(s) + E_x + F_{11}(s) + F_{22}(s)\right)\left(E(s) + E_x - F_{11}(s) - F_{22}(s)\right) \\ &= Y_d Y_x \end{aligned} \tag{3.40}$$

$$Y_x = E(s) + E_x - F_{11}(s) - F_{22}(s) \tag{3.41}$$

With Y_x, the polynomial expressions for S parameters can be found directly from admittance parameters as in (3.42). The condition in (3.40) is equivalent to the one in (3.18) and this can be proved by polynomial substitutions.

$$\begin{aligned} F_{11}(s) &= Y_d - Y_{11n} + Y_{22n} - Y_x \\ F_{22}(s) &= Y_d + Y_{11n} - Y_{22n} - Y_x \\ E(s) &= Y_d + Y_{11n} + Y_{22n} + Y_x \\ E_x(s) &= Y_d - Y_{11n} - Y_{22n} + Y_x \end{aligned} \tag{3.42}$$

For any CM regardless of the configuration, its eigenvalues and residues can be found by a Jacobi eigenvalue algorithm which is an iterate method to gradually reduce the values of the off-diagonal elements until they are small enough that the eigenvalues can be approximated by the diagonal ones. In each of the iteration, the largest off-diagonal element is set by zero by a similarity transformation with calculated pivots. As a result, any CM can be transformed back to the transversal array.

Then with the transversal array network, the rational polynomial of the admittance parameters of the network can be found according to the definition of partial expansion. Then the response of the network can be found by the transformation of admittance parameters to S parameters as given in (3.42). That is to say, rational polynomial responses of CMs can be found without matrix inversions.

3.4.2 Derivation of lossy polynomial E_x

With uniform resonator dissipations, roots of the characteristic polynomials are shifted to the left uniformly as shown section 2.4. To maintain the selectivity of lossy networks, insertion loss is tuned to be proportional to that of the lossless one as discussed in section 3.1. As a result, the roots of polynomial *E* are kept at the original positions. Correspondingly, this requires

the roots of E_x polynomial to be shifted to the left by a given amount. While this procedure is straightforward for uniform losses, for non-uniform losses, the roots need to be shifted by complex numbers which are determined by polynomial comparison. In addition, a method of iteration can be applied to deal with non-uniform losses.

3.4.2.1 Uniform losses

When dissipations of resonators are included in the filter network as shown in Fig. 2.7, its admittance parameters in (2.26) are modified to the ones in (3.43) where δ represents the amount of dissipation and can derived from resonator Q by (3.44). We can see that the inclusion of uniform dissipation is equivalent to shifting the poles of the admittance parameters to the left by the constant δ and is also equivalent to change the variable s to $s+\delta$ when the capacitors are normalized as in the synthesis of CM. Then regarding the S parameters of filter networks, lossy responses can be derived from the lossless ones by a change of variable from s to $s+\delta$.

$$\begin{aligned}[Y] &= \sum_{k=1}^{N} \frac{1}{sC_k + jB_k + \delta} \begin{bmatrix} M_{Sk}^2 & M_{Sk}M_{Lk} \\ M_{Sk}M_{Lk} & M_{Lk}^2 \end{bmatrix} \\ &= \sum_{k=1}^{N} \frac{1}{sC_k - (-jB_k - \delta)} \begin{bmatrix} M_{Sk}^2 & M_{Sk}M_{Lk} \\ M_{Sk}M_{Lk} & M_{Lk}^2 \end{bmatrix} \\ &= \sum_{k=1}^{N} \frac{1}{\left(s + \delta / C_k\right)C_k + jB_k} \begin{bmatrix} M_{Sk}^2 & M_{Sk}M_{Lk} \\ M_{Sk}M_{Lk} & M_{Lk}^2 \end{bmatrix} \end{aligned} \tag{3.43}$$

$$\delta = \frac{f_0}{BW \cdot Q} \tag{3.44}$$

The lossy filter characteristics that maintain the lossless selectivity are given in (3.45). For this lossy response, the roots of polynomial P' are shifted to the left from the original positions. As a result, the synthesized network will not give perfect transmission zeros. However, this will not have severe effect on the passband insertion loss. For this case, the polynomial E_x of the lossy response can be found directly by shifting the roots of the conjugate of the polynomial E to the left by 2δ as in (3.46).

$$\begin{aligned} E(s)' &= E^0(s) \\ P(s)' &= k_{21} \cdot P^0(s+\delta) \end{aligned} \tag{3.45}$$

$$E_x(s) = (-1)^N E^0(s)^*\Big|_{s\to s+2\delta} \tag{3.46}$$

Substituting the parameters defined in (3.45) into the general condition in (3.18), we have (3.47) with which polynomials F_{11} and F_{22} can be solved. Then CM can be synthesized from the admittance polynomials with the S to Y transformation given in (3.39) and the result has equal dissipations on resonators.

$$F_{11}(s)'\cdot F_{22}(s)' = E^0(s)\cdot E_x(s) + k_{21}\cdot P^0(s+\delta)\cdot k_{21}\cdot P^0(s+\delta) \tag{3.47}$$

(3.47) could be transformed back to a lossless case by shifting the roots of each polynomial to the right by δ as in (3.48). And it is equivalent to power conservation for lossless network due to the conditions in (3.49) for the complex conjugate pairs of characteristic polynomials.

$$F_{11}(s-\delta)\cdot F_{22}(s-\delta) = E^0(s-\delta)\cdot E_x(s-\delta) + k_{21}\cdot P^0(s)\cdot k_{21}\cdot P^0(s) \tag{3.48}$$

$$\begin{aligned} F_{22}(s)' &= F_{11}(s)'^*\Big|_{s\to s+2\delta} \\ \left(E^0(s-\delta)\right)^* &= \left(\prod\left(s-\left(r_{ei}+\delta\right)\right)\right)^* \\ &= \prod\left(-s-\left(r_{ei}{}^*+\delta\right)\right) = (-1)^N\prod\left(s+r_{ei}{}^*+\delta\right) \\ &= E^0(s)^*\Big|_{s\to s+\delta} = E_x(s-\delta) \end{aligned} \tag{3.49}$$

The example for lossy synthesis given in section 3.3 is used here to illustrate the synthesis procedures. δ is set to be -0.015 which is equivalent to a Q_u of 1100 with a centre frequency of 2 GHz and bandwidth of 0.12 GHz. k_{21} is set to be 0.8.

Table 3.5 Polynomial for the 4th order example

E'	*P'*	*F11'*	*F22'*	*Ex*
-0.7034 + 1.3183i	-0.0150 - 0.600i	-0.5186 + 1.1560i	0.4886 + 1.1560i	0.6734 + 1.3183i
-0.9291 - 0.0812i	-0.0150 - 0.200i	-0.7303 - 0.0313i	0.7003 - 0.0313i	0.8991 - 0.0812i
-0.1248 - 1.0961i	-0.0150 - 0.700i	-0.0884 - 1.0470i	0.0584 - 1.0470i	0.0948 - 1.0961i
-0.4608 - 0.8483i		-0.3703 - 0.7850i	0.3403 - 0.7850i	0.4308 - 0.8483i

First, polynomials E', E_x and P' derived using (3.45) and (3.46) are listed in Table 3.5. The multiplication of F_{11}' and F_{22}' could then be found using (3.48) and the roots on the left hand side of the complex plane are assigned to F_{11}'. The roots distribution is shown in Fig. 3.7 compared to the ones of the original general Chebyshev function. We can see the roots of E are kept at the same position. The roots of *P* are shifted to the left uniformly by a constant δ and the roots of F_{11} are now complex.

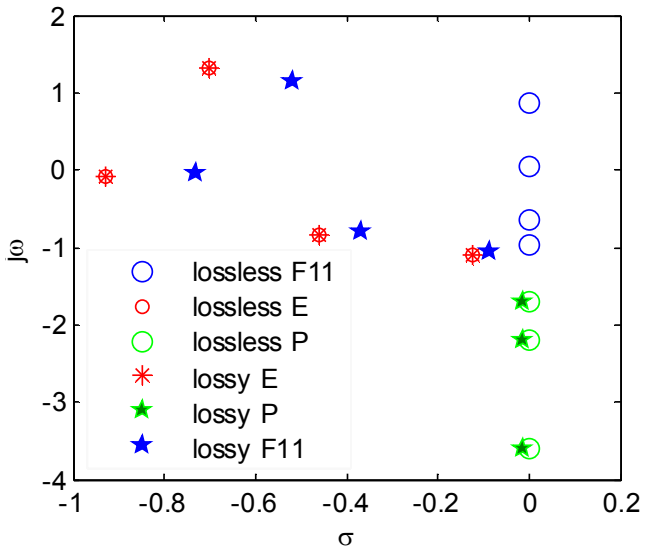

Fig. 3.7 Roots distribution of the 4th lossy network with uniform loss compared to the lossless ones.

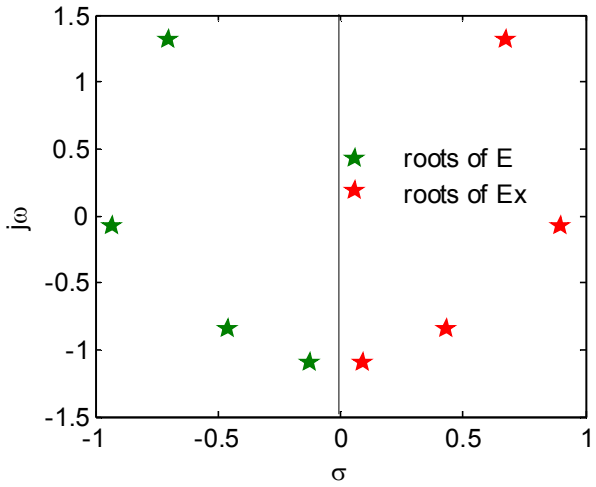

Fig. 3.8 Roots distribution for polynomials E and E_x.

The root distributions for E and E_x are compared in Fig. 3.8. For lossless cases, they form complex conjugate pair and are symmetrical regarding the imaginary axis. The uniform losses included in the networks shift the symmetrical axis to the left by a constant δ. CM synthesized using the

polynomials in Table 3.5 are shown in Table 3.6 and the response of the lossy CM is compared to the lossless ones in Fig. 3.9. This method gives a lossy filter network which is the same as one given by predistortion except that we give a lossy network with dissipation at each resonator directly.

Table 3.6 Synthesized lossy CM.

	-0.5053				
-0.5053	-0.2562 - 0.0150i	-0.8464		-0.4143	0.0873
	-0.8464	0.0679 - 0.0150i	0.2310	-0.9313	
		0.2310	0.9841 - 0.0150i	0.7653	
	-0.4143	-0.9313	0.7653	-0.0886 - 0.0150i	1.3767
	0.0873			1.3767	

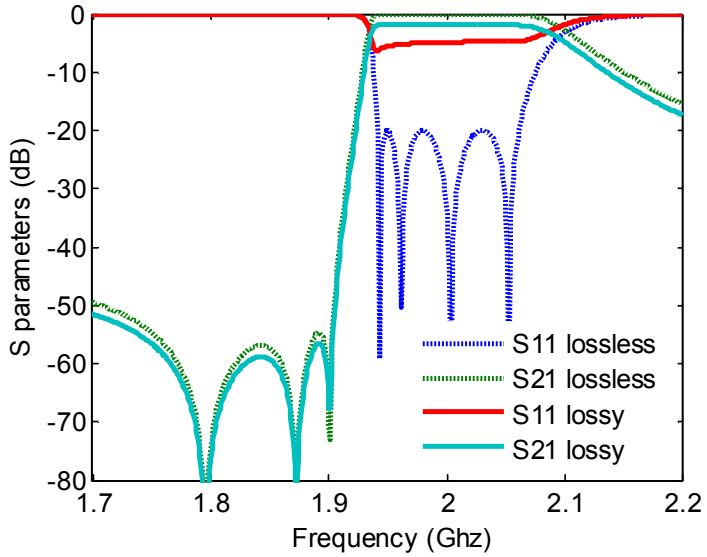

Fig. 3.9 Response of the 4th lossy network with uniform loss compared to the lossless ones.

This method of analysis explains why that for filters with transmission zeros, only the poles of the transfer function can be predistorted as in [54]. For a retrospective network, the numerator of S_{21} must be the same as the numerator of S_{12}. Assuming that we still have the perfect transmission zeros in the lossy network as in (3.50), when they are transformed to the lossless ones, we will have (3.51) which is contradicting to the power conservation

due to (3.52). As a result, the predistorted lossy network cannot have perfect transmission zeros.

$$F_{11}(s)\cdot F_{22}(s)=E^0(s)\cdot E_x(s)+k\cdot P^0(s)\cdot k\cdot P^0(s) \tag{3.50}$$

$$F_{11}(s-\delta)\cdot F_{22}(s-\delta)=E^0(s-\delta)\cdot E_x(s-\delta)+k\cdot P^0(s-\delta)\cdot k\cdot P^0(s-\delta) \tag{3.51}$$

$$P^0(s-\delta)^*\neq P^0(s-\delta) \tag{3.52}$$

In [3], a method of adaptive predistortion is given which will result in a filter network with better return loss. The circuit is actually based on the new characteristic given in section 3.1 in which the roots of E polynomial are shifted to the right. When the new characteristics are used, its roots distribution is given in Fig. 3.10 and the response is shown in Fig. 3.11 comparing to the results of the earlier case.

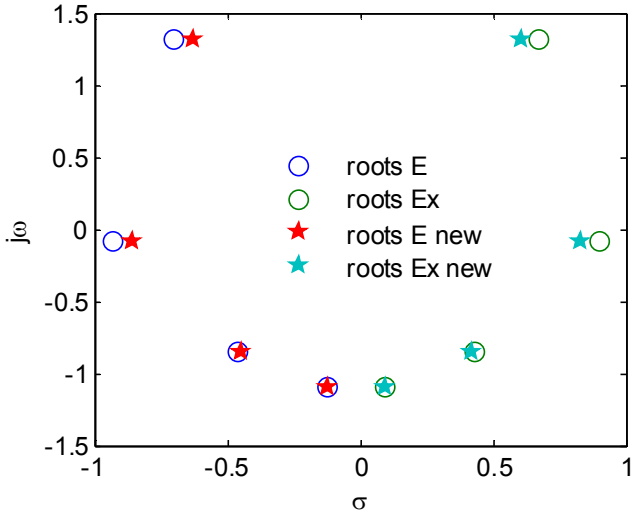

Fig. 3.10 Roots distribution of the 4th order lossy CM derived using the new characteristics comparing to the ones in Fig. 3.8.

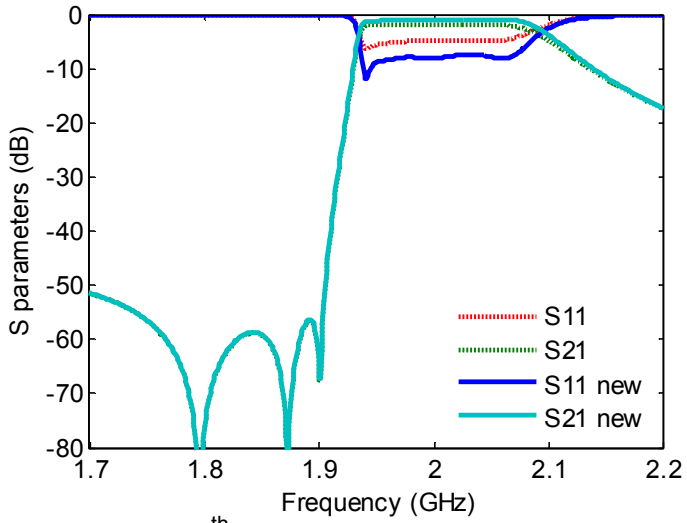

Fig. 3.11 Response of the 4th order lossy CM derived using the new characteristics.

3.4.2.2 Non-uniform losses

The method of lossy synthesis can also be applied for non-uniform Qs. In traditional method of predistortion, the loss factor δ which is used to modify the characteristic polynomials is also uniform and can be derived from resonator Q. When non-uniform Qs are applied, the effect of loss on filter characteristics is different. Loss factor δs are now non-uniform and have complex values. Comparing to (3.43), the inclusion of the non-uniform Q shifts the roots of admittance parameters as shown in (3.55), but the change of variable is no longer valid. As a result, two new parameters δ_{ei} and δ_{pi} are introduced to derive the lossy responses from the lossless ones as shown in (3.54) where r_{ei}' and r_{pi}' represent the roots of the lossless polynomials E and P.

$$[Y]=\sum_{k=1}^{N}\frac{1}{sC_k-\left(-jB_k-\delta_k\right)}\begin{bmatrix} M_{Sk}^2 & M_{Sk}M_{Lk} \\ M_{Sk}M_{Lk} & M_{Lk}^2 \end{bmatrix} \tag{3.53}$$

$$\begin{aligned} E'(s)&=\prod\left(s-r_{ei}'+\delta_{ei}\right) \\ P'(s)&=k_{21}\prod\left(s-r_{pi}'+\delta_{pi}\right) \end{aligned} \tag{3.54}$$

These complex loss factors δ_{ei} and δ_{pi} should be found first. In lossy synthesis, the lossy polynomial *E*' should be the same as the original lossless polynomial derived by Chebyshev characteristics as shown in (3.55) where r_{ei} and r_{pi} are the poles and zeros of the original Chebyshev transfer function. When a lossy CM is given, its characteristic polynomials can be found by curve fittings. The values of δ_{ei} and δ_{pi} can then be found by comparing the roots of the lossy and lossless characteristic polynomials.

$$\begin{aligned} E(s)'&=\prod\left(s-r_{ei}\right) \\ P(s)'&=k_{21}\prod\left(s-r_{pi}+\delta_{pi}\right) \end{aligned} \tag{3.55}$$

With δ_{ei}, the polynomial E_x for lossy case can be found according to(3.56). Then the synthesis process follows the same as in the case of uniform Q. Polynomials F_{11} and F_{22} can be solved according to (3.47) and then lossy CM can be derived using the admittance parameters from (3.39).

$$E_x(s)=-\prod\left(s-\left(-r_{ei}^*+2\,\mathrm{Re}(\delta_{ei})-2\,\mathrm{Im}(\delta_{ei})\right)\right) \tag{3.56}$$

The 4th order example given earlier is used here as an example. The original CM is given in Table 3.7. A Q distribution of 300, 1000, 1000 and 300 with centre frequency of 2 GHz and bandwidth of 0.12 GHz is assumed. And the

corresponding lossy CM is given in Table 3.8 by including imaginary parts from the Qs given.

Table 3.7 the original CM of the 4th order example.

	-1.0531				
-1.0531	-0.1462	-0.9303		-0.3307	0.0523
	-0.9303	0.1117	0.3232	-0.6566	
		0.3232	0.8550	0.6112	
	-0.3307	-0.6566	0.6112	-0.1133	1.0518
	0.0523			1.0518	

Table 3.8 The lossy CM of the 4th order example with non-uniform losses as imaginary parts of the diagonal elements.

	-1.0531				
-1.0531	-0.1462-0.0556j	-0.9303		-0.3307	0.0523
	-0.9303	0.1117-0.0167j	0.3232	-0.6566	
		0.3232	0.8550-0.0167j	0.6112	
	-0.3307	-0.6566	0.6112	-0.1133-0.0556j	1.0518
	0.0523			1.0518	

The lossy characteristics are found by rational polynomial fitting of the response of CM. The values of δ_{ei} and δ_{pi} could be found by comparing the roots of the fitted characteristic polynomials with the lossless ones and are given in Table 3.9.

Table 3.9 Roots of E and P of the lossy characteristic.

r_{ei} (roots of lossless E)	-0.7034 + 1.3183i	-0.9291 - 0.0812i	-0.1248 - 1.0961i	-0.4608 - 0.8483i
r_{ei}'(roots of lossy E)	-0.7448 + 1.3082i	-0.9843 - 0.0863i	-0.1418 - 1.0910i	-0.4916 - 0.8383i
r_{pi}(roots of lossless P)	- 3.6000i	- 2.2000i	- 1.7000i	
r_{pi}'(roots of lossy P)	-0.1531 - 3.6107i	0.1282 - 2.1994i	-0.0639 - 1.6899i	
δ_{ei}	-0.0413-0.0101i	-0.0552-0.0051i	-0.0170 +0.0051i	-0.0309 +0.0101i
δ_{pi}	-0.1531-0.0107i	0.1282+0.0006i	-0.0639 +0.0101i	

With the values of δ_{ei}, polynomial E_x can be found according to (3.56). The roots of E and E_x are shown in Fig. 3.12 comparing to the lossless ones. Then lossy CM with non-uniform Q can be derived using those polynomials and is given in Table 3.10. The loss distribution of the synthesized CM is not the same as the prescribed one because the CM used to calculate the values of δ_{ei} and δ_{pi} are the original lossless one. A method of iteration can be applied in which the newly calculated CM is used to find the values of δ_{ei} and δ_{pi}.

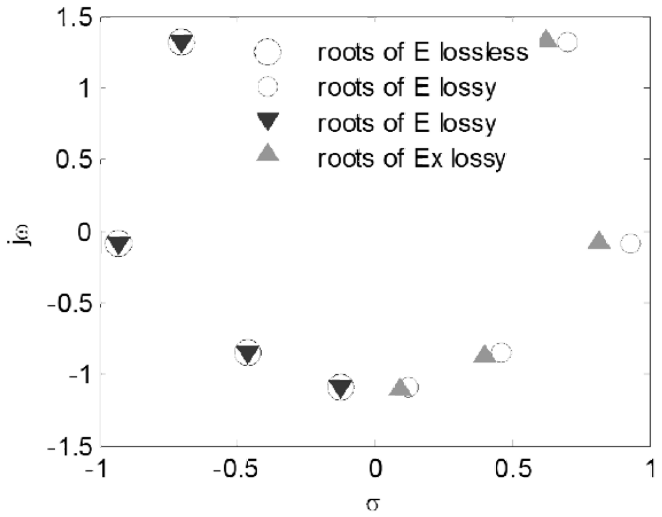

Fig. 3.12 Roots of polynomials E and E_x comparing to the lossless ones.

Table 3.10 Roots of E and P of the lossy characteristic.

	0.7631 - 0.0384i				
0.7631 - 0.0384i	-0.1212 - 0.1392i	-0.8629 + 0.0333i		-0.3548 - 0.0065i	0.0648 + 0.0033i
	-0.8629 + 0.0333i	0.0607 - 0.0206i	0.2845 - 0.0261i	-0.7764 - 0.0404i	
		0.2845 - 0.0261i	0.8963 + 0.0363i	0.6934 + 0.0049i	
	-0.3548 - 0.0065i	-0.7764 - 0.0404i	0.6934 + 0.0049i	-0.1284 - 0.0210i	1.2203 + 0.0239i
	0.0648 + 0.0033i			1.2203 + 0.0239i	

The lossy response after 10th iteration is compared to the lossless one in Fig. 3.13(a) and in Fig. 3.13(b), the lossy response is compared to the one when Q is directly applied to the original matrix.

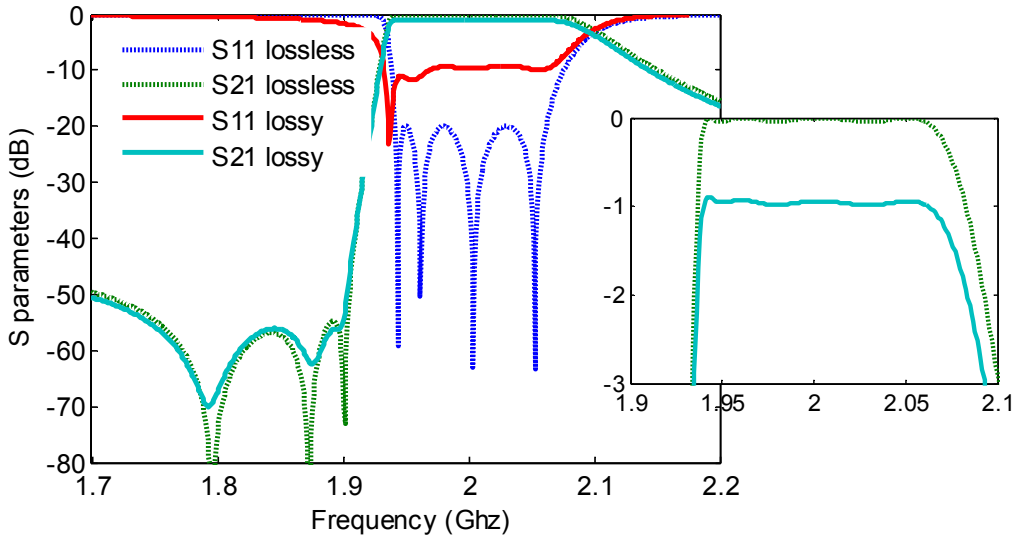

(a)

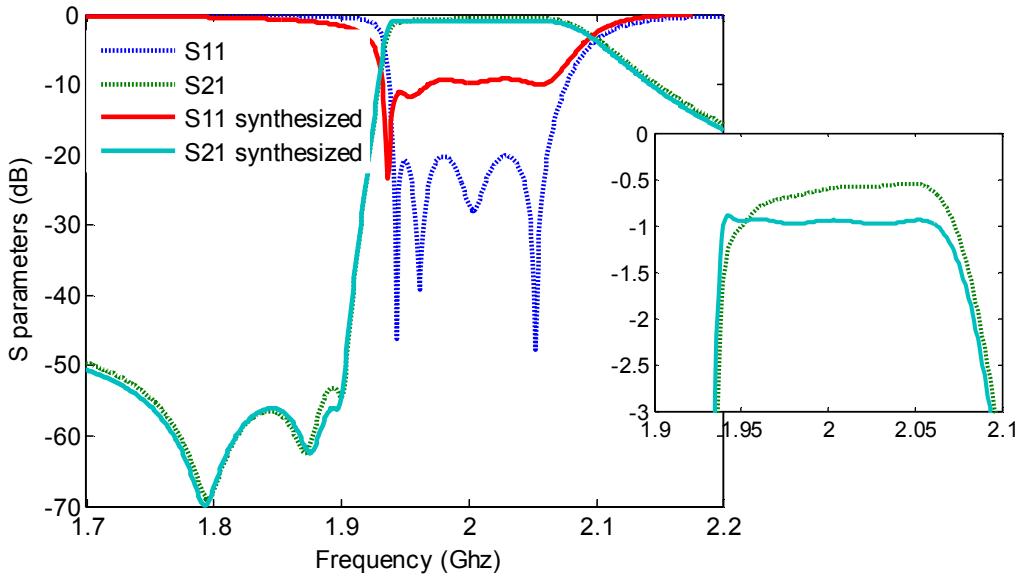

(b)

Fig. 3.13 Response of the 4[th] order example with non-uniform loss distribution (a) comparing to the lossless ones and (b) comparing to the ones when loss is applied directly to the original CM.

According to (3.55), the corresponding lossless polynomials E and P can be found as in (3.57) where r_{ei} and r_{pi} are the poles and zeros of the original Chebyshev transfer function. For these lossless functions, the polynomials F_{11} and F_{22} can be found by power conservations using E and P and a predistorted lossless CM could be synthesized.

The CM synthesis procedures can also be taken for a set of lossless polynomials. The roots of the predistorted lossless polynomial E are equal to $(r_{ei} - \delta_{ei})$. The predistorted lossless polynomial P must be the same as the

original one as discussed earlier. Then the polynomial F_{11} could be found by power conservation. The polynomials are listed in Table 3.11 with which the lossless synthesis can be applied.

$$\begin{aligned} E(s) &= \prod (s - r_{ei} - \delta_{ei}) \\ P(s) &= k_{21} \prod (s - r_{pi}) \\ k_{21} &= 1 \Big/ \max \left| \prod (s - r_{pi}) \Big/ \prod (s - r_{ei} - \delta_{ei}) \right| \end{aligned} \tag{3.57}$$

Table 3.11 Predistorted lossless polynomials.

s^i , i=	4	3	2	1	0
Predistorted E	1	2.0737 + 0.7073i	3.0606 + 1.7921i	1.8696 + 2.7298i	0.0175 + 1.3830i
Predistorted Ex	-1	2.0737 - 0.7073i	-3.0606 + 1.7921i	1.8696 - 2.7298i	-0.0175 + 1.3830i
Predistorted P	0	0.0940	0.7051i	-1.6714	- 1.2657i
Predistorted F_{11}	1	-0.4456 + 0.7127i	1.0159 + 0.3402i	-1.2507 + 0.3784i	0.3427 - 0.4436i

The procedure for non-uniform lossy synthesis given earlier contains an approximation that the loss factors derived from the lossy characteristics based on the original CM is the same as loss factors derived from responses based on the predistorted CM. The result of this approximation is that the final lossy E' is not exact the same as the Chebyshev polynomial. This problem will be discussed with more details and be solved in the next section.

3.4.3 Iterations on polynomial E_x

The problem is to synthesize a lossy CM with prescribed P' and E' for lossy responses. As discussed earlier, for uniform resonator Q, loss factor δ derived from Q is the same as the amount by which the variable s is shifted and is used directly to the modification of characteristic polynomials. With non-uniform Qs, δ_{ei} and δ_{pi} by which the roots of polynomials E and P are shifted need to be found first by curve fittings. For the synthesis method presented here, a procedure of iteration is employed, so that the polynomial P' and E_x are updated according to the response of a lossy CM.

The initial values of P' and E_x are chosen to be the lossless ones. In each iteration, they denoted as E_{xi} and P_i.

First, the polynomial for F_{11i} and F_{22i} are derived using E_{xi}, P_i and E according to (3.18). The zeros of F_{11i} and F_{22i} no longer lie on the imaginary axis as in the lossless case. Then, a lossy CM M_t is found using the characteristic polynomials.

Next, a new lossy CM M_i is defined by adding the prescribed loss distribution to the real part of M_t in which δ is an imaginary matrix with its diagonal elements representing the dissipation of each resonator and the off-diagonal ones representing the losses of invertors. Then, the new polynomials E_{xi+1} and P_{i+1} can be found by the method given in the section 3.4.1 from this lossy network M_i.

Finally, this procedure is applied iteratively until the losses of the synthesized CM are the same as the prescribed ones under a degree of precision. The loss distribution will converge to the prescribed one after about 30 iterations.

The procedure of iteration is given as follows:

1). The initial values for E_{xi} and P_i are equivalent to the ones in the lossless case.

2). Derive F_{11i} and F_{22i} using E_{xi}, P_i and E using (3.19)

3). Synthesize lossy CM M_t

4). Derive E_{xi+1} and E_{xi+1} from lossy M_i which is equivalent to $Re(M_t)+\delta$.

5). go back to 3) if the imaginary part of M_t is not close enough to δ.

The example here is the synthesis of CM of a 4th order general Chebyshev filter with three transmission zeros at -1.7j, -2.2j and -3.6j in the lowpass domain. Giving the centre frequency and bandwidth of 2 GHz and 0.12 GHz, Qs of 500, 2000, 2000 and 500 of the ladder network is given which corresponds to loss factors of 0.0333, 0.0080, 0.0080 and 0.0333.

The polynomials P, F and E of the lossless network are synthesized using the method given in [9]. For the lossy responses, E_{x0} is the complex conjugate of E. P_0 equals to P multiplied by a constant 0.91 and E' equals to E. Then F_{11i} and F_{22i} are derived. These polynomials are listed in Table 3.16. With these polynomials, M_t can be synthesized and is shown in Table 3.13.

Table 3.12 Coefficients of polynomials used in the first iteration.

	s^0	s^1	s^2	s^3	s^4
E'	0.0500 + 1.4834i	2.0477 + 2.8717i	3.2498 + 1.8931i	2.2182 + 0.7073i	1
P_0	- 1.3504i	-1.7833	0.7522i	0.1003	
E_{x0}	0.0500 - 1.4834i	-2.0477 + 2.8717i	3.2498 - 1.8931i	-2.2182 + 0.7073i	1
F_{11_0}	0.0768 + 0.6111i	0.9751 + 1.4311i	1.8930 + 1.1629i	1.4821 + 0.7073i	1
F_{22_0}	0.0768 - 0.6111i	-0.9751 + 1.4311i	1.8930 - 1.1629i	-0.9751 + 1.4311i	1

Table 3.13 CM M_t synthesized in the first iteration.

	-0.6067				
-0.6067	-0.2847	-0.8214		-0.3962	0.0827
	-0.8214	0.0736	0.2300	-0.9138	
		0.2300	0.9882	0.7537	
	-0.3962	-0.9138	0.7537	-0.0697	1.3577
	0.0827			1.3577	

Then as in the 4) step, the matrix $Re(M_t)+\delta$ is transformed to a transversal array using the Jacobi eigenvalue algorithm as discussed in section 3.4.1. The transversal array is shown in Table 3.14. Then the polynomials of the admittance parameters can be found by a reverse of partial expansion and the polynomial Y_x can be derived according to (3.40). The polynomials of the admittance parameters are listed in Table 3.15. Then the polynomials E_{x1} and P_1 updated using the Y to S transformation in (3.42) and a new round of iteration can be applied.

Table 3.14 Transversal array derived in the first iteration.

	-0.4433 - 0.0010i	0.2651 - 0.0033i	0.0139 + 0.0002i	-0.3179 - 0.0014i	
-0.4433 - 0.0010i	-0.0284 - 0.0293i				-0.6887 - 0.0031i
0.2651 - 0.0033i		0.9456 - 0.0148i			-0.3873 - 0.0050i
0.0139 + 0.0002i			1.4322 - 0.0157i		0.7360 - 0.0084i
-0.3179 - 0.0014i				-1.6421 - 0.0235i	0.8272 + 0.0025i
	-0.6887 - 0.0031i	-0.3873 - 0.0050i	0.7360 - 0.0084i	0.8272 + 0.0025i	

Table 3.15 Coefficients of the admittance parameters.

	s^0	s^1	s^2	s^3	s^4
Y_d	0.0641 + 0.0644i	0.1032 + 2.1529i	2.5737 + 0.0619i	0.0833 + 0.7073i	1
Y_{11n}	0.0043 + 0.4363i	0.5365 + 0.0159i	0.0184 + 0.3651i	0.3680	0
Y_{21n}	0.0075 + 0.6752i	0.8916 - 0.0076i	-0.0025 - 0.3761i	-0.0501	0
Y_{22n}	0.0117 + 1.0478i	1.5126 + 0.0746i	0.0925 + 1.5280i	1.8501	0
Y_x	-0.0134 + 0.0060i	0.0113 + 0.7203i	1.8930 - 1.1629i	0	0

The result will converge after about 15 iterations. Expressions for E_{xi} and P_i in last iteration are shown in Table 3.16. The lossy CM is shown in Table 3.17.

Table 3.16 Coefficients of polynomials used in the iterations.

	s0	s1	s2	*s3*	*s4*
P_n	0.0148 + 1.3497i	1.7822 - 0.0150i	-0.0050 - 0.7519i	-0.1002	
E_{xn}	0.0165 - 1.3549i	-1.8319 + 2.7055	3.0363 - 1.7732i	-2.0515 + 0.7073i	1
F_{11n}	0.0215 + 0.4885i	0.7029 + 1.2333i	1.5753 + 1.0164i	1.2227 + 0.7073i	1
F_{22n}	0.0105 - 0.3867i	-0.5413 + 1.1453i	1.4614 - 0.8965i	-1.0560 + 0.7073i	1

Table 3.17 CM M_t in the last Iteration

	-0.7054				
-0.7054	-0.1737 - 0.0336i	-0.8467		-0.3682	0.0710
	-0.8467	0.0685 - 0.0083i	0.2706	-0.8267	
		0.2706	0.9161 - 0.0082i	0.7262	
	-0.3682	-0.8267	0.7262	-0.1035 - 0.0333i	1.2776
	0.0710			1.2776	

The root distributions for lossless and lossy *P* and *F* in the complex plane are shown in Fig. 3.14. The response of the synthesized lossy network is shown in Fig. 3.15 as the solid lines and is compared with the lossless ones as the dash lines.

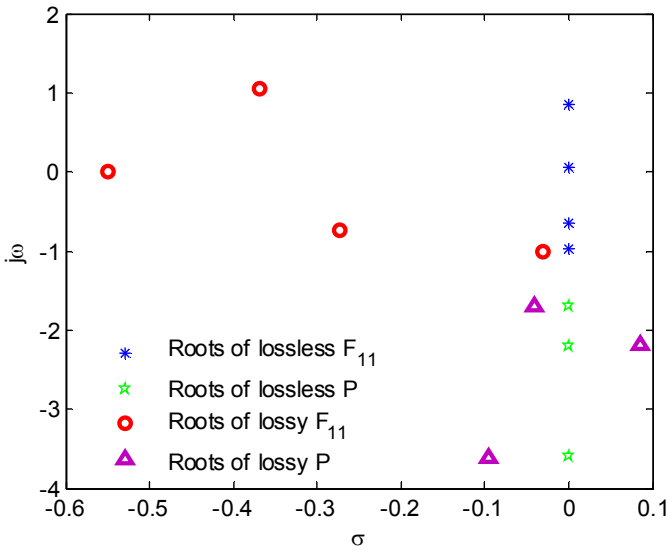

Fig. 3.14 Roots distribution of the 4th order example with non-uniform loss.

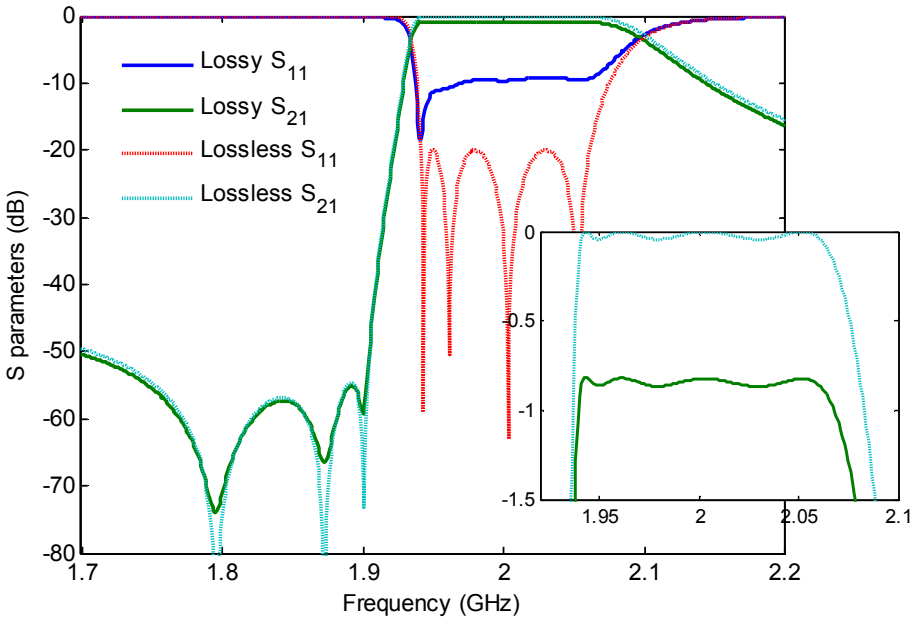

Fig. 3.15 Response of the 4th order example with non-uniform loss compared to the lossless ones.

3.4.4 Relations to the method of predistortion

In the method of predistortion, the effect of loss is compensated by designing a lossless network with the roots of its E polynomial shifted to the left in the complex plane by a constant. This network can also be solved by the lossy synthesis method given in this section.

The roots of polynomial E_x are shifted to the left by 2δ as in (3.58). Polynomials F_{11} and F_{22} can be solved according to (3.59) in which a lossy

polynomial P is used with its roots shifted from the original positions. Then by shifting the roots of the polynomials in (3.59) to the right by δ, the equation can be transformed to a lossless one which is consistent with the power conservation. This also proves that for this kind of lossy network, perfect transmission zeros which are purely imaginary can be realized

$$E_x(s) = (-1)^N E(s)^*\Big|_{s \to s+2\delta} \tag{3.58}$$

$$\begin{aligned} &F_{11}(s)' \cdot F_{22}(s)' = \\ &E(s) \cdot E_x(s) + k_{21} \cdot P(s+\delta) \cdot k_{21} \cdot P(s+\delta) \end{aligned} \tag{3.59}$$

For the resonators of non-uniform dissipation, the loss factor δ for each resonator is also non-uniform and may have complex values. However, the same procedures of designing lossy networks can be applied. The lossy polynomials given in (3.60) in which δ_{ei} and δ_{pi} represent the modifications made to the roots of polynomial E and P respectively.

$$\begin{aligned} E'(s) &= \prod (s - r_{ei} + \delta_{ei}) \\ P'(s) &= k_{21} \prod (s - r_{pi} + \delta_{pi}) \end{aligned} \tag{3.60}$$

For the CM synthesized according to the above procedures, the dissipation distribution may not be the exactly same as the required ones. The reason is that the values of δ_{ex} used don't correspond to the synthesized lossy CM. This problem can be solved using the following iteration.

The initial value is the lossless CM M_0 derived by traditional synthesis method.

1). Find the values of δ_{ex} by comparing the response of the lossless CM M_i and the one with prescribed loss.

2) Derive the polynomials $F_{11'}$ and $F_{22'}$ using (3.59).

3) Derive the complex predistorted CM M_{i+1}.

4) Go back to Step(1) using CM M_{i+1} until the loss distribution in M_{i+1} is the same as prescribed ones with a required precision.

3.4.5 Coupling matrix extraction from lossy response

In order to extract a CM based on simulated or measured data, it is important to the data is rationalized. In practice, filters have input and output

connecting sections which will introduce a phase loading effect [81] [82] that is not included in circuit models. As a result, the phase loading at input and output port should be determined and removed from the measured data before the extraction. The method given in [81] [82] provide a simple procedure for removing the phase loading. The method is based on the symmetry of the phase of S parameters in the frequency band far away from the center frequency. However, to most practical cases, it is difficult to measure the exact phase in that band and the existence of higher order mode make it impossible to retain the symmetry of phase.

A new method for removing the phase loading effect is given in this section. The method use data from the passband and is thus more reliable. For the filter response that can be modeled by a CM, its S parameters must satisfy the condition given in (3.8) and the admittance parameters must satisfy the condition given in (3.40). The first step is to remove φ_{21} so that (3.8) is maintained. The second step is to remove φ_{11} and φ_{22} so that the remaining term of partial expansion of Y can be zero.

3.5 Filter implementations

The method of lossy synthesis discussed in this chapter is capable for the synthesis of CM with any prescribed loss. Two examples of filter design are given in this section with the use of both coaxial and dielectric resonators and that requires the synthesis of CM with non-uniform Qu distributions.

3.5.1 Coaxial and dielectric resonators

Traditional design of coaxial resonator filter has the disadvantage of high loss. While the dielectric resonator has low loss, they are of poor spurious performance. The TM dielectric resonator discussed in [83] and [84] has higher Qu than coaxial resonators and when combined with coaxial resonators in the filter design, the spurious performance can also be improved [74].

The example is a 6^{th} degree filter with general Chebyshev response. The filter is symmetric with four transmission zeros at *1.6j, -1.6j, 2.4j* and *-2.4j* in the lowpass domain. The centre frequency is 2 GHz and the bandwidth is

0.12 GHz. The filter is realized by two coaxial resonators at the input and output with Q_u of 3200 and four *TM01* dielectric resonators with Q_u of 2500.

Design Step 1 CM synthesis for the lowpass prototype.

The original and designed CMs are compared in Table 3.18.

Table 3.18 CM M_t in the First and Last Iterations

M_{S1}	0.9957	M_{56}	0.8309	M_{S1}	0.6608	M_{56}	1.0458
M_{12}	0.8309	M_{6L}	0.9957	M_{12}	0.7055	M_{6L}	1.2272
M_{23}	0.5823	M_{25}	-0.1521	M_{23}	0.5548	M_{25}	-0.1595
M_{34}	0.6971	M_{16}	0.0147	M_{34}	0.7067	M_{16}	0.0174
M_{45}	0.5823			M_{45}	0.6353		

Design Step 2 Resonator design

The TM dielectric resonator to be used in the design has a diameter of 7.7 mm and height of 36.1 mm. The dielectric constant is 37. In the original design, this resonator is put into a relatively large cavity with a size of 40mm*50mm*50mm and is of low loss. The eigenmode analysis in HFSS shows the first mode has a frequency of 2.158GHz and a Qu of 122457.

In order to reduce the size of the designed filter, a smaller cavity with the dimension of 44mm*25mm*25mm is used. With the deduction in the cavity size, the resonant frequency is increased. To obtain a center frequency at 2 GHz, a cap is included in the design as shown in Fig.3.16. This will also deduce the Qu of the resonator. The new eigenmode has a frequency of 2.031GHz and a Qu of 2495.

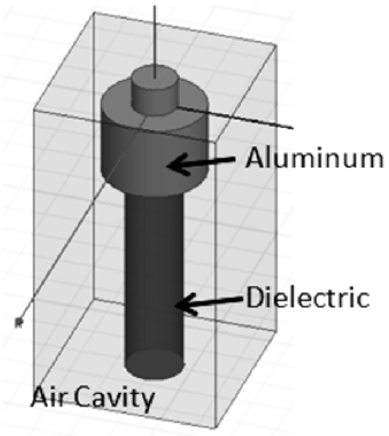

Fig. 3.16 EM model for the size reduction design.

The design of the coaxial resonator is relatively simple as shown in Fig.3.17. The first eigenmode has a resonant frequency of 2.019GHa and a Qu of 3280.

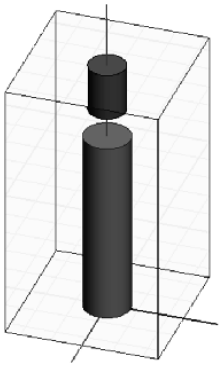

Fig. 3.17 Eigenmode (a) and EM design (b) of coaxial resonator.

Design Step 3 Design of couplings

In order to design the couplings, a 3rd order example is built first. The input/output nodes are realized by coaxial resonators and the input/output couplings are realized by probe connecting at the coaxial resonators. Couplings between resonators are realized by windows. CM extraction is applied to the simulated response for the tuning. The EM model of the 3rd order example and its response is given in Fig. 3.18. Based on the tuning information, we could make a diagram on the coupling and dimensions.

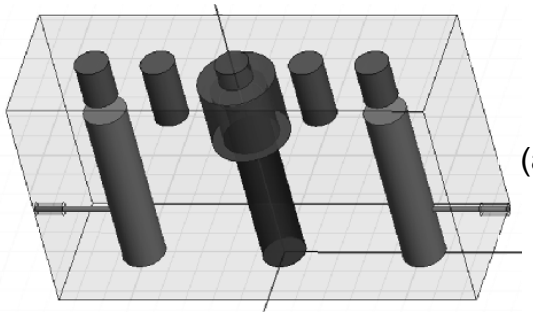

(a)

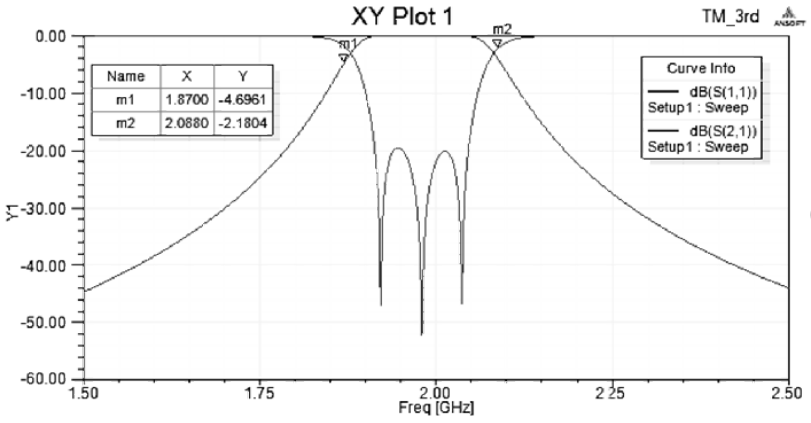

(b)

Fig. 3.18 3rd order mix mode filter and its response.

Transmission zeros are introduced into the structure by cross coupling between the first and fourth dielectric resonators. This is realized by a probe coupling as shown in Fig. 3.19 with simulated response.

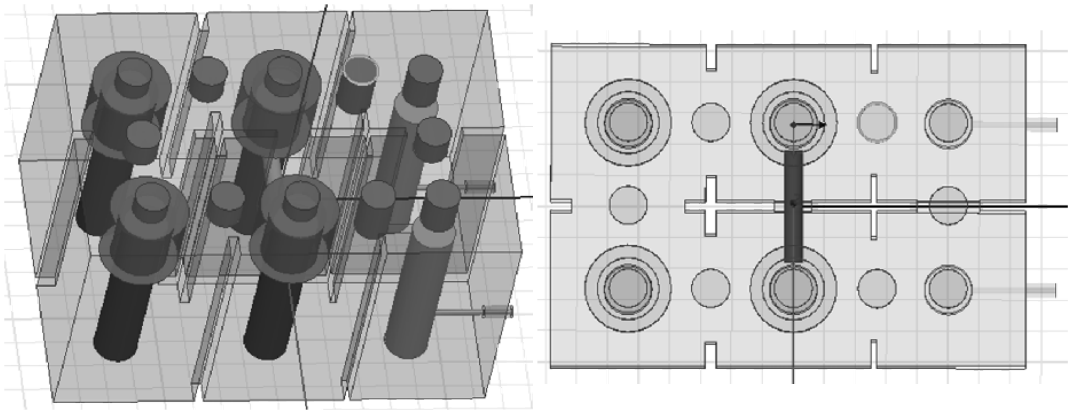

Fig. 3.19 6th order mix mode filter.

Design Step 4 Lossy design

Lossy is incorporated into the structure by modified boundary of finite conductance and replaced PEC with aluminium. Then tuning is applied by comparing the original CM and the lossy one. The response is given in Fig. 3.20.

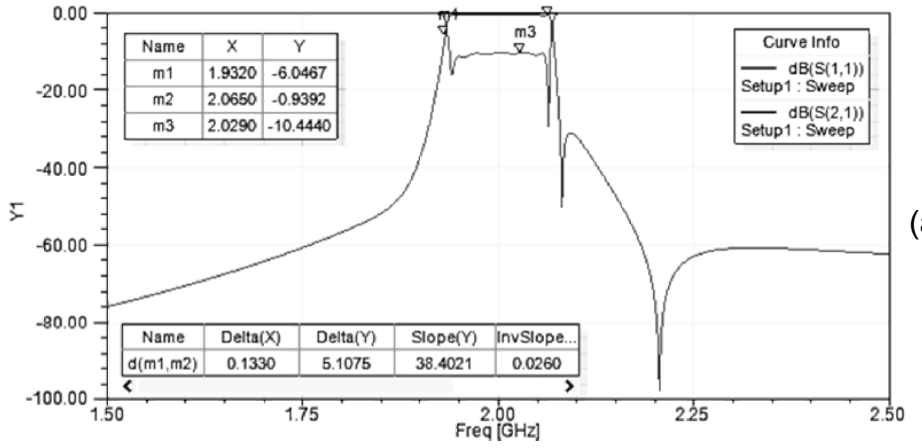

(a)

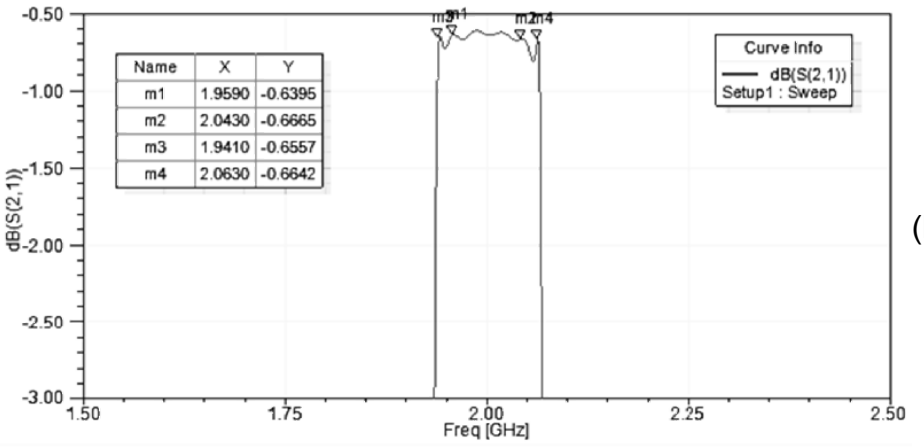

(b)

Fig. 3.20 Lossy 6th order mix mode filter and its response.

3.5.2 Coaxial and dual-mode dielectric resonators

To further reduce the size of the filter, dual mode dielectric resonators discussed in [85] and [86] can be used. The eigenmode of the coaxial resonator is 0.950 GHz with a Qu of 2483. The dielectric resonators have degenerated mode of 0.905 and 0.907 GHz with Qu of 5534 and 5497 respectively. The E and H field distribution for the two modes are given in Fig. 3.21 and Fig. 3.22.

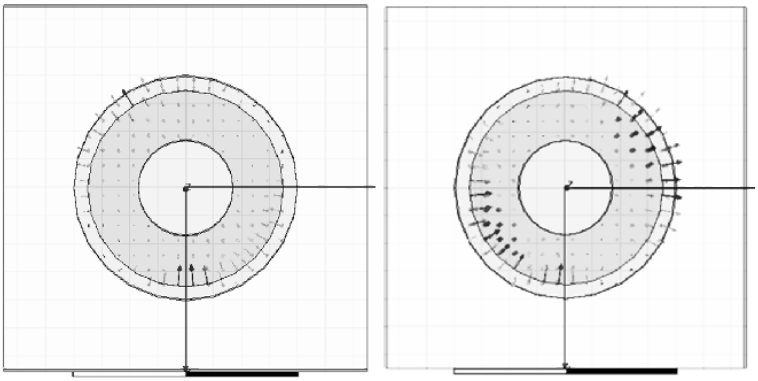

Fig. 3.21 E field distribution of the two degenerated modes.

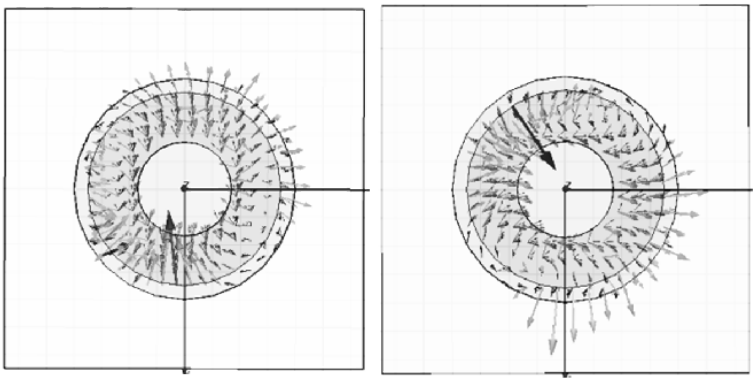

Fig. 3.22 H field distribution of the two degenerated modes.

The filter designed is of 4th order. The EM model is given in Fig. 3.23 and the response is given in Fig. 3.24. The transmission zeros are realized by spurious couplings between the two coaxial resonators.

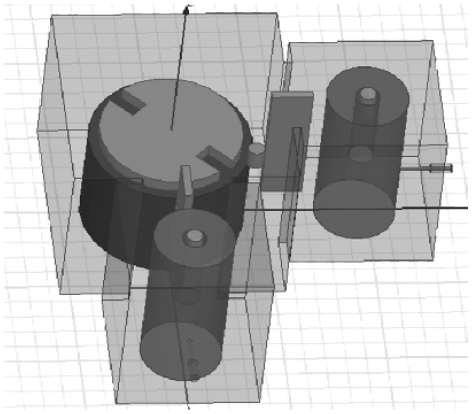

Fig. 3.23 EM model for the 4th order filter with dual mode dielectric resonator.

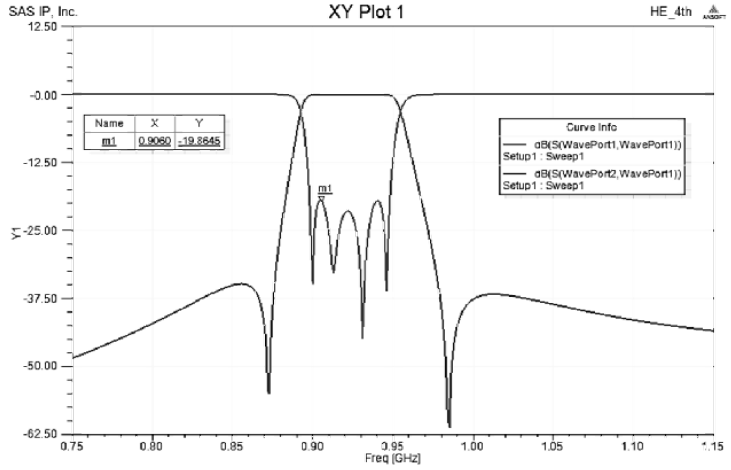

Fig. 3.24 Simulated response for the 4th order filter with dual mode dielectric resonator.

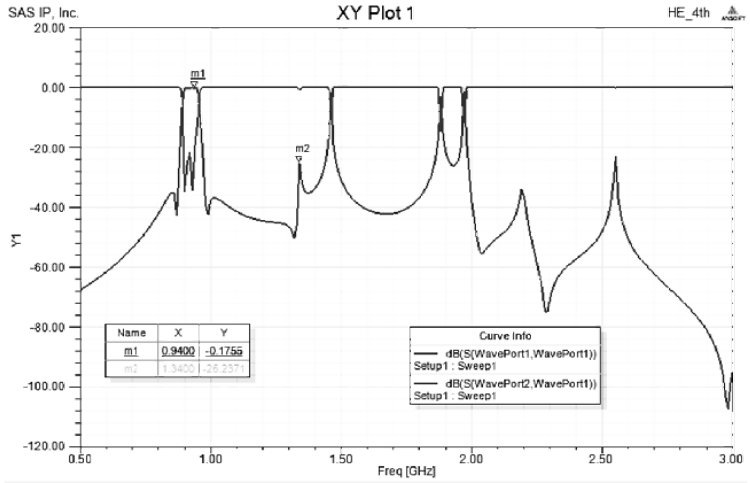

Fig. 3.25 Spurious response for the 4th order filter with dual mode dielectric resonator.

Chapter 4
Dissipations in Parallel Connected Filter Networks

The alternative approach studied in this paper is an extension on the method presented in [77][87] and it shows that it is possible to achieve a high Q performance using the correct non-uniform Q distribution. In a parallel connected network [8], each resonator represents a pole [87], as a result, each resonator Q has an independent effect on the filter response. It is shown that for resonators with smaller bandwidth and near bandedge resonant frequencies, the effect of loss is more severe than the others. As a result, these resonators are more critical in determining filter characteristics and have to be designed with high Q technologies, while the others can be designed with low Q resonators to reduce filter size and cost without deteriorating the performance.

With the first order approximation on the effect of loss of each resonator, the variation of the magnitude of S_{21} due to loss is a linear combination of the dissipation of each resonator. The Q distribution that gives a flat passband insertion loss can be derived analytically by solving a set of linear equations that enforces the insertion loss to be proportional to the lossless one at several given points. This method is suitable for the parallel connected networks with small loss.

For other cases, gradient based optimization introduced in [33] that is used for determining lossless CMs could be applied to find the Q distribution. The method presented in this paper utilizes a cost function that is defined not to get an ideal Chebyshev response but one with prescribed stopband rejection and passband insertion loss. A new lossy filter characteristic is given in this paper that is suitable to be realized by parallel connected networks with dissipations only at resonators. The variables used in the optimization are the components of a parallel connected network and the dissipation of each resonator.

The method can also be applied to configurations other than transversal arrays. Using CM rotations, transversal arrays can be transformed into other parallel connected networks by grouping the residues and poles [8]. An

example is given for the design of a 4th order filter which is then realized by a mixed coaxial and microstrip technology.

As a conclusion, it is possible to design a parallel connected filter network with unequal dissipations and have a high Q performance. Resonators with a smaller bandwidth and near band edge resonant frequency should be designed with lower loss, while the other resonators can be designed with higher loss without significantly deteriorating the performance.

4.1 The effect of loss in parallel connected networks

The traditional synthesis methods for lossy filter start with a given transfer function which is usually an ideal Chebyshev response multiplied by a constant smaller than 1, then the problem is to find a circuit to realize the response. The new approach provided in this section is based on a given lossless circuit.

Because in parallel connected networks, each resonator represents a global eigenmode, the effect of loss on each resonator is independent of each other. The effect of loss on a single resonator will be studied. Two issues arise in the design of filter with unequal Qs. First, while the existence of loss can cause the transmission to reduce, the amount of the reduction is related to the bandwidth of the resonator. A 2nd order parallel connected network is given as an example. It is shown that dissipation included in the resonator with larger bandwidth will have smaller effect on the total transmission. Second, for a higher order filter the position of the resonator frequency is also important for the total response. The resonators with resonant frequency near the bandedge have a lager effects on the rounding of insertion loss. For a circuit with order higher than 4, there are two narrow-band resonators controlling the shape of the transmission at band-edges. These two resonators have to be of high Q.

4.1.1 Loss distributions

The transversal array of a filter network is a direct representation for global eigenmode [88]. After rotations, these modes are mixed and combined. Unlike parallel connected networks, the resonators of other configurations

have indirect relations with the total characteristics. A simple 2nd order example is given to show how the loss is distributed when the network is transformed between the parallel and cascading configurations.

The CM of a 2nd order cascaded network and the pivot applied are given in (4.1). After the rotation, the CM is transformed into a parallel connect one network as in (4.2).

$$M=\begin{bmatrix} 0 & M_{s1} & 0 & 0 \\ M_{s1} & -j\delta_1 & M_{12} & 0 \\ 0 & M_{12} & -j\delta_2 & M_{2L} \\ 0 & 0 & M_{2L} & 0 \end{bmatrix} T=\begin{bmatrix} 1 & 0 & 0 & 0 \\ 0 & \frac{1}{\sqrt{2}} & \frac{1}{\sqrt{2}} & 0 \\ 0 & -\frac{1}{\sqrt{2}} & \frac{1}{\sqrt{2}} & 0 \\ 0 & 0 & 0 & 1 \end{bmatrix} \tag{4.1}$$

$$M=\begin{bmatrix} 0 & \frac{M_{s1}}{\sqrt{2}} & -\frac{M_{s1}}{\sqrt{2}} & 0 \\ \frac{M_{s1}}{\sqrt{2}} & M_{12}-\frac{j}{2}(\delta_1+\delta_2) & \frac{j}{2}(\delta_1-\delta_2) & \frac{M_{2L}}{\sqrt{2}} \\ -\frac{M_{s1}}{\sqrt{2}} & \frac{j}{2}(\delta_1-\delta_2) & -M_{12}-\frac{j}{2}(\delta_1+\delta_2) & \frac{M_{2L}}{\sqrt{2}} \\ 0 & \frac{M_{2L}}{\sqrt{2}} & \frac{M_{2L}}{\sqrt{2}} & 0 \end{bmatrix} \tag{4.2}$$

When $\delta_1 \neq \delta_2$, a lossy path between the global eigenmodes is introduced as in (4.2). When $\delta_1 = \delta_2$, the matrix is simplified to (4.3)and the Q of each resonator is not changed.

$$M=\begin{bmatrix} 0 & \frac{M_{s1}}{\sqrt{2}} & -\frac{M_{s1}}{\sqrt{2}} & 0 \\ \frac{M_{s1}}{\sqrt{2}} & M_{12}-j\delta_1 & 0 & \frac{M_{2L}}{\sqrt{2}} \\ -\frac{M_{s1}}{\sqrt{2}} & 0 & -M_{12}-j\delta_1 & \frac{M_{2L}}{\sqrt{2}} \\ 0 & \frac{M_{2L}}{\sqrt{2}} & \frac{M_{2L}}{\sqrt{2}} & 0 \end{bmatrix} \tag{4.3}$$

Similarly, for a parallel connected network of (4.4), the CM after rotations is given in (4.5). When $\delta_1 \neq \delta_2$, a lossy path between the two resonators is introduced. When $\delta_1 = \delta_2$, the Q of each resonator is not changed.

$$M=\begin{bmatrix} 0 & M_{s1} & -M_{s1} & 0 \\ M_{s1} & M_{11}-j\delta_1 & 0 & M_{2L} \\ -M_{s1} & 0 & M_{22}-j\delta_2 & M_{2L} \\ 0 & M_{2L} & M_{2L} & 0 \end{bmatrix} \tag{4.4}$$

$$M=\begin{bmatrix} 0 & \frac{2M_{s1}}{\sqrt{2}} & 0 & 0 \\ \frac{2M_{s1}}{\sqrt{2}} & -\frac{j}{2}\left(M_{11}+M_{22}+\delta_1+\delta_2\right) & -\frac{j}{2}\left(M_{11}-M_{22}+\delta_1-\delta_2\right) & 0 \\ 0 & -\frac{j}{2}\left(M_{11}-M_{22}+\delta_1-\delta_2\right) & -\frac{j}{2}\left(M_{11}+M_{22}+\delta_1+\delta_2\right) & \frac{2M_{2L}}{\sqrt{2}} \\ 0 & 0 & \frac{2M_{2L}}{\sqrt{2}} & 0 \end{bmatrix} \tag{4.5}$$

In general, for a parallel connected network, if the Qs are uniform, the transformed network will have the same Q and response. And thus is meaningless to tune the Q of each resonator. On the other hand, if the Qs are non-uniform, the circuit is equivalent to a lossless network with lossy resonators and couplings. Then it is possible to achieve a better response by a proper designed Q distribution.

4.1.2 The effect of loss on a single resonator

The admittance parameters of a parallel connected network are shown in (3.20) where r_k is a residue, λ_k is a pole and k_{21} is the value of the direct coupling between the input and output non-resonating nodes when the number of transmission zeros is the same as the filter order. Each term which provides a pole of the admittance parameters can be realized by a resonator and is a direct representation of one global eigenmode [88]. This is not the case for conventional cross-coupled ladder networks.

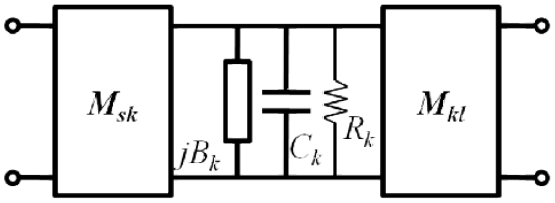

Fig. 4.1 Circuit model of a single lossy resonator.

As shown in [8], each term of the admittance parameters can be realized by a resonator. Fig. 4.1 shows the circuit model of a lossy resonator with one capacitor C_k, one frequency invariant reactance jB_k, one resistance δ_k and two invertors M_k. δ_k represents the dissipation of this resonator. The filter synthesized is a parallel connection of N single resonators with uniform capacitors.

The transmission parameter of the resonator in Fig. 4.1 is given in (4.6) with a unit capacitor and symmetric invertors. It is shown in (4.6) that the effect of

δ_k on the insertion loss is related to the magnitude of the corresponding residue, which is related to the bandwidth of the resonator. While the existence of loss can reduce the transmission, the amount of the reduction depends on the bandwidth of the resonator. As a result, dissipations included in the resonators with larger bandwidth will have smaller effects on the performance.

$$\begin{aligned} S_{11} &= \frac{-M_{sk}^2 + M_{Lk}^2 + x}{M_{sk}^2 + M_{Lk}^2 + x} = \frac{x}{2r_{11} + x} \\ S_{21} &= \frac{-2M_{sk}M_{Lk}}{M_{sk}^2 + M_{Lk}^2 + x} = \frac{-2r_{21k}}{2r_{11k} + x} \\ x &= j\omega C_k + jB_k + \delta_k = j\omega - j\lambda_k + \delta_k \end{aligned} \tag{4.6}$$

For a single resonator, the effect of loss on transmission is related to the bandwidth. As a result, the transmission of a transversal array must depend on the Qu distribution regarding the bandwidth of each branch.

A new kind of Maximum Flat filter is given in the following as an example with synthesis procedures. Resonators of this filter have a large bandwidth variation. The transfer function shown in (4.7) is maximum flat at $\omega = -1$ and has N transmission zeros at $\omega = 1$.

$$|S_{21}(s)|^2 = \frac{1}{1 + \left(\frac{1+\omega}{1-\omega}\right)^{2N}} \tag{4.7}$$

According to power conservation, we have the return loss in (4.8).

$$\begin{aligned} |S_{21}(s)|^2 &= \frac{(1-\omega)^{2N}}{(1-\omega)^{2N} + (1+\omega)^{2N}} \\ |S_{11}(s)|^2 &= \frac{(1+\omega)^{2N}}{(1-\omega)^{2N} + (1+\omega)^{2N}} \end{aligned} \tag{4.8}$$

Polynomial expressions of the numerators of S parameters in (4.8) can then be derived as in (4.9). Using the condition of power conservation, the expression for the polynomial $E(s)$ can be derived by an alternative pole method given in [9].

$$\begin{aligned} F_{11}(s) &= (-js + 1)^N \\ P(s) &= (js + 1)^N \end{aligned} \tag{4.9}$$

Synthesized circuit model for a 2nd order example is shown in Fig. 4.2. This lossless circuit is the starting point for the design of lossy filter. The response the lossless 2nd order example is shown in Fig. 4.3.

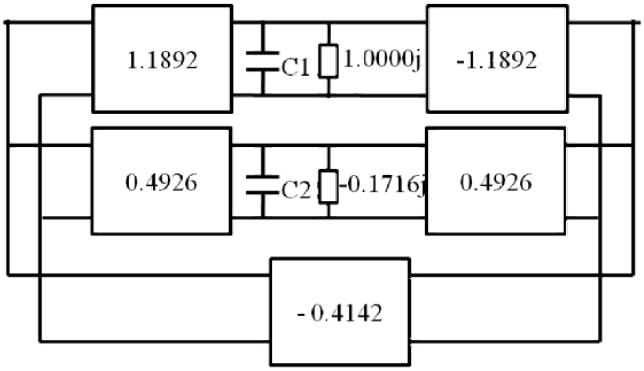

Fig. 4.2 Circuit model synthesized for the 2nd order maximum flat filter.

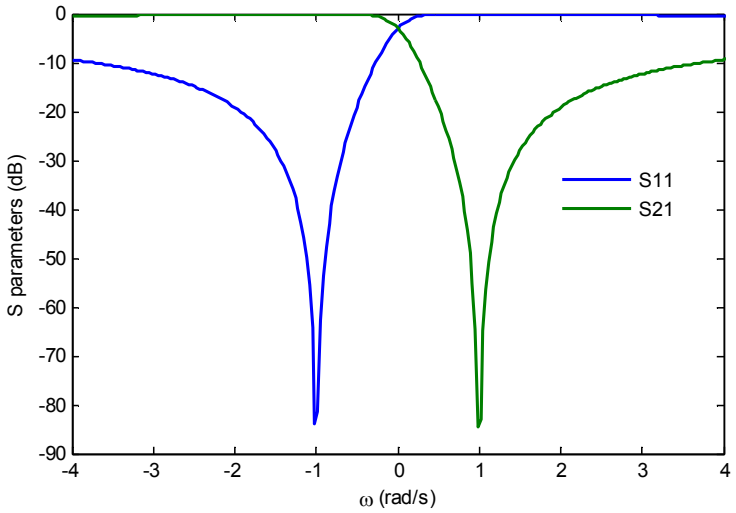

Fig. 4.3 Response of the circuit model synthesized using the above method.

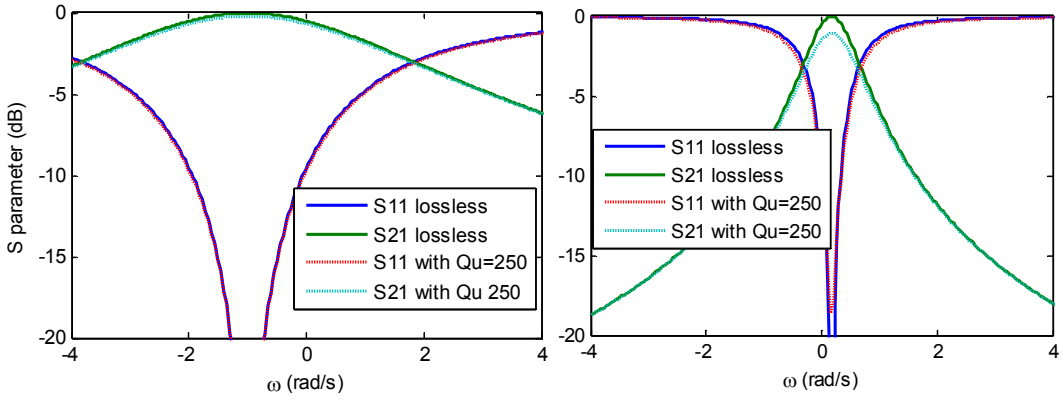

(a) (b)

Fig. 4.4 Response of a single resonator. (a) loss is included in the first resonator and (b) loss is included in the second resonator.

It can be observed from the circuit model in Fig. 4.2 that the first resonator has a larger bandwidth than the second one. The effects of loss on these resonators are compared in Fig. 4.4 which shows the responses of a single resonator with and without loss.

The responses of the total network with loss included in different resonators are compared in Fig. 4.5 with a centre frequency of 0.956 GHz and a bandwidth of 0.06 GHz. The band-edge rounding is less severe when the second resonator is of low *Qu*. It is verified that loss included in the resonator with larger bandwidth will have a smaller effect on the transmission.

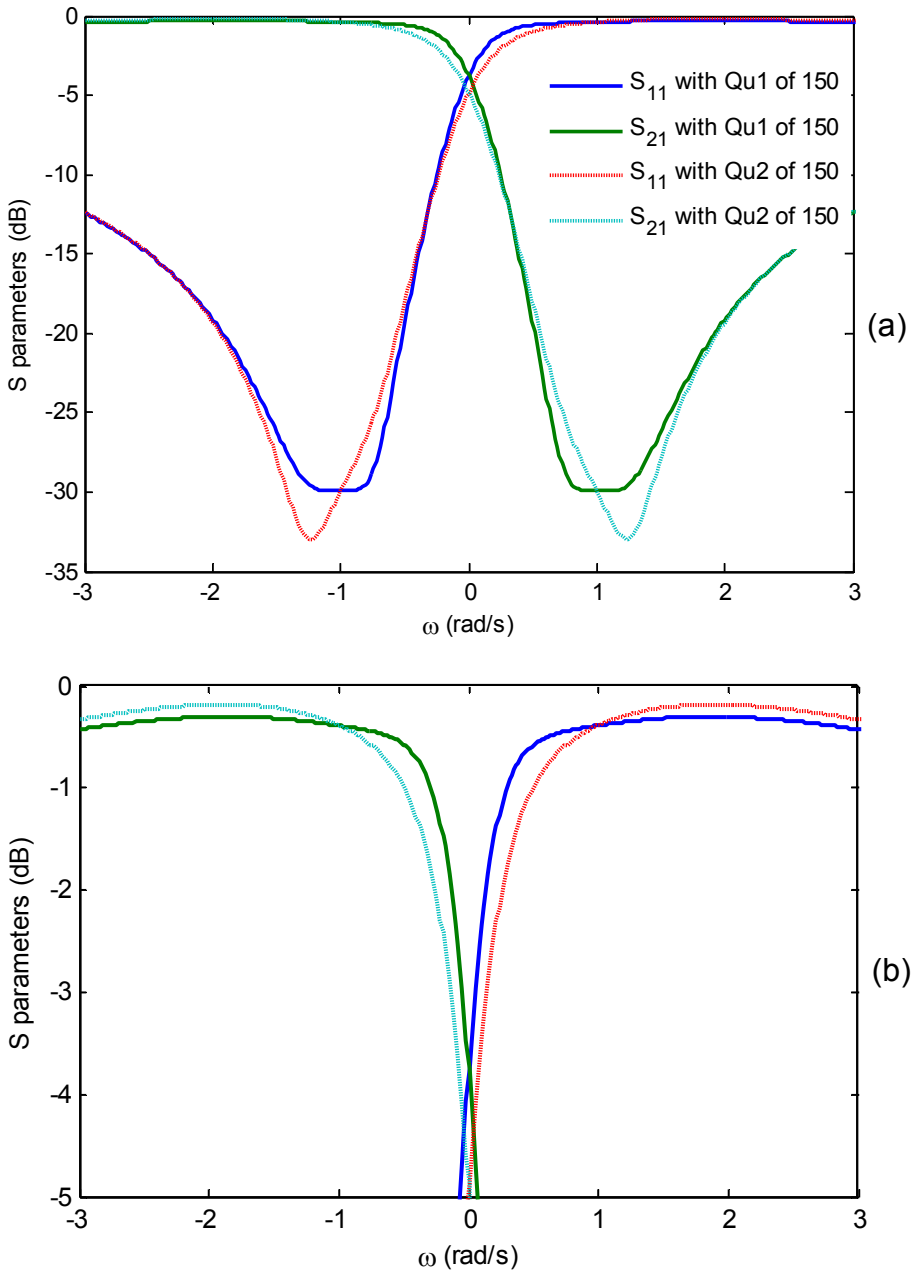

Fig. 4.5 (a) Response of the circuit model when loss is included in each resonator. (b) Zoom up of S_{21} at band edge.

4.1.3 The critical resonators

The values of the resonant frequencies should also be considered in the design. For the admittance parameters shown in (3.20), each term approaches infinity when the frequency approaches the corresponding resonant frequency as in (4.10).

$$\begin{aligned}[Y] &= j\begin{bmatrix} 0 & k_{21} \\ k_{21} & 0 \end{bmatrix} + \sum_{k=1}^{N} \frac{1}{s - j\lambda_k} \begin{bmatrix} r_{11k} & r_{12k} \\ r_{21k} & r_{22k} \end{bmatrix} \\ &\approx \left(j\begin{bmatrix} 0 & k_{21} \\ k_{21} & 0 \end{bmatrix} + \frac{1}{s - j\lambda_k} \begin{bmatrix} r_{11k} & r_{12k} \\ r_{21k} & r_{22k} \end{bmatrix} \right)_{s=j\lambda_k} \end{aligned} \tag{4.10}$$

This implies that the response at a resonant frequency is mainly determined by that specific resonator. As a result, dissipations of the resonators with resonant frequencies near the bandedge are the cause of insertion loss rounding and hence need to be reduced. This direct relation between a single resonator and the total performance does not exist for any other configuration. Generally speaking, one narrow-band and hence high Q resonator is required to control each sharp transition at the passband edges.

A 3rd order Chebyshev example with two transmission zeros at $\pm 1.5j$ is used to illustrate the effect of bandwidth variation. The synthesized circuit model is shown in Fig. 4.6.

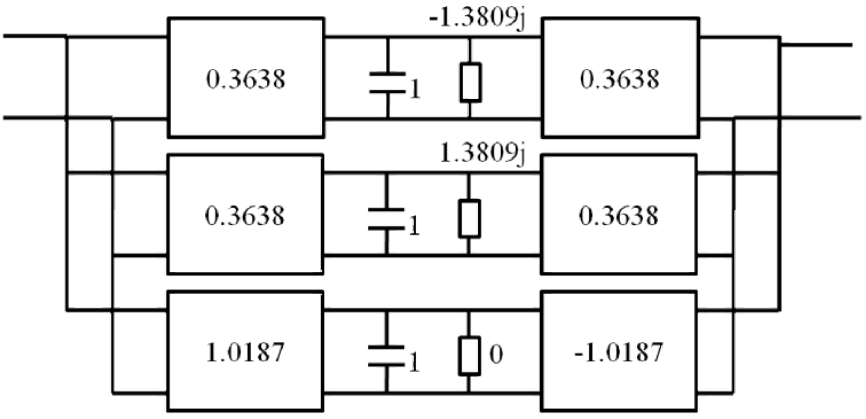

Fig. 4.6 (a) Transversal array of the 3rd order Chebyshev filter with equal capacitance.

The third resonator has a larger bandwidth. So a lower Q of 150 is assigned to the third resonator while the others have a larger Q of 2000. The designed centre frequency is 0.956 GHz and bandwidth is 0.06 GHz.

The response is compared with the one while all three resonators have equal Q of 2000 in Fig. 4.7(a). The insertion loss is proportional to the one of high Q without distortions at band edges. Fig. 4.7(b)shows the response when the resonator 1 is of lower Q. Comparing with Fig. 4.7(a)the rounding-up at band edge due to loss is much more significant thus showing the effect of loss distribution on transmission.

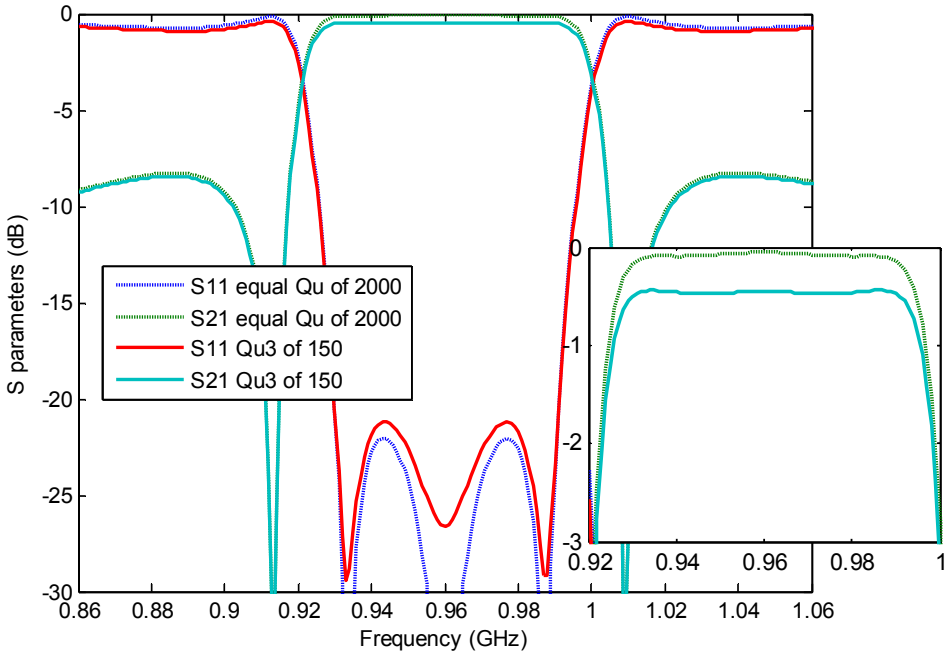

(a)

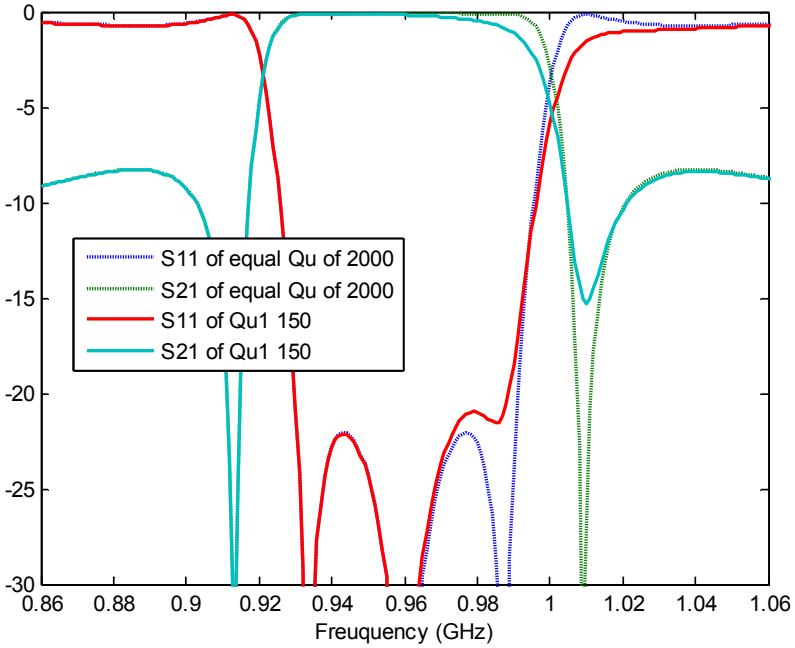

(b)

Fig. 4.7 Response of the circuit model with 3rd resonator low Qs (a) and 1st resonator low Qs (b).

So far, a design approach is proposed in which the resonators with larger bandwidth are realized with low Q techniques and the ones with narrow bandwidth are realized with high Qs.

Further analysis can be made to a 4th order example. It's a general Chebyshev filter with three transmission zeros of -1.7j, -2.2j and -3.6j in the normalized lowpass domain. The lowpass prototype network is shown in Fig. 4.8. It is synthesized using the method given in [9].

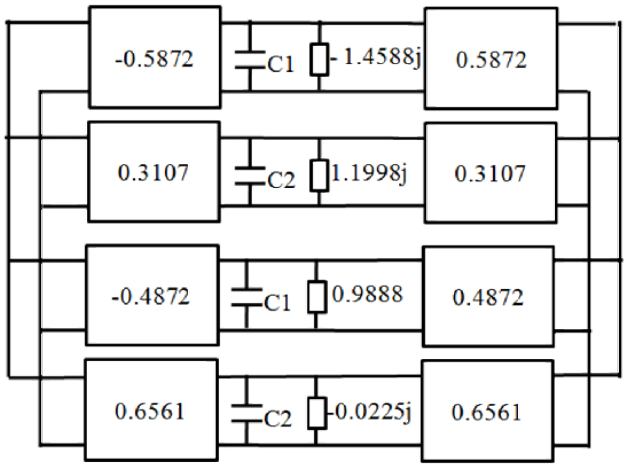

Fig. 4.8 Circuit model of the 4th order Chebyshev filter.

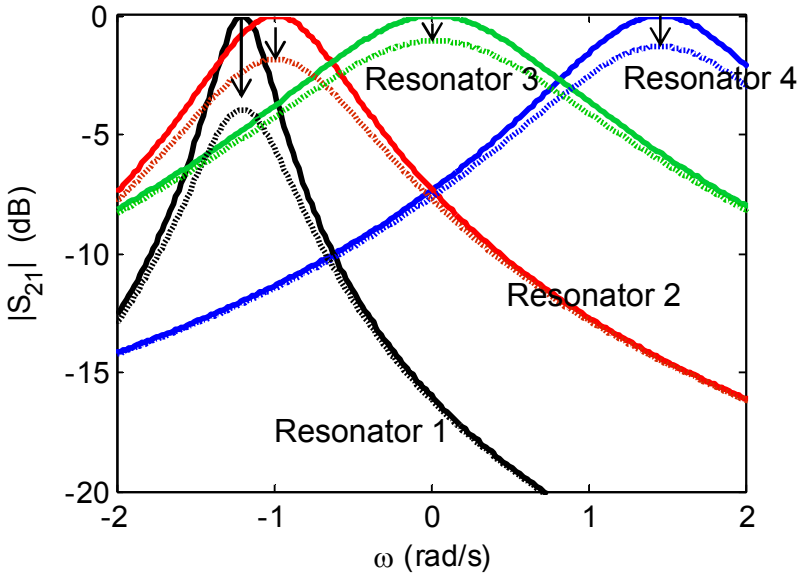

Fig. 4.9 Transmission of each lossless resonator in Fig. 4.1 is compared to the one with Q of 150. Solid lines are for the lossless case.

In Fig. 4.9 the lossless transmission of each resonator is compared to the one with Q of 150 when the center frequency and bandwidth are 2 GHz and 0.12 GHz respectively. It is shown that for resonator 2 which has the

smallest bandwidth, the effect of dissipation is much more severe than those of the other resonators. Also, resonators 2 and 3 have resonant frequencies near the selective bandedge. In order to minimize the effect of dissipation, resonators 2 and 3 should be designed with higher Q than the others.

The derivative of the absolute value of S_{21} regarding to the elements of the CM is derived in [30]. Using the complex CM shown in (4.11), we could find the derivative of $|S_{21}|$ regarding to the dissipation of each resonator which is plotted in Fig. 4.10 for this 4th order example. For each resonator, the maximum deduction of the insertion loss occurs at the corresponding resonant frequency and the amount of deduction is determined by the resonator's bandwidth.

$$\begin{bmatrix} 0 & m_{s1} & \dots & m_{sN} & 0 \\ m_{s1} & m_{11}-j\delta_1 & 0 & 0 & m_{s1} \\ \dots & 0 & \dots & 0 & \dots \\ m_{sN} & 0 & 0 & m_{NN}-j\delta_N & m_{sN} \\ 0 & m_{s1} & \dots & m_{sN} & 0 \end{bmatrix} \tag{4.11}$$

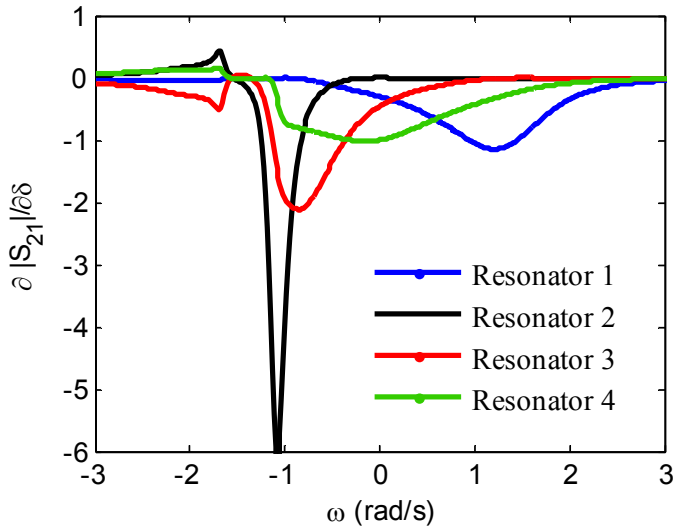

Fig. 4.10 The derivatives of the absolute values of S_{21} regarding to the dissipation of each resonator.

4.2 Synthesis of lossy parallel connected networks

In [61], a method for synthesizing parallel connected network with non-uniform Q is given. The lossy response realized is similar to the new characteristic discussed in Section 3.1.2.

According to (3.29), the roots of polynomial E_s is the same as the roots of $(1+Y_e)(1+Y_o)$ and the roots of polynomial P_s is the same as the roots of (Y_e-Y_o). When non-uniform dissipation is included in each resonator, the change of the roots of E and P could be derived as in (4.12) and (4.13) using Taylor series expansion.

$$\begin{aligned} 1+Y_e &= 1+\sum \frac{r_{ek}}{s-p_{ek}+\delta_{ek}} \\ &\approx \left(1+\sum \frac{r_{ek}}{s-p_{ek}}\right)-\sum \frac{r_{ek}\delta_{ek}}{(s-p_{ek})^2}+\sum \frac{r_{ek}\delta_{ek}^2}{(s-p_{ek})^3} \end{aligned} \tag{4.12}$$

$$\begin{aligned} Y_e-Y_o &= \sum \frac{r_{ek}}{s-p_{ek}+\delta_{ek}}-\sum \frac{r_{ok}}{s-p_{ok}+\delta_{ok}} \\ &\approx \left(\sum \frac{r_{ek}}{s-p_{ek}}-\sum \frac{r_{ok}}{s-p_{ok}}\right)-\left(\sum \frac{r_{ek}\delta_{ek}}{(s-p_{ek})^2}-\sum \frac{r_{ok}\delta_{ok}}{(s-p_{ok})^2}\right) \\ &+\left(\sum \frac{r_{ek}\delta_{ek}^2}{(s-p_{ek})^3}-\sum \frac{r_{ok}\delta_{ok}^2}{(s-p_{ok})^3}\right) \end{aligned} \tag{4.13}$$

In (4.12) and (4.13), the first terms in the expansion are the same as the ones in lossless case. The roots are modified by real second order terms and imaginary third order terms. As a result, the insertion loss of parallel connected network with loss included in each resonator is equivalent to the ones of which the poles and roots are shifted to the left in the complex plane by non-uniform complex amounts. The response achieved is a lossy version of new characteristics derived in Part II except the roots of P polynomial are complex.

4.2.1 Approximated analytical solution of Q distribution

An analytical solution for the Q distribution that gives a flat passband insertion loss could be derived with approximations on the effect of loss. For an Nth degree lossy filter network, its S parameters can be expressed by the even and odd mode parameters as in (3.29).Using the even and odd mode S and Y parameters given in (3.28), S_{21} could be derived as in (4.14).

$$S_{21} = \frac{Y_e-Y_o}{(1+Y_e)(1+Y_o)} = \frac{1}{1+Y_e}-\frac{1}{1+Y_o} \tag{4.14}$$

$$Y_e = \sum_{k=1}^{N_e} \frac{r_{ek}}{s - j\lambda_{ek}}$$
$$Y_o = \sum_{k=1}^{N_o} \frac{r_{ok}}{s - j\lambda_{ok}} \tag{4.15}$$

Using the partial expansion of the even and odd mode admittance parameters given in (4.15), the variation of $|S_{21}|$ due to loss is a linear combination of the dissipation of each resonator as in (4.16).

$$\begin{aligned}\Delta|S_{21}| &= \sum_{k=1}^{N} \frac{\partial|S_{21}|}{\partial\delta_k}\delta_k \\ &= \sum_{k=1}^{N_e} \mathrm{Re}\left[\frac{|S_{21}|}{S_{21}} \cdot \frac{1}{(1+Y_e)^2} \cdot \frac{r_{ek}}{(s-j\lambda_{ek})^2}\right] \cdot \delta_{ek} \\ &- \sum_{k=1}^{N_o} \mathrm{Re}\left[\frac{|S_{21}|}{S_{21}} \cdot \frac{1}{(1+Y_o)^2} \cdot \frac{r_{ok}}{(s-j\lambda_{ok})^2}\right] \cdot \delta_{ok}\end{aligned} \tag{4.16}$$

As a result, we can enforce the values of insertion loss at several sampling points to be proportional to the lossless ones, so that a Q distribution could be found by solving the set of linear equations analytically. A constant *m* is defined to determine the lossy insertion loss level. For an Nth degree filter, sampling points chosen as the position of reflection zeros give acceptable results.

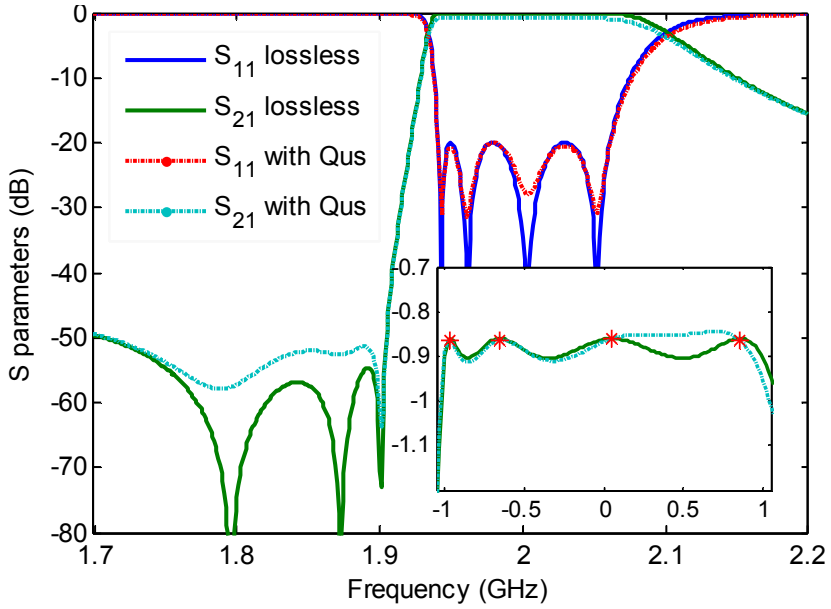

Fig. 4.11 S parameters of the 4th order filter compared to the ideal template. Markers are the sampling points. The solid line is the ideal template which is the lossless S_{21} being multiplied by a constant.

This example is the 4th order Chebyshev filter given earlier with three transmission zeros normalized at -1.7j, -2.2j and -3.6j. In the analysis, *m* is set to 0.9. With a center frequency of 2 GHz and a bandwidth of 0.12 GHz, the Q calculated are 274, 5640, 1045 and 266. The response is shown in Fig. 4.11 comparing to the ideal template. This result would be very difficult to achieve using conventional cascaded filters unless very high Q resonators are used.

Because the variation of insertion loss due to loss is a linear combination of dissipation as shown in (4.16), we could use different Q distributions that are proportional to each other to achieve different insertion loss level. With different values of m, Q distributions are calculated and listed in Table 4.1. With the decreased values of m, the Q also decreases. However, a flat passband insertion loss is still achieved as shown in Fig. 4.12 in which the passband insertion loss is compared with the ideal template for each case.

Table 4.1 Q distributions for different insertion loss level

m	Qs			
0.95	549	11281	2090	532
0.9	274	5640	1045	266
0.8	137	2820	522	133
0.7	91	1880	348	88

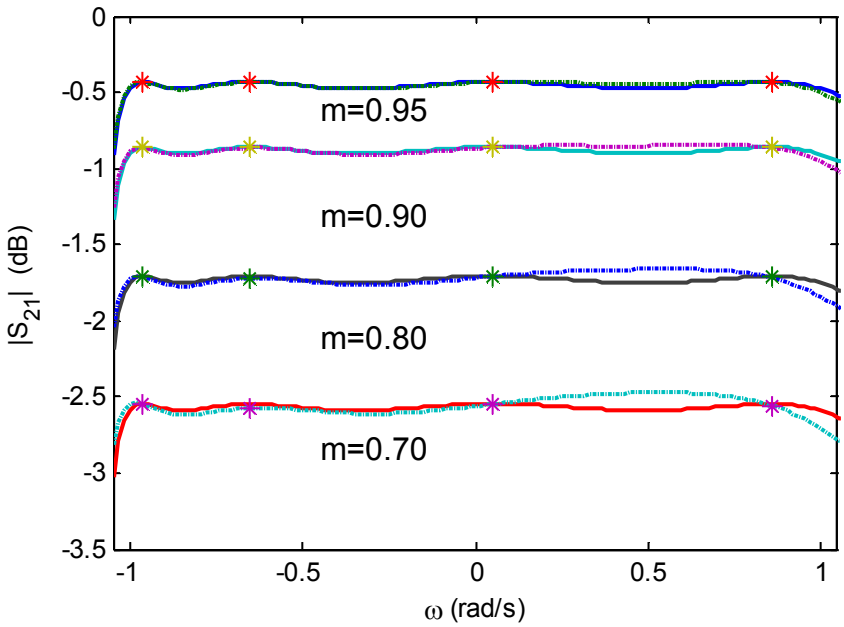

Fig. 4.12 S_{21} of the 4th order circuit with different Q distributions compared to the ideal template. Markers are the sampling points. The solid lines are the ideal template which is the lossless S_{21} being multiplied by a constant.

The S parameters with different Q distributions are shown in Fig. 4.13. For each case, the imperfect reflection and transmission zeros indicate that the characteristic realized is no longer the same as the general Chebyshev response. With the decreased Q, the return loss and rejection levels increase with respect to the lossless condition.

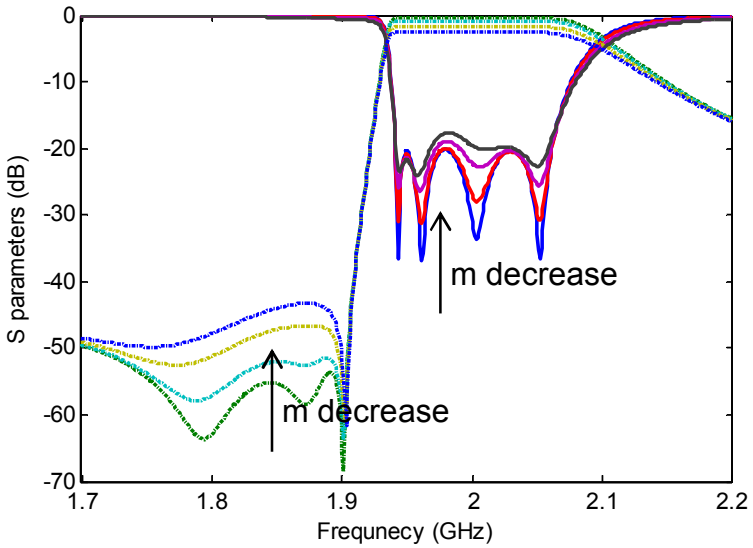

Fig. 4.13 S parameters of the 4th order circuit using different Q distributions.

4.2.2 A new lossy filter characteristic

Including loss in the filter network is equivalent to shifting the zeros and poles of the transfer function to the left in the complex plane. If the dissipation is uniform, the constant shifting of the poles and zeros will cause bandedge rounding of the insertion loss. As a result, in predistortion or the lossy circuit synthesis methods discussed earlier, the insertion loss of the lossy circuit is the same as the lossless one being multiplied by a constant, while the positions of the poles and zeros of the transfer function are the same as the lossless ones.

The lossy response synthesized in this paper is different in that the poles and zeros of the transfer function are not the same as the ideal general Chebyshev characteristic. The lossy response is derived by shifting the poles of the transfer function to the left non-uniformly. With a proper amount of shifting, a flat passband insertion loss and a good return loss can be attained with imperfect transmission zeros.Fig. 4.14 shows the poles and zeros of the 4th order example used earlier comparing to lossless ones in the complex plane.

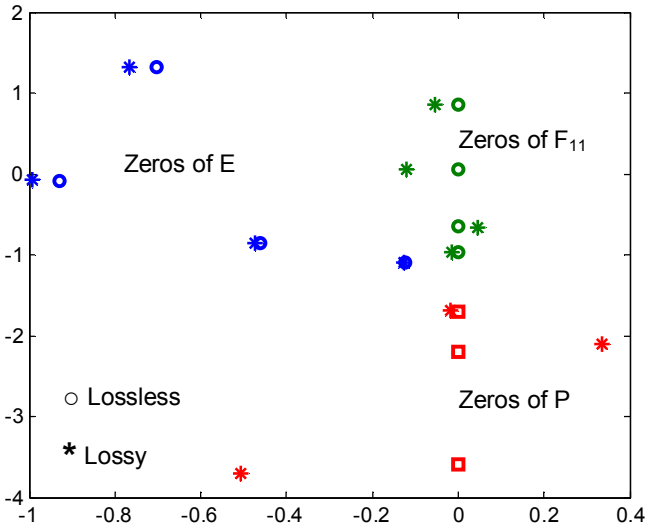

Fig. 4.14 Zeros and poles of the transfer and reflection function plotted in the complex plane.

As a conclusion, it is possible to design a parallel connected filter network with unequal dissipations and have a high Q performance. Resonators with a smaller bandwidth and near band edge resonant frequency should be designed with lower loss, while the other resonators can be designed with higher loss without significantly deteriorating the performance.

4.2.3 The gradient based optimization

For filters with configurations other than the transversal array, the optimum Q distribution can be determined by a gradient based optimization. In the optimization, the initial value of the CM is the lossless one derived by an analytical procedure [8] or by optimization [33]; then the whole or parts of the complex matrix including dissipations of resonators shown in (4.17) are used as variables. It is found that for most of the cases, acceptable results can be achieved by optimizing only the dissipation of each resonator without changing the real part of the CM. The constraints are $\delta_k > 0$ to enforce passivity or $\delta_k > \delta_{\min}$ when a minimum loss is given.

$$\begin{bmatrix} 0 & m_{s1} & \dots & m_{sN} & 0 \\ m_{s1} & m_{11} - j\delta_1 & 0 & 0 & m_{s1} \\ \dots & 0 & \dots & 0 & \dots \\ m_{sN} & 0 & 0 & m_{NN} - j\delta_N & m_{sN} \\ 0 & m_{s1} & \dots & m_{sN} & 0 \end{bmatrix} \tag{4.17}$$

Generally, the optimization consists of two procedures. First, the dissipations of resonators are used as variables to achieve different goals. Then the real part of the CM is tuned to provide an improvement on the response which is usually minor. It is noticed that for parallel connected networks, the Q distribution plays a more important role in determining the characteristics than it is in series connected networks.

There are two kinds of error functions defined later for different properties we want to achieve for the lossy filter. One focused on stopband will provide a good rejection by realizing perfect transmission zeros using Q distribution. The other can give a good insertion loss in the passband similar to the one designed by lossy circuit synthesis method.

Matlab optimization fmincon is used for the minimization of error function. Gradient is calculated numerically at each step. The algorithm used is interior-point.

4.2.3.1 For transmission and reflection zeros

Using non-uniform Q distribution, a lossy filter could have perfect transmission zeros. This is achieved by optimizing both the Q of each resonator and the real part of CM with proper setting of weights in cost function. The error function of [10] is used and is defined as in (4.18).

$$\begin{aligned} errf = {} & w_{rz}\sum_{i=1}^{N} abs\left(S_{11}(rz_i)\right)^2 + w_{tz}\sum_{j=1}^{N_{tz}} abs\left(S_{21}(tz_j)\right)^2 \\ & + w_{rl}\left\{\begin{array}{l} abs\left(abs\left(S_{11}(-1j)\right)^2 - \left(\dfrac{\varepsilon}{\sqrt{1-\varepsilon^2}}\right)^2 \right) \\ + abs\left(abs\left(S_{11}(1j)\right)^2 - \left(\dfrac{\varepsilon}{\sqrt{1-\varepsilon^2}}\right)^2 \right) \end{array}\right\} \end{aligned} \tag{4.18}$$

Where rz_i is the i[th] reflection zero, tz_j is the j[th] transmission zero. w_{rz}, w_{tz}, w_{rl} are the weights. The third term is the error of return loss at band edges ($\omega = \pm 1j$), while ε is related to the return loss level by $\varepsilon = \left(10^{RL/10} - 1\right)^{-1/2}$.

Here is a 3rd order example with two transmission zeros at $-1.6j$ and $-2.5j$. The optimized Qu are 81, 470 and 229 with a centre frequency at 2 GHz and a bandwidth of 0.12 GHz. In Fig. 4.15, the optimized response is compared to the one with uniform Qu of 470. It is shown that the zeroes of both transmission and reflection can be get using lossy resonators with decreased insertion loss.

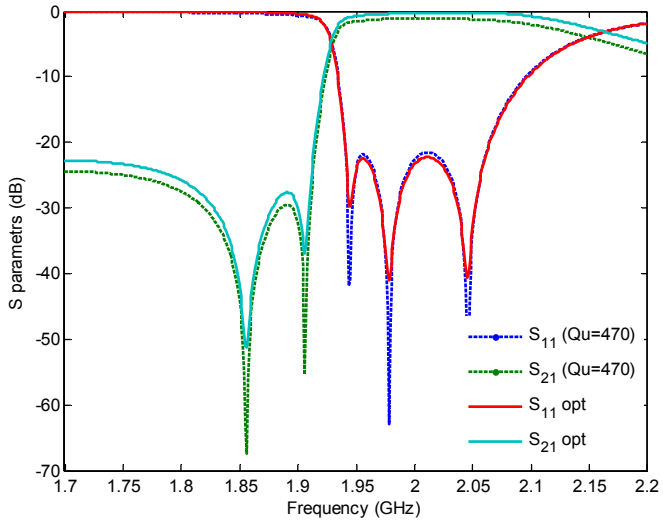

Fig. 4.15 S parameters of the optimized 3rd order circuit (Qu equal to 81, 470 and 229) compared with the ones of equal Qu of 470.

For a 4th order filter with three transmission zeros at $-1.7j$, $-2.3j$ and $-3.3j$, it is difficult to achieve the goal in one optimization due to the increased complexity of the configuration. As a result, an iteration technique is used. Keeping the cost function the same, Q and CM are optimized in iterations. The values of Qs are 92, 278, 223 and 135. The resonator with the largest Q is the one with smallest bandwidth. The response is shown in Fig. 4.16. It is shown that when the largest Q is given for a design, it is possible to have only part of the resonators high Q while the others' are lowered and still maintains the perfect transmission zeros with a decrease in insertion loss.

The largest Q of each resonator in Fig. 4.15 and Fig. 4.16 are different because the upper bounds of the Q are set with different values in optimization. New sets of Q distribution could be found with different upper bounds. This indicates that the problem of Q distribution that provides perfect transmissions have multiple solutions. As a result, an alternative approach is used in which the largest Q is fixed in the optimization. It is found that for every fixed value, a new set of Q distribution that gives perfect

transmission zeros can be found. Furthermore, these Q distributions are tending to be proportional with each other.

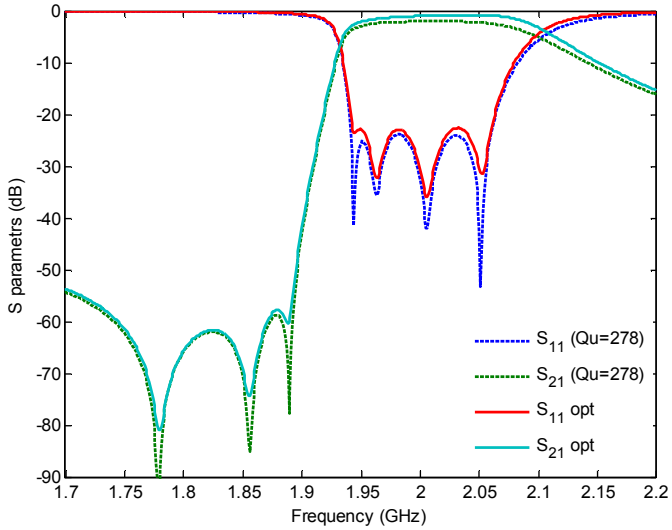

Fig. 4.16 S parameters of the optimized 4th order circuit (Q equal to 92, 278, 223 and 135) compared with the ones of equal Q of 278.

4.3.2.2 For flat passband insertion loss

For filters with configurations other than the transversal array, the optimum Q distribution can be determined by a gradient based optimization. In the optimization, the initial value of the CM is the lossless one derived by an analytical procedure [8] or by optimization [33]; then the whole or parts of the complex matrix including dissipations of resonators shown in (4) are used as variables. It is found that for most of the cases, acceptable results can be achieved by optimizing only the dissipation of each resonator without changing the real part of the CM. The constraints are $\delta_k > 0$ to enforce passivity or $\delta_k > \delta_{\min}$ when a minimum loss is required.

The error function defined in (4.19) is modified from the one given in [33] in that a new term is included to enforce the passband insertion loss to be proportional to the ideal lossless template. rz_i is the ith reflection zero and tz_j is the jth transmission zero. w_{rz}, w_{tz} and w_{il} are the weightings. m is a constant with its magnitude smaller than 1 and is used to define the loss level. $S^0{}_{21}$ is the lossless template. s_k is the k^{th} sampling points. For a Chebyshev response, the sample points are the maximums and the minimums of insertion loss in the passband and two points at bandedge.

$$errf = w_{rz}\sum_{i=1}^{N} abs\left(S_{11}(rz_i)\right)^2 + w_{tz}\sum_{j=1}^{N_{tz}} abs\left(S_{21}(tz_j)\right)^2 + w_{il}\sum_{k=1}^{N_{il}} abs\left(abs\left(S_{21}(s_k)\right)^2 - abs\left(m * S_{21}^0(s_k)\right)^2\right) \tag{4.19}$$

The same 3rd order example is used here. In the optimization, m equals to 0.8 and only w_{il} is set to a non-zero value to prove that the insertion loss level could be tuned by Q distribution. The Q optimized are 140, 2972 and 328 with only one high Q resonator. The response is compared with the lossless ones in Fig. 4.17. It is shown that the fitting of the insertion loss is not perfect, but the rounding is avoided.

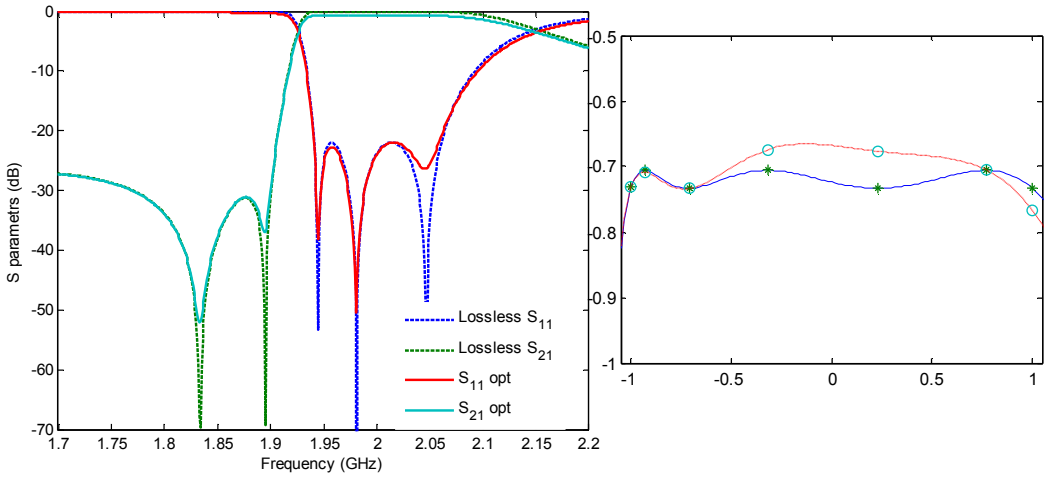

Fig. 4.17 (a) S parameters of the 3rd order filter with optimized Qu distribution compared with the loss less one. (b) Insertion loss in the passband is compared to the template which is an ideal response multiplied by 0.8.

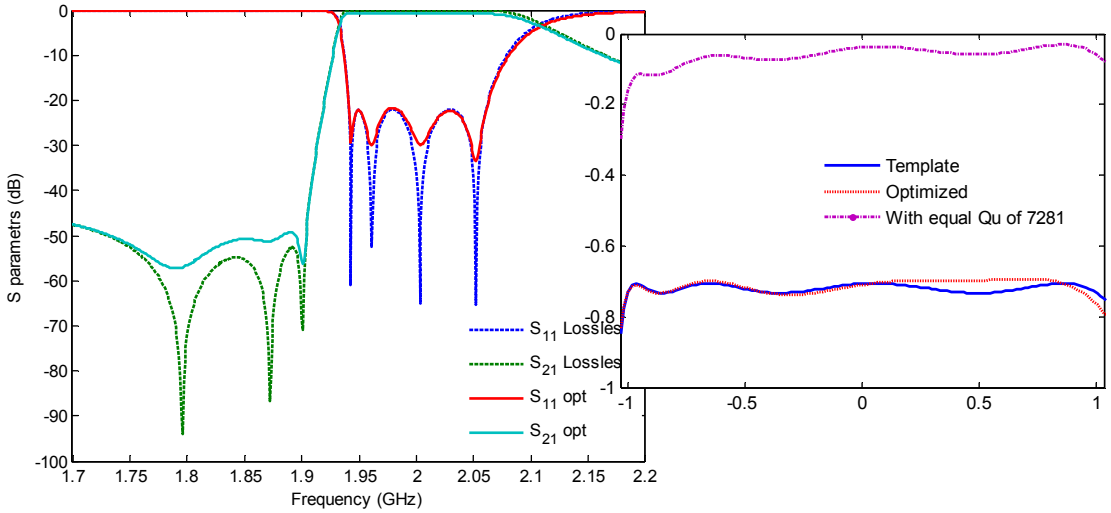

Fig. 4.18 (a) S parameters of the 3rd order filter with optimized Q distribution compared with the loss less one. (b) Insertion loss in the passband is compared to the template which is an ideal response multiplied by 0.8.

The same 4th order example is also used. The Qs are 299, 7281, 1547, 301 with one high Q resonator. The response is shown in Fig. 4.18

4.2.4 Realisation of perfect transmission zeros

A proper loss distribution could also give perfect transmission zeros. This method could be used when the requirement for rejection is severe. The solution for the 2nd order filter is exact and approximation will be used for higher order case.

According to (4.20), a transmission zero is also a zero in the admittance parameter Y_{21}. For a 2nd order filter, assuming the second residue is negative, the partial expansion of the admittance parameter is given in (4.21).

$$S_{21} = \frac{-2Y_{21}}{(1+Y_{11})(1+Y_{22}) - Y_{12}Y_{21}} \tag{4.20}$$

$$Y_{21} = \frac{(r_{21})_1}{sC_1 + jB_1 + \delta_1} - \frac{(r_{21})_2}{sC_2 + jB_2 + \delta_2} \tag{4.21}$$

At a transmission zero, the dissipation of each resonator and the values of the residues must satisfy (4.22) and (4.23).

$$(r_{21})_1(sC_2 + jB_2 + \delta_2) - (r_{21})_2(sC_1 + jB_1 + \delta_1) = 0 \tag{4.22}$$

$$\frac{\delta_1}{(r_{21})_1} = \frac{\delta_2}{(r_{21})_2} \tag{4.23}$$

When the dissipation of one resonator is given, the dissipation of the other resonator can be determined from (4.23) which guarantees that a perfect transmission zero could be get.
For an Nth order filter, when δ_i is small, each term in the admittance parameters can be replaced by its Taylor series expansion as in ((4.24).

$$\begin{aligned} Y_{21} &= \sum_{i=1}^{N} \frac{(r_{21})_i}{sC_i + jB_i + \delta_i} \\ &= \sum_{i=1}^{N} \left(\frac{(r_{21})_i}{sC_i + jB_i} + \frac{-(r_{21})_i}{(sC_i + jB_i)^2}\delta_i + \ldots \right) \end{aligned} \tag{4.24}$$

At each transmission zero, if the higher order expansions are neglected, we have (4.25).

$$\sum_{i=1}^{N}\left(\frac{-(r_{21})_i}{(tz_j C_i + jB_i)^2}\delta_i\right) = 0 \tag{4.25}$$

The linear equation can be solved when the filter has N-1 transmission zeros and one of the δ_i is given. An example is given using 4th order filter used earlier. For the perfect transmission zeros, Qu solved are 84, 277, 222 and 126 and the response is shown in Fig. 4.19.

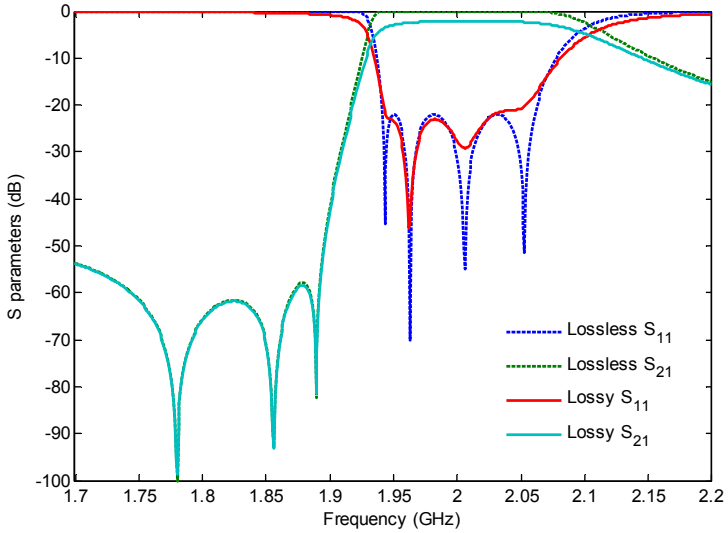

Fig. 4.19 S parameters of the 4th order example with three perfect transmission zeros.

4.3 Examples

4.3.1 Parallel connected symmetric networks

Transversal array requires the parallel connection of N networks for an Nth degree filter and is thus sometimes difficult to realize. For a symmetric network of even degree, poles and residues can be grouped. Each group can form a sub-network and can be applied with similarity transformations. The final network is the parallel connection of these sub-networks as described in [8]. In this way, the number of parallel connected branches can be reduced.

Considering the effect of loss distribution, the resonators of narrow band can be assigned to one group. In this way, each sub-network will have an equal Qu distribution. As discussed earlier, for a circuit with equal Qu distribution, similarity transformations will not change the value of Qu for each resonator and will not introduce other lossy elements at cross couplings.

1 Symmetric parallel connected 4th order example

The following is an example of symmetric 4th order Chebyshev filter with two transmission zeros at $\pm 1.5j$. The centre frequency is 2 GHz, and the bandwidth is 0.12 GHz. The transversal array model synthesized is shown in Fig. 4.20.

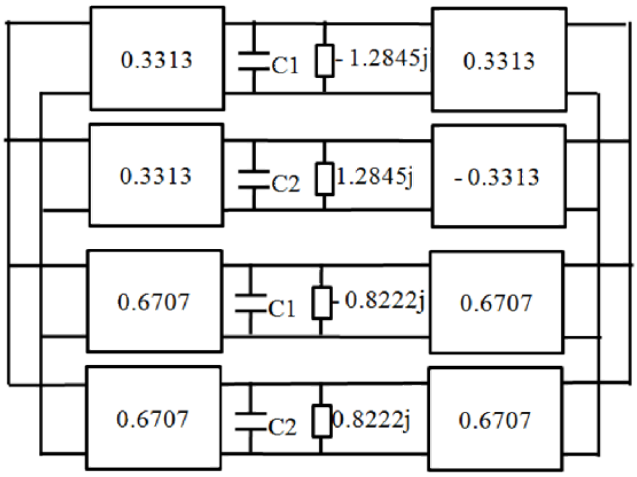

Fig. 4.20 Circuit model synthesized for the 4th order Chebyshev filter.

For this symmetric even order network, the transversal array can be transformed into the parallel connection of two 2nd order network while the response is not changed. The circuit model is shown in Fig. 4.21. The response when the resonator 3 and 4 are of low Qs is compared with the one when resonator 1 and 2 are of low Qs in Fig. 4.22. And it is shown that when the resonator 3 and 4 are of Qs of 150, the transmission of passband is proportional to the one with equal Q of 1000 and the return loss is less distorted than the other case.

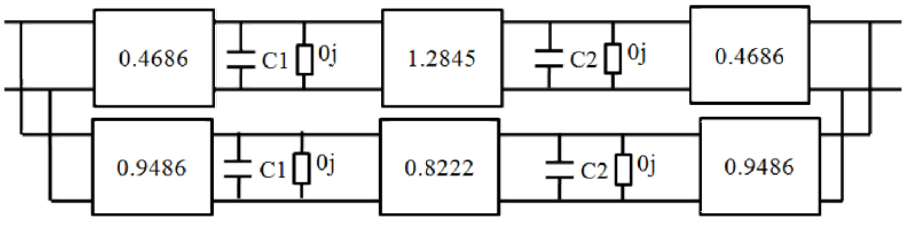

Fig. 4.21 Circuit model of the 4th order parallel connected networks.

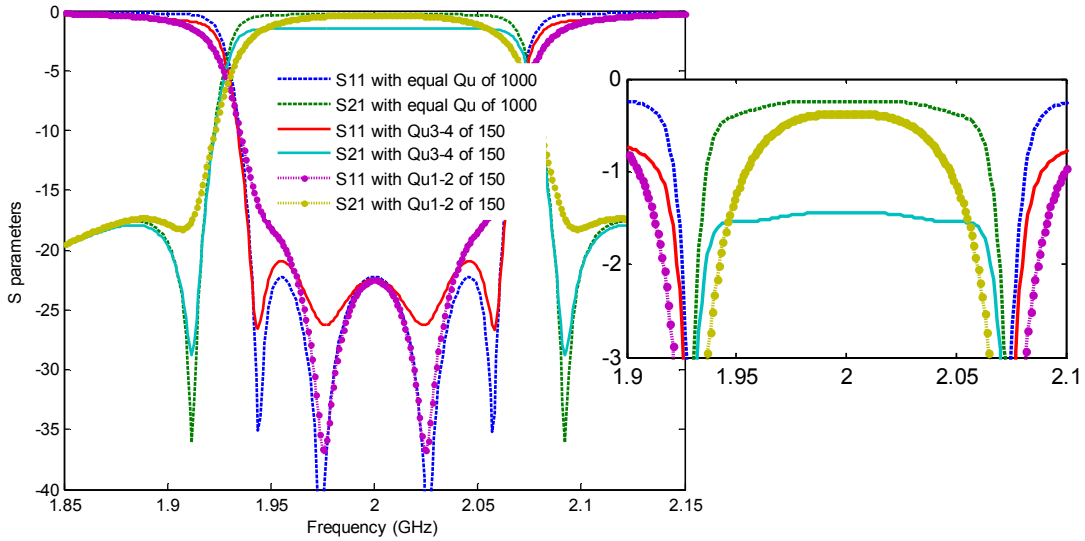

Fig. 4.22 Response of the 4th order Chebyshev filter with loss included.

It is interesting to note that when loss is included in the two symmetric resonators of one branch, the transmission of passband will be even flatter, because the degradation of transmission due to the loss of resonators with symmetric center frequencies compensates each other throughout the passband.

For the circuit with Q distribution as shown in Fig. 4.23(a) the response is the same as the one shown in Fig. 4.22. The insertion loss is shifted from lossless case by 0.7 dB. This value can be used with the method described in section I to synthesize a lossy circuit which is shown in Fig. 4.23(b). The responses of the two circuits are compared in Fig. 4.24 showing that the method of synthesizing lossy circuit presented here is as good as the one given in Fig. 4.23(b).

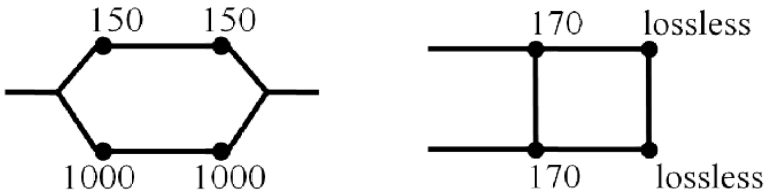

(a) (b)

Fig. 4.23 Node expression of the circuit model of (a) transversal array. (b) Folded network.

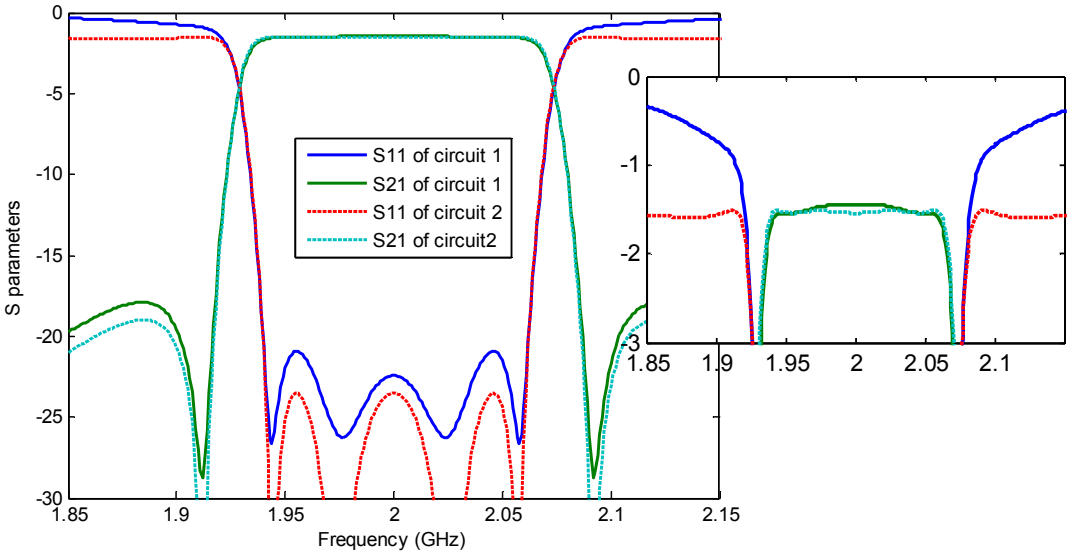

Fig. 4.24 Response of the circuit model shown in Fig. 4.23.

2 Symmetric 6th order parallel connected example

The same procedure is applied to a 6th order Chebyshev filter with four transmission zeros at 1.3958j, -1.3958j, 1.0749 and -1.0749. In the transversal array, residues and poles are grouped to form two sub-networks. The one of degree 2 is formed by narrow band resonators and are applied with lower loss. The other sub-network of 4th degree is realized with low Q resonators. The topology is shown in Fig. 4.25(a). An alternative topology is shown in Fig. 4.25(b) which is a parallel connection of three sub-networks of degree 2. The CMs for the two sub-networks are listed in Table 4.2 and Table 4.4.

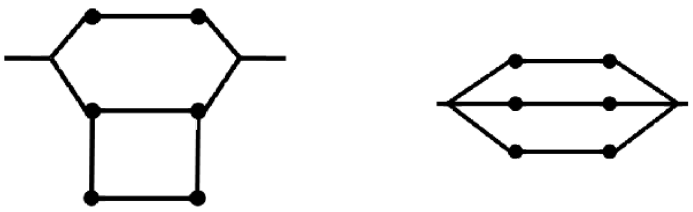

(a) (b)

Fig. 4.25 Circuit model of the parallel connected 6th order filter.

Table 4.2 CM of the sub-networks

	-0.4315		
-0.4315	-0.0080	1.2071	
	1.2071	-0.0080	0.4315
		0.4315	

	-0.9447				
-0.9447	-0.0640j	0.7032		0.3487	
	0.7032	-0.0640j	0.3277		
		0.3277	-0.0640j	0.7032	
	0.3487		0.7032	-0.0640j	-0.9447
				-0.9447	

The response is shown in Fig. 4.26. The response when the red resonators in Figure 4.33 are of low Qs of 250 is compared with the one when the blue resonators are of low Qs. The first one has a flat insertion loss and a less distorted return loss in the passband.

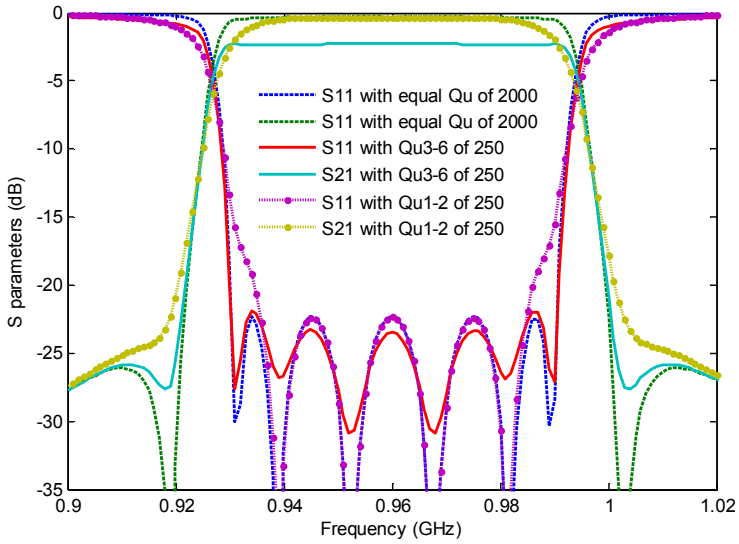

Fig. 4.26 Response of the circuit model. The response of equal Q of 2000 is compared to the one of the 3rd, 4th 5th and 6th resonators having a low Qu of 250.

4.3.3 Parallel network with input and output nodes

1. Symmetric 5th order example with input and output nodes

The following example is a 5th order Chebyshev filter with four transmission zeros at 1.4j, -1.4j, 2.2j and -2.2j. The centre frequency and bandwidth are 2 GHz and 0.12 GHz respectively. The CM is transformed according to the grouping of poles and residues.

The circuit configuration with Qs for each resonator is shown in Fig. 4.27 and the values of elements of the CM for this network are listed in Table 4.3. The circuit has three sub-networks and one of them is of high Q while the Qs of

the other two sub-networks are much smaller. The response is shown in Fig. 4.28 compared to the lossless one.

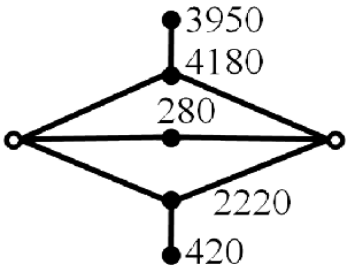

Fig. 4.27 (a) Circuit model of the 5th order symmetric filter with three parallel connected sub-networks.

Table 4.3 Values of the elements in for the 5th order network

M_{S1}	-0.4287	M_{1L}	0.4287	δ_1	0.0040
M_{12}	1.2102	M_{3L}	0.6235	δ_2	0.0042
M_{S3}	-0.6235	M_{4L}	0.7131	δ_3	0.0593
M_{S4}	0.7131			δ_4	0.0075
M_{45}	-1.0329			δ_5	0.0392

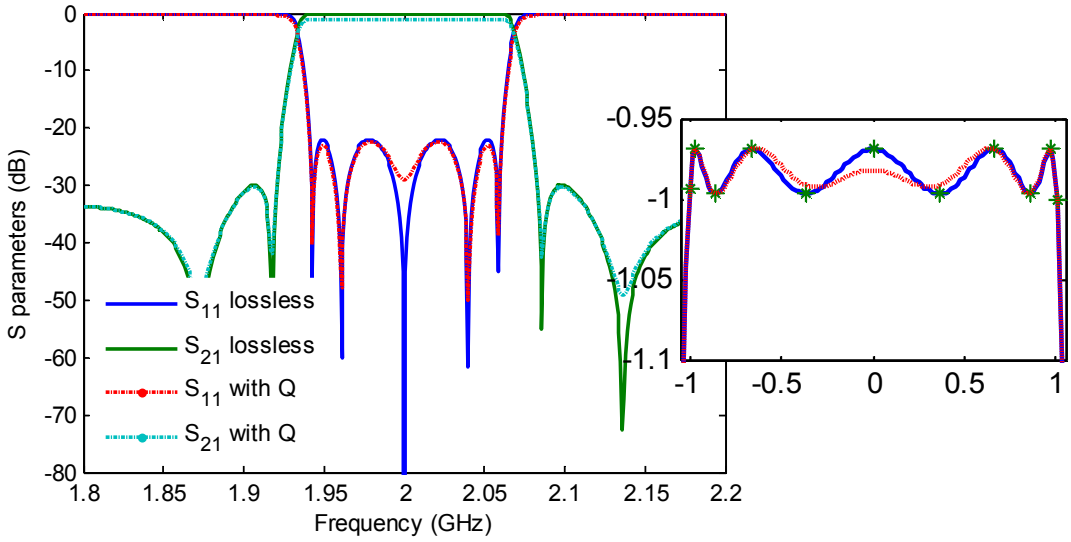

Fig. 4.28 S parameters of the 5th order filter with Q distributions compared to the lossless ones.

2. Asymmetric 7th order example with input and output nodes

A 7th order Chebyshev filter with four transmission zeros at -1.7j, -1.9j, -2.5j and -4.2j is used here with a centre frequency of 2 GHz and a bandwidth of 0.12 GHz. The configuration shown in Fig. 4.29 is different from the parallel connected network in that the input and output are resonating nodes.

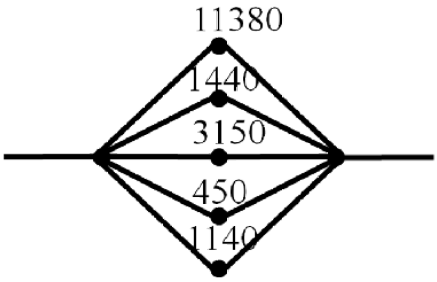

Fig. 4.29 Circuit model of the 7th order asymmetric filter with transformed configurations.

The element values of the CM are listed in Table 4.4. This is a relatively low loss design and one of the resonators is of high Q. Although the Q factors of the first and last resonators are infinity in this case, they can be scaled to any convenient level. This merely affects the absolute passband insertion but not the selectivity, flatness or return loss. The response of this circuit is shown in Fig. 4.30.

Table 4.4 Values of the elements in for the 7th order network

M_{S1}	0.9968	M_{7L}	0.9968	B_1	-0.0237	δ_1	0.00010
M_{12}	0.1610	M_{27}	0.1610	B_2	1.0165	δ_2	0.00146
M_{13}	0.3617	M_{37}	0.3617	B_3	-0.9400	δ_3	0.01157
M_{14}	-0.3058	M_{47}	0.3058	B_4	0.8189	δ_4	0.00528
M_{15}	0.4385	M_{57}	0.4385	B_5	0.3800	δ_5	0.01550
M_{16}	-0.5026	M_{67}	0.5026	B_6	-0.2889	δ_6	0.01458
				B_7	-0.0237	δ_7	0.00010

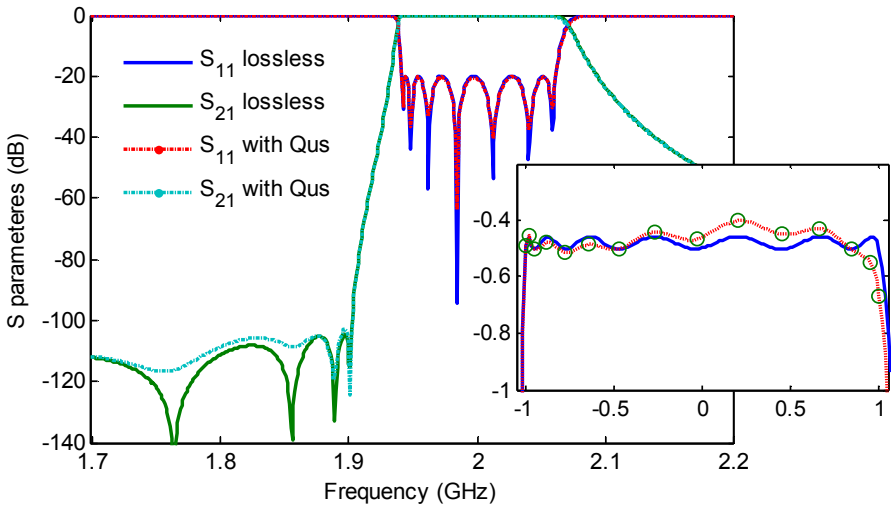

Fig. 4.30 S parameters of the 7th order filter with Q distributions compared to the lossless ones.

4.3.4 Other configurations

1. 8th order symmetric filter with transformed configuration

This example is an 8th order Chebyshev filter with 6 transmission zeros at 1.25j, -1.25j, 0.8120+0.1969j, 0.8120-0.1969j, -0.8120+0.1969j and -0.8120-0.1969j with a centre frequency of 2 GHz and a bandwidth of 0.12 GHz. CM is transformed according to the grouping of poles and residues. The two smallest residues are in one group and the other six residues are the other group. Then similarity transformations are applied to each of the sub-networks to obtain the ladder network. Optimization is applied to the final parallel connected network giving the non-uniform Qs.

The circuit configuration is giving in Fig. 4.31 with the element values in Table 4.5. The response is shown in Fig. 4.32. The insertion loss of this network overlaps with the ideal template used in the optimization.

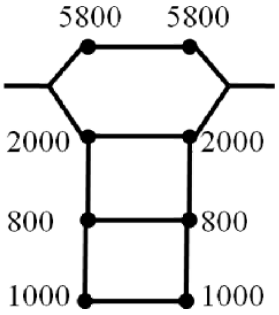

Fig. 4.31 Circuit model of the 8th order symmetric filter with two sub-networks.

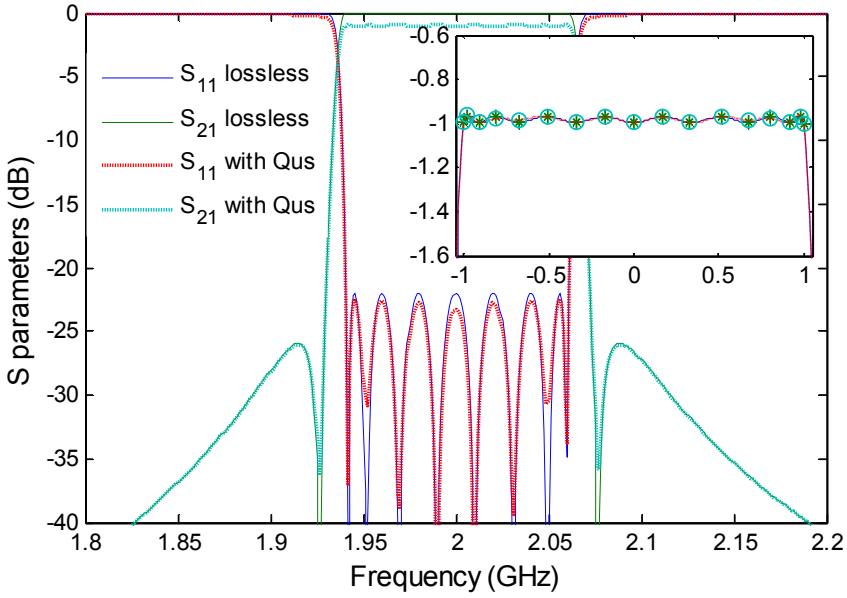

Fig. 4.32 S parameters of the 8th order filter compared to the lossless case.

Table 4.5 Values of the elements in for the 8th order network

M_{S1}	-0.4054	M_{78}	-0.7433	δ_1	0.00284
M_{12}	1.1609	M_{8L}	0.9462	δ_2	0.00284
M_{2L}	0.4054	M_{38}	0.2568	δ_3	0.00865
M_{S3}	0.9462	M_{47}	-0.1902	δ_4	0.01977
M_{34}	0.7433			δ_5	0.01640
M_{45}	0.4702			δ_6	0.01737
M_{56}	0.1945			δ_7	0.01863
M_{67}	-0.4702			δ_8	0.00857

We could assign equal Qs for each sub-network. In this case, the Qs for each sub-network are 15000 and 1000. As shown in Fig. 4.33, the ripple of insertion loss in the passband is increased. However the selective bandedge is still maintained.

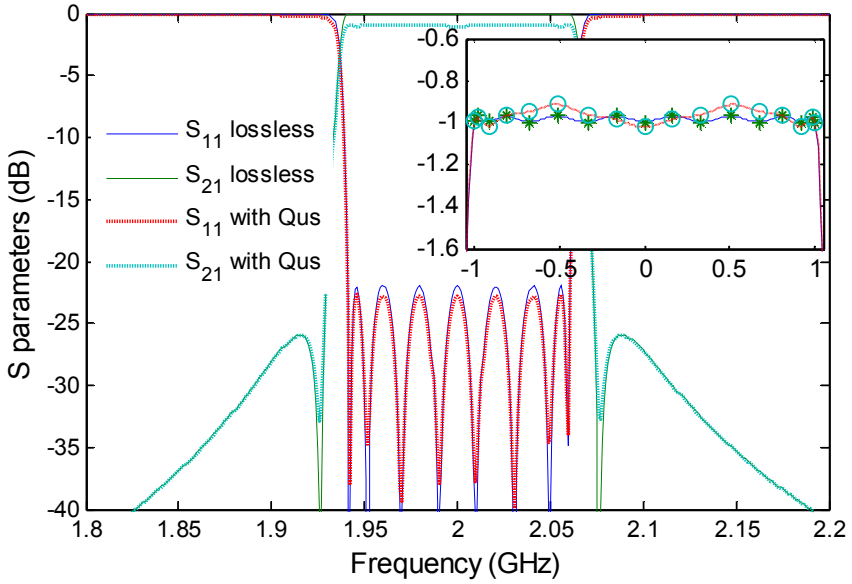

Fig. 4.33 S parameters of the 8th order filter when equal Q is assigned to each sub-network.

2. 8th order asymmetric example with transformed configuration

The parallel connected network in Fig. 4.31 could be utilized to realize asymmetric characteristic when the 6th order ladder sub-network has asymmetric couplings as shown in Fig. 4.31. The CM for this configuration is synthesized by adding a constant phase φ to the even and odd mode S parameters as in (4.26).

$$S_e' = S_e e^{j\varphi}$$
$$S_o' = S_o e^{j\varphi} \tag{4.26}$$

$$Y_e' = \frac{Y_e - j\tan\left(\varphi/2\right)}{1 - jY_e\tan\left(\varphi/2\right)}$$
$$Y_o' = \frac{Y_o - j\tan\left(\varphi/2\right)}{1 - jY_o\tan\left(\varphi/2\right)} \qquad (4.27)$$

From the even and odd mode S parameters, the even and odd mode admittance parameters could be derived as in (4.27) which are also modified by the phase φ.

Using the modified even and odd mode admittance parameters, we could derive a new set of residues and poles for each φ. In order to synthesize the network in Fig. 4.34, the poles and residues need to be divided into two groups; also the two residues that form the 2nd order sub-network should have equivalent values. A sweep of φ is used and the values of the residues are compared in each case until two of them are equal. It is noted in this step that this synthesis problem has multiple solutions. Then CM transformations are applied to each sub-network to obtain the ladder networks which are finally parallel connected. The theory of this procedure will be presented in detail in a later publication.

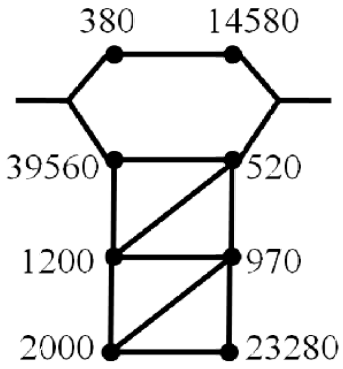

Fig. 4.34 Circuit model of the 8th order asymmetric filter with two sub-networks.

An 8th order filter with three transmission zeros at -1.7j, -1.9j and -2.5j with a centre frequency of 2 GHz and a bandwidth of 0.12 GHz is used to illustrate the idea. It is found that a phase of -1.5260 rad will give two equal residues.

The CM derived is given in Table 4.6. Because a phase shift is included in the S parameters, the reference admittances for this network are no longer

uniform but complex values dependent on φ. For this example, the values of the source and load admittance are both *1+0.9562i*. The response is shown in Fig. 4.35.

Table 4.6 Values of the elements in for the 8th order network

M_{S1}	0.5867	M_{78}	-0.7603	B_1	-0.0191	δ_1	0.04383
M_{12}	0.2782	M_{8L}	1.2992	B_2	-0.0190	δ_2	0.00114
M_{2L}	0.5867	M_{38}	-0.0568	B_3	1.2080	δ_3	0.00042
M_{S3}	1.2992	M_{47}	0.0664	B_4	-0.4486	δ_4	0.01382
M_{34}	-0.7809	M_{48}	-0.1783	B_5	0.5308	δ_5	0.00831
M_{45}	-0.5169	M_{57}	0.4619	B_6	0.8682	δ_6	0.00071
M_{56}	0.2016			B_7	-0.4797	δ_7	0.01717
M_{67}	-0.4072			B_8	1.2080	δ_8	0.02963

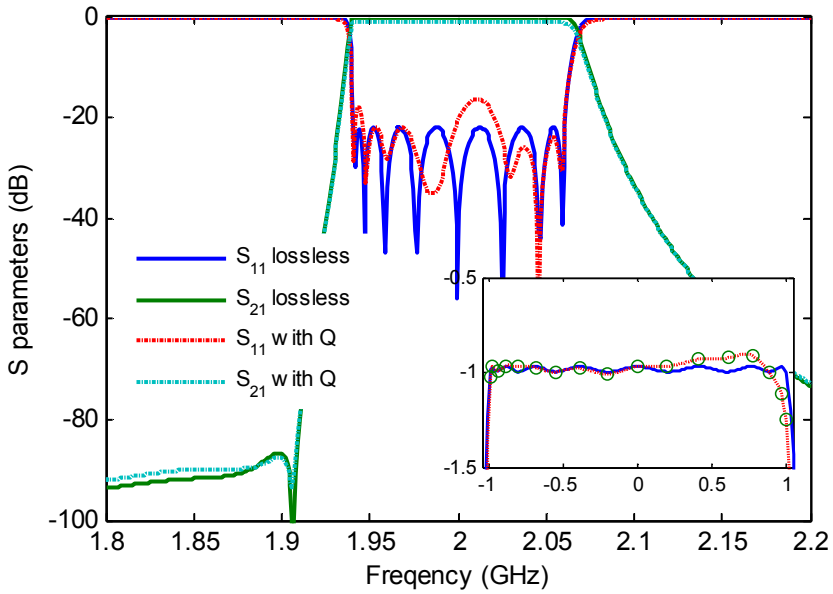

Fig. 4.35 S parameters of the 8th order asymmetric filter compared to the lossless case.

4.4 Filter implementation

A parallel connected network requires the parallel connection of N resonators for an N^{th} degree filter and is sometimes difficult to implement. For an even degree symmetric network, poles and residues can be grouped to form sub-networks which can be applied with similarity transformations independently [8]. The final network is the parallel connection of these sub-

networks. In this way, the number of parallel connected branches can be reduced.

Considering the effect of loss distribution, the critical resonators can be assigned to one group with high Q, and each sub-network can be designed with an equal Q distribution. In this way, similarity transformation applied will not introduce losses into cross couplings. The example is the design of a 4th order filter. First a mixed coaxial and microstrip design will be introduced followed by a mixed coaxial and dielectric design.

4.4.1 Mixed coaxial and microstrip design

The following is an example of a symmetric 4th order Chebyshev filter with two transmission zeros normalized at ±1.6j. The centre frequency is 2 GHz, and the bandwidth is 0.12 GHz.

Step 1 CM synthesis for the lowpass prototype

For this symmetric network, the transversal array can be transformed into the parallel connection of two 2nd order networks as in Fig. 4.36. For this network, it is found that when resonators 3 and 4 have Q of 150, and the others have high Q of 1000, the insertion loss in the passband is less distorted than the one with equal Q of 1000. The circuit could be realized by a combined coaxial and microstrip technology.

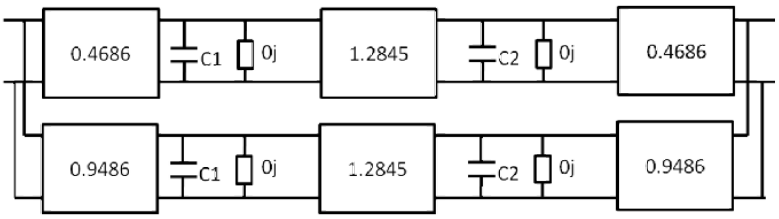

Fig. 4.36 Circuit model of the 4th order symmetric filter with two 2nd order parallel connected sub-networks with C_1=C_2= C_3=C_4=*1*.

Step 2 EM designs of branches

The high Qu branch utilizes coaxial resonators. The input couplings are realized by probes. The probes are transformed to microstrip lines. The low Qu branch is realized by hairpin microstrip resonators. The substrate used is Rogers Duroid 6010 with a thickness of 1.27 mm.

Step 3 Filter design

The final parallel network is then realized by connecting the branches using a microstrip T junction as shown in Fig. 4.37. The microstrip lines connecting each sub-network to the T junction need to be fine tuned to match the phase of the two parallel connected networks. The Q for the coaxial resonator and the microstrip resonator are 4000 and 220 respectively. The response of the EM model is shown in Fig. 4.38.

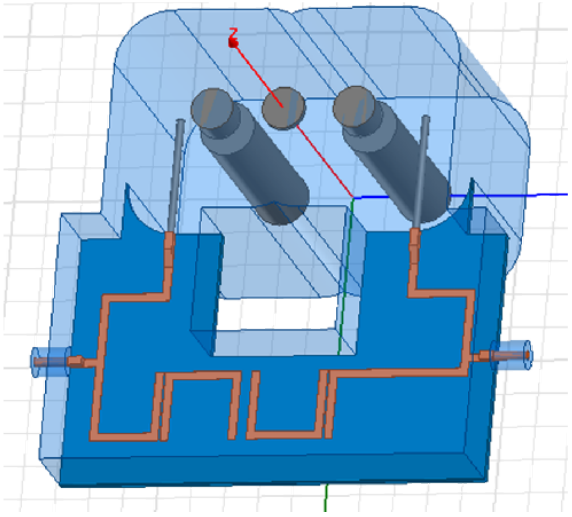

Fig. 4.37 EM model of the combined coaxial and microstrip filter.

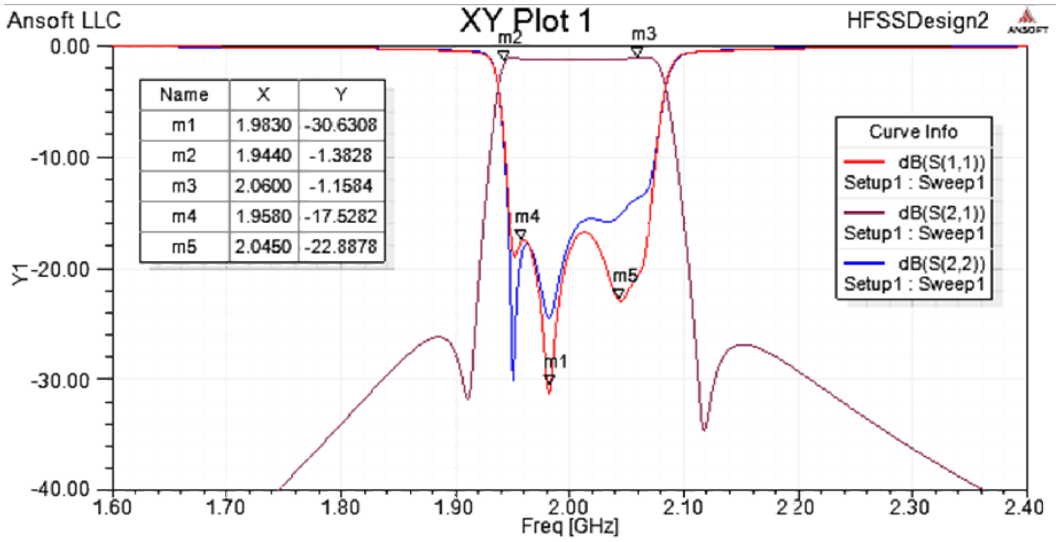

Fig. 4.38 Response of the 4th order Chebyshev filter with higher loss included in different resonators compared to one with an equal high Qu.

Step 4 Manufacture

A photo of the filter made is shown in Fig. 4.39 and the measurement result is compared with the simulation results in Fig. 4.40. The manufactured filter is tuned by tuning screws controlling the center frequency of the coaxial

resonator and the coupling between them. The deviation of the center frequency and bandwidth between the simulated and measured results is due to the mismatch of the resonant frequency of the microstrip lines. The measured passband insertion loss is 0.3 dB higher than the simulated filter. This is caused by the Q factor of the coaxial resonators being a little lower than predicted.

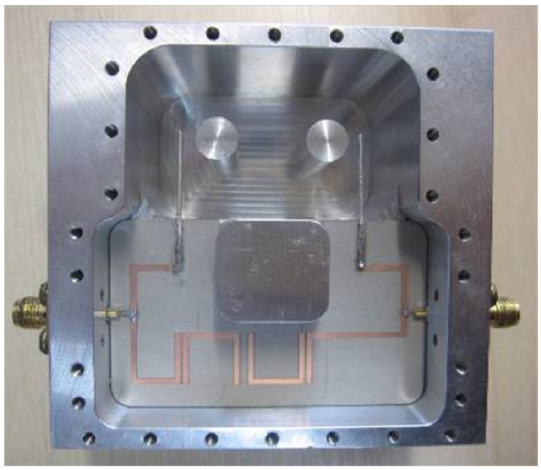

Fig. 4.39 Photo of the filter manufactured.

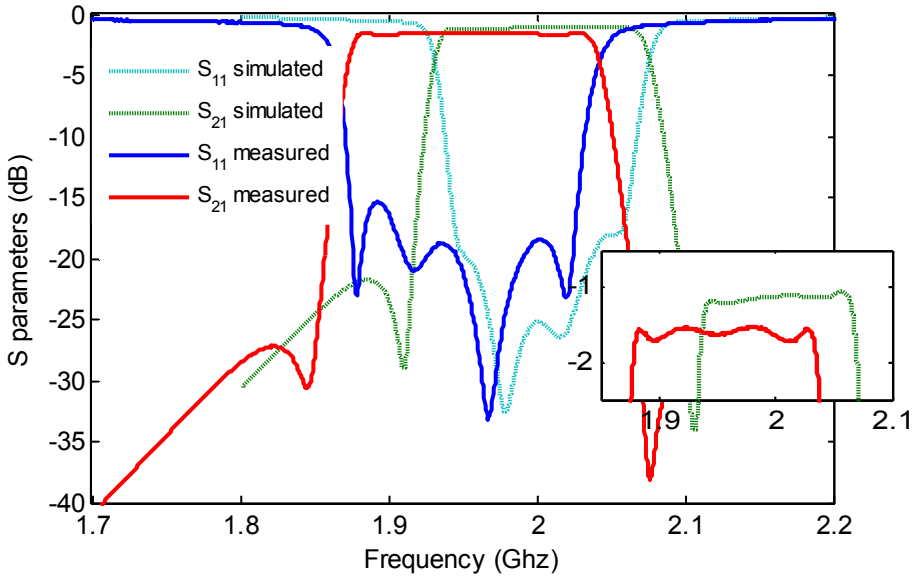

Fig. 4.40 Measurement result of the filter shown in Fig. 4.31.

4.4.2 Mixed coaxial and dielectric resonator design

The same Chebyshev response as in last section is used here for a lower loss design. The high Qu branch is realized by dielectric resonators shown in Figure and the low Qu branch is realized by coaxial resonators. The sub-

networks for the two branches are designed separately using a 2nd order coaxial network with Qu of 4000 and a 2nd order dielectric network with Q of 16000. The eigenmode analysis is applied to dielectric resonators as shown in Fig. 4.41. The effect of tuning disk is shown in Table 4.7 for the first five modes. The coupling between dielectric resonators is realized by windows and enhanced by a probe. The input and output coupling to the dielectric resonators are realized by probes.

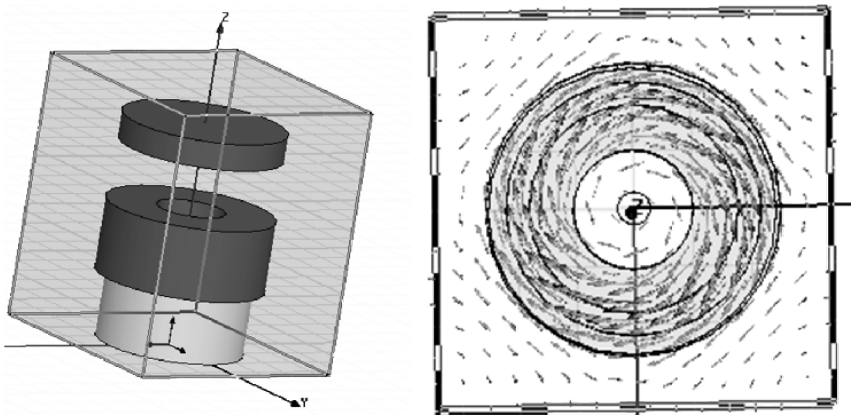

Fig. 4.41 EM model of a typical dielectric resonator and its E field distribution.

Table 4.7 The resonant frequency and Qu for the first five modes.

27	30	35
2.12, 14000	2.13, 14000	2.14, 14000
2.85, 10000	2.90, 15000	2.94, 9700
2.85, 10000	2.90, 10000	2.94, 9700
2.85, 16000	2.90, 10000	3.16, 13000
3.15, 15000	3.16, 14000	3.17, 13000

For the low Qu branch, coaxial resonators are used. The coupling between coaxial resonators is realized by a window at the top of the two resonators. A similar bottom coupling is introduced in [89]. The input and output couplings are realized by probes contacting the resonators.

The final network is then realized by connecting the branches in parallel as shown in Fig. 4.42 which is then simulated in HFSS. Because of the low loss of this design, the simulated results shown in Fig. 4.43 give perfect insertion loss.

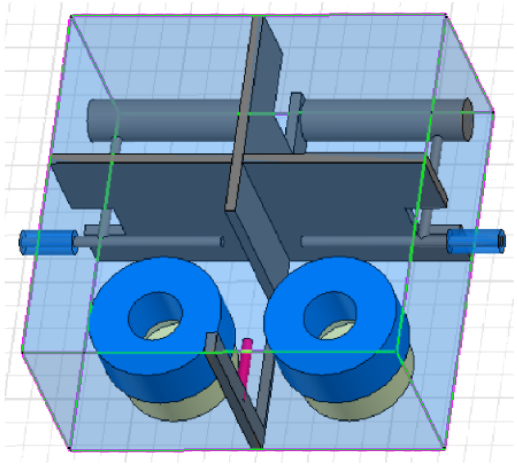

Fig. 4.42 EM model of the 4th order filter with mixed dielectric and coaxial resonators.

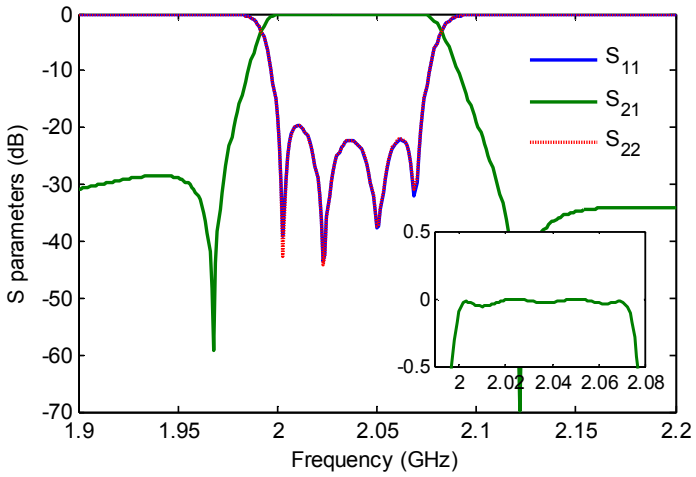

Fig. 4.43 S parameters simulated using the model in Fig. 4.42.

Chapter 5
Coupling Matrix Synthesis for Diplexers

In communication systems, microwave filters are usually assembled to form a diplexer or a multiplexer which allows signals of different frequency bands to be combined or separated. In mobile base stations, the implementation of diplexers allows signal from two different bands to be transmitted or received simultaneously on a single antenna [4]. Multiplexers are used for more complex frequency division architectures [1].

A multiplexer consisting of a manifold and several channel filters is given in [90]. The design method is based on non-linear optimization of the phase length between each channel for reduced interaction as well as the optimization of channel filters for enhanced matching. Starting from singly terminated filters [91], non-contiguous or contiguous multiplexer can be tuned to meet various specifications. A complete circuit representation of a diplexer or a multiplexer can be synthesized using the method in [92][93]. In this method, the rational polynomial expressions for the multi-port S parameters are derived first from iterations. Then CM for each filter and the circuit model for the junction is synthesized. However, the method is only valid to a limited type of junction.

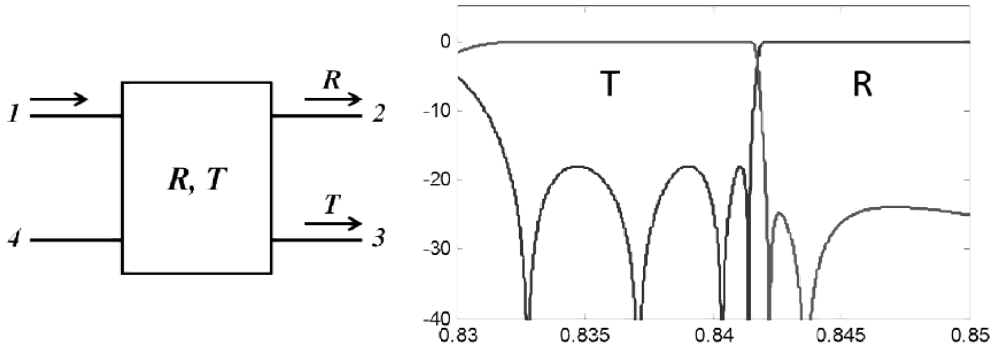

(a) (b)

Fig. 5.1 A simplified diagram for a DF (a) and its response (b) that can be used for power combining.

Diplexers or multiplexers can also be designed based on the concept of directional filters (DF) that has been presented in the literature over the past decades including the use of striplines [94]-[96] and waveguide [97]. A DF is

a matched four-port device shown in Fig. 5.1(a) with an input at port 1. Power emerges at port 2 with the frequency response of a band-pass filter and the remaining power emerges at port 3 with the complementary response of a band-reject filter as illustrated in Fig. 5.1(b). Port 4 is isolated. Because of the transmission characteristics of DF's, they may be used for signal combining or multiplexing as in [98].

In this chapter, the above two methods for the design of a diplexer are discussed with techniques introduced for improvement. In the first design method, as a channel filter is connected to a 3-port junction, the connecting port sees the junction and the other channel. For the channel filter, this effect can be interpreted as a frequency variant load impedance. After the design of common junction by optimizing phase length at each port, an analytical method is given for the synthesis of CM for a channel filter with correspondence general load impedance.

In the second method a diplexer is built from cascaded DF sections. As shown in [102], while a single section of DF realizes a first order filter characteristic, cascaded DF sections are capable of realizing any filter characteristics that can be expressed by rational polynomials. As opposed to conventional techniques of designing diplexers, this technique does not involve the design of channel filters or junctions. Instead, a single bandpass filter characteristic is used such that the insertion and return loss of this bandpass filter provides the forward transmission characteristics of each band. Because the two passbands are formed by the insertion and return loss of a single filter characteristic, the two channels of the combiner have no interaction even when the two bands are very close to each other.

5.1 CM synthesis with non-ideal load impedance

The CM synthesis method given in chapter 2 is based on a lowpass prototype network with uniform source and load impedance. However, for a filter integrated into a diplexer or a multiplexer, its output port is connected to a junction. The method of synthesis based on a uniform load is not valid in this case. The objective of this work is to find a direct approach to the design of a channel filter with a general frequency variant complex load.

5.1.1 Reference impedance for two-port filter networks

The filter network with a uniform and general frequency variant load is shown in Fig. 5.2 with two different sets of S parameters *[S']* and *[S]*.The derivation of S parameters in [78] is based on the definition of reference impedance. The filter network in Fig. 5.2(a) and (b) are the same. However, the difference of S parameters are due to the difference of reference load impedances of unitary and Z_L correspondingly.

[S'] is unknown, but since it has a unitary load impedance, it can be used for the synthesis of a CM. The filter response is given in [S]. Using the theory of power wave renormalization [78], a transformation of S parameters (5.1) with respect to reference impedance can be used to derive [S'] from [S].

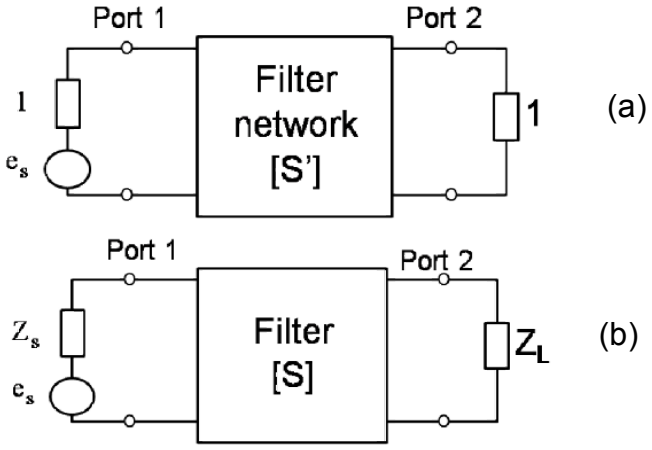

Fig. 5.2 illustration of reference impedance of (a) channel filter with response [S] and (b) ideal filter circuit model with response [S'].

$$
\begin{aligned}
s'_{11} &= s_{11} + \frac{s_{21}^2 r_2}{1 - r_2 s_{22}} \\
s'_{22} &= \frac{(1 - r_2)(s_{22} - r_2^*)}{(1 - r_2^*)(1 - r_2 s_{22})} \quad , \; r_2 = \frac{1 - Z_L}{1 + Z_L^*} \\
s'_{21} &= \frac{(1 - r_2) s_{21}}{\sqrt{\mathrm{Re}(Z_L)}(1 - r_2 s_{22})}
\end{aligned}
\tag{5.1}
$$

The procedure of earlier method [99] and [100] can be summarized as follows:

1. Designing a template of general Chebyshev filter of degree N [8] and deriving the response *[S]*.
2. Deriving the response *[S']* by renormalizing the reference impedance from complex load Z_L to unitary load.
3. Synthesizing a CM according to the response *[S']*.

The concept for the designing of a channel filter proposed in [99] focuses on a constant complex load. The method of synthesis is straightforward as the constant load gives a constant r_2 and modifications to S parameters can be found according to (5.1) without changing the degree of the polynomials. When the load is frequency variant, the load impedance at center frequency is used. As a result, the method is restricted to narrowband cases.

Frequency variant complex load is studied in [99]. Instead of only matching to constant complex impedance, the variation of the complex impedance vs. frequency is also taken into consideration in the proposed approach. The admittance matrix of a filter network is independent to the impedance reference and can be derived from the S parameters with reference impedances as in (5.2) with load impedance Z_L at output port.

$$\begin{aligned} y'_{11} &= \frac{(1-s_{11})(Z_L^* + Z_L s_{22}) + Z_L s_{21}^2}{(1+s_{11})(Z_L^* + Z_L s_{22}) - Z_L s_{21}^2} \\ y'_{22} &= \frac{(1+s_{11})(1-s_{22}) + s_{21}^2}{(1+s_{11})(Z_L^* + Z_L s_{22}) - Z_L s_{21}^2} \\ y'_{21} &= \frac{-2\sqrt{\mathrm{Re}(Z_L)}s_{21}}{(1+s_{11})(Z_L^* + Z_L s_{22}) - Z_L s_{21}^2} \end{aligned} \tag{5.2}$$

Then the polynomial expressions for the admittance parameters can be found for lossless case as in (5.3). For a frequency variant load impedance Z_L, the polynomials in (5.3) are of higher degree than the original design of S parameter. As a result, it is impossible to find the CM providing the same S parameter response with a frequency variant load.

A method of curve fitting is used in [100] to maintain the degree of admittance parameters. It is found that with proper modifications to the phase of S parameter response, the original denominator of admittance parameters can be derived. However, the accuracy of the method depends on the validation of curve-fitting. The rapid changing load impedance gives poor response for the synthesized CM.

$$\begin{aligned} y'_d &= (E(s) + F_{11}(s))Z_L^* + \left((E(s) + F_{11}(s))Z_L^*\right)^* \\ y'_{11n} &= (E(s) - F_{11}(s))Z_L^* - \left((E(s) - F_{11}(s))Z_L^*\right)^* \\ y'_{22n} &= (E(s) - F_{22}(s))Z_L^* - \left((E(s) - F_{22}(s))Z_L^*\right)^* \end{aligned} \tag{5.3}$$

5.1.2 A special case with exact solutions

Using the general expression for the rational polynomial of S parameters given in Chapter 3, the transformation of S parameters in (5.1) can be rewritten into the transformation of polynomials of S parameters as in (5.4).

$$\begin{aligned}
F_{11}(s)' &= (1+Z_2^*)F_{11}(s) - (1-Z_2)E^*(s) \\
F_{22}(s)' &= (1+Z_2)F_{22}(s) - (1-Z_2^*)E\ (s) \\
E(s)' &= (1+Z_2^*)E(s) - (1-Z_2)F_{22}(s) \\
E_x(s)' &= (1+Z_2)E^*(s) - (1-Z_2^*)F_{11}(s) \\
P(s)' &= 2\sqrt{\mathrm{Re}(Z_2)}P(s)/\varepsilon
\end{aligned} \tag{5.4}$$

Constant load Z_L can lead to a set of polynomials of $F_{11}'(s)$, $E'(s)$ and $P'(s)$ which are of the same degree as the originally designed ones. And CM synthesis can be applied without modifications. When the load impedance is frequency variant, the degrees of those polynomials must be increased. As a result, CM can only be found by least square polynomial fitting. Besides, filter topology may be changed because of the fitting to the P polynomial.

A special case is found when the load impedance has a linear imaginary part and a constant real part. For this kind of load impedance, the polynomials on the left are found to have the original degree and an exact synthesis is possible. Suppose the frequency variant part of Z_L is purely imaginary as in (5.5), substituting it into (5.4), we have (5.6). When the response is of degree N, the second term will an Nth degree polynomial when Z_x is of first order since the highest term in F_{11}-E^* is cancelled.

$$Z_L = 1 + jZ_x \tag{5.5}$$

$$\begin{aligned}
F_{11}(s)' &= 2F_{11}(s) - jZ_x\left(F_{11}(s) - E^*(s)\right) \\
F_{22}(s)' &= 2F_{22}(s) + jZ_x\left(F_{22}(s) - E(s)\right) \\
E(s)' &= 2E(s) + jZ_x\left(F_{22}(s) - E(s)\right) \\
E_x(s)' &= 2E^*(s) - jZ_x\left(F_{11}(s) - E^*(s)\right) \\
P(s)' &= 2P(s)/\varepsilon
\end{aligned} \tag{5.6}$$

The example is a fourth degree Chebyshev filter with one transmission zero at *1.7j*. The load impedance is assumed to be $Z=0.3s+(0.8j+0.5)$. The original and modified coefficients for the rational polynomials of S parameters are listed in Table 5.1.

The derived CM matched to the load is compared with the original ones in Table 5.2. When deriving the matched CM with constant complex load impedance, the elements M_{NN} and M_{NL} are changed. For this frequency variant load impedance, the element corresponds to the final resonator and the couplings to it are changed. It can be deduced that with the increase complexity of the load impedance, more elements in the CM are required to be modified to provide a matched response. The response of the CM with match load is compared with the unmatched one in Fig. 5.3.

Table 5.1 Coefficients for the rational polynomials of S parameters

F11	P	E	Ex	F11'	P'	E'	Ex'
1.0000	0	1.0000	1.0000	0.3597	0	0.3597	0.3597
- 0.3252i	0	2.1344 - 0.3252i	-2.1344 - 0.3252i	1.7506 - 1.7897i	0	2.5183 - 1.7897i	-2.5183 - 1.7897i
0.9736	0	3.2514 - 0.8101i	3.2514 +0.8101i	-1.6238 +1.1208i	0	2.9319 - 2.7409i	2.9319 + 2.7409i
- 0.2439i	0.8090	2.7013 - 1.2321i	-2.7013 - 1.2321i	2.4253 - 1.6455i	1.1441	2.9773 - 3.6218i	-2.9773 - 3.6218i
0.1118	- 1.3753i	1.0589 - 0.8847i	1.0589 +0.8847i	-1.0695 +0.3153i	- 1.9450i	0.8246 - 2.0847i	0.8246 + 2.0847i

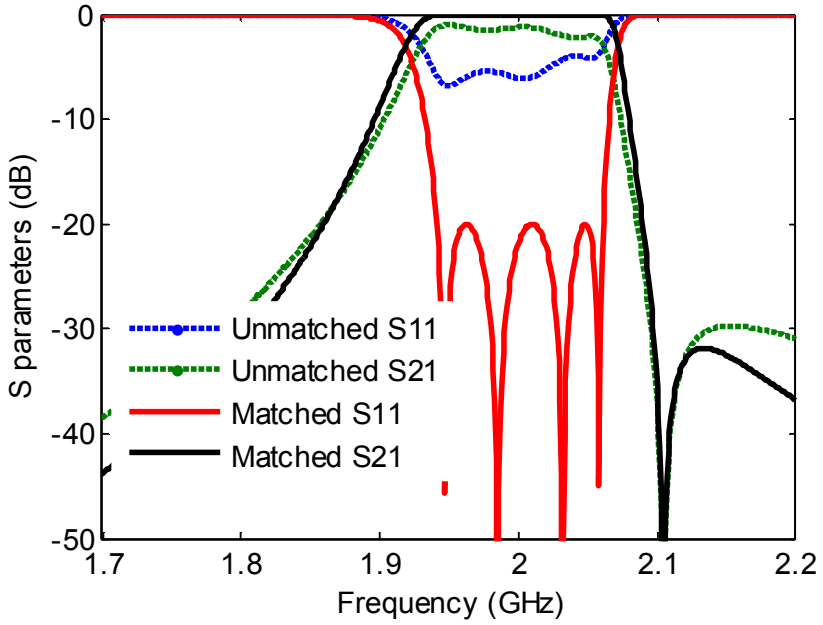

Fig. 5.3 S parameters of the network with matched and unmatched CM with frequency variant load.

Table 5.2 Original and matched CMs.

0	1.0331	0	0	0	0

1.0331	0.0543	0.9090	0	0	0
0	0.9090	0.0952	-0.6045	0.4170	0
0	0	-0.6045	-0.5290	-0.8077	0
0	0	0.4170	-0.8077	0.0543	1.0331
0	0	0	0	1.0331	0

0	1.0331	0	0	0	0
1.0331	0.0543	0.9090	0	0	0
0	0.9090	0.0952	-0.6045	0.6953	0
0	0	0.9090	-0.5290	1.3468	0
0	0	0.6953	1.3468	-4.5965	2.4360
0	0	0	0	2.4360	0

5.1.3 Synthesis with iterations

When the exact synthesis is only valid for specific load impedance, an iteration method can be derived for general load impedance. First, the inverse transformation of (5.4) can be derived where the response of matched filter ($F_{11}''(s)$ and $E''(s)$) is derived from the response of circuit model ($F_{11}'(s)$ and $E'(s)$) and load impedance as in (5.7).

$$\begin{aligned}
F_{11}''(s) &= (Z_L+1)F_{11}'(s) - (Z_L-1)E'^{*}(s) = F_{11}^0 X \\
F_{22}''(s) &= (Z_L^*+1)F_{22}'(s) - (Z_L^*-1)E'(s) = F_{22}^0 X^* \\
E''(s) &= (Z_L+1)E'(s) - (Z_L-1)F_{22}'(s) = E_0 X \\
E_x''(s) &= (Z_L^*+1)E_x'(s) - (Z_L^*-1)F_{11}'(s) = E_x X^* \\
P''(s) &= 2*(1/\sqrt{\mathrm{Re}(Z_L)})P'(s)/\varepsilon = P_0|X|
\end{aligned} \tag{5.7}$$

The degree of the polynomials in (5.7) are higher than N when Z_L is a general load impedance represented by a polynomial of degree higher than 1. If we can find a circuit model of degree N whose response is expressed by $F_{11}'(s)$, $E'(s)$ and $P'(s)$, the degree of the response of matched filter must be higher than N. The question is $F_{11}''(s)$ and $E''(s)$ are unknown.
The characteristics of a Chebyshev response are defined by its zeros and roots. We can make such a constraint that $F_{11}''(s)$ and $E''(s)$ must contain the zeros of the originally designed response F_{11}^0 and E^0. Thus the polynomial $F_{11}''(s)$ can be divided into the multiplication of two parts: the original polynomial F_{11}^0 and an additional polynomial that is represented by X in the above expression. With $F_{11}''(s)$ and $E''(s)$, the S parameters of the matched filter will be as in (5.8).

$$
\begin{aligned}
s_{11}'' &= s_{11}^0 \\
s_{21}'' &= s_{21}^0 \left| X_2 \right| / X_2 \\
s_{22}'' &= s_{22}^0 X_2^* / X_2
\end{aligned}
\tag{5.8}
$$

The magnitudes of S parameters in (5.8)are the same as the originally designed ones, while the phases are changed according to X. Conservation of energy is still satisfied because the phase of S_{11} is not changed and the amount of phase change of S_{21} is half of that of S_{22}.

With given load impedance and originally designed $F_{11}{}^0$ and E^0, an iteration method as follows is used to derive $F_{11}'(s)$, $E'(s)$ and $P'(s)$ which are used for the synthesis of CM.

1. The initial E polynomial is the original E_0 polynomial for desired response as in (5.9).

$$
E'(s) = E_0(s) \tag{5.9}
$$

2. Iteration

Since we know (1) both $F_{11}''(s)$ and $E''(s)$ have the same zeros in the passband as $F_{11}{}^0$ and E^0; (2) the highest coefficients of $F_{11}'(s)$ and $E'(s)$ are both unitary, the problem of finding other coefficients is simplified to a linear system problem.

i. Solving for $F_{11}'(s)$

The roots of $F_{11}{}^0$ are Z_{f0}. Given values of $E'(s)$ at Z_{f0}, we have the expressions in (5.10) for any of the roots of F_{11}''.

$$
\begin{aligned}
& F_{11}''(z_{f0}) \\
&= (1 + Z_L^*(z_{f0}))F_{11}'(z_{f0}) - (1 - Z_L(z_{f0}))E'^*(z_{f0}) \\
&= 0
\end{aligned}
\tag{5.10}
$$

Since $F_{11}{}^0$ has N zeros and the number of unknown coefficients is also N, an exact solution can be found.

ii. Calculating ε

ε is used for the normalization of the P polynomial. In order to keep the configuration of CM, we choose $P'(s)=P_0$. The value of ε is found in the iteration according to the required return loss level at band edge.

iii. Solving for $E'(s)$

The polynomial $E'(s)$ can be found by alternating pole method with given $P'(s)$ and $F_{11}'(s)$ as in (5.11).

$$F_{11}'(s) \cdot F_{22}'(s) + P'(s) \cdot P'^{*}(s) = E'(s) \cdot E'^{*}(s) \tag{5.11}$$

iv. Go back to i with updated $E'(s)$ until the changing of $E'(s)$ is less than a given tolerance.

5.1.4 Examples

The following is an example of designing a channel filter for waveguide diplexer. The two channel filters with general Chebyshev response are connected at a waveguide T-junction as shown in Fig. 5.4. The load impedance to one of the channel filter can be found from a combined EM simulation of the T-junction and circuit simulation of the CMs. The frequency variant load impedance is depicted in Fig. 5.5 with its real and imaginary parts.

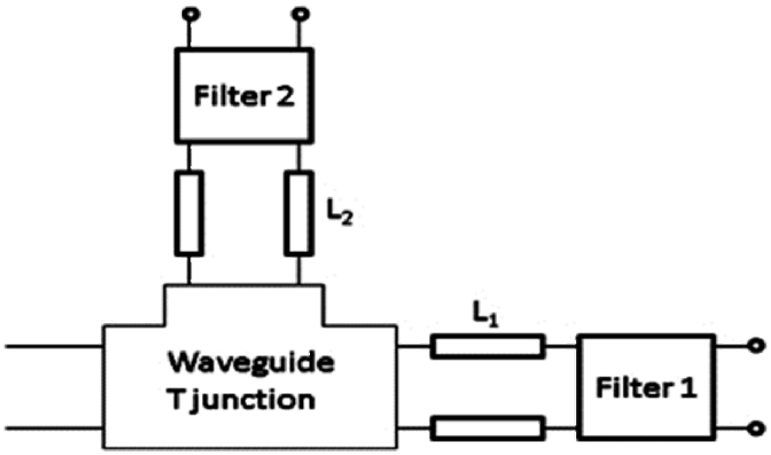

Fig. 5.4 illustration diplexer formed by two channel filter and a waveguide T-junction.

Then, a 5th degree Chebyshev filter with one transmission zero at -1.6j with the reference impedance will by synthesized using the iteration method. The

synthesized CM is given in Table 5.3 and the matched filter response is given in Fig. 5.6.

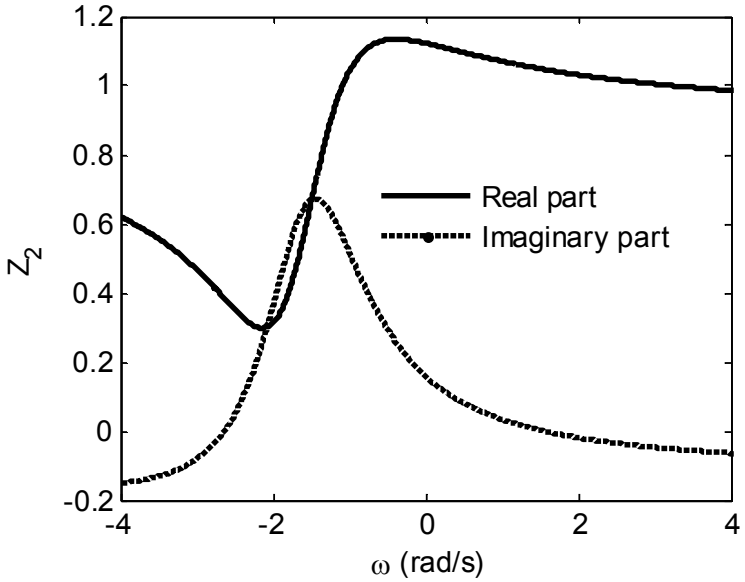

Fig. 5.5 Real and imaginary part of load impedance in the lowpass domain.

We can observe from earlier example that while the zeros of $F_{11}''(s)$ and $P'(s)$ are enforced to be the same as original, the zeros of $E''(s)$ are not exactly the same as original. As a result, reflection zeros of the network are not changed but the return loss can no longer be equal-ripple.

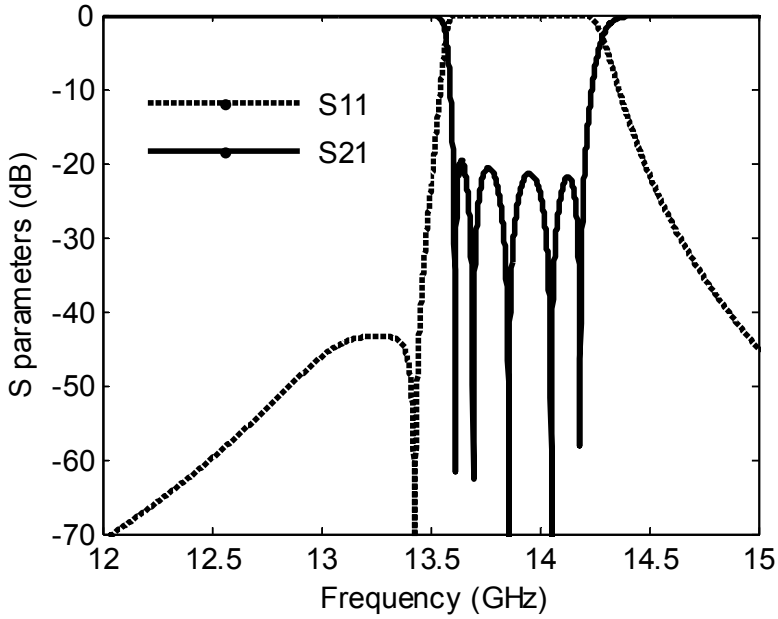

Fig. 5.6 S parameter of the network with matched S_{21}

Table 5.3 Synthesized CMs for the 5th order example.

0	1.0344	0	0	0	0	0
1.0344	-0.0548	0.8826	0	0	0	0
0	0.8826	-0.0587	-0.5777	-0.2895	0	0
0	0	-0.5777	0.4566	-0.5730	0	0
0	0	-0.2895	-0.5730	-0.0868	0.9801	0
0	0	0	0	0.9801	0.1294	1.2318
0	0	0	0	0	1.2318	0

The zeros of $F_{11}''(s)$ and $E''(s)$ can be forced to be the same as original in the iteration. In order to do this, the coefficients of $E''(s)$ will also be solved by a linear system problem similar to that of $E'(s)$. Using these new solutions, S_{11} of the matched filter are exactly the same as original but S_{21} is not. The reason is that in the equation of transformation, the value of X in the transformation of $P'(s)$ polynomial is given once the load impedance is given. The values of X derived from solving the linear system of $F_{11}''(s)$ and $E''(s)$ are not necessarily the same as the one derived from $P'(s)$. This inconsistence cannot be neglected.

A conclusion can be made here that it is impossible to match a filter with any frequency variant load impedance while restoring its original magnitude of response. However, it is possible to find a “perfect” match by the tuning of load impedance so that it satisfies certain conditions and this will be our future work.

5.2 Synthesis and design of directional filters

The principles of operation of a DF used in this section are an extension on the work presented in [101]. A synthesis method for DF’s is presented in [102]. The design is based on a pole placement method where each single section of a DF is singly tuned to provide a pole of a bandpass filter. This may be realized by inserting two resonator networks between a pair of 90º hybrids. Cascading these matched four-port sections allows a multi-pole response equivalent to the characteristics an N^{th} degree filter. As in a transversal array, each section of the network corresponds to a pole of the filter’s admittance parameters [8]; each cascaded section in a DF realizes a pole of its S parameters.

The design process starts with a lowpass filter prototype and bandpass characteristics are achieved by standard transformations. Various approximations are used to derive a simplified and realizable equivalent circuit. The final circuit contains resonators and some internal couplings that can be implemented by standard filter technologies.

The design concepts are validated with a design of a cellular combiner with specifications used in uplink 800 MHz LTE bands. The design is based on the characteristics of a 4th order general Chebyshev filter and the required selectivity is achieved by two transmission zeros placed close to the passband. The cellular combiner was fabricated using coaxial resonators. The proposed solution achieves good isolation between the input ports, return loss and minimum in-band insertion loss.

5.2.1 Theories

5.2.1.1 Directional filter networks

The original design theory [101] was based on the DF configuration shown in Fig. 5.7. The DF consists of two identical filters and a pair of 3 dB hybrids. Giving the scattering matrix the filter network as in (5.12), the power incident at port 1 emerges at port 2 with the return loss of network and at port 3 with the insertion loss while port 1 is matched and port 4 is isolated. Regarding the simplified diagram in Fig. 5.1, the response of each port is giving as in (5.13).

$$[S] = \begin{bmatrix} S_{11} & S_{12} \\ S_{21} & S_{22} \end{bmatrix} \tag{5.12}$$

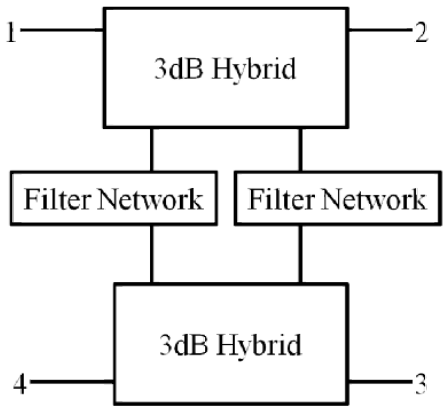

Fig. 5.7 Detailed diagram of DF with two identical filter networks inserted between a pair of 90º hybrids.

$$R = jS_{11}$$
$$T = jS_{21} \tag{5.13}$$

The complete admittances of a DF section are shown in Fig. 5.8 with the resonators be depicted as Y.

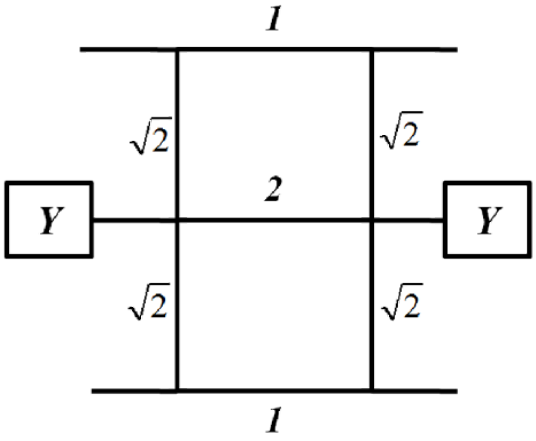

Fig. 5.8 Circuit diagram showing the admittances of a single section DF with 90º TL.

In our design, the filter network in Fig. 5.7 is a single resonator and higher order characteristics are achieved by cascading these single sections.The cascading of single section DFs are shown in Fig. 5.9. The response of a single section is shown in (5.14). For a cascade of two sections, (5.14) is the input to the second section. P_1 input at port 1 provides P_1R_1 at port 2 and P_1T_1 at port 3. Because of the symmetry of the network, Q_1 input at port 4 provides Q_1R_1 at port 3 and Q_1T_1 at port 2. So the response of two sections is the combination of those outputs as in (5.15).

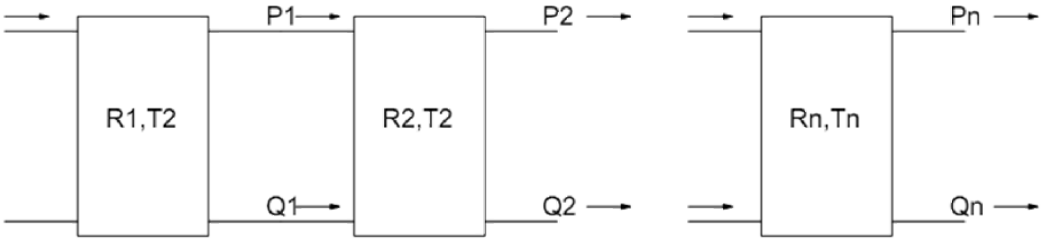

Fig. 5.9 Cascading of n single section DF's.

$$P_1 = R_1$$
$$Q_1 = T_1 \tag{5.14}$$

$$P_2 = R_1R_2 + T_1T_2 = P_1R_2 + Q_1T_2$$
$$Q_2 = R_1T_2 + T_1R_2 = P_1T_2 + Q_1R_2 \tag{5.15}$$

With (5.14) being the initial values, a recurrence formula in (5.16) can be derived for the cascading of n sections. From the expression for P_n+Q_n, we can derive the equation in (5.17) which represents an all-pass response.

$$\begin{aligned} P_n &= P_{n-1}R_n + Q_{n-1}T_n \\ Q_n &= P_{n-1}T_n + Q_{n-1}R_n \end{aligned} \tag{5.16}$$

$$P_n + Q_n = \prod_{i=1}^{n}\left(R_i + T_i\right) \tag{5.17}$$

5.2.1.2 Node diagram

As DF is a four-port network with admittances shown in Fig. 5.7, the analysis is usually done by a circuit simulator of connected transmission lines. It is noticed that the response of a DF network can be easily derived using a node diagram as shown in Fig. 5.10.

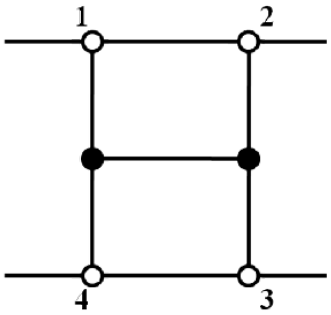

Fig. 5.10 Node diagram for a single section DF with lines representing invertors. The empty node represents non-resonating nodes.

The node diagram is obtained by replacing the 90º TL in Fig. 5.7 with admittance invertors. As a node diagram of a conventional filter, the lines represent couplings; the dark dots represent resonators and the empty dots represent non-resonating nodes. The couplings realized by invertors are related to the characteristic impedance of the TLs. For each DF section, a four port CM with six nodes could be derived from the node diagram. The response of the DF network can then be found using the multi-port CM analysis method given in [103].

An alternative configuration for single section DF may be found as shown in Fig. 5.11, while the dashed line represent negative couplings. This network is derived by scaling nodes in one of the hybrids in Fig. 5.10 and the two couplings in the center of the network cancel with each other. The response

of this network remains the same except the port 3 and port 4 are exchanged.

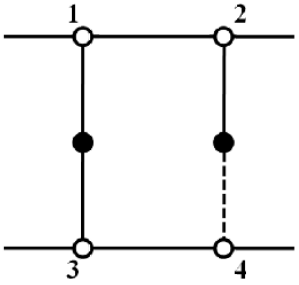

Fig. 5.11 The alternative configuration of the single section DF of Fig. 5.10.

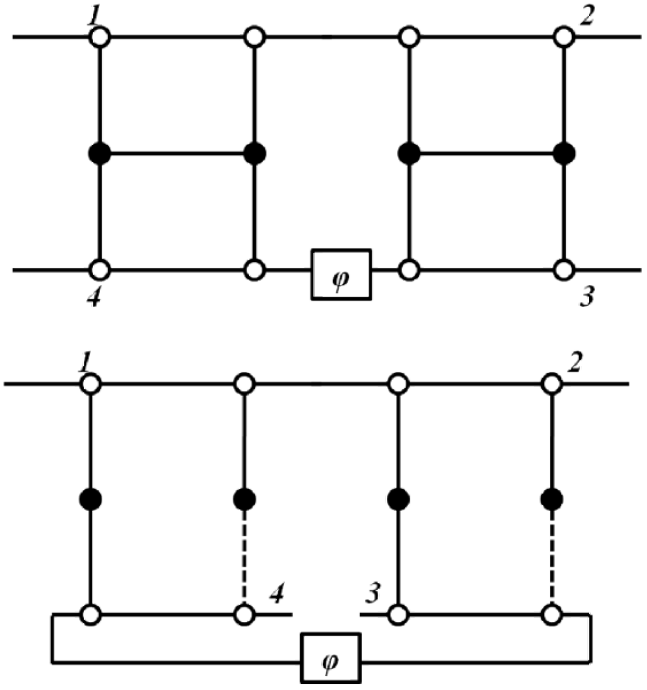

Fig. 5.12 Cascading of the single section DF (a) and its alternative (b).

An N^{th} degree DF is derived by cascading N sections. Unlike a conventional filter, sections can be cascaded in any order. Fig. 5.12 shows the connection of two sections for the two configurations with the 180º phase shifter which should be added after the section when the corresponding z_i is the same as the conjugate of p_i.

5.2.1.3 Circuit Realization

The S parameters of a lossless filter network may be expressed as rational polynomials and the sum of these parameters is given in (5.18) which is also

an all-pass response and n is the filter order, z_i represents a zero and p_i represents a pole.

$$S_{11} + S_{21} = \frac{F_{11} + P}{E} = \frac{\prod_{i=1}^{n}(s - z_i)}{\prod_{i=1}^{n}(s - p_i)} \tag{5.18}$$

From power conservation, we can derive (5.19), which states that p_i is the same as either z_i or its conjugate.

$$E \cdot E^* = (F_{11} + P) \cdot (F_{11} + P)^* \tag{5.19}$$

By equating the two all-pass responses in (5.17) and (5.18), for a given filter characteristics, P_n+Q_n are known as in (5.20). By the decomposition of poles, R_i and T_i of each section can be derived according to (5.21) which states that R_i and T_i have the same pole p_i and the zeros of the numerator of R_i+T_i are z_i. As a result, each pole of a filter characteristic may be realized by a single DF section and a higher order response may be formed by cascading DF's. The next problem is to find the network realisation with reflection coefficient R_i and transmission coefficient T_i.

$$P_n + Q_n = \frac{F_{11} + P}{E} \tag{5.20}$$

$$R_i + T_i = \frac{s - z_i}{s - p_i} \tag{5.21}$$

A simple resonator network as shown in Fig. 5.13 is used to provide the characteristics of R_i and T_i. The network consists of a capacitance C and a frequency invariant reactance B which is included for complex poles. The S parameters of this network are given in (5.22).

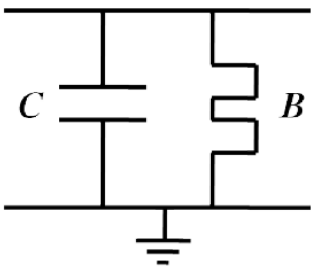

Fig. 5.13 Filter network to provide the required pole of a DF.

$$S_{11} = -\frac{s + jB/C}{s + jB/C + 2/C}$$
$$S_{21} = -\frac{2/C}{s + jB/C + 2/C} \tag{5.22}$$

Comparing (5.22) with (5.21), we obtain the values for the capacitance and frequency invariant reactance according to the values of poles as in (5.23). It should be noted that in the case when z_i is of the complex conjugate of p_i, a 180º phase shifter should be introduced after the i^{th} section.

$$C_i = -\frac{2}{\mathrm{Re}(p_i)}$$
$$B_i = \frac{2\,\mathrm{Im}(p_i)}{\mathrm{Re}(p_i)} \tag{5.23}$$

The final circuit for a section may be derived after some scaling and simplifications. Standard lowpass to band-pass transformations are applied. The branches for the 90º hybrid are replaced by an equivalent π network of inductances. Elements of the inductances of the π network are then merged with the resonators. The 90º TL with unit Z_0 at the input and output is replaced by an equivalent TL. The final circuit for the single section DF is given in Fig. 5.14. L' and C' can be realized by conventional resonators such as coaxial and dielectric resonators. The inductances L_v represents the input coupling to the resonators and L_m represents inter coupling between the resonators.

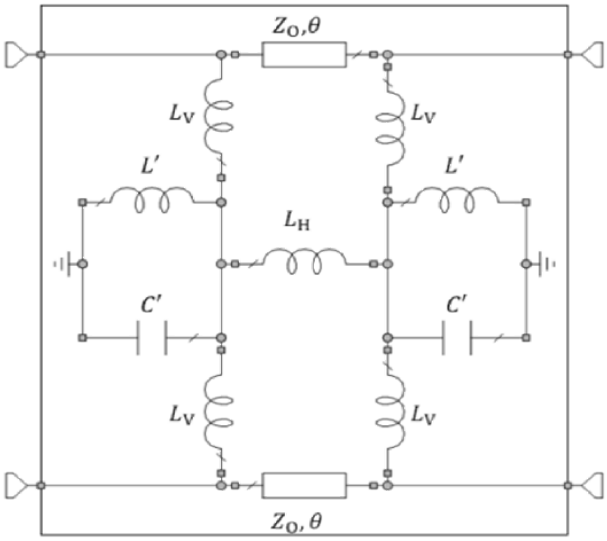

Fig. 5.14 Simplified circuit for a single section DF.

An N[th] degree DF is derived by cascading $n=N$ sections. A 180º phase shifter should be added after the section in which the corresponding z_i is the same as the conjugate of p_i as illustrated in Fig. 5.15. Unlike a conventional filter, sections of DFs can be cascaded in any order.

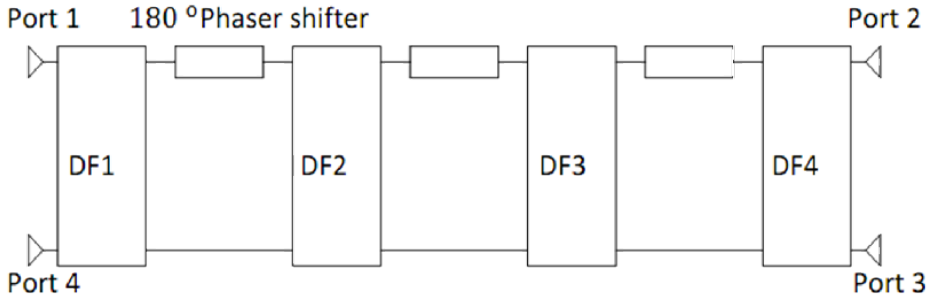

Fig. 5.15 Cascaded single section DFs with phase shifters.

5.2.2 Considerations of dissipations

As discussed in Chapter 4, different Qs can be assigned to parallel connected networks without deducing the selectivity. Each resonator in parallel connected network is independent of each other and is realizing one corresponding eigenmode. In the design of directional filter, each section of DF is realizing a pole of S parameters and can also be assigned with different Qs. The same optimization method as in Chapter 4 is applied to find the optimum Q distribution for directional filter.

1. N=4 symmetric example

This example is an $N=4$ Chebyshev filter with symmetric response. The two transmission zeros are at 1.6j and -1.6j in the lowpass domain. The optimized Q are 1455.7, 234.5, 234.0 and 1473.8 with two low-Q resonators and two medium Q resonators. The S parameter response is shown in Fig. 5.16(a) and is compared to the one with equal Q of 600 in Fig. 5.16(b).

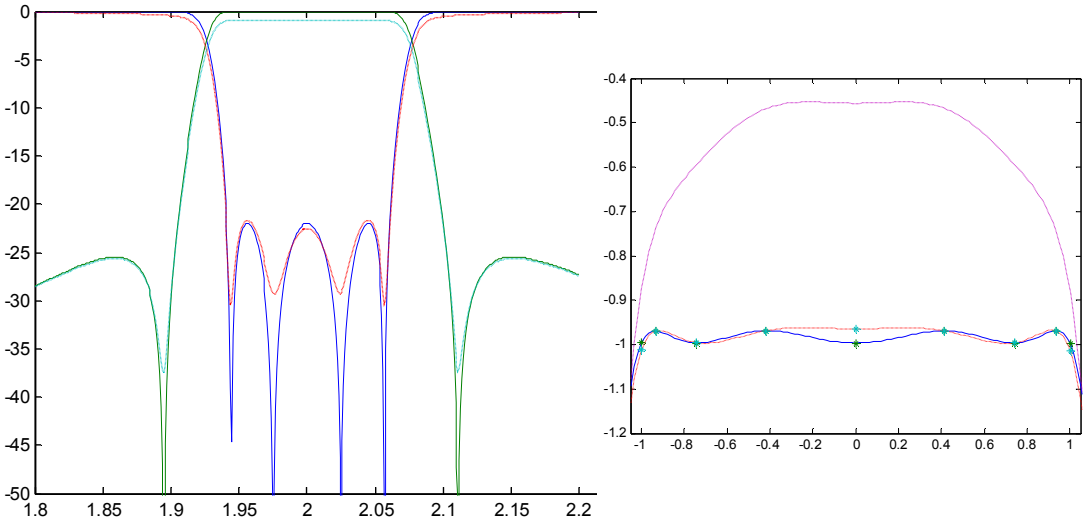

(a)(b)

Fig. 5.16 Response for N=4 filter with Qu distribution (a) compared to the one with equal Q of 600 (b).

Lower Q resonators could be used in the structure with lowered insertion loss levels. When the highest Q is confined to 400, the response is shown in Fig. 5.17(a). The insertion loss in the passband is reduced to -3 dB compared to -1 dB in the earlier example. The optimized Q are 400.5558, 78.1153, 78.0794 and 405.1020. The response is compared to the one with equal Qu of 160 in Fig. 5.17(b).

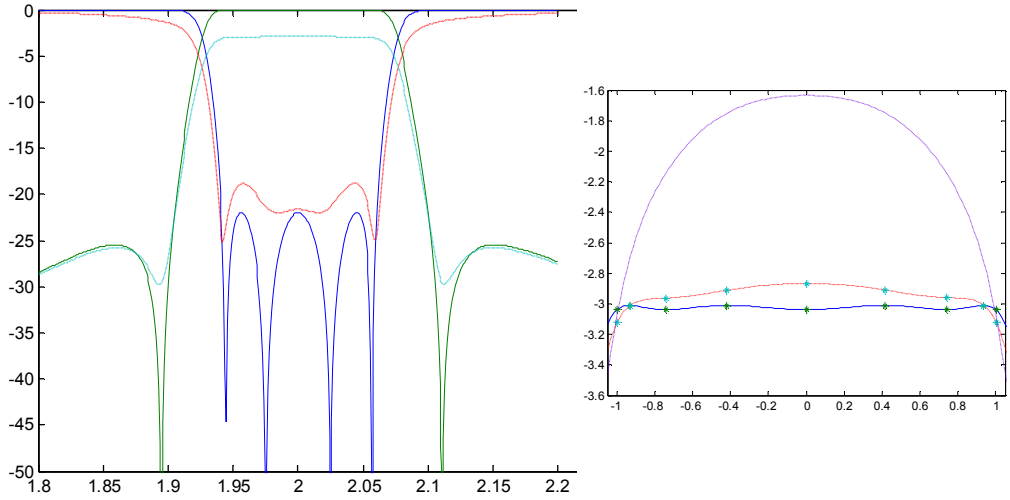

(a) (b)

Fig. 5.17 Response for N=4 filter with lowered Qu distribution (a) compared to the one with equal Qu of 160 (b).

2. N=4 Asymmetric example

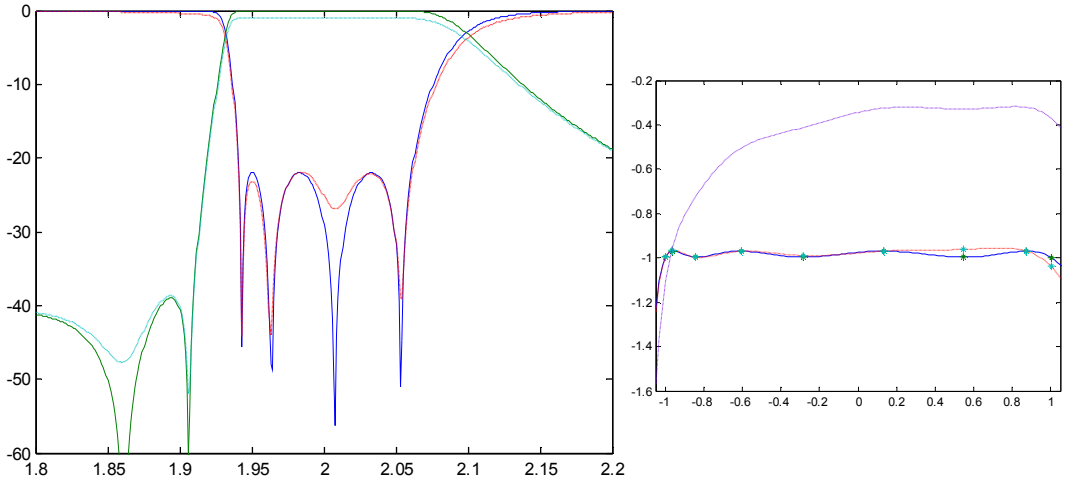

(a) (b)

Fig. 5.18 Response for the asymmetric 4th order filter with Q distribution (a) compared to the one with equal Q of 800 (b).

The optimization method is valid for asymmetric response. For this 4th order example, the transmission zeros are at -2.4j and -1.6j. The optimized Q are 291.0, 195.9, 4076.1 and 567.8. The high Qu resonator is due to the high selectivity of this response at the lower bandedge. The response has similar selectivity as the one with equal Q of 800 as shown in Fig. 5.18.

For the cascading of DFs, a phase shifter can be inserted between sections. This provides an addition parameter that can be used in optimization. The response of the 4th order filter is shown in Fig. 5.19 with the optimized phase shifters. It can be seen that perfect transmission zeros could be realized. The Qus optimized in this example are 307.6, 197.2, 3819.0 and 562.6. The optimized phase shifters are -1.3694, 1.7074, 2.4064 and 2.6700 in degree.

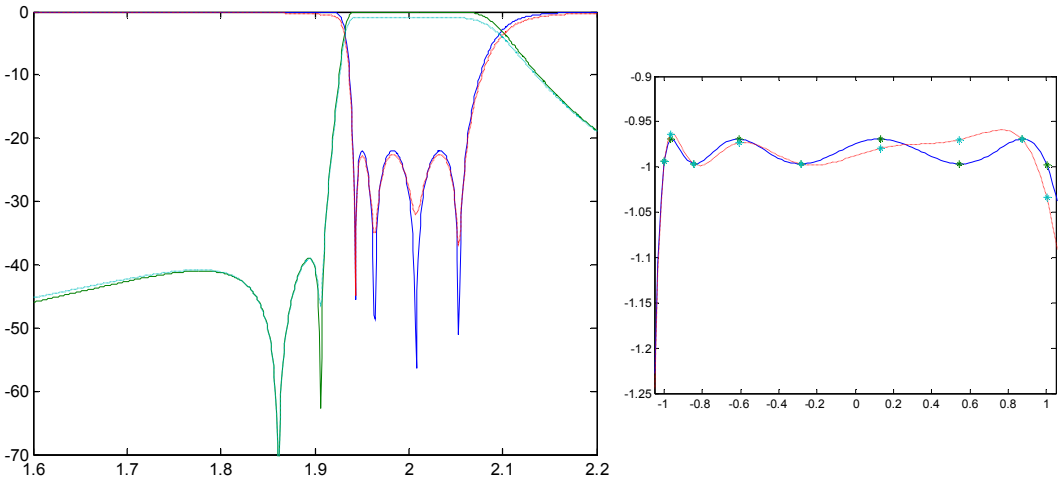

Fig. 5.19 Response for asymmetric 4th order filter with optimized Q distribution and phase shifter(a) compared to the one with equal Q of 800 (b).

3. N=5 asymmetric

This example is a 5th order Chebyshev filter with three transmission zeros at 1.8j, -2.6j and -4j. The optimized Q are 589.8, 306.4, 418.4, 3666.3 and 1017.4. The response is compared to the one with equal Q of 1200 in Fig. 5.20.

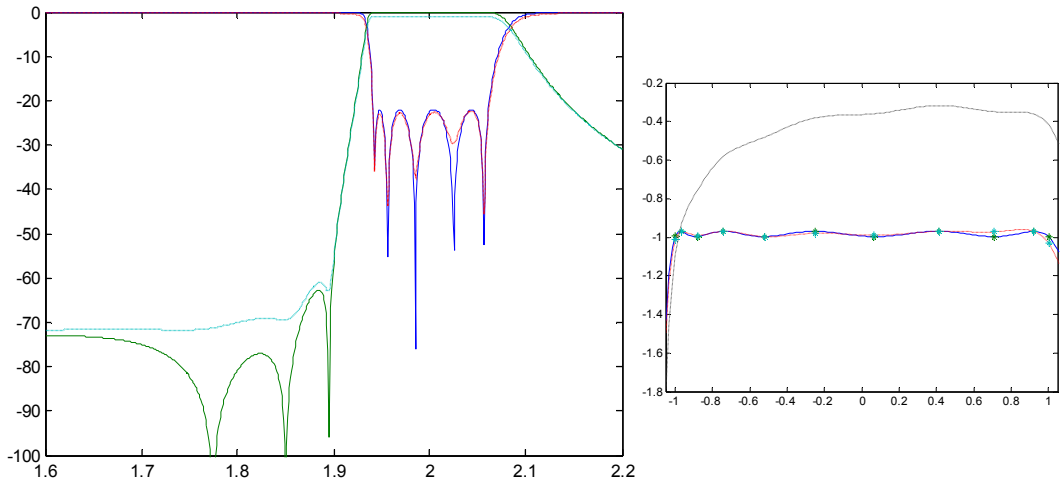

Fig. 5.20 Response for 5th order filter with Q distribution (a) compared to the one with equal Q of 1200 (b).

When optimized with phase shifter, the response is given in Fig. 5.21. The response shown has perfect transmission zeros. The optimized Q are 615.8 304.8 424.6 3638.5 985.3. The optimized values for phase shifters are -0.8193 0.6990 1.7361 0.8136 1.5699 in degree.

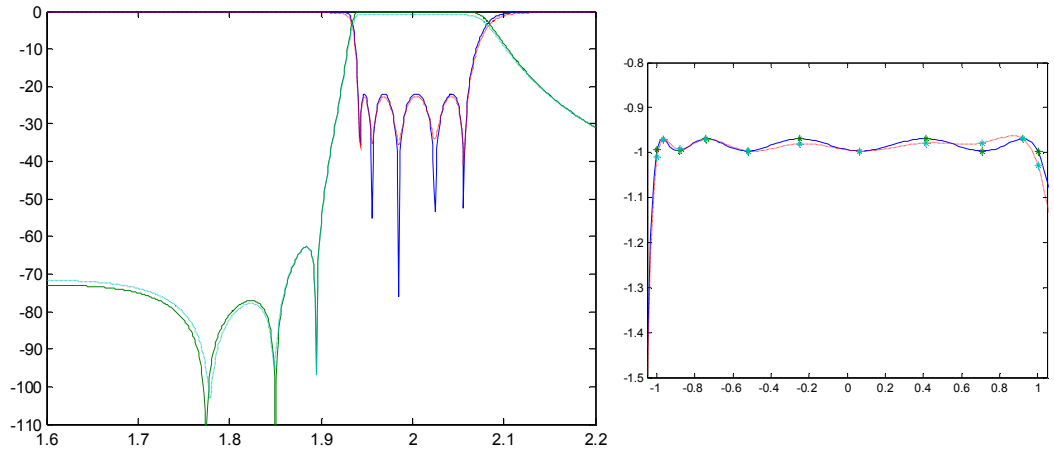

Fig. 5.21 Response for 5th order filter with optimized Q and phase shifters (a) compared to the one with equal Q of 1200 (b).

4. N=5 asymmetric

For this Chebyshev filter with transmission zeros at -1.8j -2.2j -3.8j, the response has equal rippled stop band and various parameters are used in the optimization. The response with the optimization of phase shifter is given in Fig. 5.22. The Qs are 594, 289, 444, 4508 and 997. The phase shifters are -0.4742, 0.8497, 1.6045, -0.1084 and 1.1680 in degree.

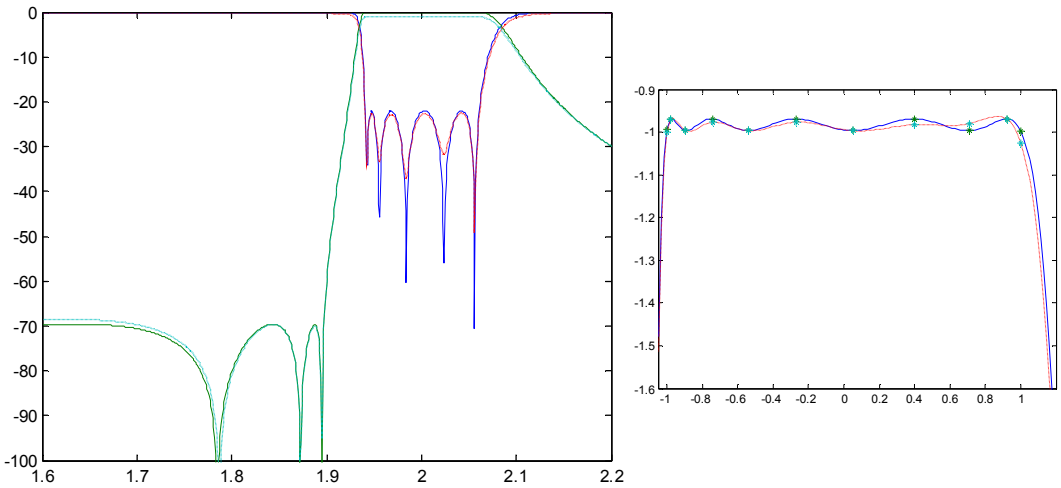

Fig. 5.22 Response for the 5th order filter with optimized Q and phase shifters.

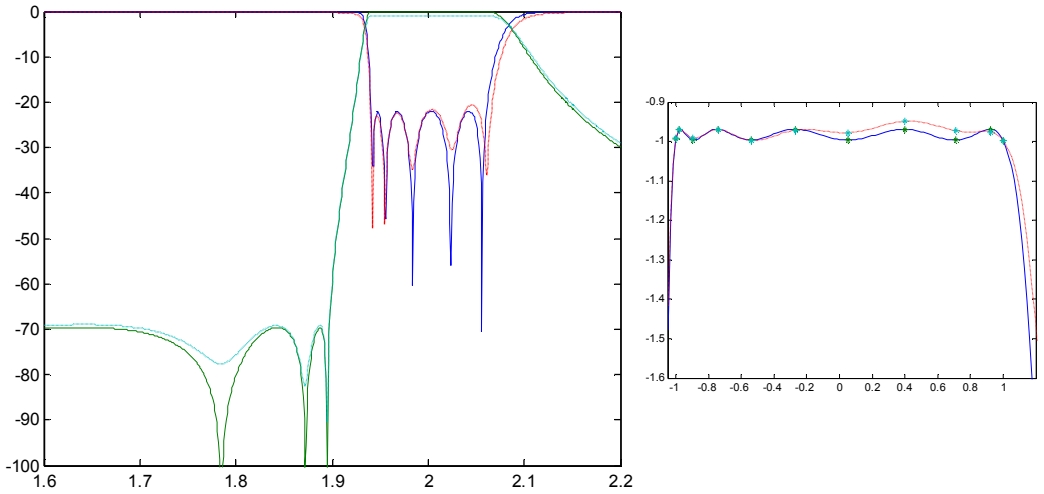

Fig. 5.23 Response for the 5th order filter with optimized Q, phase shifter and FIR.

For each resonator in DF, its center frequency is shifted from 0 in the lowpass domain by the additional frequency invariant reactance denoted by B. When B is used in the optimized as a variable, the response is given in Fig. 5.23. The optimized Qus are 486, 311, 414, 4098 and 1064. The original Bs are -6.6024, -1.1585, 1.2254, 20.8042 and 5.0813. The optimized frequency invariant reactances are -6.9279, -1.2364, 1.2098, 20.9139 and 5.1038.

Optimization of the asymmetric invertors with Qs of 649, 282, 428, 4810 and 1086 and Invertors K of 1.0901, 1.0775, 1.0587, 1.0345 and 1.0427 is shown in Fig. 5.24.

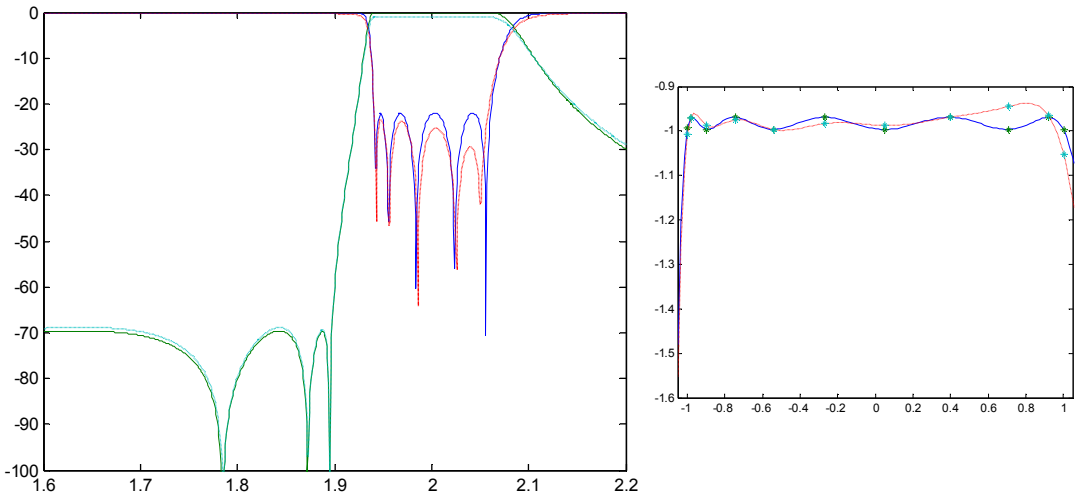

Fig. 5.24 Response for the 5th order filter with optimized Qs, phase shifters, FIRs and invertors.

5.2.3 Filter implementations

With cascaded sections, high performance combiners may be designed. A combiner with two passbands of 832-841.5 MHz and 842.5-852 MHz is used as an example to illustrate the design theory. The requirements are: passband return loss >18 dB, the insertion loss <1 dB and isolation between input ports >30 dB.

Design Step 1 – chosen filter characteristics

A 4th order general Chebyshev filter is used. Because the two bands are close to each other, the filter characteristic should have a steep transition and is realized by two transmission zeros close to the passband. The transmission zeros are at 1.15j and 1.45j in the lowpass domain. After synthesizing the general Chebyshev response using the method given in [9], we have the polynomials F_{11} and E of the lowpass prototype and Ri and Ti of each section are found according to (5.20). Values of the capacitors and frequency invariant reactances are calculated according to (5.22) and are listed in Table 5.4.

Table 5.4 Element Values for the DF Sections

Roots of F_{11}	Roots of E	Roots of F_{11}+P	C	B

-0.8366i	-0.7005-1.2885i	0.7005-1.2885i	0.9636	3.6787
0.9805i	-0.9531+0.2651i	-0.9531+0.2651i	0.7021	3.6787
0.7632i	-0.3062+0.9603i	0.3062+0.9603i	2.1762	-6.2716
0.0751i	-0.0537+1.0451i	-0.0537+1.0451i	2.1762	-38.9048

Design Step 2 – transformation to a band-pass circuit

A lowpass to bandpass transformation is applied to each resonator and the network is combined with the equivalent circuit of the 90º hybrid. For the design of mainline TL, because of the transformation used, its characteristic impedance cannot remain as 50 ohm. However, by choosing a scaling factor, the characteristic impedance can be set as 50.5 ohm and it is then replaced by 50 ohm TL in the circuit design with little effect on the response. The element values for the circuit model are given in Table 5.5.

Table 5.5 Element Values for the Circuit Model

L' (nH)	*C' (pF)*	L_v *(nH)*	L_H*(nH)*	*Θ (deg)*
4.4055	9.4932	67.7524	482.6675	*98.0693*
6.2435	*6.9168*			
1.7620	*21.4403*			
0.2954	*122.1489*			

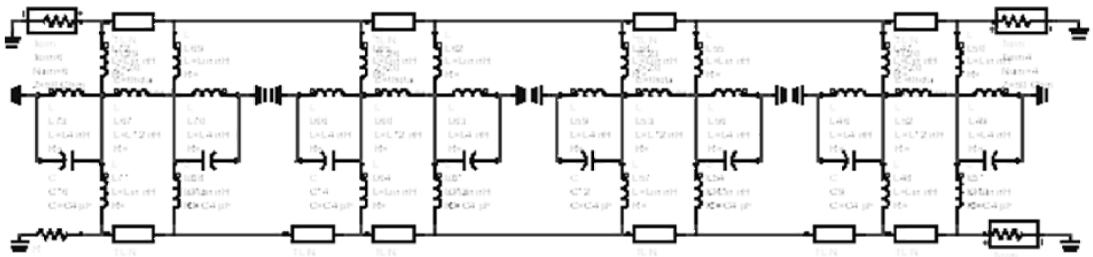

Fig. 5.25 Circuit model of cascaded DFs simulated in ADS.

Then four DF sections are cascaded. The final complete circuit model is then simulated in ADS as shown in Fig. 5.25. The result is shown in Fig. 5.26 and it is the same as synthesized Chebyshev response. The simulated isolation is shown in Fig. 5.27.

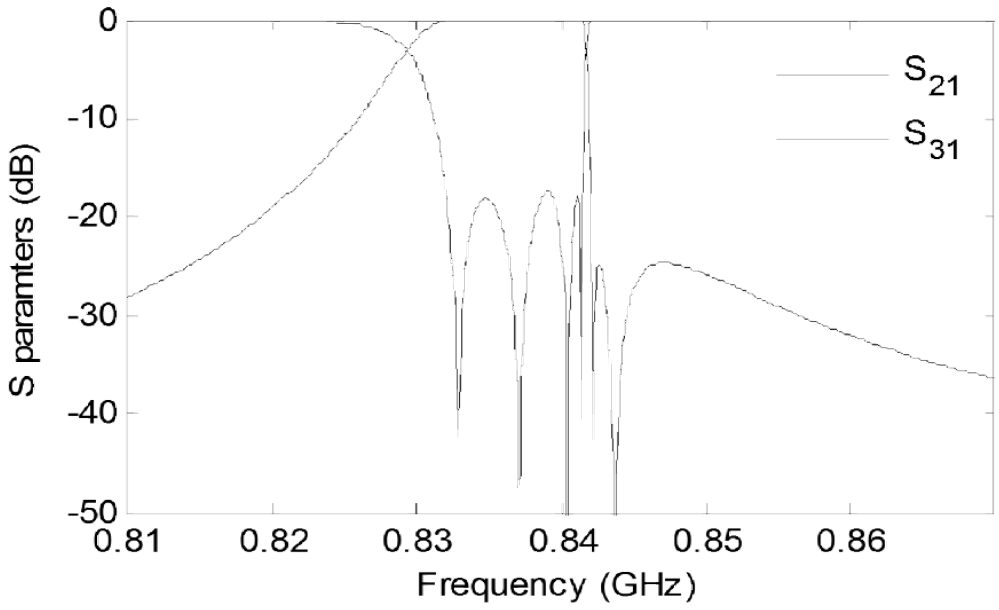

Fig. 5.26 Simulated response is exactly the same as the designed Chebyshev filter.

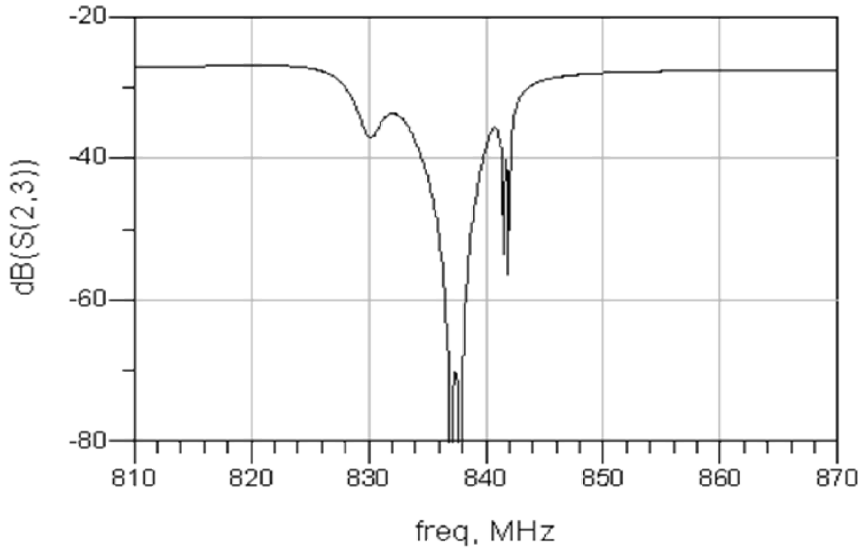

Fig. 5.27 Simulated response of the isolation.

Design Step 3 – circuit realization by an EM model

For this 4th order filter, there are four sections and each of them contains two coupled resonators. The input and output are non-resonating nodes. Each section is designed and tuned in HFSS. The Fig. 5.28 and Fig. 5.29 are the first and fourth sections. Couplings realized by windows. The input couplings are realized by non-resonating stubs and the inter resonator coupling is realized by a window. For this lossless design, we used PEC for conductors.

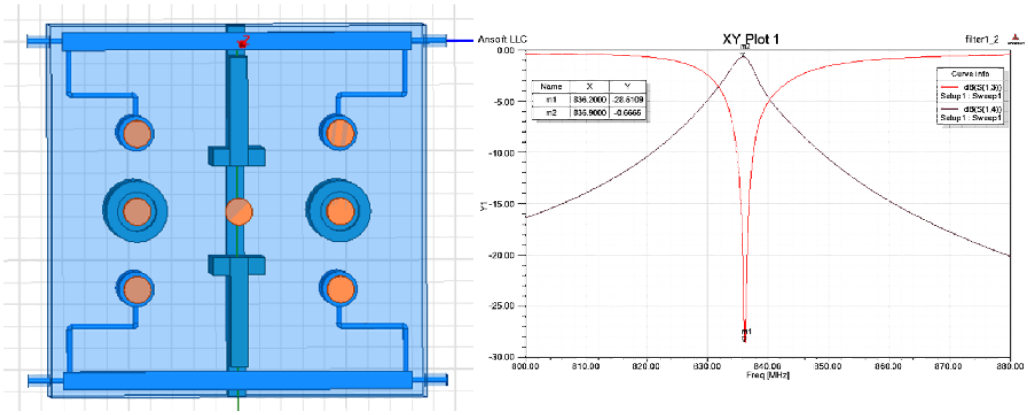

(a) (b)

Fig. 5.28 EM design of the first DF section in HFSS (a) andits response (b).

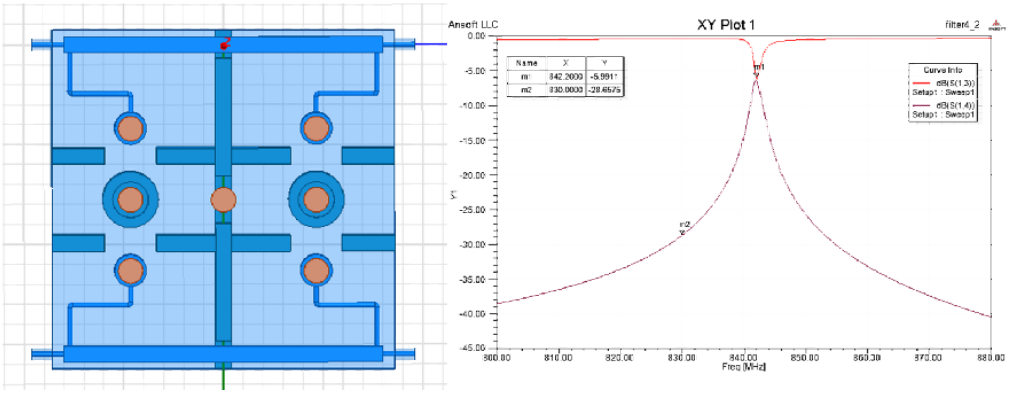

(a) (b)

Fig. 5.29 EM design of the last DF section in HFSS (a) and its response (b).

The main branch of the hybrid is realized by a 50 Ω line. 50 Ω line is achieved by adjusting the distance between the probe and cavity as shown in Fig. 5.30 for the modal and response.

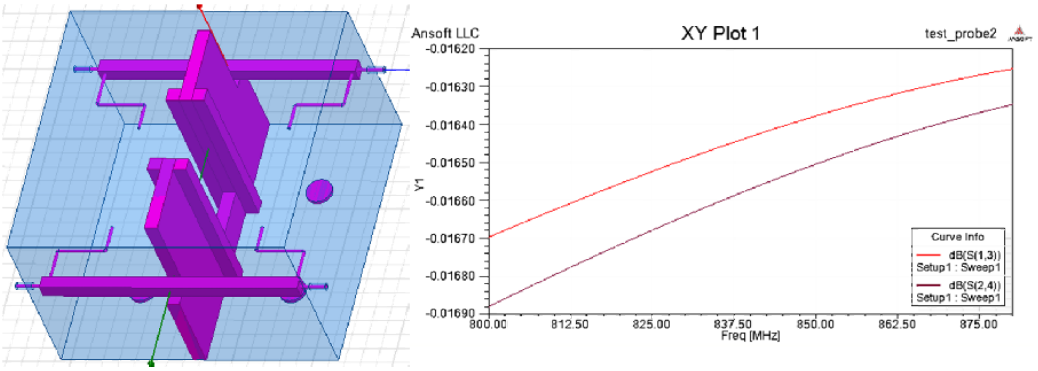

(a) (b)

Fig. 5.30 EM design of the 50Ω transmission line (a) and its response (b).

Design Step 4 – combined simulation of the whole structure

An EM model for each DF section was built and tuned in HFSS. Each section has a different resonant frequency and couplings as illustrated in Fig. 5.28(b) and Fig. 5.29(b). The S parameters of each section were then put in ADS and connected by TLs. The result of this combined EM and circuit simulation is given in Fig. 5.31 as the dashed line response.

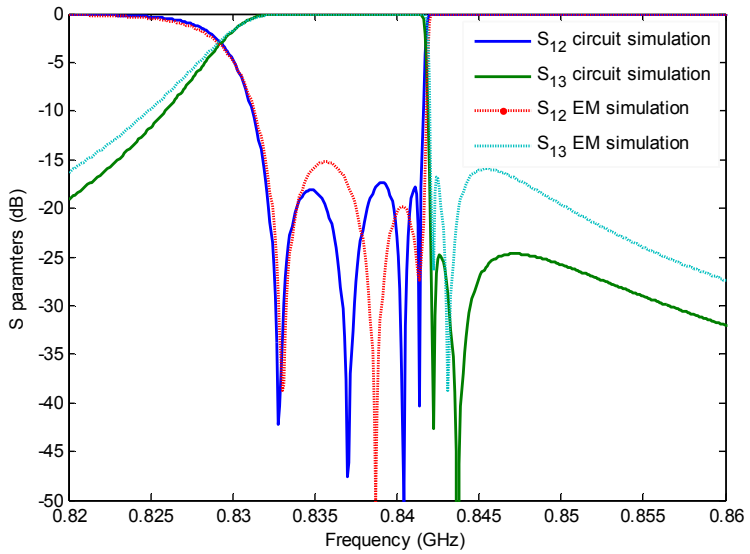

Fig. 5.31 Simulation result for the combiner (Solid line for the circuit simulation and dashed line for the combined EM/circuit simulation)

The EM model of the whole structure is shown in Fig. 5.32. Because each DF section controls one pole of filter characteristic, they may be tuned independently. No cross couplings are required when realizing transmission zeros and thus through tuning, different kinds of responses may be achieved by the same structure.

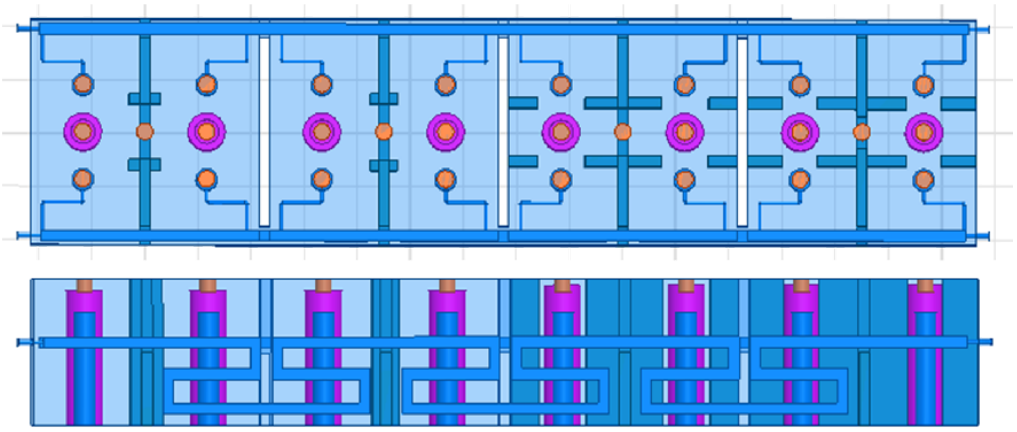

Fig. 5.32 EM model for the combiner (top view and side view).

Chapter 6
Circuit Analysis of Uniform 2D Lumped Element Networks

The problem wave propagation in N-wire line structure is studied using generalized telegrapher's equation in [104]. It is shown that the structure supports the propagation of N de-coupled modes [105][106]. However, in the field of metamaterial, many papers have been published claiming to have constructed metamaterials with two-dimensional cross section which demonstrate effective negative constitutive parameters and hence negative refraction at an interface. All these papers .have made the same fundamentally incorrect assumption that if the dimensions of the individual circuit elements are small with respect to the wavelength then one can assume a single mode of propagation [107].

The 2D lumped element network is a special case of N wire line with uniform cross sections in xy-plane and finite length in z-axis. With the definition of characteristic impedance and admittance matrices, the modes of propagation in this structure can be found by the diagonalization of the transfer matrix. The method can be applied to the analysis of waffle-iron filter [108][109].

6.1 Wave propagation in multi-wire line

This section provides a review for the analysis of wave propagation in multi-wire line structure.

6.1.1 Generalized telegrapher's equation

The N-wire line structure is illustrated in Fig. 6.1. The wires are one-dimensional and are defined by self-inductance. Each wire is coupled to the ground and other wires by coupling capacitance.

A transverse field component $E(z-vt)$satisfies the wave equation everywhere in the transverse plane even after the introduction of the lossless N-wire line structure shown in Fig. 6.1. Assuming there is a ground conductor then the

voltages on each of the remaining N wires can be calculated from a line integral along any path to each of the conductors producing a unique set of voltages *Vr* for r=1 to n. Since the E field has the solution *E(z-vt)* everywhere in the cross sectional plane then each voltage has the same argument and hence the voltage column vector is [*V(z-vt)*].

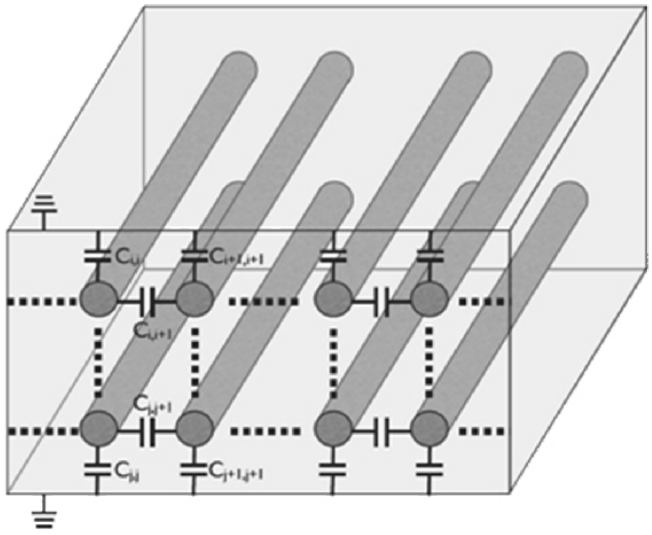

Fig. 6.1 Illustration of the N-wire line with coupling capacitance.

Let the current flow on each conductor be described by the vector [*I*]. The loss of charge on the wires over an incremental length *dz* is given in (6.1) where [C] is the capacitance matrix with the necessary and sufficient conditions on realisability being that [C] is hyperdominant i.e. all off diagonal terms are negative and the sum of all rows and columns are non-negative. In the limit, (6.1) is equivalent to (6.2).

$$\partial[Q] = \partial z[C][V] \tag{6.1}$$

$$\frac{\partial[Q]}{\partial z} = [C][V] \tag{6.2}$$

With the definition of current, (6.2) is equivalent to the differential equation in (6.3a) which gives the loss of current along the lines. A new matrix which can be called an inductance matrix is defined with respect to loss of voltage along the lines as in (6.3b).

$$\frac{\partial[I]}{\partial z} = [C]\frac{\partial[V]}{\partial t} \tag{6.3a}$$

$$\frac{\partial[V]}{\partial z} = [L]\frac{\partial[I]}{\partial t} \tag{6.3b}$$

Eliminating [I] and [V] in (6.3a) and (6.3b), we obtain (6.4) which can then be expressed as in (6.5) since [V] and [I] have the argument *(z-vt)*.

$$\begin{aligned} \frac{\partial^2[V]}{\partial z^2} &= [L][C]\frac{\partial^2[V]}{\partial^2 t} \\ \frac{\partial^2[I]}{\partial z^2} &= [C][L]\frac{\partial^2[I]}{\partial^2 t} \end{aligned} \tag{6.4}$$

$$\begin{aligned} [V]'' &= \nu^2[L][C][V]'' \\ [I]'' &= \nu^2[C][L][I]'' \end{aligned} \tag{6.5}$$

6.2.2 Modes of propagation

Assuming there is a single mode of propagation in the N-wire line, (6.5) is equivalent to in (6.6). For a solution of V'' we have (6.7) which defines the relation between L and C.

$$\left(\nu^2[L][C]-[1]\right)[V]'' = [0] \tag{6.6}$$

$$[L] = \frac{1}{\nu^2}[C]^{-1} \tag{6.7}$$

Considering case of multi-mode propagation, since wave propagation along the z axis can be expressed by the generalized form of $e^{-\gamma z}$, voltage in (6.5) is derived as in (6.8).

$$\gamma^2[V] = \nu^2[L][C][V] \tag{6.8}$$

We can now define characteristic impedance and admittance matrices as in (6.9). Using the characteristic admittance and impedance matrices, the general telegrapher's equation in (6.5) can be written as in (6.10).

$$\begin{aligned} [Z] &= \nu[L] \\ [Y] &= \nu[C] \end{aligned} \tag{6.9}$$

$$\begin{aligned} [V]'' &= [Z][Y][V]'' \\ [I]'' &= [Y][Z][I]'' \end{aligned} \tag{6.10}$$

In general, a solution of V requires the condition in (6.11) that the propagation constant of each mode is the corresponding eigenvalue of matrix YZ.

$$\left|[Z][Y]-\gamma^2[1]\right|=0 \tag{6.11}$$

Thus for a single mode of propagation, $[Z]=[Y]^{-1}$ apart from a scalar multiplier. In general this is not the case and (6.11) is a complex multi-valued function with N solutions for γ all connected by branch points of the square root variety. The modes must all exist simultaneously with N positive solutions representing forward waves and N negative solutions representing waves travelling in the opposite direction [110].

Since there are multimode propagations, the column vector of voltage [V] can be expressed in (6.12) which states that each node voltage V is a linear combination of N mode voltages V_e. The same applies to the node current [I] which is a combination of N mode current I_e.

$$\begin{aligned}[V]&=[X_V][V_e]\\ [I]&=[X_I][I_e]\end{aligned} \tag{6.12}$$

Each V_e and I_e corresponds to a mode of propagation along the z axis of the form $e^{-\gamma z}$. Substituting (6.12) into (6.10), we have (6.13) in which $[\gamma^2]$ is a diagonal matrix and $[e^{-\gamma z}]$ is a column vector.

$$\begin{aligned}[X_V][\gamma^2][e^{-\gamma z}]&=[Z][Y][X_V][e^{-\gamma z}]\\ [X_I][\gamma^2][e^{-\gamma z}]&=[Y][Z][X_I][e^{-\gamma z}]\end{aligned} \tag{6.13}$$

The solution of (6.13) is found in (6.14) which is transformed into (6.15)by matrix inversion which shows that $[\gamma^2]$ and $[X_V]$ are the eigenvalues and normalized eigenvector of matrix of [Z][Y].

$$\begin{aligned}[X_V][\gamma^2]&=[Z][Y][X_V]\\ [X_I][\gamma^2]&=[Y][Z][X_I]\end{aligned} \tag{6.14}$$

$$\begin{aligned}[Z][Y]&=[X_V][\gamma^2][X_V]^{-1}\\ [Y][Z]&=[X_I][\gamma^2][X_I]^{-1}\end{aligned} \tag{6.15}$$

When the N-wire line have uniform cross section which means that the network have equivalent self-inductance (L_1=L_2=…L_n), matrix *[Y][Z]* is equivalent to *[Z][Y]*, so that $[X_v]$ is equal to $[X_I]$. The N-wire line structure is equivalent to a network of N separated wire connected at the input and output by combiners.

6.2 Lumped element analysis for generalized 2D network

This section shows the method for the analysis of 2D lumped element networks by the separation of mode. The response of the network can be found by equivalent circuits based on propagating modes.

A generalized circuit model is given with defined characteristic matrices Y and Z. First, the transfer matrix of network is derived. Then the mode separation method for N-wire line is applied to the network and an equivalent circuit can be found according to the equivalence of single mode and input/output combiner. The transfer matrix of the network can then be block diagonalized and is found to be the multiplication of three sub-networks. For the cascading of the networks, the response can be found by method of image parameters. A 3rd order example is given to show the analysis procedures.

6.2.1 Method of analysis

1. Circuit model and Y Z

The circuit in Fig. 6.1 could be viewed as the cascading of M basic blocks along z-axis and the cascading is most easily described by the multiplication of transfer matrices. In this section, the transfer matrix of a single block along z-axis is derived. The circuit model for the basic block is shown in Fig. 6.2. It is a 2N port network consisting N shunt admittance Yi coupled to the adjacent one by Y_{ij}. In the figure, we define the input node voltages and currents as $V_1, V_2, \ldots V_n$ and $I_1, I_2, \ldots I_n$. The output node voltages and currents are $V_1', V_2', \ldots V_n'$ and $I_1', I_2', \ldots I_n'$ respectively. For this diagram, its impedance and admittance matrices are given in (6.16) and (6.17).

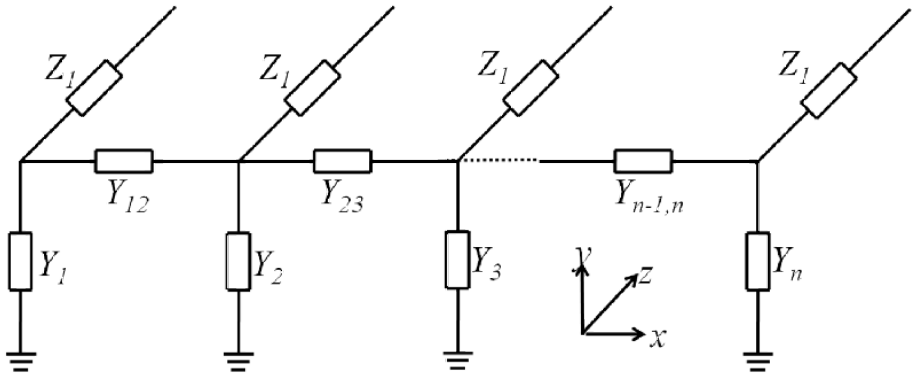

Fig. 6.2 Generalized circuit model.

$$[Z]=\begin{bmatrix} Z_1 & 0 & & \\ 0 & Z_2 & .... & \\ & ... & ... & 0 \\ & & 0 & Z_n \end{bmatrix} \tag{6.16}$$

$$[Y]=\begin{bmatrix} Y_1+Y_{12} & -Y_{12} & 0 & \\ -Y_{12} & Y_2+Y_{12}+Y_{23} & .... & 0 \\ 0 & ... & ... & -Y_{n-1,n} \\ & 0 & -Y_{n-1,n} & Y_n+Y_{n-1,n} \end{bmatrix} \tag{6.17}$$

2. Transfer matrix

The input and output node voltages satisfy the equations in (6.18) and the node currents satisfy the conditions in (6.19). I_{Yij} represent current in inductance L_{ij}.

$$\begin{aligned} V_1'-V_1 &= Z_1 I_1' \\ V_2'-V_2 &= Z_2 I_2' \\ &... \\ V_n'-V_n &= Z_n I_n' \end{aligned} \tag{6.18}$$

$$\begin{aligned} I_1'-I_1 &= Y_1 V_1 + I_{Y12} \\ I_2'-I_2 &= Y_2 V_2 + I_{Y23} - I_{Y12} \\ &... \\ I_n'-I_n &= Y_n V_n + I_{Yn-1,n} \end{aligned} \tag{6.19}$$

Substituting the inductance currents in (6.20) into (6.19), we have (6.21).

$$\begin{aligned} V_1 - V_2 &= Y_{12} I_{Y12} \\ V_2 - V_3 &= Y_{23} I_{Y23} \\ &... \\ V_{n-1} - V_n &= Y_{n-1,n} I_{Yn-1,n} \end{aligned} \tag{6.20}$$

$$\begin{aligned} I_1'-I_1 &= \left(Y_1+\frac{1}{Y_{12}}\right)V_1 - \frac{1}{Y_{12}}V_2 \\ I_2'-I_2 &= \left(Y_2+\frac{1}{Y_{12}}+\frac{1}{Y_{23}}\right)V_2 - \frac{1}{Y_{12}}V_1 - \frac{1}{Y_{23}}V_3 \\ &... \\ I_n'-I_n &= \left(Y_n+\frac{1}{Y_{n-1,n}}\right)V_n - \frac{1}{Y_{n-1,n}}V_{n-1} \end{aligned} \tag{6.21}$$

Re-organizing (6.18) and (6.21), we have (6.22) in which V and I are vectors of voltages and currents at the input nodes. Y and Z are matrices defined in (6.16) and (6.17). *D* is an N by N identity matrix. By simple matrix operation,

(6.23) can be derived which is a description of the transfer matrix of the network shown in Fig. 6.2.

$$\begin{bmatrix} D & 0 \\ Y & D \end{bmatrix}\begin{bmatrix} V \\ I \end{bmatrix}=\begin{bmatrix} D & -Z \\ 0 & D \end{bmatrix}\begin{bmatrix} V' \\ I' \end{bmatrix} \tag{6.22}$$

$$\begin{bmatrix} V \\ I \end{bmatrix}=\begin{bmatrix} D & -Z \\ -Y & YZ+D \end{bmatrix}\begin{bmatrix} V' \\ I' \end{bmatrix} \tag{6.23}$$

3. Decoupling of modes

It is shown in the analysis of N wire line that node voltages and currents can be expressed by the linear combination of mode voltages and currents. The relation is shown in (6.24) and (6.25) in matrix form where V_{mi} and V_{mo} are the input and output voltages of each mode.

$$\begin{bmatrix} V \\ I \end{bmatrix}=\begin{bmatrix} X_V & 0 \\ 0 & X_I \end{bmatrix}\begin{bmatrix} V_{mi} \\ I_{mi} \end{bmatrix} \tag{6.24}$$

$$\begin{bmatrix} V' \\ I' \end{bmatrix}=\begin{bmatrix} X_V & 0 \\ 0 & X_I \end{bmatrix}\begin{bmatrix} V_{mo} \\ I_{mo} \end{bmatrix} \tag{6.25}$$

Substituting (6.24) and (6.25) into the transfer matrix in (6.23), we have (6.26), which can be derived as in (6.27) according to (6.15).

$$\begin{aligned}\begin{bmatrix} V_{mi} \\ I_{mi} \end{bmatrix}&=\begin{bmatrix} X_V^{-1} & 0 \\ 0 & X_I^{-1} \end{bmatrix}\begin{bmatrix} D & -Z \\ -Y & YZ+D \end{bmatrix}\begin{bmatrix} X_V & 0 \\ 0 & X_I \end{bmatrix}\begin{bmatrix} V_{mo} \\ I_{mo} \end{bmatrix} \\ &=\begin{bmatrix} D & -X_V^{-1}ZX_I \\ -X_I^{-1}YX_V & X_I^{-1}YZX_I+D \end{bmatrix}\begin{bmatrix} V_{mo} \\ I_{mo} \end{bmatrix}\end{aligned} \tag{6.26}$$

$$\begin{bmatrix} V_{mi} \\ I_{mi} \end{bmatrix}=\begin{bmatrix} D & -X_V^{-1}ZX_I \\ -X_I^{-1}YX_V & [\gamma^2]+D \end{bmatrix}\begin{bmatrix} V_{mo} \\ I_{mo} \end{bmatrix} \tag{6.27}$$

When the matrix Z has uniform elements, that is $Z=z_0*D$, (6.28) can be derived from (6.15). Then (6.27) is equivalent to (6.29). Since the four block matrices in (6.29) are all diagonalized, it represents the transfer matrix of the de-coupled network in which the transfer matrix of a mode is independent of the other modes.

$$X_I^{-1}YX_V = X_I^{-1}YX_I = [\gamma^2]/z_0 \tag{6.28}$$

$$\begin{bmatrix} V_{mi} \\ I_{mi} \end{bmatrix}=\begin{bmatrix} D & -z_0D \\ -[\gamma^2]/z_0 & [\gamma^2]+D \end{bmatrix}\begin{bmatrix} V_{mo} \\ I_{mo} \end{bmatrix} \tag{6.29}$$

With (6.24), (6.25) and (6.29), the transfer matrix of the network is given in (6.29) which is the multiplication of three sections.

$$\begin{aligned}\begin{bmatrix} V \\ I \end{bmatrix} &= \begin{bmatrix} X_V & 0 \\ 0 & X_I \end{bmatrix}\begin{bmatrix} V_{mi} \\ I_{mi} \end{bmatrix} \\ &= \begin{bmatrix} X_V & 0 \\ 0 & X_I \end{bmatrix}\begin{bmatrix} D & -z_0 D \\ -[\gamma^2]/z_0 & [\gamma^2]+D \end{bmatrix}\begin{bmatrix} V_{mo} \\ I_{mo} \end{bmatrix} \\ &= \begin{bmatrix} X_V & 0 \\ 0 & X_I \end{bmatrix}\begin{bmatrix} D & -z_0 D \\ -[\gamma^2]/z_0 & [\gamma^2]+D \end{bmatrix}\begin{bmatrix} X_V^{-1} & 0 \\ 0 & X_I^{-1} \end{bmatrix}\begin{bmatrix} V' \\ I' \end{bmatrix}\end{aligned} \tag{6.30}$$

4. Equivalent circuit

According to the definition of transfer matrix in (6.31), the matrix in (6.23) can be re-organized so that the transfer matrix of the 2N-port network can is as shown in (6.32).

$$[V_1\ I_1\ V_2\ I_2\ \ldots\ V_n\ I_n]^t = [T][V_1'\ I_1'\ V_2'\ I_2'\ \ldots\ V_n'\ I_n']^t \tag{6.31}$$

$$[T] = \begin{bmatrix} 1 & -Z_1 & 0 & 0 & & \\ -Y_1 - Y_{12} & 1+Z_1(Y_1+Y_{12}) & Y_{12} & -Z_2 Y_{12} & & \\ 0 & 0 & 1 & -Z_2 & & \\ Y_{12} & -Z_1 Y_{12} & -Y_2 - Y_{12} - Y_{23} & 1+Z_2(Y_2+Y_{12}+Y_{23}) & \ldots & \\ & & & & 1 & -Z_n \\ & & & & -Y_n - Y_{n-1,n} & 1+Z_n(Y_n+Y_{n-1,n}) \end{bmatrix} \tag{6.32}$$

The transfer matrix T in (6.32) can be viewed as a block matrix of N by N elements. Each element consists of a 2 by 2 sub-matrix. When the circuit has uniform elements, the transfer matrix T can be block diagonalized. Then the matrix T is a multiplication of the block eigenvector matrix and the diagonalized matrix T_{c1} as in (6.33).

$$[T] = [T_{in}][T_{c1}][T_{out}] \tag{6.33}$$

The multiplication of transfer matrices represents the cascading of networks. In this way, the network in Fig. 6.2 can be viewed as the cascading of three sections. The first and last sections can be viewed as input and output combiners whose transfer matrices are T_{in} and T_{out}. These transfer matrices satisfy the condition in (6.34). They can be derived from the eigenvector matrix X_v as in (6.35)according to (6.30) and V_{ij} represent the element in row i and column j of matrix X_v.

$$[T_{in}][T_{out}] = [D] \tag{6.34}$$

$$[T_{in}]=\begin{bmatrix} V_{11} & 0 & V_{21} & 0 & & & \\ 0 & V_{11} & 0 & V_{21} & & & \\ V_{21} & 0 & V_{22} & 0 & & & \\ 0 & V_{21} & 0 & V_{22} & & & \\ & & & & \cdots & & \\ & & & & & V_{nn} & 0 \\ & & & & & 0 & V_{nn} \end{bmatrix} \tag{6.35}$$

The matrix T_{c1} is given in (6.36). Each diagonal block of matrix T_{c1} is a 2 by 2 matrix which is the transfer matrix of a 2-port network as shown in Fig. 6.3.

$$[T_{c1}]=\begin{bmatrix} 1 & Z_1 & 0 & 0 & & \\ -Y_1-Y_{12}' & 1+Z_1(Y_1+Y_{12}') & 0 & 0 & & \\ 0 & 0 & 1 & Z_1 & & \\ 0 & 0 & -Y_1-Y_{23}' & 1+Z_1(Y_1+Y_{23}') & & \\ & & & & \cdots & \\ & & & & 1 & Z_1 \\ & & & & -Y_1-Y_{n-1,n} & 1+Z_1(Y_1+Y_{n-1,n}') \end{bmatrix} \tag{6.36}$$

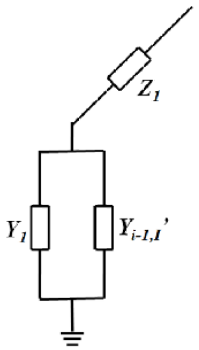

$$[T_i]=\begin{bmatrix} 1 & Z_1 \\ -Y_1-Y_{i-1,i} & 1+Z_1(Y_1+Y_{i-1,i}) \end{bmatrix}$$

Fig. 6.3 Equivalent circuit of a mode.

The values for $Y_{i-1,1}'$ can be derived from the corresponding eigenvalue γ^2 in as in (6.37).

$$(Y_1+Y_{i-1,i}')Z_1=\gamma_k^2 \tag{6.37}$$

As a result, the circuit in Fig. 6.2 which has N shunt admittance along x-axis is divided into N 2-port sub-networks combined by input and output combiners. These 2-port networks have no interaction with each other and are a direct representation of propagating modes.

5. Image parameters

The total transfer matrix for M blocks along the z direction is given in (6.38) with simplifications. The transfer matrix in (6.38) is equivalent to a network

consisting of N branches combined at the input and output by 2N-port combiners whose transfer matrices are T_{in} and T_{out}. Because each of the T_{ci}matrix is block diagonalized, each branch supports the propagation of one mode and the equivalent circuit is shown in Fig. 6.4. For each branch, the method of image parameter can be applied.

$$\begin{aligned}[T] &= [T_{in}][T_{c1}][T_{out}]\cdot[T_{in}][T_{c2}][T_{out}]\cdot\ldots\cdot[T_{in}][T_{cn}][T_{out}] \\ &= [T_{in}][T_{c1}][T_{c2}]\cdot\ldots\cdot[T_{cn}][T_{out}]\end{aligned} \tag{6.38}$$

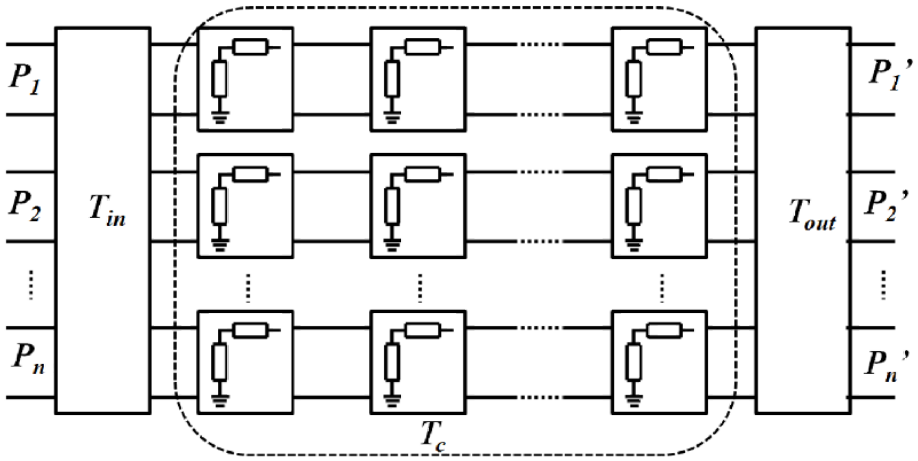

Fig. 6.4 Illustration of the equivalence of 2-D waffle-iron filter.

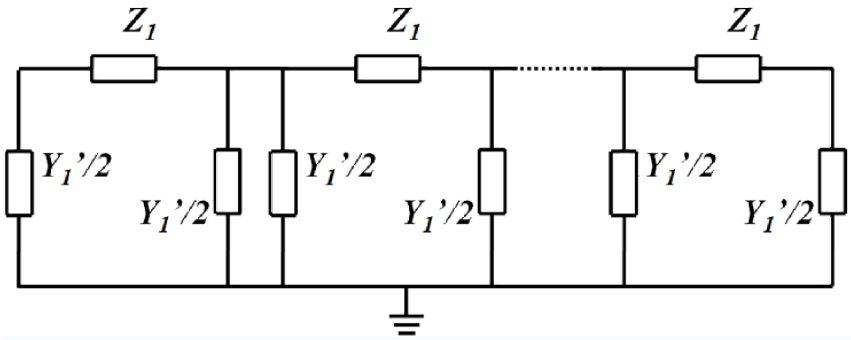

Fig. 6.5 Illustration of the network for each branch.

As each branch in Fig. 6.4 is periodic, the transfer matrix of each branch can be found by the method of image parameter. The equivalent circuit of such a branch is shown in Fig. 6.5.

Y_i' and Z_i can be derived according to Fig. 6.3. With the even and odd mode admittance defined in Fig. 6.6, the transfer matrix of M cascaded section is given in (6.39) with γ and Z_i given in (6.40).

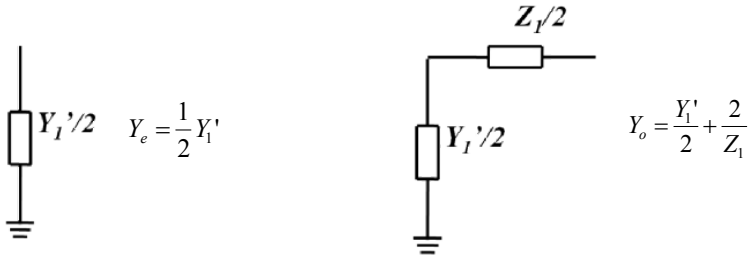

Fig. 6.6 Even and odd mode admittance of a basic section.

$$\left[T^m\right]=\begin{bmatrix}\cosh m\gamma & Z_I \sinh m\gamma \\ Y_I \sinh m\gamma & \cosh m\gamma\end{bmatrix} \tag{6.39}$$

$$\gamma=\cosh^{-1}\frac{Y_e+Y_o}{Y_e-Y_o},\ Y_I=\frac{1}{Z_I}=\sqrt{Y_eY_o} \tag{6.40}$$

6. S parameters

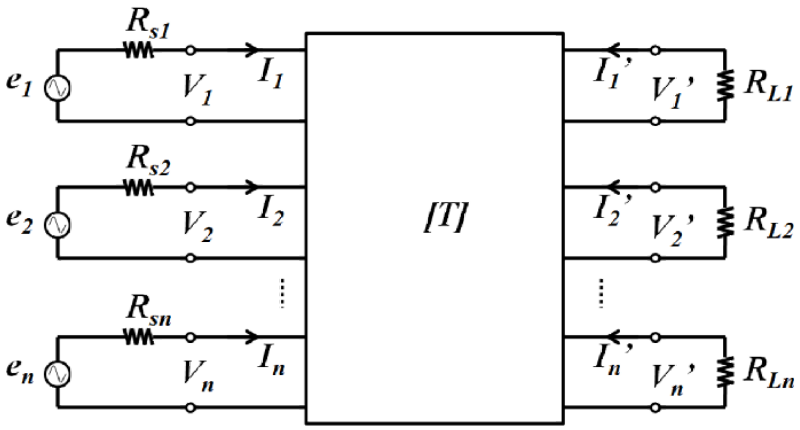

Fig. 6.7 Illustration of the node voltage and current for waffle-iron filter with 2N nodes.

With the total transfer matrix *[T]* of the 2N-port network, its S parameter can be derived with given source and load resistances. The complete circuit is illustrated in Fig. 6.7 with source voltage e_i, source resistance R_s and load resistance R_l. The source voltages and port voltages are related as in (6.41) while the load voltages and load currents are related as in (6.42). With the 2N port transfer matrix in (6.38), we can substitute the equations in (6.41) and (6.42) to replace V_i and I_i'. Then after some re-arrangement, an N by N matrix T' could be derived as in (6.43) which states the voltage transfer ratio.

$$V_i = e_i - I_i R_{si} \tag{6.41}$$

$$I_i' = V_i' / R_{Li} \tag{6.42}$$

$$\begin{bmatrix} e_1 \\ e_2 \\ \dots \\ e_n \end{bmatrix} = [T'] \begin{bmatrix} V_1' \\ V_2' \\ \dots \\ V_n' \end{bmatrix} \tag{6.43}$$

Considering the 2N port network in Fig. 6.7, the output voltage V_i' can be found when source voltage e_i is given according to (6.43). From the previous discussion we know that when input voltages are equivalent to an eigenvector of matrix [Y][Z], the 2D network support a single mode of propagation whose propagation constant is equivalent to the corresponding eigenvalues. To study this single mode of propagation, the network in Fig. 6.7 can be viewed as a 2-port network and its power transfer ratio can be found as in (6.44) where the total input and output power are the summation of the input and output power of each discrete port. Then an equivalent S_{21} can be found as in (6.45).

$$pt = \frac{\sum (e_i - R_{si} I_i) I_i}{\sum V_j'^2 / R_j} \tag{6.44}$$

$$S_{21} = 10 \log (pt) \tag{6.45}$$

6.2.2 N=3 example

It is instructive to imagine constructing a metamaterial which supports a single mode of propagation. Consider the simplest metamaterial where the transverse network is an array of three capacitors to ground with coupling constrained to adjacent capacitors as shown in Fig. 6.8. The capacitance matrix is given by (6.46).

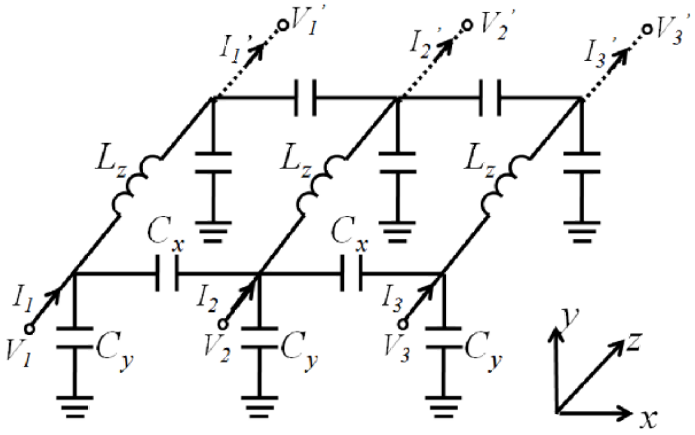

Fig. 6.8 Circuit model of the metamaterial with 3 transversal nodes.

$$[C]=\begin{bmatrix} C_{11} & -C_{12} & 0 \\ -C_{12} & C_{22} & -C_{23} \\ 0 & -C_{23} & C_{33} \end{bmatrix} \tag{6.46}$$

And the inverse matrix is given in (6.47)where $\Delta = |C| = C_{11}C_{22}C_{33} - C_{33}C_{12}^2 - C_{11}C_{23}^2$.

$$[C]^{-1} = \frac{1}{\Delta}\begin{bmatrix} C_{22}C_{33}+C_{23}^2 & C_{12}C_{33} & C_{12}C_{23} \\ C_{12}C_{33} & C_{11}C_{33} & C_{11}C_{23} \\ C_{12}C_{23} & C_{11}C_{23} & C_{11}C_{22}+C_{12}^2 \end{bmatrix} \tag{6.47}$$

Thus although the capacitance matrix is sparse the inductance matrix is full, with each inductor coupling to all the others. Any attempt to construct a metamaterial with a single mode of propagation would require the construction of this complex matrix with all inductors coupling all the others despite the capacitors not coupling. This is impossible to achieve in practice and indeed none of the metamaterials published in the literature attempt to do this. Consequently all must support multiple modes of propagation. It is the interference between these modes which creates negative refraction as we demonstrated in [111].

Considering the case of multimode propagation, the network in Fig. 6.8 has 3 nodes in the transversal plane and infinity sections cascading along the z direction. The vertical capacitances C_y represent the couplings to ground. The horizontal capacitances C_x represent the couplings between adjacent nodes. The inductance along z direction represents self inductance of the wire. The admittance and impedance matrices of a basic section are given in (6.48) and (6.49).

$$[Y]=p\begin{bmatrix} C_y+C_x & -C_x & 0 \\ -C_x & C_y+2C_x & -C_x \\ 0 & -C_x & C_y+C_x \end{bmatrix} \tag{6.48}$$

$$[Z]=p\begin{bmatrix} L_z & 0 & 0 \\ 0 & L_z & 0 \\ 0 & 0 & L_z \end{bmatrix} \tag{6.49}$$

When C_x=1, C_y=2 and L_z=2, the characteristic matrix is given in (6.50).

$$[Y][Z]=2p^2\begin{bmatrix} 3 & -1 & 0 \\ -1 & 4 & -1 \\ 0 & -1 & 3 \end{bmatrix} \tag{6.50}$$

The eigenvalues of (6.50) are $4p^2$, $6p^2$ and $10p^2$ which corresponding to propagating constant of $\pm 2p$, $\pm\sqrt{6}p$ and $\pm\sqrt{10}p$ for the three existing modes. The normalized eigenvectors are given in (6.51).

$$[V]=\begin{bmatrix} -\frac{1}{\sqrt{3}} & -\frac{1}{\sqrt{2}} & \frac{1}{\sqrt{6}} \\ -\frac{1}{\sqrt{3}} & 0 & -\frac{2}{\sqrt{6}} \\ -\frac{1}{\sqrt{3}} & \frac{1}{\sqrt{2}} & \frac{1}{\sqrt{6}} \end{bmatrix} \tag{6.51}$$

For sinusoidal wave, the eigenvectors represent the input voltage at the three nodes which will excite the eigenmode with corresponding eigenvalues.

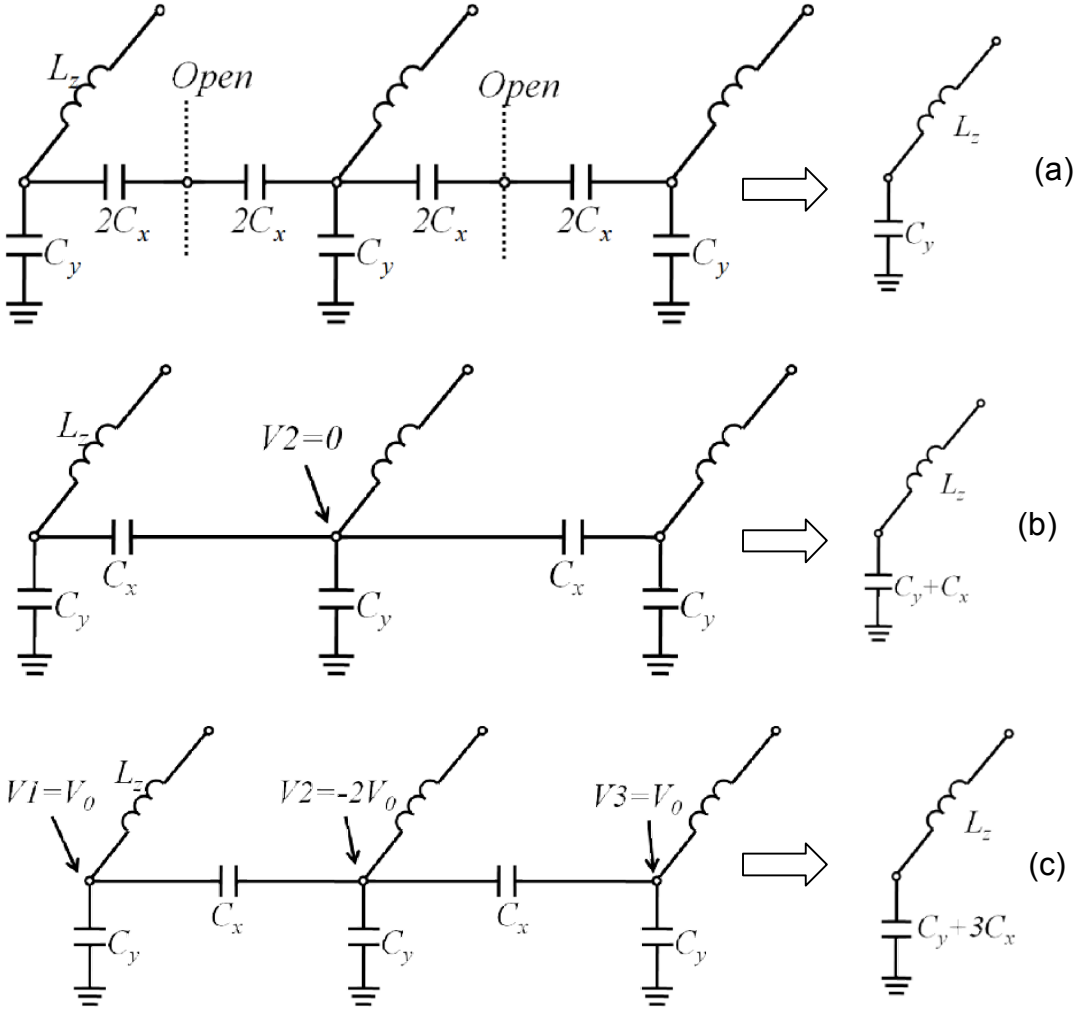

Fig. 6.9 Equivalent circuit model 3 nodes network with the excitation to three modes.

The first eigenvector represents equal voltages at the three input nodes. This case is equivalent to an even mode excitation, so that an even mode

analysis can be applied as shown in Fig. 6.9(a) providing the equivalent circuit with propagation constant of $\gamma = \pm \mathrm{p}\sqrt{L_z C_y} = \pm 2\mathrm{p}$.

The second eigenvector represents a zero voltage at the second node and the equivalent circuit is shown in Fig. 6.9(b). The propagation constant of this mode is $\gamma = \pm \mathrm{p}\sqrt{L_z(C_y + C_x)} = \pm\sqrt{6}\mathrm{p}$.

For the third eigenvector, the voltage across C_y is V_0 and the voltage across C_x is $3V_0$ which provides an equivalent capacitance of $3C_x$. As a result, the propagation constant is $\gamma = \pm \mathrm{p}\sqrt{L_z(C_y + 3C_x)} = \pm\sqrt{10}\mathrm{p}$.

6.3 Waffle-iron filter

Waffle-iron was invented by S.B. Cohn in the 1950s [112] and developed by Leo Young in the 1960s [108]. It is a waveguide lowpass filter which has a wide stop band. Due to the effect of cut-off frequency of waveguide, the filter exhibits a bandpass characteristic. The design is developed from ridged waveguide filter and has the advantage of little spurious mode in the stop band. A photo of waffle-iron filter is shown in [109].

6.3.1 Simplified circuit model

The circuit model of waffle-iron filter is shown in Fig. 6.10. It consists of bandpass resonators similar to those of combline filters that extend in 2 dimensional. It has N resonators along x-axis connected by inductance L_x and has M blocks along z-axis connected by inductance L_z.

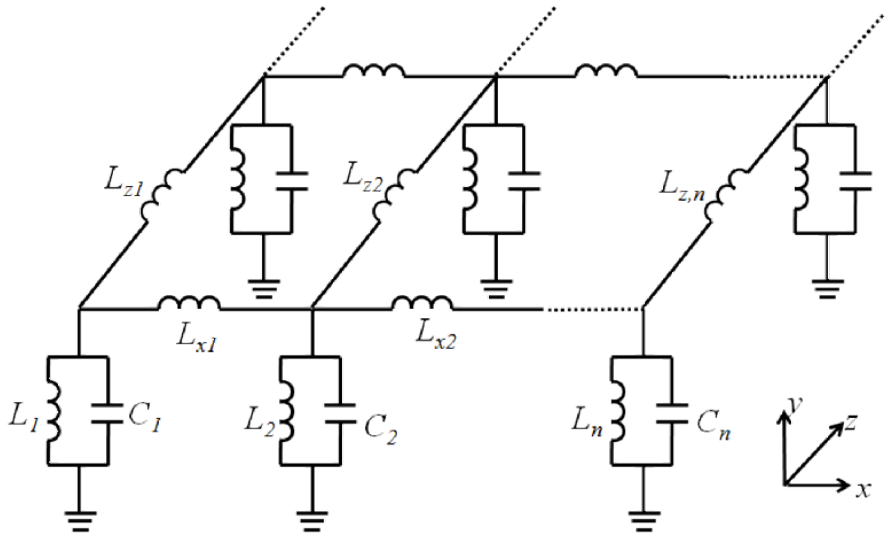

Fig. 6.10 Circuit model for waffle-iron filter with N transversal sections and M longitudinal sections.

The impedance and admittance matrices of this circuit are given in (6.52) and (6.53).

$$[Y]=\begin{bmatrix} pC_1+\frac{1}{pL_1}+\frac{1}{pL_{x1}} & -\frac{1}{pL_{x1}} & 0 & \\ -\frac{1}{pL_{x1}} & pC_2+\frac{1}{pL_2}+\frac{1}{pL_{x1}}+\frac{1}{pL_{x2}} & .... & 0 \\ 0 & ... & ... & -\frac{1}{pL_{x,n-1}} \\ & 0 & -\frac{1}{pL_{x,n-1}} & pC_n+\frac{1}{pL_n}+\frac{1}{pL_{x,n}} \end{bmatrix} \tag{6.52}$$

$$[Z]=\begin{bmatrix} pL_{z1} & 0 & & \\ 0 & pL_{z1} & .... & \\ & ... & ... & 0 \\ & & 0 & pL_{z1} \end{bmatrix} \tag{6.53}$$

6.3.2 N=5 example

The example is a waffle-iron filter with 5 sections in x direction and 10 sections in z direction. For a practical design, a half inductance is added to the basic section at both ends along x-axis. Such a network is illustrated in Fig. 6.11. The resonator is denoted as inductance *L* and capacitance *C*. The transversal coupling is represented by inductance L_x and the longitudinal coupling is represented by inductance L_z. There are two inductances at the end of transversal plane with the values of $L_x/2$.

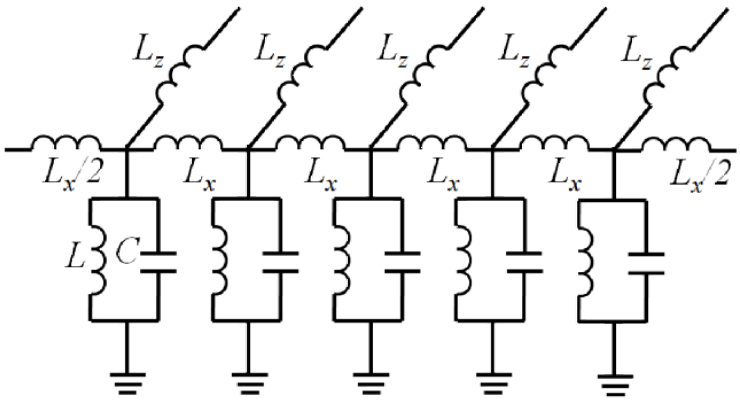

Fig. 6.11 Circuit model of N=5 waffle-iron filter

For a five section waffle iron filter with the illustrated configuration, its eigenvectors are listed below and the values of the eigenvectors are independent of the values assigned to L, C, L_x and L_z.

V1=-0.1954, -0.5117, -0.6325, -0.5117, -0.1954

V2=-0.3717, -0.6015, 0, 0.6015, 0.3717

V3=-0.5117, -0.1954, 0.6325, -0.1954, -0.5117

V4=-0.6015, 0.3717, 0, -0.3717, 0.6015

V5=0.4472, -0.4472, 0.4472, -0.4472, 0.4472

The values of the eigenvector represent to five sinusoidal waves which correspond to the five initial modes of a rectangular waveguide. The values of the five eigenvectors are plotted in Fig. 6.12 with fitted sin waves.

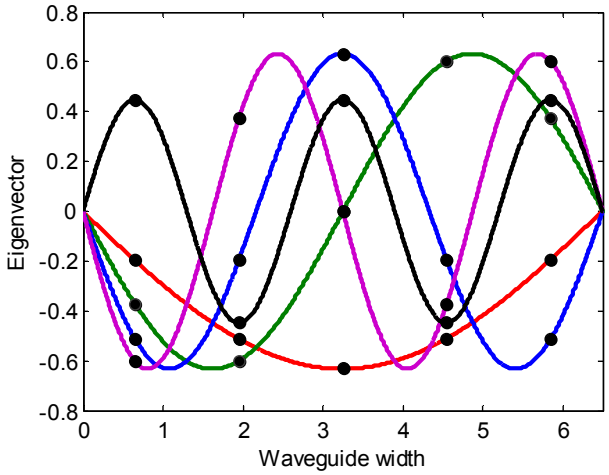

Fig. 6.12 Plot of 5 sets of eigenvectors with fitted sine waves.

When the input voltage is the same as a set of eigenvector, there should be only one corresponding mode propagating in the network. We choose C=2, L=2, Lx=1 and Lz=1. The S_{21} of these five modes are compared in Fig. 6.13. Each of these five modes has a passband and a different center frequency.

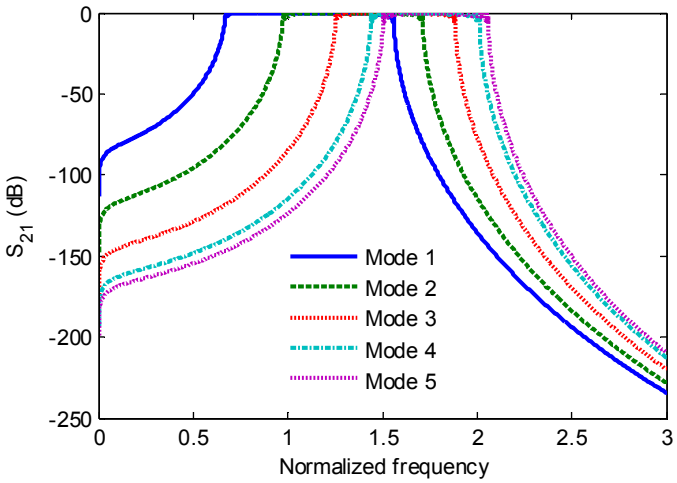

Fig. 6.13 S_{21} of the five modes.

For any other input voltage, the resulting S_{21} is a combination of the five eigenmodes. For example, when V_input=[1, 2, 3, 0, -2], the S_{21} is given in Fig. 6.14. The modes are combined to provide a wider passband.

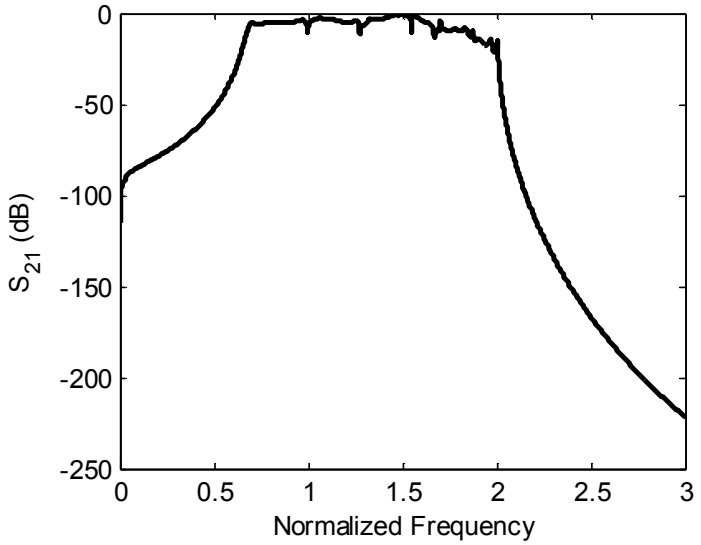

Fig. 6.14 S21 with input voltage 1, 2, 3, 0, -2.

When the input voltage has the magnitude of the first eigenvector with a phase difference, the S_{21} is compared to that of the first mode in Fig. 6.15. This S_{21} is the same to that of the first mode but distorted in the stopband due to the existence of other modes.

$V1 = -0.1954e^{j\theta}$, $V2 = -0.5117e^{j2\theta}$, $V3 = -0.6325e^{j3\theta}$, $V4 = -0.5117e^{j4\theta}$, $V5 = -0.1954e^{j5\theta}$

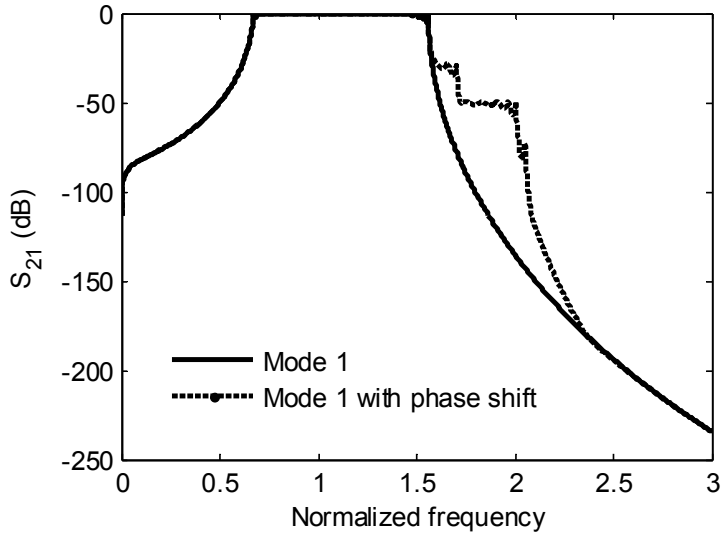

Fig. 6.15 S_{21} of the first mode with input voltage at an angle.

6.3.3 EM model and simulation

An EM model of a waffle iron filter with five section in the transversal plane and ten sections in the longitudinal plane is simulated in HFSS as shown in Fig. 6.16. There are five propagating mode in this structure. The transfer functions of the first and fifth mode are shown as green lines in figures below. As the five propagating modes have little interaction with each other as shown in Fig. 6.17, the response of the EM simulation is quite similar to that of a circuit model.

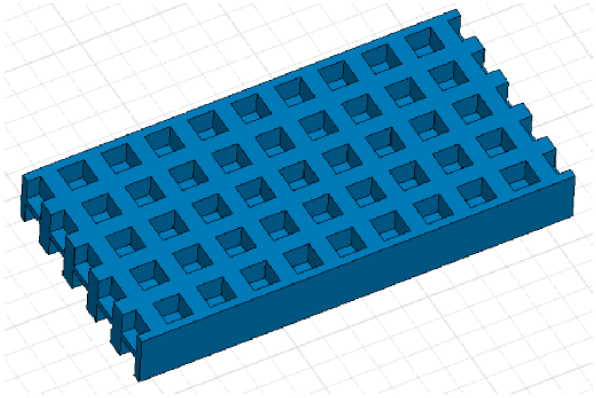

Fig. 6.16 HFSS model of waffle-iron filter.

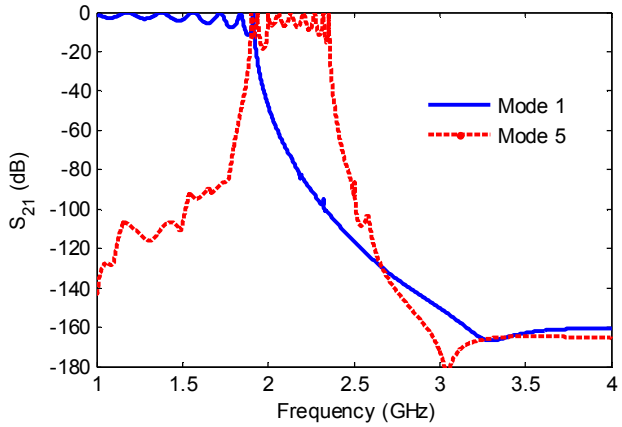

Fig. 6.17 Simulated S parameter of the first and fifth mode.

In actual design, input and output matching waveguides are included as shown in Fig. 6.18. As the size of the input and output waveguide is determined by the first mode, only the first mode maintains a flat passband as shown in Fig. 6.19. The responses of higher order mode are distorted due to the mis-matching. And these distortions of higher order modes cause the spikes in the first mode.

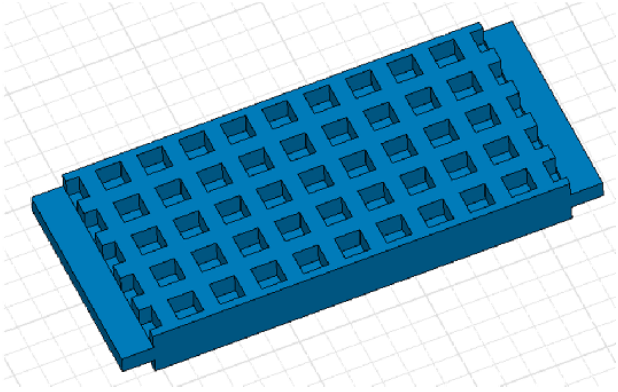

Fig. 6.18 HFSS model of waffle-iron filter with input and output waveguide.

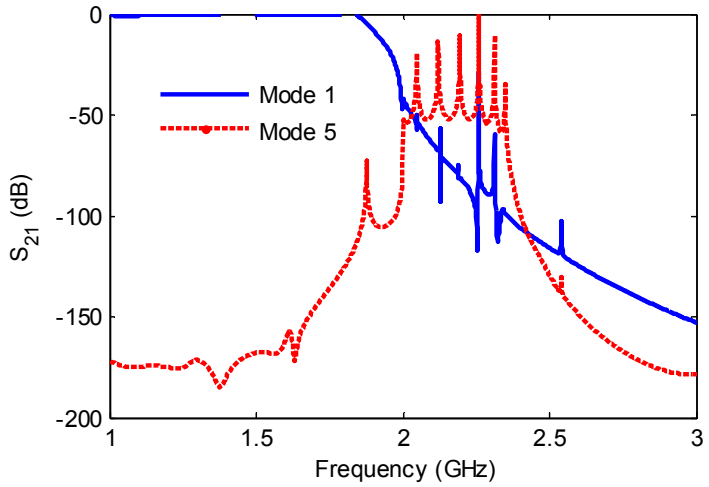

Fig. 6.19 Simulated S parameter of the first and fifth mode.

6.3.4 Improved configuration

To enhance the performance of a waffle iron filter, one way is to get better matching with the input and output rectangular waveguide. And the other is to modify the structure so that the higher order modes having the same bandedge leaving the stop band completely spurious free.

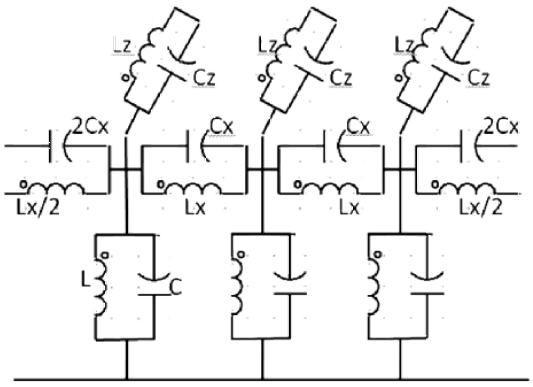

Fig. 6.20 Circuit model for an alternative waffle-iron filter configuration

The second option can be achieved by a structure based on a modified circuit model as shown in Fig. 6.20. In this circuit, each of the inductance couplings is modified to include a capacitance coupling.

When L=2, C=2, Lx=1, Cx=0.5, Lz=1, Cz=0.5, the response of the circuit model is shown in Fig. 6.21. All the five modes have a similar bandage in the higher frequency side. When the input voltage corresponds to that of the first mode with a phase shifter, the insertion loss is shown in Fig. 6.22.

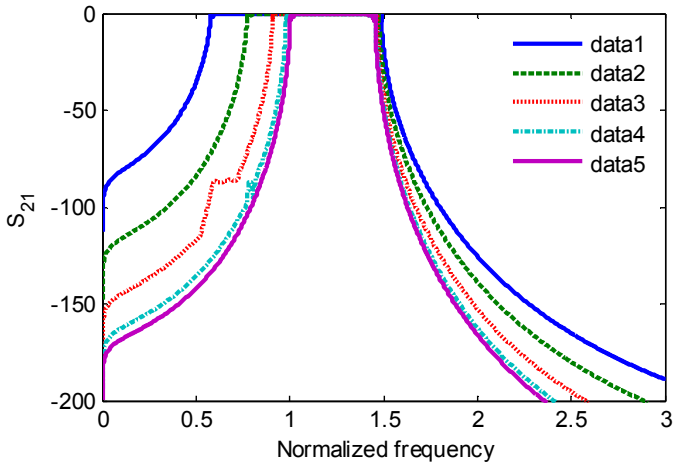

Fig. 6.21 S_{21} of the five modes of the modified configuration.

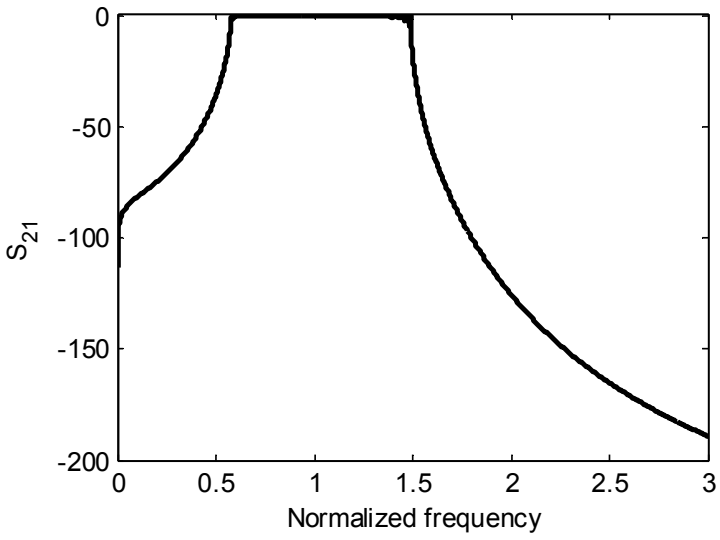

Fig. 6.22 S_{21} of the first mode when the input has a phase shift.

Chapter 7
Conclusions and Future work

The study for the theories of filter design and synthesis started in 1930s. Over the decades, the commonly used procedures begin with defined specifications. Then proper characteristic functions can be chosen. Various circuit networks can then be synthesized according to the applications. EM models are derived from the networks by direct transformation and EM tuning. Finally, physical structures can be built based on the EM models.

Even though these procedures are well-defined in the literature, the development of communication systems requires filters of high performance and more complicated architectures while the issues of size and cost are also critical. The work in the thesis consists of four parts, which are extensions to different aspects of filter synthesis. In the first two parts, various ways of incorporating dissipations are considered. Resonator loss is important in filter design because it determines its overall size. The method of filter synthesis with non-uniform Qs provides an effective way of reducing filter size.

The lossy synthesis method in Chapter 3 is an extension to the lossless coupling matrix synthesis given in [7] and [8] which first derives the admittance parameters from the characteristic functions using the equation of power conservation, then generate a canonical CM that can be transformed to required configurations. The lossy synthesis method presented is based on a new condition for the lossy characteristic polynomials to replace the power conservation. When the lossy transfer function is defined, solutions to the characteristic polynomials are found under two conditions. In the first one, S11 equals to k·S22 where k is a constant. This an even and odd mode of analysis applied to asymmetric filter responses. In the second one, the loss distribution is given and thus is a non-uniform predistortion. The method can 1) find the reflection function from the transfer function when unitary condition is not satisfied; 2) derive the expressions for the complex admittance parameters and 3) synthesize the lossy CM with prescribed loss distribution.

As the method is completely based on the given transfer function and loss distribution, future work can be concentrated on deriving the optimum lossy transfer function and Q distribution so that the filter designed has the small dimensions with varied cavity sizes.

Alternatively, an optimum lossy transfer function can be defined considering the return loss. As with loss compensation, the return loss is usually increased, transfer functions can be tuned to deliver the required return loss level.

For the method of lossy synthesis presented in section 3.3, the synthesis starts with a defined passive insertion loss and the derived CM has a positive imaginary part which represents dissipation. When various transformations of CM are applied, the imaginary part might be negative which is non-realistic. It is thus desired to include additional conditions on the transformation so that the passivity of the network can be guaranteed.

Generally speaking, the method of lossy synthesis can be used as a starting point for lossy filter design as it provide more variables tunable for filter performance and size. While the method presented considers only the resonator loss, the coupling loss can also be taken into consideration. While two specific solutions are discussed in the thesis, it is also possible that there are other solutions that can be used for a specific design.

The design of parallel connected network in Chapter 4 begins with discussions on the effect of dissipation on a single resonator with consideration of bandwidth and resonant frequency. Then for parallel connected networks, an approximated analytical solution to the loss distribution that gives a specific transfer function is given. Gradient based optimizations can also be applied for perfect transmission and reflection zeros and an optimum passband insertion loss.

The method presented can deliver good return loss and insertion loss with non-uniform Q distributions based on non-perfect Chebyshev functions. As a general rule, for better performance, high Qu resonators are the ones with a smaller bandwidth or the ones with near bandedge resonant frequencies.

The future work is to improve the applicability of the method to cavity filters as the parallel connected network is usually difficult to implement for such filters using coaxial or dielectric resonators. One way of doing this is to replace the couplings to the non-resonating nodes at the input and output by

a resonator since multiple couplings to a resonator are much easier to achieve.

Examples are given in the thesis for filters with a low loss path and a high loss path. Since the two paths can be realized using coaxial and microstrip technologies, a proper arrangement of the structure can save much size. Another future work is to implement the method to higher order filters.

Chapter 5 is on the coupling matrix synthesis for diplexers. In the first method, diplexers are designed using common junctions and channel filters. While the port length of common junction can be tuned to deliver optimum channel isolation and insertion, CMs are synthesized with a frequency variant load.

While the method of iteration guarantees the position of reflection zeros of the original Chebyshev responses, the return loss may not be equal ripple with a varied load. A further algorithm can be applied to change the position of reflection zeros so that equal rippled return loss can be found.

The method may be extended to derive the network for a diplexer or multiplexer when proper circuit models are used to represent junctions and connections. As the load is general, the method may also find application in designing a filter connecting to other devices such as an amplifier.

In the second method, directional filters are used for the design of diplexers. Methods are given for the synthesis of single and cascaded DF sections. Example of DF with coaxial resonators are also given. One of the advantage of designing diplexers with DFs is that it provide good isolation between the two channels as they are realized by the return loss and insertion loss of a filter response.

Since each DF section is coupled externally to other sections by specific length of 50Ohm transmission lines and is coupled internally to the resonators by non-resonating nodes, it is possible to replace the non-resonating nodes by resonators so that the phase length between sections can be realized by couplings. Also, different arrangement for the cascading can be experimented for the best performance.

Chapter 6 is on the circuit analysis of uniform 2D lumped element networks. The work presented here is a supplement to the study of metamaterial in

[111]. First, wave propagation in multi-wire line is studied. Then method of analysis is given for lumped element networks 2D networks and it is shown that for a 2D network with N by M nodes, there exist N mode of propagation within the structure. The input and output response of the structure is a combination of the propagating modes. Finally, the method of analysis is verified by the simulation of waffle-iron filters. It is thus shown that for a general non-uniform 2D structure that can be modelled by a lumped element network, there are always multiple mode of propagation. Single mode of propagation used in much of the discussion of metamaterial occurs only with a specific arrangement of input voltages or when the inductance matrix is the inverse of the capacitance matrix.

The method of analysis may be used for the synthesis of lowpass filter networks using waveguide or waffle-iron structures. And the spikes at stop band due to a misalignment at input and output port can be eliminated by a varied filter structure as discussed in section 6.3.4.

List of References

[1] G.L. Matthaei, L. Young, and E.M.T. Jones, Microwave Filters, Impedance-Matching Networks and Coupling Structures. New York: McGraw-Hill, 1964.

[2] Hunter, I.C.; Billonet, L.; Jarry, B.; Guillon, P., "Microwave filters-applications and technology," *Microwave Theory and Techniques, IEEE Transactions on* , vol.50, no.3, pp.794,805, Mar 2002

[3] M. Yu, W. C. Tang, A. Malarky, V. Dokas, R. Cameron, and Y. Wang, "Predistortion technique for cross-coupled filters and its application to satellite communication systems," IEEE Trans. Microwave Theory Tech., vol. 51, no. 12, pp. 2505–2515, Dec. 2003

[4] Mansour, R.R., "RF filters and diplexers for wireless system applications: state of the art and trends," *Radio and Wireless Conference, 2003. RAWCON '03. Proceedings* , vol., no., pp.373,376, 10-13 Aug. 2003

[5] Mansour, R.R., "Filter technologies for wireless base stations," *Microwave Magazine, IEEE* , vol.5, no.1, pp.68,74, Mar 2004

[6] Saal, R.; Ulbrich, E., "On the Design of Filters by Synthesis," *Circuit Theory, IRE Transactions on* , vol.5, no.4, pp.284,327, Dec 1958

[7] A. Atia and Williams, "New type of waveguide bandpass filters for satellite transponders," *COMSAT Tech. Rev.*, vol. 1, no. 1, pp. 21–43, 1971.

[8] R. J. Cameron, "Advanced Coupling Matrix Synthesis Techniques for Microwave Filters" *IEEE Trans. Microw. Theory Tech.*, vol.51 , no.1 , pp.1-10, Jan. 2003.

[9] Pozar, David M, Microwave engineering; 3rd ed. Hoboken, NJ , Wiley, 2005

[10] Swanson, Dan; Macchiarella, G., "Microwave filter design by synthesis and optimization," *Microwave Magazine, IEEE* , vol.8, no.2, pp.55,69, April 2007

[11] Advanced Simulation/Design Techniques for Microwave Filters. Ming Yu, IEEE MTTS 2001 workshop

[12] Cameron, R.J., Kudsia, C. M., Mansour, R. R., "Characterization of lossless lowpass prototype filter functions", Microwave filters for Communication systems, 1st ed, New Jersey, USA, John Wiley & Sons, Inc, 2007, Chapter 3, pp 97-101

[13] Cohn, Seymour B., "Direct-Coupled-Resonator Filters," *Proceedings of the IRE* , vol.45, no.2, pp.187,196, Feb. 1957

[14] Cameron, R.J., Kudsia, C. M., Mansour, R. R., “Design and physical realization of coupled resonator filter”, Microwave filters for Communication systems, 1st ed, New Jersey, USA, John Wiley & Sons, Inc, 2007, Chapter 14, pp 502-524

[15] 2002 Microwave filter applications and technologies-I.C.Hunter

[16] Cameron, R.J., "General coupling matrix synthesis methods for Chebyshev filtering functions," *Microwave Theory and Techniques, IEEE Transactions on* , vol.47, no.4, pp.433-442, Apr 1999

[17] Rhodes, J.D., "The Design and Synthesis of a Class of Microwave Bandpass Linear Phase Filters," *Microwave Theory and Techniques, IEEE Transactions on* , vol.17, no.4, pp.189,204, Apr 1969

[18] Rhodes, J.D., "The Generalized Direct-Coupled Cavity Linear Phase Filter," *Microwave Theory and Techniques, IEEE Transactions on* , vol.18, no.6, pp.308,313, Jun 1970

[19] Chapter 4. G. L. Matthaei, Leo Young, and E. M. T. Jones, Microwave filters, Impedance Matching Networks, and Coupling structures. New York: McGraw-Hill, 1964

[20] P. I. Richards, “Resistor-transmission-line circuits, ” .Proc. IRE, vol. 36, pp. 217–220, February 1948.

[21] Dishal, M., "Alignment and Adjustment of Synchronously Tuned Multiple-Resonant-Circuit Filters," *Proceedings of the IRE* , vol.39, no.11, pp.1448,1455, Nov. 1951

[22] Levy, R.; Cohn, Seymour B., "A History of Microwave Filter Research, Design, and Development," *Microwave Theory and Techniques, IEEE Transactions on* , vol.32, no.9, pp.1055,1067, Sep 1984

[23] A. E. Atia and A. E. Williams, “Narrow-bandpass waveguide filters,” *IEEE Trans. Microwave Theory Tech.*, vol. MTT-20, pp. 258–265, Apr. 1972.

[24] A. E. Atia, A. E. Williams, and R. W. Newcomb, “Narrow-band multiple-coupled cavity synthesis,” *IEEE Trans. Circuit Syst.*, vol. CAS-21,pp. 649–655, Sept. 1974.

[25] Levy, R., "Synthesis of general asymmetric singly- and doubly-terminated cross-coupled filters," *Microwave Symposium Digest, 1994., IEEE MTT-S International* , vol., no., pp.719,722 vol.2, 23-27 May 1994

[26] Fathelbab, W.M., "Synthesis of Cul-De-Sac Filter Networks Utilizing Hybrid Couplers," *Microwave and Wireless Components Letters, IEEE* , vol.17, no.5, pp.334,336, May 2007

[27] G. Macchiarella, “Accurate synthesis of in-line prototype filters using cascaded triplet and quadruplet sections,” IEEE Trans. Microwave Theory Tech., vol. 50, no. 7, pp. 1779–1783, July 2002.

[28] S. Tamiazzo and G. Macchiarella, “An analytical technique for the synthesis of cascaded N-tuplets cross-coupled resonators microwave filters using matrix rotations,” IEEE Trans. Microwave Theory Tech., vol. MTT-53, no. 5, pp. 1693–1698, May 2005

[29] R. J. Cameron, A. R. Harish and C. J. Radcliffe, “Synthesis of advanced microwave filters without diagonal cross-couplings,” IEEE Trans. Microwave Theory Tech., vol. MTT-50, pp. 2862-2872, Dec. 2002.

[30] Amari, S.; Macchiarella, G., "Synthesis of inline filters with arbitrarily placed attenuation poles by using nonresonating nodes," *Microwave Theory and Techniques, IEEE Transactions on* , vol.53, no.10, pp.3075,3081, Oct. 2005

[31] W. A. Atia, K. A. Zaki and A. E. Atia, “Synthesis of general topology multiple coupled resonator filters by optimization”, IEEE Microwave Theory Tech. Dig., pp821-824, 1998

[32] Amari, S.; Harscher, P.; Vahldieck, R.; Bornemann, J.; , "Novel analytic gradient evaluation techniques for optimization of microwave structures," Microwave Symposium Digest, 1999 IEEE MTT-S International , vol.1, no., pp.31-34 vol.1, 1999

[33] S. Amari, “Synthesis of cross-coupled resonator filter using an analytical gradient-based optimization technique” IEEE Trans. Microw. Theory Tech., vol.48 , no.9 , pp.1559-1564, Sep. 2000.

[34] Amari, S.; Rosenberg, U.; Bornemann, J.; , "Adaptive synthesis and design of resonator filters with source/load-multiresonator coupling," Microwave Theory and Techniques, IEEE Transactions on , vol.50, no.8, pp. 1969- 1978, Aug 2002

[35] Kozakowski, P.; Lamecki, A.; Sypek, P.; Mrozowski, M.; , "Eigenvalue approach to synthesis of prototype filters with source/load coupling," Microwave and Wireless Components Letters, IEEE , vol.15, no.2, pp. 98- 100, Feb. 2005

[36] Nicholson, G.L.; Lancaster, M.J., "Coupling matrix synthesis of cross-coupled microwave filters using a hybrid optimisation algorithm," *Microwaves, Antennas & Propagation, IET* , vol.3, no.6, pp.950,958, September 2009

[37] Manseok Uhm; Sangho Nam; Jeongphill Kim, "Synthesis of Resonator Filters With Arbitrary Topology Using Hybrid Method," *Microwave Theory and Techniques, IEEE Transactions on* , vol.55, no.10, pp.2157,2167, Oct. 2007

[38] Hunter, I.C.; Chandler, S.R.; Young, D.; Kennerley, A., "Miniature microwave filters for communication systems," *Microwave Theory and Techniques, IEEE Transactions on* , vol.43, no.7, pp.1751,1757, Jul 1995

[39] Ming Yu; Miraftab, V., "Shrinking microwave filters," *Microwave Magazine, IEEE* , vol.9, no.5, pp.40,54, Oct. 2008

[40] J. D. Rhodes, I. C. Hunter, "Synthesis of reflection-mode prototype networks with dissipative circuit elements," *Microwaves, Antennas and Propagation, IEE Proceedings*, vol.144, no.6, pp.437-442, Dec 1997

[41] Fathelbab, W.M.; Hunter, I.C.; Rhodes, J.D., "Synthesis of lossy reflection-mode prototype networks with symmetrical and asymmetrical characteristics," *Microwaves, Antennas and Propagation, IEE Proceedings* , vol.146, no.2, pp.97,104, Apr 1999

[42] Hunter, I.; Guyette, A.; Pollard, R.D.; , "Passive microwave receive filter networks using low-Q resonators," *Microwave Magazine, IEEE* , vol.6, no.3, pp. 46- 53, Sept. 2005

[43] Levy, R.; Snyder, R.V.; Matthaei, G., "Design of microwave filters," *Microwave Theory and Techniques, IEEE Transactions on* , vol.50, no.3, pp.783,793, Mar 2002

[44] Thal, H.L., Jr., "Microwave Filter Loss Mechanisms and Effects," *Microwave Theory and Techniques, IEEE Transactions on* , vol.30, no.9, pp.1330,1334, Sep. 1982

[45] Cohn, Seymour B., "Dissipation Loss in Multiple-Coupled-Resonator Filters," *Proceedings of the IRE* , vol.47, no.8, pp.1342,1348, Aug. 1959

[46] L. Young, “Group delay and dissipation loss in transmission line filters, ” IEEE Trans. on Microwave Theory and Techniques (Correspondence), vol. MTT- 11, pp. 2 15–2 17, May, 1963

[47] Papoulis, A., "Perturbations of the Natural Frequencies and Eigenvectors of a Network," *Circuit Theory, IEEE Transactions on* , vol.13, no.2, pp.188,195, Jun 1966

[48] S. Darlington, “Synthesis of reactance-Four pole which prescribed insertion loss characteristics” *Math. Phys.,* vol. 18, Sept. 1939.

[49] Desoer, C.A., "Network Design by First-Order Predistortion Technique," *Circuit Theory, IRE Transactions on* , vol.4, no.3, pp.167,170, Sep 1957

[50] Temes, G., "First-Order Estimation and Precorrection of Parasitic Loss Effects in Ladder Filters," *Circuit Theory, IRE Transactions on* , vol.9, no.4, pp.385,399, Dec 1962

[51] MacDonald, J.; Temes, G., "A Simple Method for the Predistortion of Filter Transfer Functions," *Circuit Theory, IEEE Transactions on* , vol.10, no.3, pp.447,450, Sep 1963

[52] MacDonald, J., "Lossy Low-Pass Network Design by Iteration," *Circuit Theory, IEEE Transactions on* , vol.13, no.3, pp.329,330, Sep 1966

[53] Gadenz, R., "Iterative compensation techniques for lossy or mismatched two-ports," *Circuit Theory, IEEE Transactions on* , vol.20, no.5, pp.599,603, Sep 1973

[54] A. E. Williams, W. G. Bush and R. R. Bonetti, “Predistortion Techniques for Multicoupled resonator” *IEEE Trans. Microw. Theory Tech.*, vol.33 , no.5 , pp.402-408, May. 1985.

[55] B. S. Senior, I. C. Hunter and J. D. Rhodes, “Synthesis of lossy filters,” in *32nd Eur. Microw. Conf.*, Milan, Italy, 2002, pp.401-404.

[56] Guyette, AC.; Hunter, IC.; Pollard, Roger D., "A new class of selective filters using low-Q components suitable for MMIC implementation," *Microwave Symposium Digest, 2004 IEEE MTT-S International* , vol.3, no., pp.1959,1962 Vol.3, 6-11 June 2004

[57] A. C. Guyette, I. C. Hunter and R. D. Pollard, “The Design of Microwave Bandpass Filters Using Resonators With Nonuniform Q” *IEEE Trans. Microw. Theory Tech.*, vol.54 , no.11 , pp.3914-3922, Nov. 2006.

[58] A. C. Guyette, I. C. Hunter and R. D. Pollard , Design of highly selective bandpass filters with non-uniform dissipations, 3rd EMRS DTC Technical Conference, Edinburgh, 2006.

[59] Guyette, A.C.; Hunter, I.C.; Pollard, Roger D., "Exact Synthesis of Microwave Filters with Nonuniform Dissipation," *Microwave Symposium, 2007. IEEE/MTT-S International* , vol., no., pp.537,540, 3-8 June 2007

[60] Oldoni, Matteo; Macchiarella, G.; Gentili, G., "A novel approach to lossy filter synthesis," *Microwave Conference, 2009. EuMC 2009. European* , vol., no., pp.444,447, Sept. 29 2009-Oct. 1 2009

[61] Oldoni, Matteo; Macchiarella, G.; Gentili, G.G.; Ernst, C., "A New Approach to the Synthesis of Microwave Lossy Filters," *Microwave Theory and Techniques, IEEE Transactions on* , vol.58, no.5, pp.1222,1229, May 2010

[62] V. Miraftab and M. Yu, “Generalized Lossy Microwave Filter Coupling Matrix Synthesis and Design Using Mixed Technologies” *IEEE Trans. Microw. Theory Tech.*, vol.56 , no.12 , pp.3016-3027, Dec. 2008.

[63] V. Miraftab and M. Yu, “Advanced Coupling Matrix and Admittance Function Synthesis Techniques for Dissipative Microwave Filters” *IEEE Trans. Microw. Theory Tech.*, vol.57 , no.10 , pp.2429-2438, Oct. 2009.

[64] Desoer, C.; Mitra, S.; , "Design of Lossy Ladder Filters by Digital Computer," *Circuit Theory, IRE Transactions on* , vol.8, no.3, pp. 192-201, Sep 1961

[65] Lasdon, L.; Waren, A.; , "Optimal Design of Filters with Bounded, Lossy Elements," *Circuit Theory, IEEE Transactions on* , vol.13, no.2, pp. 175- 187, Jun 1966

[66] Lamperez, A.G.; Salazar-Palma, M.; Padilla-Cruz, M.J.; Carpintero, I.H.; , "Synthesis of cross-coupled lossy resonator filters with multiple input/output couplings by gradient optimization,"*Antennas and Propagation Society International Symposium, 2003. IEEE* , vol.2, no., pp. 52- 55 vol.2, 22-27 June 2003. – opt of cm only, equal Qu for resonators

[67] Szydlowski, L.; Lamecki, A.; Mrozowski, M.; , "Synthesis of Coupled-Lossy Resonator Filters," *Microwave and Wireless Components Letters, IEEE* , vol.20, no.7, pp.366-368, July 2010. – matrix with complex cross couplings

[68] Improved Synthesis for the Design of Microwave Filters With a Minimum Insertion-Loss Configuration Abdallah Nasser, Stéphane Bila, Serge Verdeyme, Member, IEEE, and Fabien Seyfert

[69] Advanced Simulation/Design Techniques for Microwave Filters- An Engineering Perspective Dr. Ming Yu

[70] G. L. Matthaei, “Comb-line filters of narrow or moderate bandwidth,” Microwave J., vol. 6, pp. 82–91, Aug. 1963

[71] S. J. Fiedziuszko, I. C. Hunter, T. Itoh, Y. Kobayashi, T. Nishikawa, S. N. Stitzer, and K. Wakino, “Dielectric materials, devices, and circuits,” IEEE Trans. Microwave Theory Tech., vol. 50, pp. 706–720, Mar. 2002

[72] W. G. Lin, “Microwave filters employing a single cavity excited in more than one mode,”J. Appl. Phys., vol. 22, pp. 989–1001, Aug. 1951.

[73] MENG, M..*An analytical approach to computer aided diagnosis and tuning of lossy microwave coupled resonator filters*. Thesis (M.Phil.)--Chinese University of Hong Kong, 2009.

[74] Chi Wang, *Senior Member, IEEE,* Kawthar A. Zaki, *Fellow, IEEE,*Ali E. Atia, *Fellow, IEEE,* and Tim G. Dolan, Dielectric Combline Resonators and Filters

[75] Michael Höft and Thore Magath, "Compact Base-Station Filters Using TM-Mode Dielectric Resonators", German Microwave Conference GeMIC, Karlsrhue, 2006.

[76] HFSS, Version 13, Ansoft Corporation LLC, 225 West Station, Square Suite 200, Pittsburgh, PA 15219-1119, 2011.

[77] Meng Meng; Hunter, Ian C., "The design of parallel connected filter networks with non-uniform Q resonators," *Microwave Symposium Digest (MTT), 2012 IEEE MTT-S International* , vol., no., pp.1,3, 17-22 June 2012

[78] K. Kurokawa, "*Power Waves and the Scattering Matrix*", *IEEE Trans. Microwave Theory & Tech.,* Mar. 1965, pp194-202

[79] F. Seyfert “From S to M” tutorial. [Online]. Available:http://www-sop.inria.fr/apics/Dedale/Doc/S2M.html

[80] Abunjaileh, A.I.; Hunter, I.C., "Direct Synthesis of Parallel-Connected Symmetrical Two-Port Filters," *Circuits and Systems II: Express Briefs, IEEE Transactions on* , vol.57, no.12, pp.971,974, Dec. 2010

[81] Meng Meng; Ke-Li Wu, "An analytical approach of extracting coupling matrix and unloaded Q of A bandpass filter," *Microwave Symposium Digest, 2009. MTT '09. IEEE MTT-S International* , vol., no., pp.1345,1348, 7-12 June 2009

[82] Meng Meng; Ke-Li Wu, "An Analytical Approach to Computer-Aided Diagnosis and Tuning of Lossy Microwave Coupled Resonator Filters," *Microwave Theory and Techniques, IEEE Transactions on*, vol.57, no.12, pp.3188,3195, Dec. 2009

[83] Hoft, M., "Bandpass filter using TM-mode dielectric rod resonators with novel input coupling," *Microwave Symposium Digest, 2009. MTT '09. IEEE MTT-S International* , vol., no., pp.1601,1604, 7-12 June 2009

[84] Zhang Zhongxiang; Chen Chang; Wu Xianliang, "A compact cavity filter with novel TM mode dielectric resonator structure," *Microwave Technology & Computational Electromagnetics (ICMTCE), 2011 IEEE International Conference on* , vol., no., pp.111,113, 22-25 May 2011

[85] Hunter, I.C.; Rhodes, J.; Dassonville, V., "Dual-mode filters with conductor-loaded dielectric resonators," *Microwave Theory and Techniques, IEEE Transactions on* , vol.47, no.12, pp.2304,2311, Dec 1999

[86] Hunter, I.C.; Walker, V., "Ceramic filters in mobile communications," Microwave Filters and Multiplexers, IEE Colloquium on , vol., no., pp.5/1,5/3, 2000

[87] Meng Meng; Hunter, I.C.; Rhodes, J.D., "The Design of Parallel Connected Filter Networks With Nonuniform Resonators," *Microwave Theory and Techniques, IEEE Transactions on* , vol.61, no.1, pp.372,381, Jan. 2013

[88] Amari, S.; Bekheit, M.; , "Physical Interpretation and Implications of Similarity Transformations in Coupled Resonator Filter Design," *IEEE Trans. Microw. Theory Tech.,* vol.55, no.6, pp.1139-1153, June 2007

[89] Bottom Coupling of Combline Resonators for Hybrid Dielectric / Air-Cavity Bandpass Filters, Michael Hoft

[90] R.J. Cameron, Ming Yu, "Design of manifold-coupled multiplexers," *Microwave Magazine, IEEE* , vol.8, no.5, pp.46-59, Oct. 2007

[91] R.J. Wenzel, W.G. Erlinger, "Narrowband Contiguous Multiplexing Filters with Arbitrary Amplitude and Delay Response," *Microwave Symposium Digest, MTT-S International* , vol.76, no.1, pp. 116-118, Jun 1976

[92] G. Macchiarella, S. Tamiazzo, "Novel Approach to the Synthesis of Microwave Diplexers," *IEEE Trans. Microwave Theory & Tech*, vol.54, no.12, pp.4281-4290, Dec. 2006

[93] Macchiarella, G.; Tamiazzo, S., "Synthesis of Star-Junction Multiplexers," *Microwave Theory and Techniques, IEEE Transactions on* , vol.58, no.12, pp.3732,3741, Dec. 2010

[94] Matthaei G. L., Young L., and Jones E. M. T., *Microwave Filters, Impedance Matching Networks and Coupling Structures*, Norwood, MA: Artech House, 1964, pp. 165–173, 243–252.

[95] Wanselow, R.D. and Tuttle, L.P. Jr., “Practical design of strip transmission line half-wavelength resonator directional filters”, *Trans. IRE*, Jan. 1959, vol. MTT-7, pp. 168-173

[96] Coale, F.S., “A Travelling-Wave Directional Filter”, *Trans. IRE*, Oct. 1956, vol. MTT-4, pp. 256-260

[97] Wing, O., “Cascade Directional Filter”, *Microwave Theory and Techniques, IRE Transactions*, 1959, vol. 7, vo. 2, pp. 197-201

[98] Cohn, S.B.; Coale, F.S., "Directional Channel-Separation Filters," *Proceedings of the IRE* , vol.44, no.8, pp.1018,1024, Aug. 1956

[99] K.-L. Wu, W. Meng, "A Direct Synthesis Approach for Microwave Filters With a Complex Load and Its Application to Direct Diplexer Design," *IEEE Trans. Microwave Theory & Tech*, vol.55, no.5, pp.1010-1017, May 2007

[100] Meng Meng; Ke-Li Wu, "Direct synthesis of general Chebyshev bandpass filters with a frequency variant complex load," *Microwave Symposium Digest (MTT), 2010 IEEE MTT-S International* , vol., no., pp.433,436, 23-28 May 2010

[101] Rhodes, J. D. and Mobbs C.I., “Explicit Design of remote-tuned combiner for GSM and WCDMA signals”, *International Journal of Circuit Theory and Applications*, September – December 2007, vol. 35, no.5-6, pp. 547-564

[102] I. C. Hunter, E. Musonda, R. Parry, M. Guess, M. Meng, “Transversal Directional Filters for Channel Combining”, *Microwave Symposium Digest, 2013 IEEE MTT-S International*, June 2013.

[103] Garcia-Lamperez, A.; Salazar-Palma, M.; Sarkar, T.K., "Analytical synthesis of microwave multiport networks," *Microwave Symposium Digest, 2004 IEEE MTT-S International*, vol.2, no., pp.455,458 Vol.2, 6-11 June 2004

[104] Pipes, Louis A., "Steady-State Analysis of Multiconductor Transmission Lines," *Journal of Applied Physics* , vol.12, no.11, pp.782,799, Nov 1941

[105] Chang, Fung-Yuel, "Computer-aided characterization of TEM transmission lines," *Circuits and Systems, IEEE Transactions on*, vol.27, no.12, pp.1194,1205, Dec 1980

[106] Scanlan, J.O., "Theory of microwave coupled-line networks," *Proceedings of the IEEE* , vol.68, no.2, pp.209,231, Feb. 1980

[107] Nature, August 2008, pg4

[108]Young, Leo; Schiffman, Bernard M., "New and improved types of waffle-iron filters," *Electrical Engineers, Proceedings of the Institution of* , vol.110, no.7, pp.1191,1198, July 1963

[109]. Chapter 7. G. L. Matthaei, Leo Young, and E. M. T. Jones, Microwave filters, Impedance Matching Networks, and Coupling structures. New York: McGraw-Hill, 1964

[110] J.D Rhodes “General Constraints on Propagation Characteristics of Electromagnetic Waves in Uniform Inhomogeneous Waveguides” Proc. IEE, Vol.118, No.7, July 1971.

[111] I.C.Hunter, A.I.Abunjaileh, J.D.Rhodes, R.V. Snyder, M.Meng, “Propagation and Negative Refraction”, IEEE Microwave Magazine, Vol.13, No.5, July/Aug 2012, pp. 58-65.

[112] Cohn, S. B., Jones, E. M. T., Shimizu, J. K., Schiffman, B. M., and Coale, F. S., ‘Research on design criterialfor microwave filters’, Final report, June 1957, Project 1331, Stanford Research Institute